

Mechanisms and Clinical Implications of Human X Chromosome Inactivation



Bas de Hoon

Mechanisms and Clinical Implications of Human X Chromosome Inactivation

Bas de Hoon

**Mechanisms and Clinical Implications
of Human X Chromosome Inactivation**

PhD thesis, Erasmus University, The Netherlands

ISBN: 978-94-6299-264-1

Cover design: Rian van de Wiel

Layout: Bas de Hoon

Printing: Ridderprint BV, Ridderkerk, The Netherlands

The research described in this thesis was performed at the department of Developmental Biology and the department of Obstetrics and Gynaecology at the Erasmus MC, Rotterdam, The Netherlands.

The printing of this thesis has been financially supported by the department of Developmental Biology at the Erasmus MC, Rotterdam, The Netherlands and the Maatschap Gynaecologie Albert Schweitzer Ziekenhuis, Dordrecht, The Netherlands.

Copyright © 2015

Bas de Hoon, The Netherlands

All rights reserved. No part of this thesis may be reproduced in any form or by any means without written permission from the author.

Mechanisms and Clinical Implications of Human X Chromosome Inactivation

De mechanismes en klinische implicaties
van humane X chromosoom inactivatie

Thesis

to obtain the degree of Doctor
from the Erasmus University Rotterdam
by command of the rector magnificus

Prof.dr. H.A.P. Pols
and in accordance with
the decision of the Doctorate Board.

The public defense shall be held on
Tuesday the 12th of January 2016 at 15:30 hrs.

by
Bas de Hoon
born in Oosterhout, The Netherlands

Doctoral committee

Promotors: Prof.dr. J.H. Gribnau
Prof.dr. J.S.E. Laven

Other members: Prof.dr. D. Huylebroeck
Prof.dr. R.M.W. Hofstra
Prof.dr.ir. S.M. van der Maarel

Paranymphs: A. Kenter
E. Rentmeester

Contents

List of abbreviations		6
Chapter 1	Introduction	8
Chapter 2	The probability to initiate X chromosome inactivation is determined by the X to autosomal ratio and X chromosome specific allelic properties	84
Chapter 3	The human X-inactivation center comprises a cis-acting and a trans-acting region	118
Chapter 4	Mutations in <i>RNF12</i> segregate with X-linked intellectual disability and result in hypomorphic alleles	134
Chapter 5	Buccal swab as a reliable predictor for X-inactivation ratio in inaccessible tissues	154
Chapter 6	Stable X Chromosome Reactivation in Female Human Induced Pluripotent Stem Cells	172
Chapter 7	General Discussion	194
Appendix	Summary	216
	Samenvatting	219
	List of publications	223
	Curriculum Vitae	224
	PhD portfolio	225
	Dankwoord	226

List of Abbreviations

3C	chromosome conformation capture
4C	chromosome conformation capture on-chip
AITD	Auto Immune Thyroid Disease
AR	androgen receptor
BAC	bacterial artificial chromosome
CEU	Utah residents with ancestry from northern and western Europe
EPI	epiblast
epiSC	epiblast derived stem cell
ES cell	embryonic stem cell
FISH	fluorescent in-situ hybridisation
GWA	genome wide association
ICM	inner cell mass
iPS cell	induced pluripotent stem cell
iXCI	imprinted X chromosome inactivation
LCL	lymfoblastoid cell line
lncRNA	long non coding RNA
LIF	leukemia inhibitory factor
LINE	long interspersed nuclear element
PAR	pseudo-autosomal region
PCOS	polycystic ovary syndrome
PE	primitive endoderm
RNA pol II	RNA polymerase II
RNA-seq	RNA-sequencing
rXCI	random X chromosome inactivation
TAD	topologically associated domain
TE	trophectoderm
Tsix	gene antisense of Xist
Xa	active X chromosome
Xi	inactive X chromosome
Xm	X chromosome from maternal origin
Xp	X chromosome from paternal origin
Xce	X choosing element
XCI	X chromosome inactivation
XCR	X chromosome reactivation

XIC	X-inactivation center
XIST	X-Inactive Specific Transcript
XIR	X-inactivation ratio
YRI	Yoruban, in Ibadan, Nigeria

CHAPTER 1



Introduction

Parts of this chapter will be published as:

Fitting the puzzle pieces: the bigger picture of XCI
Cheryl Maduro, Bas de Hoon, and Joost Gribnau

Submitted



The need for X chromosome inactivation was created by the evolution of the Y chromosome

Sex determination systems

Sexual reproduction offers the advantage of increased genetic variation in offspring, which creates detrimental mutations, but also an increased adaptability for a species to select for fitness in a changing environment. As a result of sexual reproduction a variety of sex determination systems have evolved, that either use environmental conditions or genetic factors to determine sexual differentiation of an individual. Environmental sex determination is used by many egg-laying reptile species, where the temperature during embryonic development permanently determines the sex of the embryo. A disadvantage of environmental sex determination is that the balance between the sexes is not guaranteed and might be disturbed by changes in the environment.

In genetic sex determination, which is the topic of this PhD research, sexual differentiation of an individual is determined by a sex-determining gene, or by the ratio between sex chromosomes and autosomes. In the non-parasitic worm *Caenorhabditis elegans* the X: autosome ratio is used for sex determination. Males have one X chromosome and hermaphrodites have two X chromosomes and both have a similar set of autosomes. The ratio between autosomal factors and X chromosomal factors determines the expression of the male-specifying gene *xol-1* (Carmi et al., 1998; Miller et al., 1988). In the fruit fly *Drosophila melanogaster* sex is also determined by the X: autosome ratio, with males being heterogametic, having an X and a Y chromosome, and females being homogametic, having two X chromosomes. Again the ratio between X-encoded factors and autosomal factors regulates the expression of a sex-determining gene. In this case, the sex-determining gene *SXL* promotes female differentiation (Cline, 1983; Salz et al., 1989).

In birds, sex is determined by the Z and W chromosomes, with females being heterogametic, carrying a Z and a W chromosome, and males having two Z chromosomes. Whether the Z chromosome or W chromosome is sex determining in birds is still unresolved. A role for the Z chromosome as male sex-determining chromosome is supported by the presence of the male sex determining gene *Dmrt1* on the Z chromosome, with a double dose of *Dmrt1* resulting in male gonadal development. A sex determining role for the W chromosome in females is hypothesized based on the location of the *Fet1* and *Asw* genes, which are expressed during female development (Pace and Brenner, 2003; Reed and Sinclair, 2002). The avian ZW sex-chromosomes and mammalian XY sex-chromosomes are unrelated, as they have probably evolved from a different pair of autosomes (Nanda et al., 2002; Nanda et al., 1999).

In placental mammals, including humans, males are heterogametic carrying an X and Y chromosome, whereas females carry two X chromosomes. Sex is determined by the presence of the Y-chromosomal gene *Sry*, for Sex Determining region on the Y. The *Sry* gene is critical for induction of male sexual differentiation, leading embryonic development away from female development, which occurs by default. The requirement of *Sry* for sex determination is shown by XY mice lacking a functional copy of *Sry*, which develop a female phenotype, and XX mice carrying a *Sry* transgene, which develop a male phenotype (Kato et al., 2013). The location of *Sry* on the Y chromosome made it the sex-determining chromosome in mammals.

At present, the X and Y chromosome are two heteromorphic chromosomes, with the human X chromosome being the larger chromosome, containing 819 coding genes. The human Y chromosome contains 72 coding genes, of which most are involved in sex determination and male fertility. The heteromorphic nature of the X and Y chromosome creates a potential imbalance for X chromosomal gene dosage between XY males and XX females. To correct this imbalance in number of X-chromosomal genes a dosage compensation mechanism has evolved, involving (i) the two-fold upregulation of X-chromosomal genes in males and (ii) the subsequent inactivation of one of the X chromosomes in females (Lyon, 1961; Ohno, 1967). The mechanism of X chromosome inactivation (XCI) has been subject of study for decades, and still has not revealed all its secrets.

Dosage compensation evolved parallel to the degeneration of the Y chromosome

Although the X and Y chromosome are remarkably different at present, it is commonly accepted that they find their origin in a single set of identical autosomes. This hypothesis is based on studies comparing sex-chromosomal sequences between eutherian mammals, other eutherians, marsupials, and monotremes. The diversion of two identical autosomes into the current X and Y chromosomes has driven the evolution of XCI. It is thought that the diversion of the ancestral autosomes started 160-180 million years ago with the acquisition of *Sry* by one of the autosomes, together with an inversion involving the *Sry* region (Lahn and Page, 1999). By acquiring *Sry* this autosome became the future Y chromosome (Fig. 1). In addition, the inversion that occurred must have served the prevention of meiotic recombination of the *Sry* region with the future X chromosome. As the inverted region was no longer able to recombine, this region on the future Y chromosome became susceptible to acquiring mutations and as a consequence started to lose genetic material. To compensate the loss of genetic material in the *Sry* region in males, dose-sensitive homologous genes on the future X were upregulated twofold. Simultaneously in females, the upregulated region on the future X chromosome became subject to XCI (Gribnau and Grootegeod, 2012).

As the *Sry* region accumulated the aforementioned mutations, the region that was unable to recombine must have expanded (Bachtrog, 2013; Ellegren, 2011). This did not only

result in the additional loss of genetic material, but also in the acquisition of male-beneficial genes (Rice, 1987). As more genes were disrupted or deleted on the future Y, their homologous counterparts on the future X were upregulated in males, and became subject to female specific silencing. During the accumulation of deletions and mutations the Y chromosome lost most of its genes (Skaletsky et al., 2003). Since the X chromosome remained able to recombine during female meiosis it was not subject to the degeneration observed for the Y chromosome, but it became almost completely subject to XCI.

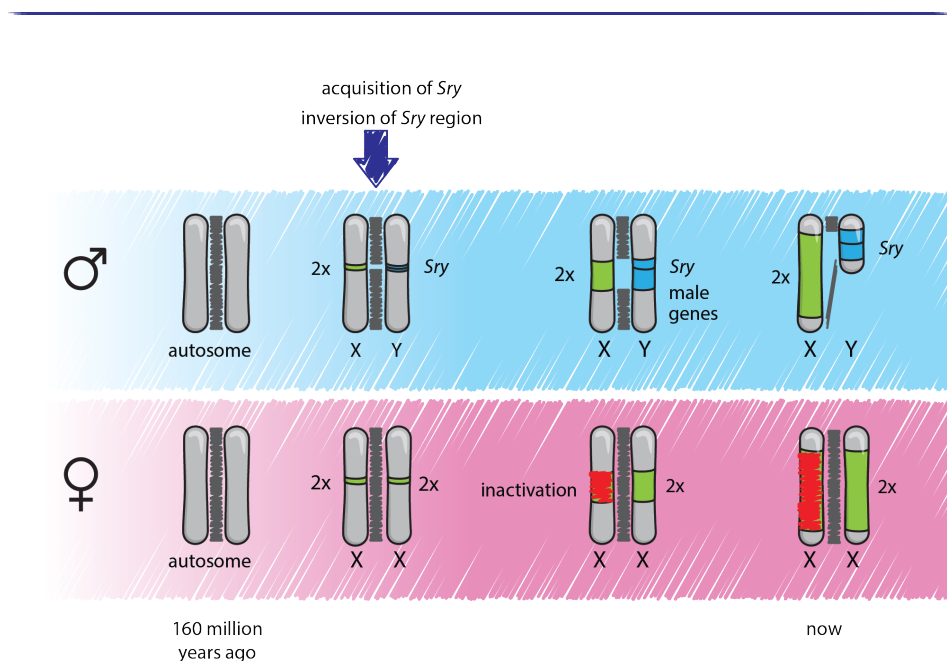


Figure 1.

The need for dosage compensation evolved in parallel with the degeneration of the Y chromosome.

The X and Y chromosome in their current state originate from a single set of identical autosomes. On one of the ancestral autosomes *Sox3* mutated into *Sry*, thereby designating this autosome as the future Y chromosome. On the future X chromosome the remaining *Sox3* allele was upregulated twofold to compensate for the loss of the Y chromosomal allele. As the *Sry*-containing region on the future Y was no longer able to recombine with the future X during male meiosis, this region started to lose genetic material, thereby expanding the non-homologous region between X and Y. The loss of functional genes in the non-homologous region between X and Y prompted the compensatory upregulation of X chromosomal genes. Finally the X and Y chromosome are able to recombine only at the pseudoautosomal region (PAR, see main text). The X-chromosomal genes outside the PAR are upregulated twofold, and are subject to inactivation in females.

In its current status the X and Y chromosomes are still able to recombine at one or two small segments, named PseudoAutosomal Regions (PARs). In humans there are two PARs at the distal tips of both the X and Y chromosomes. The human PAR1 at the tip of the short arm is 2,6 Mb in size and contains at least 24 genes. The human PAR2 at the tip of the long arm is 330 kb and contains 4 genes (Ross et al., 2005). In mouse there is one PAR only, which varies in size between different strains of laboratory mice. The mouse PAR is between 700 kb and 1100 kb long and contains at least two genes.

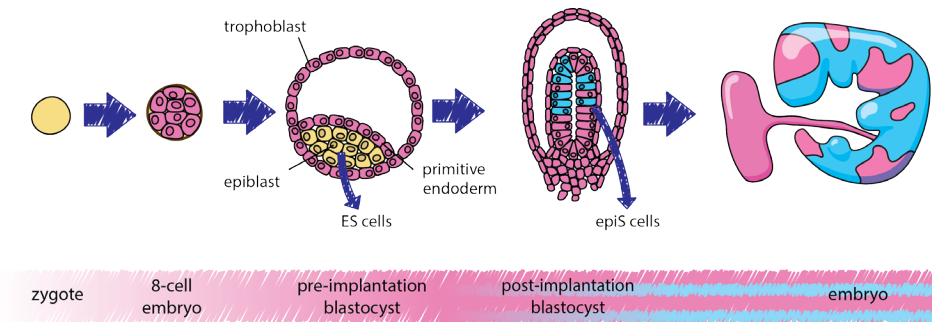
X chromosome inactivation

XC occurs early in embryogenesis. In mouse two forms of XCI take place successively, which results in different XCI patterns in the embryo and extraembryonic tissues (Fig. 2). First, from the 2 to the 16 cell stage imprinted XCI is initiated, resulting in the exclusive inactivation of the paternal X chromosome (Xp) in all cells of the slowly cleaving embryo (Huynh and Lee, 2003; Nesterova et al., 2001a; Okamoto et al., 2004; Sheardown et al., 1997; Takagi and Sasaki, 1975). At the blastocyst stage the different cell lineages that have emerged will exhibit different forms of XCI. Cells of the trophectoderm (TE) and the primitive endoderm, which both contribute to the extraembryonic tissues, will maintain imprinted XCI. In contrast, the remaining cells of the inner cell mass (ICM) that will make up the embryo proper, reactivate the inactive Xp to prepare for the second round of XCI (Mak et al., 2004). This second round of XCI is initiated around day 5.5 of development and is random with respect to the parental origin of the X chromosomes, meaning that both X chromosomes will have an equal probability to be inactivated. Once the inactive state is established, this will be maintained for a near infinite number of cell divisions. As a result of this random choice which X chromosome is inactivated the female embryo is a mosaic of cells with either an inactive maternal X chromosome (Xm) and cells with an inactive Xp.

Pluripotent cells as model system for XCI

Embryonic stem cells

XCI occurs during early embryogenesis, which is an obstacle for functional studies of the underlying mechanisms for XCI in humans. *In vivo* studies would require the use of human embryos, which are sometimes available as surplus material from IVF procedures, but only in a very limited amount (Van den Berg 2009). Given the limited amount of material to study human XCI and the lack of a good human *in vitro* system, most of our knowledge regarding XCI

**Figure 2.****XCI occurs during early mouse embryogenesis**

In the zygote of the mouse both X chromosomes are active after zygotic genome activation. Around the morula stage imprinted inactivation of the Xp takes place, resulting in the exclusive expression of the Xm in all cells. In the pre-implantation blastocyst the cells of the epiblast reactivate the Xp to prepare for subsequent random XCI. The cells of the hypoblast and and trophoblast maintain an inactive Xp. In the post-implantation blastocyst the cells of the epiblast initiate a second round of XCI, which is random with respect to the parental origin of the X chromosomes. After the cells of the epiblast have selected and inactivated one of their X chromosomes, the inactive state of this chromosome is passed on to all daughter cells. As a result the female embryo is a mosaic of cells that express either the Xp or the Xm. The cells of the extra-embryonic tissues will maintain the imprinted inactive state of the Xp throughout female embryonic development.

comes from mouse model systems. Especially mouse Embryonic Stem (ES) cell lines have been of great importance to study XCI in the past decades, as female mouse ES cells carry two active X chromosomes and, when induced to differentiate *in vitro*, these cells undergo random XCI. Mouse ES cells are derived from the epiblast of (E3,5-4,5) pre-implantation blastocysts (Fig. 2). In the pre-implantation blastocyst three morphologically different cell types can be distinguished. The trophoblast (TE) is a monolayer of cells on the outside of the blastocyst, that serves implantation, and will later give rise to most of the fetal part of the placenta. Located on the inside of the blastocyst are the epiblast (EPI) cell population and the cells of the primitive endoderm (PE). The cells of the epiblast will form the entire fetus and contribute to the yolk sac and amnion. The cells of the epiblast are covered by a layer of the primitive endoderm cells, which will later cover the entire cavity of the fluid-filled blastocyst. After implantation of the blastocyst, the primitive endoderm will give rise to parietal and visceral

endoderm, of which the latter will form the endodermal layer of the yolk sac. From the pre-implantation stage embryo, epiblast cells can be isolated and cultured and kept in an undifferentiated pluripotent state as mouse ES cells (Boroviak 2014). Due to their capability of self-renewal, the ability to undergo XCI during differentiation, and the possibility to perform genetic targeting, mouse ES cells have been instrumental as an *in vitro* system for studying the mechanisms of XCI.

Human ES cells

Unfortunately a similar human model system as the aforementioned mouse ES cells is not available, as human ES cells seem to represent a more differentiated pluripotent stem cell than mouse ES cells. Most human ES cell lines carry an inactivated X chromosome (Xi), and those that have two active X chromosomes (Xa's) do not always undergo XCI upon differentiation (Silva et al., 2008). This dissimilarity between human and mouse ES cells in this respect is striking, given that they are both isolated from a pre-implantation blastocyst. Over the last few years it has become clear that human ES cells are more resembling mouse epiblast stem cells (epiSC), which are a more differentiated type of pluripotent stem cell. EpiSCs can be derived from the epiblast of the mouse post-implantation blastocyst, where ES cells are derived from mouse a pre-implantation blastocyst. As a result, epiSCs represent the cells of the epiblast that are primed for differentiation, where ES cells represent the naïve epiblast. As a consequence epiSCs cannot contribute to the germline of chimaeric mice, while ES cells can. Mouse epiSCs carry an inactive X chromosome, like most human ES cells. Human ES cells and mouse epiSCs are grown in similar culture conditions, as both depend on Activin/Nodal and FGF signaling for self-renewal. In contrast, mouse ES cells require Leukemia Inhibitory Factor (LIF) and Wnt signaling for staying undifferentiated *ex vivo* and for self-renewal (Brons et al., 2007; Smith et al., 1988; Tesar et al., 2007). When kept in culture both mouse epiSCs and human ES cells grow in colonies with a flat morphology, while mouse ES cell colonies are dome-shaped. The transcriptome of human ES cells overlaps more with that of mouse epiSCs, instead of mouse ES cells (Huang et al., 2014).

The identified differences between cultured pluripotent mouse ES cells and human ES cells can be the result of the derivation itself, an adaptation to culture conditions or intrinsic differences between human and mouse early embryogenesis. An interesting phenomenon in mouse embryos, which might facilitate isolation of ES cells is embryonic diapause. Mouse embryos have the ability to arrest their development at the late blastocyst stage, when entering an unfavorable uterine environment. When restored into an estrogen-rich environment, these blastocysts resume their arrested development normally. In diapause the embryos thus cease to develop and remain un-implanted in the uterus, which can persist for several weeks without losing the ability to continue development. Interestingly, mouse ES cells

were in fact first derived from such diapause embryos and appear to be derived more efficiently from diapause embryos than from normal blastocysts (Brook and Gardner, 1997; Evans and Kaufman, 1981). Interestingly, diapause is dependent on LIF, which is required for mouse ES cells establishment (Nichols and others 2001). Altogether, it seems that the window of naïve pluripotency can be extended for a longer period of time in the mouse, facilitating the derivation of ES cell lines. In human, the existence of diapause is unlikely, although this is still under debate (Ptak 2012, Ptak 2013). The absence of diapause in humans would explain why the derivation of naïve human ES cells carrying two active X chromosomes is difficult.

Mouse induced pluripotent stem cells

Another type of pluripotent stem cell frequently used to study the mechanism of XCI is the induced pluripotent stem (iPS) cell. iPS cells have first been generated from somatic cells (e.g. fibroblasts) by forced expression of the transcription factors Klf4, Sox2, Oct4 and c- Myc (Takahashi and Yamanaka, 2006). Forced expression of these pluripotency factors in somatic cells resulted in reversion of these cells into a pluripotent state morphologically and functionally indiscernible from ES cells. When injected into a mouse blastocyst iPS cells can contribute to all germ layers, including the germ line (Maherali et al., 2007; Okita et al., 2007; Wernig et al., 2007). Moreover, when injected into a mouse tetraploid blastocyst, iPS cells can generate a complete embryo proper (Boland et al., 2009; Stadtfeld et al., 2008; Zhao et al., 2009). In mouse, the reversion of female somatic cells to such a pluripotent state is accompanied by reactivation of the Xi. This reactivation occurs late during the reprogramming process, around the moment where iPS cells become independent of the expression of exogenous pluripotency transcription factors (Stadtfeld et al., 2008). Interestingly, the numerous events that take place during XCI do not happen in the reverse order during reprogramming, as some of the events that occur late during XCI are not reversed early during reactivation (Pasque et al., 2014). Importantly, when mouse iPS cells are induced to differentiate they undergo random XCI like ES cells, making them suitable for studying the mechanisms underlying XCI (Maherali et al., 2007).

Human induced pluripotent stem cells

Human iPS cells hold great promise as a model system for studying human XCI (Takahashi et al., 2007). Unfortunately the generation of human iPS cell lines containing two active X chromosomes turned out to be difficult. Since the first human iPS cells were derived by many research groups, iPS cells have been generated using different reprogramming strategies (e.g. using other combinations of transcription factors). These studies reported different results with respect to X chromosome status. Although a number of studies indicated X chromosome reactivation (XCR) in all or a limited number of generated iPS cell lines, a comparable number

of studies found no XCI at all (Amenduni et al., 2011; Ananiev et al., 2011; Bruck and Benvenisty, 2011; Cheung et al., 2011; Kim et al., 2011; Marchetto et al., 2010; Tchieu et al., 2010). Importantly, iPS cell lines that reactivated their Xi initiated random XCI upon differentiation (Bruck and Benvenisty, 2011; Kim et al., 2011; Marchetto et al., 2010). To force human iPS cells to reactivate the Xi, new culture conditions have been developed to induce a naïve state (Hanna et al., 2010; Lengner et al., 2010; Silva et al., 2008; Ware et al., 2009). Two studies successfully and efficiently generated naïve iPS cell lines containing two active X chromosomes, using a combination of different cytokines and small molecule inhibitors (Gafni et al., 2013; Hanna et al., 2010). Upon differentiation, these iPS cells upregulate the gene *Xist*, suggestive of random XCI, although additional studies need to confirm this. Although these results seem promising with respect to the usefulness of iPS cells to model human XCI *in vitro*, these findings still need to be reproduced in independent studies before human iPS cells can be used on a large scale for human XCI studies.

The X-inactivation center (XIC)

The X-inactivation center (XIC)

From genetic studies of X chromosome rearrangements and translocations it was deduced that a single region on the X chromosome is required for XCI to occur. This region, termed the X-inactivation center (XIC in humans and *Xic* in mouse), was defined as “the minimal required region that was both necessary and sufficient to induce XCI” (Rastan and Robertson, 1985). As the *Xic* was defined by naturally occurring X chromosome alterations it was redefined several times, with newly identified translocations or rearrangements reducing the size of the *Xic* (Rastan, 1983; Rastan and Robertson, 1985; Russell and Montgomery, 1970). The mouse *Xic* was finally narrowed down to the breakpoints of the Searle’s t(X;16) translocation, and the HD3 truncation (Rastan, 1983; Rastan and Robertson, 1985). It was hypothesized that the single *Xic* locus was not only required for the *cis*-inactivation of the X chromosome it is located on, but also for *trans*-inactivation of the other X chromosome, as deletion of the *Xic* region resulted in the inability of the unaffected X chromosome to inactivate (Rastan, 1983; Rastan and Robertson, 1985). Inherent properties of the *Xic* therefore include counting the number of X chromosomes in a cell, determining which X chromosome will be inactivated, and next the implementation of this choice along the entire X chromosome.

Similar to the mouse *Xic*, the human XIC was also defined by naturally occurring X chromosome rearrangements and translocations. The human XIC was first limited to a size of at least 0.8 Mb and maximally would be 2.89 Mb long. This region was defined by the

breakpoints of a X;14 translocation in a male individual, and an isodicentric X chromosome in a female Turner patient (Allderdice et al., 1978; Brown et al., 1991b; Pettigrew et al., 1991). Later, the distal breakpoint was redefined by a complex rearrangement of the X chromosome in a female individual, now leading to an estimated human XIC of 0.68 to 1.2Mb in size (Leppig et al., 1993).

As the genes of the Xic and their function in XCI were identified one by one, it became clear that the Xic is not a single locus, but rather that its genetic elements are spread across the entire X chromosome. Consequently, the Xic can currently be separated in a *cis*-acting part and a *trans*-acting part (Fig. 3) (Gribnau and Grootegoed, 2012). The *cis*-acting Xic comprises the genes and elements that exert their function in XCI in-*cis*, on the X chromosome they are located on. The *cis*-acting elements are involved in the inactivation of an X chromosome, and determine which X chromosome will be inactivated, by generating an X chromosome-specific chance to inactivate. In contrast, the genes that comprise the *trans*-acting Xic have an effect on both X chromosomes. They are involved in counting the number of active X chromosomes in a cell and dictate whether inactivation of additional X chromosomes is required. The *trans*-acting Xic comprises X-encoded activators of XCI that are required for counting the number of active X chromosomes, but also encompasses autosomally encoded inhibitors of XCI, which prevent premature initiation of XCI. At this moment identification of elements of the Xic is still ongoing.

Xist

XIST, for *X-Inactive Specific Transcript* is perhaps the most iconic gene in the *cis*-Xic, as it is absolutely required for XCI to take place (Brown et al., 1991a). *XIST* was identified as the first gene expressed from the inactive X chromosome and silenced on the active X chromosome. In both human and mouse, *XIST/Xist* is a non-coding gene that is expressed from the Xi and produces an RNA that strongly associates with the Xi. Accumulation of *XIST/Xist* RNA on the Xi is required for inactivation, as X chromosomes lacking a functional copy of *Xist* are unable to inactivate (Marahrens et al., 1997; Penny et al., 1996).

In undifferentiated ES cells *Xist* is expressed extremely lowly, with at maximum 10 *Xist* RNA molecules per nucleus (Sun et al., 2006). Upon differentiation, *Xist* is upregulated. Initially, undifferentiated female ES cells display a small focus of *Xist* RNA molecules at its transcription site, using RNA-FISH. Upon ES cell differentiation, *Xist* RNA molecules accumulate over time and spread across the entire future Xi. As *Xist* transcripts accumulate, chromatin modifiers are recruited that silence gene expression. During *Xist* accumulation on the future Xi the *Xist* RNA concentration in the nucleus increases 30-fold, which is the result of increased transcription rather than transcript stabilization (Panning et al., 1997; Sheardown et al., 1997; Sun et al., 2006).

Human *XIST* appears to function comparable to mouse *Xist*, as the Xi in human female somatic cells is similarly covered by a large domain of *XIST* RNA molecules (Brown et al., 1991a; Chureau et al., 2002). Human *XIST* contains 8 exons and produces a 19.3 kb full-length transcript (Hong 2000), while mouse *Xist* contains 7 exons and produces a 17.4 kb transcript (Hong et al., 1999). Both human and mouse *XIST/Xist* transcripts contain alternative splice variants (Brockdorff et al., 1992; Brown et al., 1992; Hong et al., 1999; Hong et al., 2000). While *XIST* is conserved between mouse and human, the overall *XIST* sequence conservation between

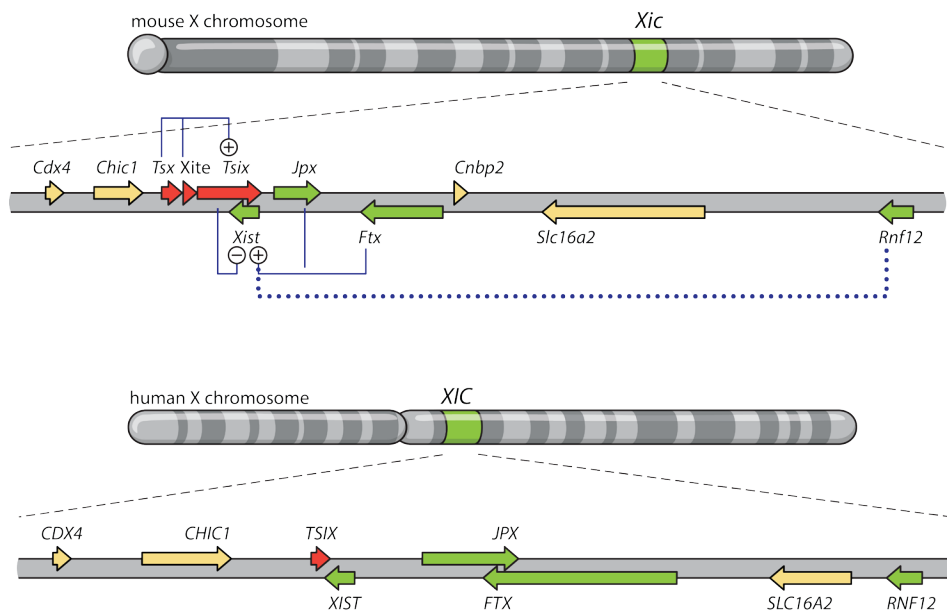


Figure 3.

The X inactivation center

The top shows a schematic overview of the mouse X chromosome, with the location of the Xic indicated in green, and below a schematic representation of the genes located in the Xic. *Tsix* and its positive regulators are indicated in green, *Xist* and its positive regulators in red. Arrows indicate the regulatory effect and the target genes of cis-acting elements. The stippled line indicates the trans-acting effect of *Rnf12*.

At the bottom a schematic overview of the human X chromosome and XIC is shown. Whether the cis-acting and trans-acting elements perform similar functions as in mouse is currently unknown.

human and mouse is relatively poor with 48-60% similarity (Brown et al., 1992; Hendrich et al., 1993; Nesterova et al., 2001b). Instead, human *XIST* shows higher sequence homology to bovine *Xist* (76%), or leptine *Xist* (73%) (Hendrich et al., 1993). Conservation of *XIST* is not homogeneous across its entire sequence, but shows regions that are more conserved and regions that are not conserved at all. The strong conserved regions involve a number of repeat regions and *XIST* intron 4, suggesting that these regions were subject to a more stringent selective pressure, possibly because they are required for the function of *XIST*. Although the exact mechanisms by which *XIST* RNA exerts its function and the regions that are required to perform its function are still subject of ongoing studies, it is clear that *XIST* RNA is central to XCI in both mouse and human.

Tsix

The second gene that is central to the *cis*-acting Xic is *Tsix*, which is a non-coding gene, that acts as a negative regulator of *Xist*. *Tsix* completely overlaps with *Xist*, but is transcribed in the antisense direction (Fig. 3) (Lee et al., 1999). In mouse, *Tsix* contains 4 exons and is transcribed from 2 promoters, producing a 40kb-long transcript. In undifferentiated female mouse ES cells *Tsix* is expressed from both active X chromosomes. The transcripts stay in close proximity of the Xic, as can be seen by the presence of two pinpoints when performing RNA-FISH (Lee et al., 1999). When XCI takes place, *Tsix* first becomes silenced on the future Xi. On the Xa *Tsix* remains expressed for a longer period and becomes silent between day 4 and 11 of general ES cell differentiation (Lee et al., 1999). *Tsix* silencing on the future Xi correlates with the onset of *Xist* RNA coating. However, in some cells with immature *Xist* domains *Tsix* transcripts can still be detected inside these domains, indicating transcription of *Xist* and *Tsix* is not mutually exclusive (Lee et al., 1999; Sado et al., 2001).

The function of *Tsix* as negative regulator of *Xist* was shown by deleting the *Tsix* promoter region. Mouse ES cells carrying this deletion exclusively inactivate the mutant X chromosome (Clerc and Avner, 1998; Lee and Lu, 1999). How *Tsix* exactly exerts its repressive function on *Xist* transcription is still unknown, although several hypotheses exist. One possibility is that *Tsix* affects *Xist* transcription through transcriptional interference, a process that has been observed for a number of antisense positioned genes (Palmer et al., 2011). This hypothesis is supported by the observation that *Tsix* transcripts are present in a decreasing gradient from the *Tsix* promoter towards the *Xist* promoter. At the *Tsix* 5' region there is 100-fold more *Tsix* compared to *Xist*, while at the 3' region this is only 10-fold (Shibata and Lee, 2003; Sun et al., 2006). Furthermore, *Tsix* transcription through the *Xist* promoter seems required for its silencing, as a truncated form of *Tsix* is no longer able to induce silencing (Ohhata et al., 2008).

Another mechanism by which *Tsix* might repress *Xist* is through RNA mediated recruitment of chromatin remodelers (Shibata and Lee, 2004). If antisense *Tsix* transcription is disrupted, inactive chromatin marks at the *Xist* promoter are reduced (Navarro et al., 2006; Ohhata et al., 2008; Sado et al., 2005; Sun et al., 2006). However, this finding might also be explained by a model where an actively transcribed promoter is targeted for inactivation by chromatin remodelers that target histone modifications associated with transcribed sequences.

Lastly, *Tsix* has been proposed to repress *Xist* expression through a RNA-interference (RNAi) mechanism. Indeed, small RNA molecules of 25-37 nucleotides from the *Xist/Tsix* locus have been detected and are hypothesized to be the result of RNAi (Ogawa et al., 2008). However, genetic inactivation of *Dicer*, which encodes an endonuclease that is a critical component of the RNAi machinery, has yielded contradictory results. One study observed *Xist* up-regulation after *Dicer* inactivation, while others found no effect on XCI (Kanellopoulou et al., 2009; Nesterova et al., 2008). Whatever the mechanism by which *Tsix* represses *Xist*, it will not depend on *Tsix* splicing, as around 50% of the *Tsix* transcripts remains unspliced, and a mutant *Tsix* gene defective in splicing is still able to repress *Xist* (Sado et al., 2006).

In humans, *TSIX* is poorly conserved and seems to be inactive. Several studies have compared the human and mouse *Tsix* region and found little sequence conservation. The little sequence conservation that was found, is mostly explained by the strong conservation of *XIST*. Importantly, the conserved sequences are found in the region overlapping with exons 5-8 of *XIST*, but not in the *XIST* promoter region (Chureau et al., 2002; Lee et al., 1999; Migeon et al., 2001). For mouse *Tsix*, transcription through the *Xist* promoter seems required for its silencing capability (Ohhata et al., 2008). Also, the *DXPas34* region, that has been shown to be important for proper *Tsix* expression in mouse, is not conserved in humans (Chureau et al., 2002). Interestingly, despite the poor sequence conservation for *TSIX*, transcription antisense to *XIST* was detected from the *TSIX* region (Migeon et al., 2001; Migeon et al., 2002). However, when performing RNA-FISH on human fetal cells, transcription of *TSIX* was detected only from the Xi and never from the Xa, which is contradictory to expression patterns observed in mouse (Migeon et al., 2002). Since human *TSIX* is expressed in-cis with *XIST* it can be concluded that in humans *TSIX* might not be functional as a repressor of *XIST* (Migeon, 2003).

Other non-coding genes

The Xic contains several other non-coding genes that positively regulate either *Xist* or *Tsix* in-cis. Located upstream of *Xist* are *Jpx* and *Ftx*, which positively regulate *Xist* (Fig. 3) (Chureau et al., 2011; Sun et al., 2013; Tian et al., 2010). *Jpx* (also named *Enox*, for *Expressed neighbor of Xist*) is a non-coding gene located 10kb upstream of *Xist* that is transcribed in the opposite direction of *Xist*, and escapes from XCI (Johnston et al., 2002). Several studies have shown that

Jpx RNA is involved in the regulation of *Xist* promoter activity. *Jpx* is thought to achieve this by altering the occupancy of the chromatin insulator CTCF (for CCCTC-binding factor) at the *Xist* P2 promoter. Low-level *Xist* expression is characterized by high CTCF occupancy at the *Xist* promoter, while *Xist* upregulation is accompanied by CTCF eviction. *Jpx* RNA has been shown to directly bind to CTCF and is thought to titrate CTCF away from the *Xist* promoter, thereby inducing *Xist* expression (Sun et al., 2013). Interestingly, deletion of *Jpx* abolishes *Xist* expression, but can be rescued by a *trans*-acting autosomal copy, arguing that *Jpx* is a *trans*-acting activator rather than a *cis*-regulatory element (Tian et al., 2010). However, the *trans*-acting effect of *Jpx* on *Xist* expression needs to be considered with care, for the observation that a *Jpx* transgene induces low frequencies of ectopic *Xist* expression could not be reproduced in an independent study (Jonkers et al., 2009; Sun et al., 2013).

Ftx (for *Five prime to Xist*) is less well investigated than *Jpx*. Like *Jpx*, *Ftx* is also a non-coding gene, which partially escapes XCI, but is located 150 kb upstream of *Xist*. *Ftx* affects expression of genes in its downstream region, suggesting that extended transcription from the *Ftx* promoter is involved in this regulation. This is further supported by the observation that sense transcription in the downstream region of *Ftx* is reduced after *Ftx* deletion, but antisense transcription is unaffected. One of the genes that is negatively affected by deletion of *Ftx* is *Xist* (Chureau et al., 2011). To date, the function of *Ftx* has only been investigated by deletion in male ES cells, where the effect of deleting an *Xist*-activator will not be obvious as male cells do not upregulate XCI. A *trans*-acting effect of *Ftx* RNA seems unlikely, as *Ftx* transgenes in male mouse ES cells did not induce ectopic XCI (Jonkers et al., 2009). Both *Ftx* and *Jpx* are conserved between mouse and human, suggesting they might have a similar role in human *XIST* regulation (Chureau et al., 2002).

Upstream of *Tsix* reside the non-coding genes *Tsx* and *Xite*, which positively regulate *Tsix* (Fig. 3). *Xite* (for *X chromosome Intergenic Element*) is a non-coding element that is located around 10 kb upstream of the *Tsix* major promoter and is transcribed in the same direction (Ogawa and Lee, 2003). *Xite* is thought to act as an enhancer of *Tsix* transcription, as deletion of *Xite* results in reduced *Tsix* expression and preferential inactivation of the mutated X chromosome (Ogawa and Lee, 2003; Stavropoulos et al., 2005). How *Xite* enhances *Tsix* transcription remains poorly understood, but this might involve the formation of an active chromatin domain through chromatin looping, as Chromatin Conformation Capture (3C) experiments identified a physical interaction between *Xite* and *Tsix* (Tsai et al., 2008). This interaction is present before XCI is initiated and is reduced after XCI, which is consistent with a change in interactions within the *Tsix*-TAD after initiation of XCI. Despite these results suggesting a role as enhancer of *Tsix*, the possibility that *Xite* acts as a minimal promoter of *Tsix*, cannot be excluded.

Tsx (*Testes-Specific X-linked*) is located around 36 kb upstream of *Tsix* and *Xite*, and is transcribed in the same direction, antisense to *Xist* (Simmler et al., 1996). *Tsx* functions as a positive regulator of *Tsix*, and deletion of *Tsx* in mouse ES cells results in ectopic XCI (Anguera et al., 2011). Originally, *Tsx* was thought to be protein coding, but later experiments suggested *Tsx* is non-coding, as the original immunostainings for TSX protein did not coincide with mRNA expression (Cunningham et al., 1998; Simmler et al., 1996). Furthermore, experiments testing several putative open reading frames for *Tsx* could not detect any protein, leading to the conclusion that *Tsx* is non-coding (Anguera et al., 2011). Apart from its potential role in XCI, *Tsx* might also be implicated in silencing of unpaired chromatin during male meiosis, as it is also expressed in meiotic cells and one of the few genes escaping from male sex chromosome inactivation (MSCI) (Anguera et al., 2011; Namekawa et al., 2006). In humans, *TSX* is poorly conserved and *XITE* is not conserved at all, which is coherent with the poor conservation and possible absence of a functional *TSIX*.

One of the intriguing questions of gene regulation in general is how the genome is three dimensionally organized within the nucleus. Recent advances in a series of chromatin conformation capture techniques have made analysis of the spatial organization of the genome possible, and have shown that the genome is organized into *topologically associated domains* (TADs). These TADs are up to a Megabase in size and are characterized by an increased frequency of internal spatial interactions (Nora et al., 2012). Genes that are located within the same TAD not only show an increased frequency of interaction, but also a correlation in their expression, suggesting that genes located within the same TAD are co-regulated (Giorgetti et al., 2014; Nora et al., 2012). In the mouse the *Xic* maps as having two TADs, with *Xist* and its positive regulators located in one TAD and *Tsix* and its positive regulators in the other TAD. The boundary between the TADs is located in between the *Xist* and *Tsix* promoters, with transcription crossing the boundary (Nora et al., 2012). It is not surprising that *Xist* and its positive regulators are located in the same TAD, and also *Tsix* and its positive regulators are located in a single TAD.

Apart from the abovementioned mechanisms by which the respective positive regulators of *Xist* and *Tsix* function, they are likely to regulate *Xist* and *Tsix* expression also by altering the transcriptional status of their respective TADs. After initiation of XCI the location and size of the TADs remain similar, but the internal contacts within each TAD are altered (Nora et al., 2012). The boundary between the *Xist* and *Tsix* TAD is characterized by a CTCF-binding site and acts as an insulator (Spencer et al., 2011). Deletion of the boundary region compromises the separation of the two TADs and results in ectopic interactions between the respective *Xist* and *Tsix*-TADs (Nora et al., 2012). Another study showed that deletion of the boundary element in female mouse ES cells results in reduced initiation of XCI, accompanied by low *Xist* expression and high *Tsix* expression (Spencer et al., 2011). This might implicate that

in absence of the boundary element the TADs of the Xic are unable to switch from a pre-XCI configuration to a configuration where *Xist* is activated. Altogether these data indicate that the *cis*-regulation of *Xist* and *Tsix* not only involves single gene regulation, but likely involves the *cis*-organization of entire, discernable chromatin domains.

RNF12

Where the elements of the *cis*-Xic are required for the *cis*-inactivation of an X chromosome and generating an X chromosome-specific threshold for XCI, several *trans*-acting factors are required to coordinate XCI between the two X chromosomes. These *trans*-acting factors ensure that the correct number of X chromosomes will be inactivated, and involves activators of XCI that are X-encoded and inhibitors that are autosomally encoded. The X-encoded activators are required to count the number of active X chromosomes in a cell. To date, the only identified *trans*-acting activator is *Ring finger protein 12* (*Rnf12*, also named *Rlim* for *Ring finger protein LIM domain interacting*), which was identified in the mouse. *Rnf12* is an X-encoded E3 ubiquitin ligase that induces XCI indirectly, by marking the pluripotency factor REX1 for proteasomal degradation (Gontan et al., 2012). REX1 is a transcription factor that is exclusively expressed in pluripotent stem cells, acting as an inhibitor of XCI. REX1 represses *Xist* and activates *Tsix* by binding their respective gene regulatory sequences. REX1 is encoded by the autosomally located *Zfp42*. In undifferentiated ES cells REX1 is present in high concentrations, thereby preventing preemptive *Xist* activation, while *Rnf12* is moderately expressed. When differentiation is induced, *Rnf12* mRNA and protein levels are upregulated, accompanied by a quick down regulation of REX1 protein levels (Fig. 4.). In female XX cells the concentration of REX1 is sufficiently low to result in activation of *Xist* and initiation of XCI (Gontan et al., 2012). Transgenic overexpression of *Rnf12* in male and female ES cells results in aberrant XCI (Jonkers et al., 2009).

The gene encoding *Rnf12* is located 500kb upstream of *Xist* on the X chromosome, and this chromosomal location seems essential for performing its function. Its location on the X chromosome allows *Rnf12* to induce XCI in a female-specific manner, due to the twofold dosage of *Rnf12* in females compared to males. Furthermore, its close proximity to *Xist* allows a rapid feedback mechanism for XCI, preventing inactivation of a second X chromosome. As *Xist* RNAs spread along the X chromosome and induce silencing, *Rnf12* will be one of the genes that is silenced early during the XCI process. After silencing one copy of *Rnf12*, the concentration of RNF12 protein will decrease to a level comparable to the level in male cells, which is insufficient to induce XCI on the second X chromosome (Gontan et al., 2012). Another essential requirement for the feedback loop of *Rnf12* on XCI is the short half-life of both REX1 and RNF12 proteins, as RNF12 degradation is mediated by auto-ubiquitination (Gontan et al., 2012).

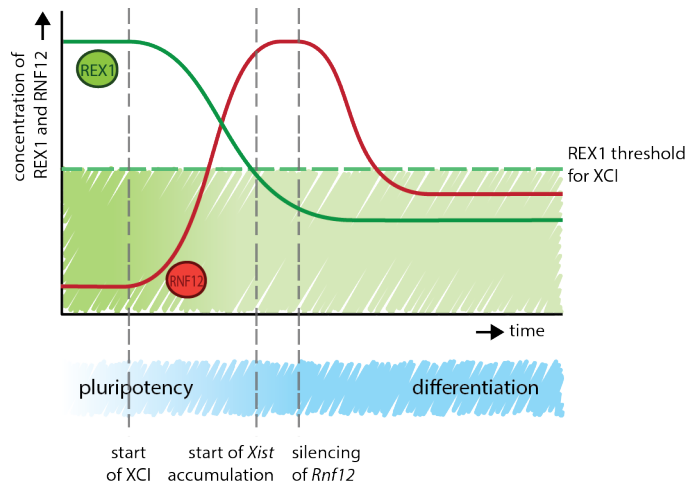


Figure 4.

RNF12 functions as a trans-acting activator of XCI by targeting the pluripotency factor REX1 for proteasomal degradation.

In pluripotent ES cells the concentration of the pluripotency factor REX1 is relatively high, and prevents *Xist* activation. When differentiation is induced *Rnf12* transcription is upregulated. The increasing amount of RNF12 targets poly-ubiquitinates REX1 and thereby targets REX1 for degradation by the ubiquitin-proteasome. The resulting decrease in REX1 permits *Xist* activation on both X chromosomes, resulting in *Xist* RNA spreading and silencing. While *Xist* RNA spreads on both X chromosomes, it is thought that that this does not occur synchronous. As a result *Rnf12* will likely be silenced on one X chromosome, resulting in a decrease in RNF12. This decrease in RNF12 is thought to prevent further degradation of REX1 and inactivation of the second X chromosome.

The function of *Rnf12* has been extensively studied using loss-of-function approaches in mouse ES cells and mice. In mouse ES cells a heterozygous deletion of *Rnf12* results in a clear XCI phenotype, in which the mutant allele is preferentially inactivated, and XCI is initiated at a reduced rate (Barakat et al., 2011; Shin et al., 2010). As *Rnf12*^{+/-} ES cells are still able to initiate XCI, where male ES cells with one allele of *Rnf12* do not initiate XCI, it is likely that other *trans*-acting activators exist. ES cells carrying a homozygous deletion of *Rnf12* almost do not initiate XCI (Barakat et al., 2011). When the effect of *Rnf12* deletion was studied *in vivo*, a severe phenotype for imprinted XCI was observed, in a parent-of-origin specific manner. Since the paternal allele is always inactivated during imprinted XCI, a maternally inherited *Rnf12* deletion, results in complete functional loss of *Rnf12* in extraembryonic tissue.

As a result *Rnf12*^{+/-} females inheriting a maternally transmitted knockout allele display severe developmental defects of the extraembryonic tissues and as a result are not born. In contrast, *Rnf12*^{+/-} females inheriting a paternal deletion of *Rnf12* do not show any phenotype of imprinted XCI, and develop normally. When random XCI is analyzed in these females they show exclusive inactivation of the mutant X chromosome, comparable to ES cells (Shin et al., 2010).

To circumvent the imprinted XCI phenotype, a recent study used a ICM-specific conditional deletion of *Rnf12* to create *Rnf12*^{-/-} embryos. Unexpectedly, *Rnf12*^{-/-} embryos were viable, and seem to be able to undergo XCI, as *Xist* domains could be detected by RNA-FISH (Shin et al., 2014). These results are highly contradictory with results from ES cells, where one allele of *Rnf12* needs to remain active to establish proper silencing of the Xi (Barakat et al., 2014). The difference between these mice and ES cells is most likely caused by the use of different knockout approaches, targeting different critical exons and different genetic backgrounds. This is further illustrated by the observation that *Rnf12*^{-/-} ES cells that are genetically similar to the *Rnf12*^{-/-} embryos, were also able to undergo XCI, and did so at a rate comparable to *Rnf12*^{+/-} ES cells (Shin et al., 2010). In addition to the different genetic background, the cell type specificity of the conditional knockout can be questioned, as well as the non-allele-specific methods that were used to analyze XCI in *Rnf12*^{-/-} embryos. Therefore, the discussion whether embryonic *Rnf12*^{-/-} cells are able to undergo XCI is still ongoing.

While REX1 seems to be the primary target of RNF12 during XCI, several other proteins have been identified as such targets of RNF12. These are unlikely to be involved in XCI as they have not been identified in affinity purification experiments with mouse ES cells undergoing XCI (Gontan et al., 2012). Instead, they are involved in different cellular functions and signaling cascades. Among the targets of RNF12 are SMAD7 (for Mothers Against Decapentaplegic homolog 7) and SMURF2 (for SMAD Ubiquitination Related Factor 2). These proteins are both involved in the Transforming Growth Factor (TGF)- β family signaling pathway, and act as inhibitors of this pathway. This signaling system is essential for regulation of many cellular processes including proliferation, differentiation, and apoptosis, but is also involved in regulating embryonic development. The TGF- β pathway is activated by a broad range of cytokines and hormones, including TGF- β s, Bone Morphogenic Proteins (BMP), Growth and Differentiation Factors (GDF), Activin, Nodal and Anti-Mullerian Hormone (AMH). These ligands activate signaling by binding a complex of TGF- β Receptor type I and type II, with different ligands being recognized by different receptor complexes. Ligand binding to the receptor complex results in activation of the type I receptor, which on its turn selectively phosphorylates the receptor activated SMAD proteins (R-SMADs, including SMAD1, SMAD2, SMAD3, SMAD5 and SMAD8). These R-SMADs form a complex with the co-factor SMAD4 to act as transcription factors and regulate target genes. To date, several inhibitors of the TGF- β family signaling pathway have been identified, that inhibit signaling at different levels. These include SMAD6

and SMAD7, which were identified as inhibitory SMADs (I-SMAD), and the E3 ubiquitin ligase SMURF2. SMURF2 inhibits the TGF- β family signaling by targeting its receptor complex for proteasomal degradation. In addition, SMURF2 is implicated in the targeted degradation of the R-SMAD SMAD2 (Huang et al., 2011). SMAD7 inhibits TGF- β family signaling by multiple mechanisms, involving inhibition and degradation of type I receptors, and disruption of functional SMAD transcription factor complexes (Stolfi et al., 2014). RNF12 has been shown to increase signaling by targeting both SMAD7 and SMURF2 for proteasomal degradation (Huang et al., 2011; Zhang et al., 2012). In mouse ES cells depletion of RNF12 using RNAi affects differentiation fates, through decreased sensitivity of signaling by BMPs and Activin (Zhang et al., 2012). A dysregulation of TGF- β family signaling by RNF12 could hypothetically also be involved in tumorigenesis and subsequent invasion and metastasis of tumor cells, as the TGF- β system is involved in these processes. Notably, SMAD7 was found to have both pro-tumor and anti-tumor actions, depending on the type of cancer analyzed and the tumor stage, similar to the known bimodal effects of other components of the TGF- β system in initial cancer suppression compared to later promotion (Stolfi et al., 2014). Through modulation of the TGF- β system, dysregulation of RNF12 might have profound effects on a number of important cellular and biological processes.

RNF12 can also interact with the LIM domain of nuclear proteins. LIM domains are highly conserved protein domains that consist of two zinc fingers, and serve protein-protein interactions. These domains have been found in a variety of proteins, some of which consist of little more than two LIM domains, and these were therefore termed LIM domain only (LMO) proteins. LMO proteins are thought to regulate transcription by mediating interactions between proteins in transcriptional complexes. They are reported mainly to be involved in cell differentiation (Bach, 2000; Matthews et al., 2013). Of the four known LMO proteins, LMO2 and LMO4 interact with RNF12, resulting in their poly-ubiquitination, and likely in their degradation (Bach, 2000; Ostendorff et al., 2002). Since overexpression of LMO proteins is associated with cancer development and progression, RNF12 might have a tumor-suppressive function by degrading LMO proteins. Another group of LIM domain containing proteins are the LIM-hd proteins that contain a homeodomain in addition to their two LIM domains. LIM-hd proteins act as transcription factors and are involved in regulating embryogenesis and specifying the body plan. Of the LIM-hd proteins, LHX1, LHX2, LHX3 and ISL1 have been shown to directly interact with RNF12, although this interaction does not result in their ubiquitination (Bach et al., 1999; Ostendorff et al., 2002). Nevertheless, RNF12 inhibits the transcription of target genes of LHX3, through recruitment of the SIN3A-Histone Deacetylase (HDAC) complex (Ostendorff et al., 2002). The recruitment of the SIN3A/HDAC complex by RNF12 indicates that not all interactions of RNF12 serve targeting the interacting protein(s) for proteasomal degradation. Two co-factors of LIM-hd transcription factors have been identified and were

termed LDB1 (for LIM Domain Binding protein 1, also known as Clim2 for Carboxy terminal LIM domain-binding protein 2, or NLI for Nuclear LIM Interactor) and LDB2 (for LIM Domain Binding protein 2, also known as Carboxy terminal LIM domain-binding protein 1). Both these LIM-hd co-factors directly interact with RNF12, resulting in their poly-ubiquitination and proteasomal degradation. In addition, RNF12 competes with LIM co-factors for binding of LMO proteins and DNA bound LIM-hd proteins, making RNF12 a negative co-regulator of LIM domain proteins (Bach et al., 1999; Ostendorff et al., 2002). The variety of processes LIM co-factors are involved in is illustrated by the phenotype of *Ldb1*^{-/-} mice, which are not born and display severe developmental defects, including truncated head structures, posterior axis duplication, and lack of heart and foregut formation. In addition, conditional knockout studies have shown that *Ldb1* is essential for erythropoiesis and for neuronal development in the central nervous system (Li et al., 2010; Zhao et al., 2014). Interestingly, RNF12 seems not only capable of targeting LDB1 for proteasomal degradation by poly-ubiquitination, but also of stabilizing LDB1 by mono-ubiquitination. (Bach et al., 1999; Howard et al., 2010). Taken together, RNF12 is an important negative co-regulator of LIM protein regulated transcription.

Another target of RNF12 is the telomeric protein TRF1 (for Telomeric Repeat binding Factor 1), which is also targeted for proteasomal degradation by poly-ubiquitination. TRF1 is involved telomere length regulation, and promotes telomere shortening by inhibiting the access of telomerase to telomere termini. TRF12 directly binds to telomeric DNA, thereby preventing telomerase in adding telomeric repeats. Upon depletion of RNF12 in a human cell line TRF1 levels increase, resulting in gradual telomere shortening and reduced cell proliferation (Her and Chung, 2009). Notably, another E3 ubiquitin ligase, Fbx4 (for F-box protein 4), is also capable of targeting TRF1 for proteasomal degradation through poly-ubiquitination, independent of RNF12 (Lee et al., 2006).

Another protein that is involved in cell proliferation and is targeted for proteasomal degradation by RNF12 is STMN1 (for Stathmin 1). STMN1 is a cytosolic protein involved in regulating microtubule dynamics, and promotes destabilization of microtubules by direct interaction with microtubule ends, and sequestration of tubulin heterodimers (Belmont et al., 1996; Curmi et al., 1997). Upon depletion of Rnf12 STMN1 concentrations increase, while overexpression of RNF12 results in a decrease in STMN1 and inhibits cell proliferation (Chen et al., 2014).

RNF12 also interacts with the Estrogen Receptor alpha (ER α), which is a nuclear hormone receptor that is activated by the sex-hormone estrogen. The activated ER relocates from the cytosol to the nucleus, where ER-dimers regulate gene transcription either by binding to genomic Estrogen Responsive Elements (ERE) or by association with other DNA-binding factors to induce ERE-independent transcription. Estrogen signaling is essential for sexual development, but is also involved in tumorigenesis. RNF12 is capable of poly-ubiquitinating

ER α , but this does not seem to alter its stability, indicating ER α ubiquitination does not result in its degradation by the ubiquitin-proteasome. The interaction with RNF12 is specific for ER α , as other steroid hormone receptors like the Estrogen Receptor β (ER β), the androgen receptor (AR), or glucocorticoid receptor (GR) do not interact with RNF12. RNF12 enhances estrogen signaling, as ERE-driven transcription increases in the presence of RNF12. Like for LIM-hd regulated transcription, RNF12 and Ldb1/2 seem to antagonize each other in ERE-driven activation (Johnsen 2009). Given the involvement of estrogen signaling in breast cancer, with ER+ tumors generally having a better prognosis, LDB1/2 expression were documented in human breast cancer samples. Increased expression of *LDB1/2* was found to correlate with ER+ status, and poor prognostic tumor characteristics. Unfortunately, analysis of RNF12 protein levels in breast cancer was not performed in this study (Johnsen et al., 2009).

Presently, several interaction partners of RNF12 have been identified, and it is likely that more will be identified in the future. A number of the abovementioned interaction partners of RNF12 were identified in studies that were not truly aimed at identifying them. Instead, they were directed to identify the interacting partners of another protein of interest, which identified RNF12 as an interactor (Bach et al., 1999; Chen et al., 2014; Zhang et al., 2012). Several other directed studies were performed to identify interaction partners of RNF12, but used a candidate-based approach (Her and Chung, 2009; Huang et al., 2011; Johnsen et al., 2009). Therefore, it is unlikely that all proteins interacting with RNF12 have been identified. To date, only one study investigated the proteins interacting with RNF12 in mouse ES cells, using co-immunoprecipitation (Gontan et al., 2012). However, as not all previously identified interaction partners were co-purified, it seems that some interactions of RNF12 might be cell-type specific.

Inhibitors of XCI

Where XCI activators are required to count the number of active X chromosomes present in a cell, XCI inhibitors prevent premature initiation of XCI during development as well as ES cell differentiation. Therefore it is not surprising that most XCI inhibitors identified to date are pluripotency associated genes, as loss of pluripotency is accompanied by down-regulation of pluripotency factors and initiation of XCI. This relation between pluripotency and XCI is further illustrated by experiments showing that ES cells with two active X chromosomes have difficulties exiting their pluripotent state without performing XCI. The presence of two active X chromosomes blocks the exit from the pluripotent state by inhibition of the MAPK and GSK3 β pathways (Schulz et al., 2014).

Different pluripotency factors inhibit XCI by repressing *Xist*, or by stimulating *Tsix*, or both. The pluripotency factors NANOG, OCT4, SOX2 and PRDM14 have been shown to repress *Xist* in undifferentiated ES cells by binding to a region in *Xist* intron 1 (Ma et al., 2011; Navarro

et al., 2008). *Tsix* is repressed by OCT4, KLF4, REX1 and C-Myc (Donohoe et al., 2009; Navarro et al., 2010). Although C-Myc is in fact not a pluripotency factor, it is used as a factor to reprogram differentiated cells back to a pluripotent state. Finally, OCT4, SOX2 and NANOG act as negative regulators of *Rnf12* transcription, adding another constraint on the XCI system (Navarro et al., 2011; Payer et al., 2013). These inhibitory mechanisms act synergistically to prevent initiation of XCI in pluripotent cells. The redundancy of these mechanisms is demonstrated by deleting *Xist* intron 1. Even if this abolishes pluripotency factor binding to *Xist*, it does not result in clear *Xist* activation (Barakat et al., 2011; Minkovsky et al., 2013; Nesterova et al., 2011).

Initiation of XCI: Models for counting and choice

Counting and choice

The process of XCI can be divided into several phases. During the “initiation” phase a cell determines if it needs to inactivate an X chromosome and which X chromosome is inactivated. After an X chromosome is chosen to be inactivated it is silenced in the “establishment” phase. Finally, during the “maintenance” phase the silent state of the inactive X chromosome is clonally passed-on to all daughter cells.

Shortly after discovering the phenomenon of XCI, it was recognized that the mechanism of XCI must function in such a way that it keeps only one X chromosome active per diploid genome. If additional X chromosomes are present, like in 47, XXX females or 47, XXY Klinefelter patients, all X chromosomes except but one are inactivated, while in 45, XO Turner patients the single X chromosome is never inactivated (Grumbach et al., 1963; Jacobs et al., 1959; Maclean and Mitchell, 1962). In tetraploid embryos 2 of the 4 X chromosomes are inactivated, indicating that the number of X chromosomes that is kept active is also dictated by the ploidy of the cell (Carr, 1970; Webb et al., 1992). To explain how XCI invariably results in one active X chromosome per diploid genome, its mechanism should involve properties that allow it to count both the number of X chromosomes and the ploidy of a cell. Several models have been proposed to explain for the counting property in XCI (Fig. 5). All these models have to take into account not only that one X chromosome per diploid genome set stays active, but also that XCI is random with respect to the parental origin of the X chromosomes. Notably, most of these models were proposed before the identification of RNF12 as a *trans*-acting activator.

The blocking factor model

The blocking factor model proposes that every diploid cell contains a blocking factor, which is only present as a single molecule in every nucleus. This blocking factor randomly associates with one of the two X chromosomes and protects it from inactivation. The blocking factor was hypothesized to bind the X chromosome at a region termed the “counting element”. From studies analyzing X chromosome truncations and translocations the counting element was thought to be located within the Xic. The nature of the blocking factor is not specified so far, and could be protein or nucleic-acid. However, the location of the blocking factor gene was hypothesized, as it should be autosomally encoded to relate cell ploidy to the number of X chromosomes (Rastan, 1983). An extension to the blocking factor model was proposed in the form of the symmetry breaking model. In this model the blocking factor is not present as a single molecule in a diploid nucleus, but instead is assembled on one of the X chromosomes from a larger number of diffusible blocking factor molecules (Nicodemi and Prisco, 2007).

The competence factor model

In the competence factor model, an X-encoded competence factor was introduced in addition to the blocking factor. In this model the X chromosome that initiates XCI is selected by association with the competence factor. The competence factor model was proposed after experiments with *Xist*^{+/−} ES cells yielded results that could not be explained by a model featuring only a blocking factor. In these ES cells the wildtype X chromosome was exclusively inactivated, which is incompatible with the blocking factor model, as deletion of the counting element should result in exclusive inactivation of the mutant X chromosome as it can no longer associate with the blocking factor. These results could be explained by the introduction of a competence factor, which should associate with the deleted *Xist* region and therefore always selects the wildtype X chromosome for inactivation. The competence factor is X-encoded to allow counting of the number of X chromosomes. The blocking factor is required in addition to count the ploidy of a cell (Marahrens et al., 1998).

The transvection model

The transvection model does not rely on diffusible factors to mark the X chromosomes as active or inactive, but proposes that counting and choice are regulated by a transient interaction between the Xic's of the two X chromosomes. This model is based on the observation that during initiation of XCI the Xic's of the two X chromosomes move in closer proximity to each other (<2μm) (Bacher et al., 2006; Xu et al., 2006). This pairing event lasts for approximately 45 minutes, and is accompanied by a decrease in nuclear mobility of the two Xic's. Although pairing is defined as a distance of <2μm between Xic's, and complete overlap of the two Xic's could be observed in 7% of cells (Masui et al., 2011). It is thought that during

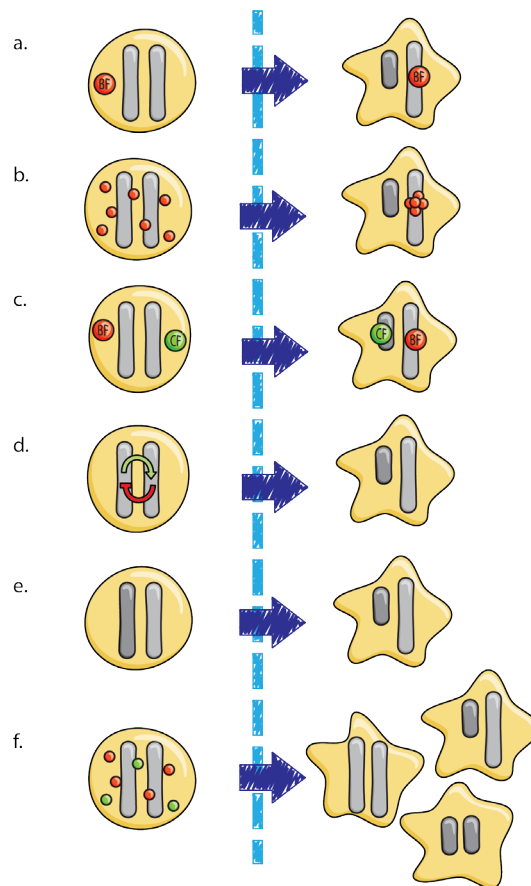


Figure 5.

Models explaining XCI counting and choice

- The blocking factor model: a blocking factor is present as a single entity in the nucleus and prevents one of the two X chromosomes from inactivating.
- The symmetry breaking model: the blocking factor is a complex of diffusible molecules that assembles on one of the two X chromosomes and prevents it from inactivating.
- The competence factor model: a competence factor promotes inactivation of one of the two X chromosomes, while the other X chromosome is protected from inactivation by the blocking factor.
- The transvection model: the two X chromosomes transiently co-localize in the nucleus to determine the future active and inactive X chromosome.
- The model of alternate states: the two X chromosomes differ epigenetically already before the onset of XCI.
- The stochastic model: XCI is stochastic, with both X chromosomes having a probability to inactivate. As a result all combinations of inactive and active X chromosomes occur after a single “choice round” of inactivation (XaXa, XaXi, XiXi). Cells that retained two active X chromosomes are subject to another “choice round”.

pairing transcription factors are asymmetrically distributed between the two Xic's resulting in mono-allelic silencing of *Tsix* and the consequent upregulation of *Xist*. Interestingly, not all cells show asymmetric *Tsix* expression after pairing, which might indicate that some cells require multiple rounds of pairing (Masui et al., 2011). Several regions of the Xic were identified as required for co-localization, and included *Tsix*, *Xite* and a region overlapping with *Slc16a2* that was termed the X-pairing region (Xpr) (Augui et al., 2007; Bacher et al., 2006; Xu et al., 2006).

However, several subsequent studies argue against a functional effect of co-localization in counting and choice. In ES cells carrying a deletion of all the elements involved in co-localization of the Xic's, counting is unaffected (Barakat et al., 2014). Also, in heterokaryons obtained by fusion of male and female ES cells, XCI is initiated on the single X chromosome in the male nucleus upon differentiation, indicating that co-localization of the Xic's does not require a physical interaction (Barakat et al., 2014). Instead, counting and XCI initiation seem dependent on diffusible factors. Together, these results suggest that the observed transient co-localization during initiation of XCI is a consequence of the XCI process, in which the spatial movement of the Xic's might be caused by the changes in gene transcription that occur at the two Xic's. Gene transcription occurs in the nucleus at foci that are enriched for RNA polymerase II (RNA pol II), and are termed transcription factories. When a gene is actively transcribed it relocates to a transcription factory, and multiple genes located *in-cis* or *in-trans* can share the same transcription factory (Osborne et al., 2007). Therefore, the observed co-localization of the two Xic's might be the consequence of their change in transcriptional activity, as they co-localize at the same or neighboring transcription factories.

The alternative states model

The alternative states model hypothesizes that the two X chromosomes are epigenetically marked prior to XCI. As the two X chromosomes switch between these two epigenetic states, a random choice for XCI is generated (Mlynarczyk-Evans et al., 2006). This model was based on the observation that in undifferentiated ES cells the two X chromosomes differ in sister chromatid cohesion after DNA replication. Thus far an epigenetic mark distinguishing the two states the X chromosomes adopt has not been identified.

The stochastic model

The abovementioned models all hypothesize that XCI is a deterministic process, in which one X chromosome is determined to remain active and in which every cell inactivates exactly the correct number of X chromosomes. The stochastic model however, proposes that XCI is not deterministic, but instead is a stochastic process in which each X chromosome has its own probability to inactivate within a developmental time window (Monkhorst et al., 2008). This model was based on the observation that tetraploid XXXX ES cells preferably inactivate two X

chromosomes, but a significant number of these cells inactivate more or less X chromosomes during ES cell differentiation (Monkhorst et al., 2008). Also, diploid ES cells show a small proportion of cells that initiate XCI on both X chromosomes (Lee, 2005; Monkhorst et al., 2008). This outcome of XCI is unexpected if XCI would be regulated by a deterministic process. A stochastic mechanism for XCI is further supported by observations in mouse tetraploid embryos, where a significant number of cells inactivate one or three X chromosomes, similar to the *in vitro* ES cell differentiation studies (Webb et al., 1992). In this model the probability for an X chromosome to inactivate depends on the relative concentrations of XCI activators and inhibitors. The genes encoding XCI inhibitors are autosomally located to facilitate counting the ploidy of a cell. The genes encoding XCI activators are X-chromosomally encoded and subject to XCI to provide feedback that prevents inactivation of too many X chromosomes in most cells. This feedback mechanism is not completely foolproof, as both *in vivo* and *in vitro*, a small percentage of cells was found to initiate *XIST/Xist* spreading on too many X chromosomes, despite this feedback mechanism. With the identification of RNF12 as a trans-acting activator of XCI and several pluripotency factors as XCI inhibitors this model seems most plausible to date.

Establishment of XCI

Establishing the Xi

After the initiation phase, where a cell determines whether XCI needs to be initiated and which X chromosome will be inactivated, the inactive state of the X chromosome must be established. During establishment of the Xi a cascade of molecular events take place to ensure that the active X chromosome is silenced and kept so. A number of epigenetic modifications are applied to ensure that the Xi stays inactive during subsequent cell divisions. These epigenetic modifications stay on the inactive Xi during mitosis (Chaumeil et al., 2002; Jeppesen and Turner, 1993; Jonkers et al., 2008; Mak et al., 2002). Most of the studies analyzing the establishment of the inactive state have used mouse ES cells to determine the order in which these modifications are acquired, however the use of immunocytochemistry precludes fair conclusions about the precise order of events.

XCI initiation starts with the accumulation of *Xist* RNA along the entire X chromosome. The earliest event that follows *Xist* RNA accumulation is the cessation of active transcription as RNA pol II and transcription factors are excluded from the Xi (Chaumeil et al., 2006; Smeets et al., 2014). This exclusion is first established in the center of the Xi, where repetitive elements are clustered, while genes at the border of the Xi are still transcribed and silenced at a later

stage (Chaumeil et al., 2006). As active transcription stops, a number of histone modifications associated with active chromatin are removed from the Xi (Chaumeil et al., 2002; Heard et al., 2001; Jeppesen and Turner, 1993). Histone modifications are an important mechanism to regulate gene transcription in an inheritable, but reversible way. They are generally covalent modifications of the histone tails, including methylation, acetylation and phosphorylation. Combinations of different histone modifications may act synergistic or antagonistic to regulate gene expression (Strahl and Allis, 2000). After the removal of histone modifications that mark active chromatin, the Xi acquires many repressive histone modifications. Of these trimethylation of lysine27 of histone H3 (H3K27me3), and monoubiquitination of lysine 119 of histone H2 (H2AK119Ub1) are most extensively studied (Chadwick and Willard, 2003). These modifications are catalyzed by the polycomb repressive complexes PRC2 and PRC1, respectively (de Napoles et al., 2004; Mak et al., 2002; Plath et al., 2003; Silva et al., 2003).

After acquiring these modifications the Xi becomes late-replicating during mitosis, which is a hallmark of inactive chromatin. To maintain the inactive state several other epigenetic modifications are applied to the Xi. The histone variant macro H2A becomes incorporated (Costanzi and Pehrson, 1998). This variant is thought to be involved in maintenance of XCI rather than establishment, because it is acquired late during XCI. One of the last modifications established on the Xi is DNA methylation of gene promoters and regulatory sequences like CpG islands (Lock et al., 1987). DNA methylation seems to permanently lock in the silent state of the Xi (Sado et al., 2000). Interestingly, *in vivo* deletion of macroH2A does not result in obvious X reactivation however, but requires the additional treatment with the demethylating agent 5-AZA-DC or the histone deacetylase inhibitor trichostatin A, indicating that multiple epigenetic layers are involved in maintained repression of the Xi (Hernandez-Munoz et al., 2005; Pehrson et al., 2014).

The developmental time window of establishing the Xi

In mouse, *Xist* can establish the silent state of the Xi only during a specific developmental time window. This time window was defined by experiments in differentiating mouse ES cells carrying an inducible *Xist* transgene. These experiments showed that *Xist* transcription must be induced within 48 hours of differentiation to result in gene silencing. When *Xist* is induced after 72 hours *Xist* RNA still accumulates along the chromosome, but no longer results in gene silencing (Wutz and Jaenisch, 2000).

In contrast to mouse *Xist*, which is unable to induce silencing outside its developmental window, it is likely that human *XIST* can induce silencing at later stages of development. In human somatic cells (human fibrosarcoma HT-1080) induction of an *XIST* transgene results in silencing of gene transcription and accumulation of silent chromatin marks, including histone hypoacetylation, H3K27me3 and H4K20me1, incorporation of the histone variant macroH2A,

late replication of DNA and chromatin condensation (Chow et al., 2007; Chow et al., 2002; Hall et al., 2002; Smith et al., 2004). However, this silent state is lost over the subsequent passages, probably due to selection against the cells that have become functionally hemizygous for the inactivated autosomal region (Chow et al., 2002; Hall et al., 2002).

Whether this difference in timing of *XIST/Xist* functionality between human and mouse is caused directly by properties of the *XIST/Xist* RNA remains to be seen. It is very well possible that the observed difference is the result of a difference in permissive chromatin state or the species-specific requirement of co-factors, rather than species-specific properties of *XIST/Xist* RNA. The studies analyzing human *XIST* transgenes used HT-1080 cells and Human Embryonic Kidney (HEK) cells, which may have a nuclear environment that is more supportive to active epigenetic remodeling, compared to the differentiating ES cells that were used to analyze mouse *Xist*.

The role of Xist in Xi establishment

One of the most intriguing questions is how *Xist* RNA molecules induce gene silencing with accompanying epigenetic modifications and maintain the silent state of genes along an entire chromosome. Many studies have assessed the role of different regions of the *Xist* RNA, and the involvement of other chromatin modifiers in inducing silencing. The repeat regions of *Xist* are most highly conserved and have therefore been the focus point of functional studies. Both mouse and human *Xist/XIST* RNA contain 5 repeat regions, termed repeat element A-E (Brockdorff et al., 1992; Brown et al., 1992). Of these repeats the first two repeat elements are conserved in sequence and repeat number, while the other three have been differentially amplified. Stronger conservation of the first two repeats might indicate a functional significance. Indeed, repeat A, located in exon1, is required for the silencing function of *Xist*, as deletion of this repeat still allows proper localization of *Xist* RNA, but completely abolishes its silencing capacity (Chaumeil et al., 2006; Wutz et al., 2002). Several studies have suggested that the A repeat directly recruits PRC2, that is required for the establishment of the H3K27me3 mark (Maenner et al., 2010; Zhao et al., 2008). The silencing capacity of the A repeat is independent of its position in *Xist* RNA as moving the A repeat to the 3' end of *Xist* does not affect silencing capability (Wutz et al., 2002). However, while *Xist* RNA lacking the A repeat region cannot induce gene silencing, it still induces exclusion of RNA pol II, repression of *Cot-1* transcription, accumulation of H3K27me3 and macroH2A incorporation, suggesting that these effects are mediated by other elements of *Xist* RNA, and indicate that H3K27me3 accumulation is not sufficient for silencing the X (Chaumeil et al., 2006; Wutz et al., 2002). Even more puzzling are the observations from two recent studies using superresolution microscopy which did not observe any co-localization of *Xist* RNA with PRC2 or H3K27me3, arguing against a direct recruitment of PRC2 by *Xist* (Cerase et al., 2014; Smeets et al., 2014).

The human repeat A region has similar silencing properties as the mouse repeat A, as deletion of human repeat A also abolishes silencing. However, unlike mouse *Xist* which still can properly localize without A repeat A, human *XIST* lacking the A repeat form smaller *XIST* RNA domains (Chow et al., 2007). Although this effect might be due to defective localization, another study suggests that the human A repeat is required for proper *XIST* RNA transcription levels as insertion of the human repeat A sequence into a luciferase reporter gene increased transcription >3 fold (Hendrich et al., 1997). The human repeat A consists of 9 palindromic repeats, of which the number of repeats correlates with the silencing capabilities of this repeat region. A minimum of two repeats still induces silencing of a flanking EGFP reporter gene, but not of more distally located genes (Minks et al., 2013).

The C repeat region of mouse *Xist* seems required for correct localization of *Xist* RNA, as it is required for interaction with the matrix attachment protein hnRNP, also known as SAF-A (Pullirsch et al., 2010). hnRNP is essential for proper localization of *Xist* as knockdown of hnRNP results in dispersed *Xist* clouds (Hasegawa et al., 2010). Also the properties of the C repeat seem conserved between mouse and human as deletion of the human C repeat also results in dispersed *XIST* RNA domains (Chow et al., 2007). Interestingly, the silencing properties of *XIST* RNA do not seem to depend on the C repeat as human *XIST* lacking repeat C is still able to induce silencing of a neighboring GFP transgene (Chow et al., 2007).

Apart from the repeat regions, another conserved region between mouse and human is *XIST* exon4, a region that also shows homology to the Marsupial *Ln timer*, from which *Xist* might have been evolved (Duret et al., 2006; Elisaphenko et al., 2008). Deleting *Xist* exon 4 *in vivo* only affected *Xist* expression, which was lower compared to wildtype *Xist* expression, but did not affect *Xist* silencing, localization, or skewing of XCI (Caparros et al., 2002). Another *Xist* disruption, involving the same deletion of exon 4 and in addition a large inversion involving most of *Xist* exon 1 up to the deleted exon 4, showed impaired silencing capabilities and reduced localization to the X chromosome (Senner et al., 2011). Altogether these results indicate that *Xist* RNA contains several elements that have overlapping and redundant functions for the localization and silencing properties of *XIST* RNA.

Xist spreading along the Xi

Several models have been put forward to explain how *Xist* RNA spreads along the X chromosome. According to the LINE-1 hypothesis *Xist* RNA uses Long Interspersed Elements (LINE) as way stations to spread over the X chromosome (Lyon, 1998). Way stations along the X chromosome were proposed to facilitate *Xist* spreading based on observations that *Xist* RNA could efficiently spread over X chromosomal sequences, but not over autosomal sequences (Gartler and Riggs, 1983). Studies with mouse cells carrying X; autosome translocations or *Xist* transgenes on autosomes showed that when flanked by autosomal sequences *Xist* is unable to

completely spread across the autosomal sequence (Lee and Jaenisch, 1997; Rastan, 1983). Also silencing of flanking autosomal sequences is incomplete and takes place along a gradient with most effective silencing closest to the breakpoint. Also in human X; autosome translocations *XIST* RNA spreading and silencing was found less efficient on autosomal sequences. The proposed way stations were hypothesized to be present on the X chromosome but to a lesser extent on autosomes. As LINE-1 sequences are relatively enriched on the X chromosome, it was proposed that LINE-1 sequences act as these way stations (Lyon, 1998). As both the human and mouse the X chromosome are relatively enriched for LINE-1 sequences, this might explaining why *XIST/Xist* spreads more efficiently along the X chromosome (Bailey et al., 2000). Moreover, LINE-1 sequences are distributed unevenly along the X chromosome with a lower density at escaping genes, providing an explanation why certain genes might escape XCI (Bailey et al., 2000).

However, there are several studies that provide observations arguing against the LINE-1 hypothesis. An important observation arguing against the LINE-1 hypothesis is the occurrence of XCI in the marsh rice rat, a rodent that lacks LINE-1 repeats (Cantrell et al., 2009). Also, the low efficiency by which *Xist* RNA spreads into autosomal sequences can also be explained by selection against cells that did successfully inactivate autosomal sequences and as a consequence became functional hemizygous. Indeed, a recent study managed to successfully inactivate a complete chromosome 21 in human iPS cells derived from a patient with trisomy 21, further arguing that *Xist* spreading into autosomal sequences is hampered by functional hemizygosity (Jiang et al., 2013).

Recent studies using next generation sequencing and pull-down assays provide a complete different picture of *Xist* RNA spreading and silencing. Two studies used an oligonucleotide-based pull-down of *Xist* RNA to determine its way of spreading. From these studies it seems that *Xist* uses the three-dimensional organization of the X chromosome to spread to sequences that are in close proximity to its own locus of transcription, and do not need to be close by on the linear chromosome. As a result *Xist* first localizes to active genes and from there spreads into adjacent intergenic regions. In support of this proximity based way of spreading, no specific sequences were identified to characterize *Xist* binding sites (Engreitz et al., 2013; Simon et al., 2013). These two studies however are based on analyses of cell populations, and do not completely correspond with observations of single cells using superresolution microscopy. Where these cell population analyses showed a uniform distribution of *Xist* RNA, super resolution microscopy detected a focal pattern of *Xist* localization. From this discrepancy it can be hypothesized that *Xist* RNA does not stably bind to specific sites, but instead temporarily associates with potential binding sites in a stochastic way (Smeets et al., 2014).

Maintenance of Xi

While *Xist* is required for the initiation of XCI, its role in maintaining the silent state of an X chromosome is less clear. Originally, it was thought that *Xist* was essential for initiation of XCI, but became dispensable after establishment of the Xi. This was based on the observation that in cultured cells deletion of *Xist* after establishment of the Xi did not result in robust reactivation of the Xi (Csankovszki et al., 1999; Splinter et al., 2011). Also, autosomal sequences that were silenced by *Xist* transgenes did not show reactivation after switching of *Xist* (Wutz and Jaenisch, 2000). Although these experiments suggest that *Xist* is not required for maintenance of the silent state, *Xist* remains expressed after establishment of the Xi during all subsequent cell divisions. Moreover, *Xist* remains transcribed throughout the cell cycle and *Xist* RNA molecules actually remain attached to the Xi throughout mitosis (Jonkers et al., 2008). The continuous association of *Xist* with the Xi suggest that *Xist* RNA is required for maintaining the inactive state, and indeed several recent studies have shown that loss of *Xist* expression results in Xi reactivation (Bhatnagar et al., 2014; Yildirim et al., 2013). In mice, *in vivo* deletion of *Xist* in hematopoietic stem cells results in reactivation of X-encoded genes and eventually leads to hematologic cancer (Yildirim et al., 2013). In addition, a RNA interference screen identified several factors required for maintaining the Xi. Inhibition of these factors in mouse liver cells resulted in *Xist* silencing and reactivation of X-linked genes (Bhatnagar et al., 2014). Moreover, mice defective for Stanniocalcin 1 (*Stc1*), which was one of the factors identified as a maintenance factor also show two active X chromosomes (Bhatnagar et al., 2014). It needs to be noted that in this study only four genes were analyzed to assess X chromosomal activity. Together it seems that in mice continuous *Xist* expression is required for long term maintenance of the silent state of the Xi. For human *XIST* there is only one study addressing this issue. In this study deletion of the XIC in somatic cell hybrids containing a human inactive X chromosome on a mouse background did not result in reactivation of X-encoded genes, suggesting that human *XIST* is dispensable for maintenance (Brown and Willard, 1994).

Barr body organization

A question that has intrigued researchers for years is how DNA is organized within the nucleus of a cell. For long it has been recognized that chromosomes occupy their own distinct territory within the nucleus and do not intermingle too much. How a chromosome is structurally organized within its territory has been studied extensively using a variety of techniques, and it is only with the recent development of techniques like super-resolution microscopy and Chromatin Conformation Capture that this organization is being further dissected. Also the three dimensional organization of the Xi has been subject of many studies and it seems that the structural organization of the Xi is not that different from active chromosomes.

In general, the three dimensional organization of chromatin seems to differ with the transcriptional activity of a cell (Derenzini et al., 2014). In active cells, with enhanced transcription rates, the borders of the chromosome territories are less well defined, and chromatin of different chromosomes intermingles. The chromatin of a chromosome does not contain a specific region where transcription takes place, as gene transcription is thought to take place throughout the entire chromosome territory (Branco and Pombo, 2006). In contrast, the chromosomes of resting cells, with a low transcription rate, occupy more distinct territories. Silent heterochromatin is located on the inside of a chromosome territory, while gene transcription takes place on the outside of the chromosome. In addition, chromosome territories are pervaded by a network of channels. These channels facilitate access of transcription factors to the chromatin, allowing gene transcription to occur not only at the outer rim of, but also inside a chromosomal territory (Cremer and Cremer, 2010; Fakan and van Driel, 2007; Markaki et al., 2010).

The studies that have investigated the organization of the Xi have reported contradictory results, although in general the Xi seems to have an organization similar to autosomes and the Xa, with a core of silent heterochromatin, and gene transcription of XCI escaping genes taking place at the periphery of the Xi. As only a few genes escape from XCI the number of genes transcribed from the Xi is much lower compared to autosomes or Xa. The location of genes subject to XCI and genes escaping from XCI has been studied using DNA-FISH and RNA-FISH. While early studies agreed that XCI escaping genes are found at the periphery of the Xi territory, they disagreed on the localization of genes subject to XCI. While one study found that silenced genes are located at the periphery of the Xi together with escaping genes, another study found silenced genes in the core of the Xi (Chaumeil et al., 2006; Clemson et al., 2006). This study demonstrated that during establishment of XCI active genes relocate from the periphery of the Xi towards the interior, as they are being silenced (Chaumeil et al., 2006). The organization of the Xi in a transcriptionally silent core and active transcription at the periphery is supported by Chromatin Conformation Capture on Chip (4C) experiments that analyzed the long range interactions of X-chromosomal loci with other DNA segments. These experiments showed that within the Xi, inactive genes preferentially interact together and active genes also preferentially interact together. As active genes were more frequently engaged in interactions with other chromosomes, they are likely to be located on the periphery of the Xi territory (Splinter et al., 2011). In contrast to these studies that suggest that XCI escaping genes are located at the periphery of the Xi territory, several other studies observed gene transcription of escaping genes throughout the Xi territory (Calabrese et al., 2012).

Like other chromosomal territories, the chromosome territory of the Xi is also completely pervaded by a channel-like network, but the channels of the Xi have a reduced diameter. *Xist* RNA molecules are located inside these channels and interact with the

surrounding chromatin, that is thought to be active (Smeets et al., 2014). This is in line with the observation that *Xist* seems to spread to active genic regions first (Engreitz et al., 2013).

Interestingly, the organization of the inactive compartment of the Xi shows a high degree of variability between cells compared to other chromosomes. In 4C experiments the inactive compartment of autosomes and the Xa displays preferential interactions, indicating that these interactions were present in a substantial proportion of the cell population that was analyzed (Simonis et al., 2009; Splinter et al., 2011). In contrast, the inactive chromatin of the Xi is devoid of preferential interactions, indicative of a variable structural organization between cells. This lack of preferential interactions is induced by *Xist* RNA rather than by the larger amount of silent chromatin, as deletion of *Xist* results in a conformation of the Xi that more resembles that of the Xa (Splinter et al., 2011). Altogether, our understanding of the structural organization of the Xi still holds some contradictories, and completely understanding this organization might require the analysis of a larger number of X-encoded genes as the RNA-FISH studies performed to date have analyzed four genes at most.

Extraembryonic XCI

Extraembryonic XCI in human and mouse

XCI differs between human and mouse in several ways. One of the most striking differences is the mechanism of XCI in extraembryonic tissues. As mentioned above, the cells of the early mouse embryo undergo imprinted XCI, resulting in the exclusive inactivation of the Xp. In contrast to mouse, XCI in human extraembryonic tissues does not seem to be imprinted, and silencing is not as strict (Moreira de Mello et al., 2010). A number of studies observed random XCI patterns in human placenta (Looijenga et al., 1999; Migeon and Do, 1978, 1979; Zeng and Yankowitz, 2003). In contrast, several other studies concluded that in human extraembryonic tissues Xp is preferentially inactivated (Goto et al., 1997; Harrison, 1989; Harrison and Warburton, 1986; Ropers et al., 1978).

These seemingly contradictory results can be explained by the relatively large patch size of the placenta, with 8mm³ biopsies consisting of a single patch (Looijenga et al., 1999; Moreira de Mello et al., 2010). In perspective, the patch size of human muscle and liver is smaller than 0.008mm³ (unpublished results). A large patch size, as in placenta, can confound XCI analysis if the patch size approaches the size of the sample taken for XCI analysis. Interestingly, almost all studies reporting preferential Xp inactivation in placenta, did observe random XCI in a subset of samples. Moreover, expression analysis of multiple X-chromosomal loci shows that silencing of the inactive X chromosome in human extraembryonic tissues is not as stringent as in mouse

(Moreira de Mello et al., 2010). This is further underscored by the observation that the human Xi is relatively easily reactivated in hybrids from human chorionic villi and mouse A9 cells (Migeon et al., 2005; Migeon et al., 1986).

The difference between mouse and human extraembryonic XCI is further underscored by the difference in coping with supernumerary maternal X chromosomes. In mouse, an additional Xm cannot be inactivated, resulting in almost absence of extraembryonic tissues (Takagi and Sasaki, 1975). In humans in contrast, additional X chromosomes from either paternal or maternal origin can be inactivated, and instead of being embryonic lethal lead to Klinefelter syndrome (Jacobs and others 1988)

Mouse imprinted XCI

Several locations for the imprint responsible for exclusive Xp inactivation during imprinted XCI have been considered. This imprint could be located on Xp, marking it for future inactivation, on Xm, preventing it from inactivating itself, or both. For a long time it was assumed that at least the maternal X chromosome contains an imprint preventing it from inactivation, as parthenogenetic embryos carrying a double maternal genome (XmXm) embryos do not initiate XCI in extra-embryonic tissues until the late blastocyst stage (Kay et al., 1994). Although considered a likely candidate, DNA methylation is not the main epigenetic mark characterizing the maternal imprint, because mice deficient for de novo methyltransferase (DNMT3a/b) still show *Xist* repression on Xm (Chiba et al., 2008).

A recent report identified H3K9me3 at the *Xist* promoter region on the maternal X chromosome as the imprint preventing inactivation of the maternal X chromosome (Fukuda et al., 2014). Whether additional imprints in maternal repression of *Xist* are involved remains to be seen. The imprint on Xm is established during late oogenesis, as was shown in nuclear transfer experiments using nuclei from different stages of germ cell development (Oikawa et al., 2014). Interestingly the maternal *Xist* repressing imprint is not only erased in the epiblast, prior to random XCI, but also in the trophectoderm at E4.5, explaining initiation of XCI in XmXm blastocysts after initial repression of *Xist* (Oikawa et al., 2014).

An imprint on the paternal X chromosome is considered unlikely, as this would require an imprint that silences *Xist* repressing elements, the most likely candidate being *Tsix*. However, *Tsix* is not expressed in the mouse embryo until the blastocyst stage, well after the implementation of imprinted XCI (Fukuda et al., 2014; Sado et al., 2001). Interestingly, a deletion of *Tsix* on the maternal X chromosome is lethal during post-implantation development, as this result in ectopic upregulation of *Xist* from the Xm in extra-embryonic tissues (Ohhata et al., 2011).

Order of events during mouse extraembryonic XCI

In both mouse and human, XCI seems to coincide with activation of the embryonic genome. In mouse embryonic genome activation occurs at the 2-cell stage, while in human this occurs a little bit later, around the 4-8 cell stage (Dobson et al., 2004; Huynh and Lee, 2003; Schultz and Heyner, 1992). Embryonic genome activation does not occur simultaneously in all cells, nor does *Xist* accumulation (Huynh and Lee, 2003).

In mice, both X chromosomes are active at the two cell stage (Kalantry et al., 2009; Namekawa et al., 2010; Okamoto et al., 2004; Patrat et al., 2009) and *Xist* is transcribed at a low level. Using RNA-FISH *Xist* RNA is visible as a small pinpoint signal on one or two X chromosomes. From the 2-cell stage to the 16-cell stage the *Xist* pinpoint of the Xp enlarges and spreads along the X chromosome (Namekawa et al., 2010; Okamoto et al., 2004). Spreading of *Xist* coincides with repression of *Cot-1* transcription and exclusion of RNA pol II (Namekawa et al., 2010; Okamoto et al., 2004). The future inactive X chromosome first loses its active histone modifications, and subsequently acquires repressive histone modifications, similarly to random XCI. Immunofluorescent studies showed that the loss of active histone modifications and accumulation of repressive chromatin marks does not happen simultaneously in all cells of the early embryo (Mak et al., 2004; Okamoto et al., 2004). This heterogeneity in the early embryo probably explains why early studies using pools of embryos and cells to define the time-point of actual gene silencing concluded imprinted XCI to start at a later time-point, compared to studies that have used single cell analyses (Hadjantonakis et al., 2001; Kalantry et al., 2009; Latham and Rambhatla, 1995; Lebon et al., 1995; Okamoto et al., 2004; Singer-Sam et al., 1992; West et al., 1977). RNA-FISH analysis of X-linked expression in single cells showed Xp silencing occurring from the 8-cell stage onwards (Kalantry et al., 2009; Okamoto et al., 2004). During silencing, repeat regions are silenced first, followed by silencing of genes (Namekawa et al., 2010). Furthermore, genes located closer proximity to the *Xist* locus on the linear chromosome, including *Rnf12*, are silenced earlier compared to gene located further away (Huynh and Lee, 2003; Namekawa et al., 2010).

Order of events during human extraembryonic XCI

Few studies have investigated the onset of human XCI, because of the ethical restrictions on studies of human embryos. Two studies that have been able to analyze human embryos from the 8-cell stage onwards have yielded contradictory results. One study found that XCI starts from the 8-cell stage onwards and shows much similarity to mouse XCI, as *XIST* RNA accumulation was observed on one X chromosome, which coincided with repression of *COT-1* transcription and accumulation of H3K27me3 and macroH2A enrichment (van den Berg et al., 2009). Another study analyzed embryos from the 8-cell stage to the blastocyst stage and detected two *XIST* RNA clouds from the 8-cell stage onwards. Interestingly, in this study *XIST*

accumulation did not coincide with silencing, as no H3K27me3 methylation was observed and several X-encoded genes were found to be biallelically expressed using RNA-FISH (Okamoto et al., 2011). A third study also did not observe any H3K27me3 foci in early blastocysts. Only after prolonged culture of embryos on decasualized endometrium stromal cells, H3K27me3 foci were detected in late blastocysts. These H3K27me3 foci were never detected in cells of the ICM, only in trophoctoderm and to lesser extend in the hypoblast (Teklenburg et al., 2012). These latter two studies suggest that human XCI is executed differently from mouse XCI, as *XIST* accumulation does not lead to gene silencing, not even in the late blastocyst.

The observation of two *XIST* clouds in human embryonic cells might have interesting implications for the choice which X chromosome will be inactivated in random XCI. In mouse, random XCI is tightly regulated ensuring mono-allelic *Xist* expression and factors influencing *Xist* up-regulation or *Xist* spreading will determine the choice which X chromosome will be inactivated. However, when two *Xist* clouds are present prior to actual silencing, the choice which X chromosome will be inactivated will not be determined by *Xist* spreading anymore, but instead by factors effecting silencing. Also the observation that in early embryos *XIST* clouds are more dispersed compared to somatic cells, might indicate that to effect silencing *XIST* needs to associate with the X chromosome and factors recruiting *XIST* to the X chromosome are instructive in the regulation of a mutual exclusive outcome of the XCI process.

In mouse, feedback of XCI, that prevents inactivation of too many X chromosomes, is tightly controlled by *Xist* mediated-silencing of its own activator *Rnf12*. However, if *Xist* is accumulated over the entire X chromosome prior to inactivation, a trans-acting factor regulating XCI feedback does not necessarily needs to be in close proximity to the *XIST* locus, allowing other factors than *Rnf12* to have taken over this role during evolution. Until now it is not known whether the trans-activating function of *Rnf12* is conserved from mouse to man. The observation that male human embryos also contain an *XIST* cloud, suggests that in the initial phase *XIST* upregulation is independent of the presence of two X chromosomes (Okamoto et al., 2011).

Skewed XCI

Skewed XCI

As a result of XCI every female individual consists of two cell populations that have a different active X chromosome. These two cell populations are intermingled and make every female a mosaic of cells with an active Xp or an active Xm. The relative size of these two populations can be expressed as the X-inactivation ratio (XIR). Most female individuals have an XIR of 50:50, but

deviations from this 50:50 ratio are common. In general, an XIR greater than 80:20 is termed “skewed” XCI, while an XIR of more than 90:10 is termed “extremely skewed” XCI.

Primary vs Secondary skewed XCI

Two different mechanisms causing skewed XCI can be distinguished. Primary skewed XCI is a result of processes influencing the choice which X chromosome is inactivated, while secondary skewed XCI is a result of post-XCI cell selection (Fig. 6). Primary skewed XCI can be the result of mutations in genes involved in XCI, but could also occur naturally. Since the choice which X chromosome is inactivated is random, most cells of the early embryo might inactivate the same X chromosome by chance, thus resulting in primary skewed XCI. The chance of this happening, increases if a smaller number of cells is present at the time of XCI. Unfortunately, the number of stem cells present at the time of human XCI is unknown, as studies of XCI in human embryos can only be performed up to day 8 of embryonic development, which is insufficient to analyze post-implantation random XCI (Teklenburg et al., 2012). Therefore, the chance of spontaneous primary skewed XCI in humans is unknown. Several studies have tried to deduce the number of cells at the time of XCI from the distribution of XIR's in a female population, assuming that the number of skewed individuals reflects the number of stem cells during XCI. However, as these studies used blood samples to determine an XIR, they only allow an estimation of the number of hematopoietic stem cells at the time of XCI, and not the total number of stem cells during XCI. These studies estimated that there are 8-16 hematopoietic stem cells present when XCI is initiated (Amos-Landgraf et al., 2006; Puck et al., 1992). Another study used the intra-individual difference for XIR between blood cell lineages to calculate the number of stem cells and estimated there are 14-16 hematopoietic stem cells during XCI (Tonon et al., 1998). However, all the above mentioned studies do not take into consideration the effects of secondary skewing. Instead, they assume that the frequency of skewed XCI among newborns or adults is comparable to embryos at the time of XCI. Also, when comparing different blood cell populations within an individual, secondary skewing specific for these cell populations cannot be taken into consideration. Therefore, the reported numbers are likely an underestimation of the true number of hematopoietic stem cells, and the total number of cells during XCI remains unknown.

Primary skewed XCI can also be caused by mutations in genes involved in XCI, as is illustrated by mutations in the *XIST* promoter that showing exclusive activation or inactivation (Plenge et al., 1997; Pugacheva et al., 2005). Although only two mutations in the *XIST* promoter are reported to date, it is not unlikely that many more mutations occur in the *XIST* promoter or *XIST* regulatory elements without being discovered as they are not accompanied by a clinical phenotype. From mouse studies involving deletion of different parts of the *Xic*, it can be deduced that mutations involving *Tsix*, *Xite* and *Rnf12* will also result in primary skewed XCI ,

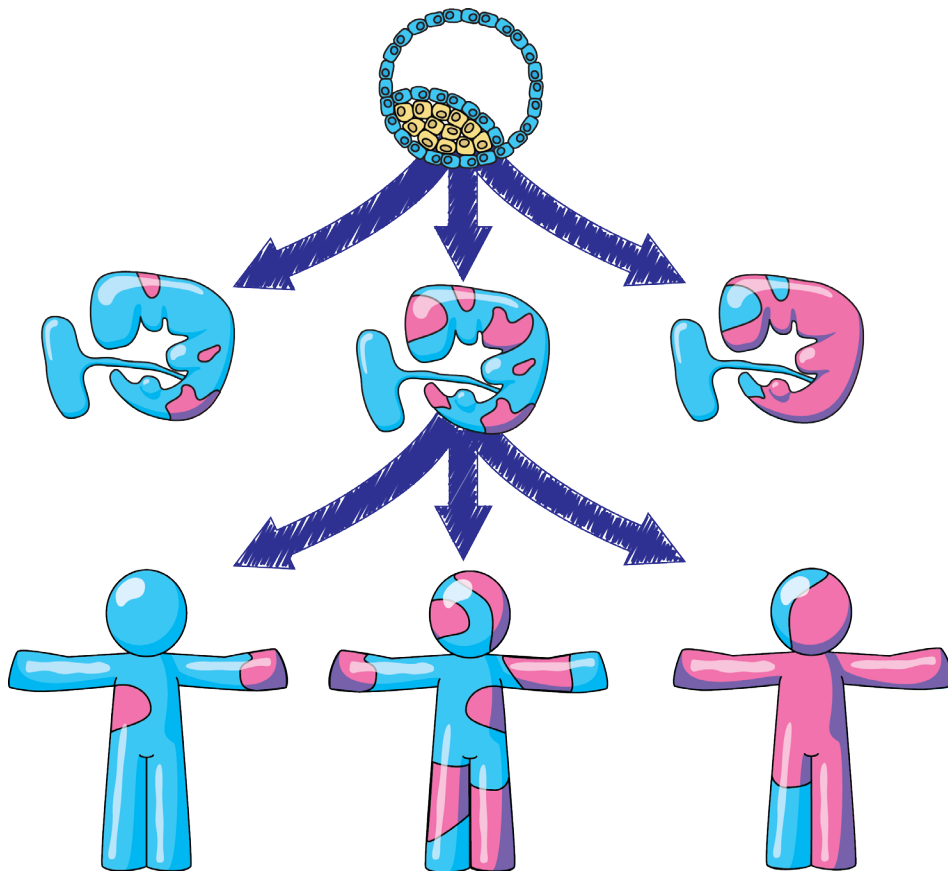


Figure 6.

Skewing of X chromosome inactivation

Two forms of skewing of X chromosome inactivation exist. The top part of the figure shows primary skewed XCI: cells of the epiblast randomly inactivate the paternal or the maternal X chromosome. As a result most embryos will have an X-inactivation ratio around 50:50, but by chance some embryos may consist of cells where the majority cells has inactivated the same X chromosome, resulting in skewed XCI. The lower part of the figure shows secondary skewed XCI: as a result of post-inactivation cell selection, one cell population might have an advantage in cell growth or differentiation, resulting in a relative increase of this cell population over the other.

either by affecting *Xist* expression directly or by impacting on *Xist* through feedback mechanisms.

Secondary skewed XCI is the result of a selective pressure applied to a heterozygous X-encoded gene, resulting in a proliferative or differentiating advantage of one X chromosome over the other. Such a selection can theoretically occur at any age and can be tissue-specific.

Skewed XCI in a healthy female population

In a healthy human female population the XIR follows a normal distribution. Most females have an XIR around 50:50, but deviations from 0:100 up to 100:0 occur. The proportion of females displaying skewed XCI in a healthy population varies between studies from 0% to 58% (Amos-Landgraf et al., 2006; Bolduc et al., 2008; Busque et al., 1996; El Kassas et al., 1998; Hatakeyama et al., 2004; Mossner et al., 2013; Sharp et al., 2000; Tonon et al., 1998). This variation between studies is partially explained by the age of females that were included in the studies, as skewing of XCI seems to increase with age and especially above the age of 60 years. Many studies have analyzed the putative association of skewed XCI in blood with increasing female age, and reported varying results. In general, the proportion of females with skewed XCI increases throughout female life. This increase in females with skewed XCI is thought to be small below the age of 30-60 years, but increases substantially after this age (table 1). Where the increase in skewed XCI in elder women is obvious, and reported by all studies, the increase during early female life is small and remains controversial. The studies that have compared skewed XCI in neonates to adult women, mostly found that skewing increases from neonatal life onwards (Amos-Landgraf et al., 2006; Bolduc et al., 2008; Busque et al., 1996; El Kassas et al., 1998; Tonon et al., 1998). However, studies that did not include a large number of neonates, but a smaller number of children from 0 years and older did not detect any obvious increase in skewed XCI before the age of 30 years (Fey et al., 1994; Hatakeyama et al., 2004; Mossner et al., 2013). This might indicate that a large number of subjects is required to detect the small increase in skewed XCI during early female life. Where almost all these studies are cross-sectional, one study performed an elaborate longitudinal analysis of 178 females by measuring XCI ratios with an interval of 13 to 21 years. This analysis confirmed the small increase in skewed XCI during female life (with a maximum increase of 12% during 16.5 years), and the more dramatic increase after the age of 60 (Sandovici et al., 2004).

Several hypothesis have been postulated to explain the increase in skewed XCI during female life. It might be possible that with increasing age the number of stem cells decreases, which will result in an oligoclonal expansion and an increased chance that the majority of these cells has the same inactive X chromosome (Amos-Landgraf et al., 2006). This is supported by a recent report of a 115-year old women where the majority of peripheral white blood cells originate from two hematopoietic stem cell clones (Holstege et al., 2014). Although this

Table 1
Summary of studies analyzing skewness of XCI in healthy female individuals of various age

cross sectional studies					
study	year	population	assay	skewed XCI	conclusion
Busque	1992	162 neonates, 67 females (28-32 years), 66 females (>60 years)	methylation	75% and 90%	skewing increases from neonates to young women to elderly women
Fey	1994	105 females (2-96 years)	methylation	80%	skewing increases above 75 yrs
Gale	1994	100 females (12-86 years)	methylation	75%	skewing does not increase with age
Tonon	1998	36 neonates, 34 females (25-32 years), 34 females (>75 years)	methylation	75%	skewing increases from neonates to young women to elderly women
Kassar	1998	40 neonates, 49 females (22-50 years), 34 females (50-80 years)	methylation and transcription	75%	skewing increases above 50 yrs
Sharp	2000	148 females (<25 years), 106 females (>60 years)	methylation	75% and 90%	skewing increases above 25 years
Hatakeyama	2004	350 females (0-88 years)	methylation	75% and 90%	skewing increases above 30 years
Kristiansen	2005	258 dizygotic twin pairs, 200 monozygotic twin pairs, 391 singletons (18-101 years)	methylation	80%	skewing increases above 50 years
Amos	2006	590 neonates, 415 adults (no age reported)	methylation	80% and 90%	skewing increases from neonates to adults
Bolduc	2008	454 neonates, 448 mothers (18-43 years)	methylation	75%	skewing increases from neonates to adults
Mossner	2013	139 females (0-93 years)	transcription	80%	skewing increases above 40 yrs
longitudinal studies					
study	year	population	assay	skewed XCI	conclusion
Sandovici	2004	178 females (0-74 years)	methylation	-	skewing increases throughout life, but dramatically above 60 yrs
Wong	2011	twins (5 years)	methylation	75%	skewing increases already during childhood

number is extremely low, and therefore can be disputed, it supports the idea of a decreasing stem cell pool during female life. In addition, the increase of skewed XCI at later age could also be caused by secondary cell selection during female life.

Although many studies have reported an age-related increase in skewed XCI, it has also been proposed that the detected increase in skewed XCI does not represent actual X-inactivation, but rather is the result of changes in DNA methylation patterns in elderly women. Most studies analyzing skewing of XCI use methylation of the Androgen Receptor locus to determine the XIR, and one study found a discrepancy between AR methylation and expression in their study population (Swierczek et al., 2008). In contrast, other studies found a good agreement between DNA methylation and expression (Amos-Landgraf et al., 2006; El Kassas et al., 1998).

In laboratory mice the distribution of the XIR is different from human due to the inbred nature of these mice. Although the XIR is still normally distributed, it has a much smaller variation. The inbred nature of laboratory mouse strains allowed the identification of genetic elements that affect the XIR, which is most clearly observed when analyzing an F1 of different mouse strains. In for example the F1 of *Mus musculus domesticus* (C57BL/6) and *Mus musculus castaneus* mice, the average XIR is 70:30 favoring the *Mus musculus castaneus* X chromosome for inactivation. The genetic element responsible for this difference has been termed the X choosing element (Xce) (Cattanach, 1975). Different mouse strains carry different Xce alleles that affect the probability of an X chromosome to initiate XCI. As a result, an F1 with homozygous Xce alleles will result in an XIR around 50:50, while heterozygosity for the Xce results in an XIR deviating from 50:50. Originally, four Xce alleles, termed Xce^a - Xce^d, were identified and are ordered by their probability to initiate XCI, with Xce^a having the largest probability and Xce^d the lowest (Cattanach, 1991, 1994; Cattanach and Isaacson, 1967; Cattanach et al., 1969; Cattanach and Williams, 1972; Forrester and Ansell, 1985; Fowles et al., 1991). Recently, a fifth Xce allele has been identified, termed Xce^e, with a probability intermediate to Xce^a and Xce^b (Calaway et al., 2013). It has been suggested that the probability of an X chromosome to initiate XCI is not only determined by the Xce, but also by its parental inheritance and by autosomal factors (Chadwick and Willard, 2005). However, the general consensus is that the effect of a parent of origin effect and autosomal factors is relatively small compared to that of the Xce allele (Chadwick et al., 2006; Chadwick and Willard, 2005; Forrester and Ansell, 1985). The location of the Xce was first mapped to the Xic and a recent study narrowed down the region of the Xce to a 194 kb interval centromeric of *Xist* and *Tsix* (Calaway et al., 2013). The identification of a human Xce seems unlikely, as the variation of a human Xce will be too extensive to identify individual Xce alleles. Furthermore, a study comparing 500 mother-neonate pairs did not detect any heritability of skewed XCI, further arguing against a human Xce (Bolduc et al., 2008).

Skewed XCI and human disease

Skewing of XCI becomes of clinical importance when an X-encoded disease or trait is involved. It can easily be envisioned that in case of a heterozygous mutation, skewed XCI in which the affected allele is predominantly inactivated, or kept active, modulates disease phenotype. This has been established for Rett syndrome, a neurodevelopmental disorder that is caused by mutations in the MECP2 gene. Rett syndrome occurs almost exclusively in females, as males do not survive until birth (Amir et al., 1999). The phenotype of Rett syndrome females is modulated by their XIR, and results in an increased prevalence of skewed XCI among Rett syndrome patients (Archer et al., 2007; Huppke et al., 2006; Weaving et al., 2003). The same modulating effect has been established for Fragile X syndrome, a neurodevelopmental disorder caused by a loss of function of the FMR1 gene due to a CGG repeat expansion (Fryns and Van den Berghe, 1988; Heine-Suner et al., 2003; Martinez et al., 2005; Martorell et al., 2011; Schmidt et al., 1990).

Skewing of XCI does not only affect disease phenotype, but X-linked mutations can also induce secondary skewing. This is clearly illustrated in Incontinentia Pigmenti, a genodermatosis that is caused by a mutation in the IKBKG gene. Cells that lack IKBKG are more prone to undergo apoptosis, resulting in a completely skewed XCI pattern in females carrying a mutation in IKBKG (Smahi et al., 2000).

Skewed XCI and autoimmunity

Generally, skewed XCI is associated with diseases for which a causative X-chromosomal locus is identified. Interestingly, also a number of diseases for which no X-linked disease causing locus is known, have been associated with skewed XCI. Despite the lack of a causative X-chromosomal locus, an increased prevalence of skewed XCI is found in patient populations for these diseases. Among these diseases are several autoimmune disorders, including Rheumatoid Arthritis, Multiple Sclerosis and Autoimmune Thyroiditis (AITD) (Chabchoub et al., 2009; Ozbalkan et al., 2005; Uz et al., 2008). The association between these autoimmune disorders and skewed XCI has been explained by an increased autoimmunity against X-encoded antigens. This hypothesis states that in females with skewed XCI several X-encoded antigens escape from presentation in the thymus or other peripheral sites, leading to inadequate deletion of self-reactive T-cells and loss of T-cell tolerance. As a result, autoimmunity will occur more frequently among women with skewed XCI. This hypothesis is based on two observations. First, autoimmune disorders occur more frequently in females compared to males (Whitacre, 2001). Although this sex-bias for autoimmunity could also be explained by immune modulating effects of sex hormones, involvement of XCI in the pathogenesis of autoimmunity cannot be ruled out. Second, mouse studies have shown that a lack of exposure to self-antigens increases the risk of autoimmune reactions (Klein et al., 2000; Laufer et al.,

1996). To date, this hypothesis is not confirmed and alternatively the association between autoimmunity and skewed XCI might be explained by X-encoded genes that regulate immune processes.

Although for these diseases no X-linked locus has been identified yet, Genome Wide Association (GWA) studies might identify the X-chromosomal loci responsible for their association with skewed XCI. Unfortunately, the X chromosome has been poorly analyzed in GWA studies until now, as analysis of the X chromosome requires sex-specific analysis for X-chromosomal sequences is required. Of the GWA studies performed between 2010 and 2014, only 33% analyzed the X chromosome (Wise et al., 2013). Attention for this hiatus in GWA analysis and the consequential missing data is growing, and two recent studies have re-analyzed published GWA data sets from autoimmune disorders for X-chromosomal involvement. One study focused on GWA data sets for Graves' disease, that together with Hashimoto's disease comprises AITD, and identified an X-chromosomal variant in the G-protein coupled receptor GPR174 (Chu et al., 2013). This variant is validated in an independent study and although the function of GPR174 still needs to be investigated, it provides an explanation for the association of skewed XCI and Graves' disease (Szymanski et al., 2014). Another study that analyzed published X-chromosomal GWA data and found several X-encoded variants associated with different autoimmune disorders, including rheumatoid arthritis (Chang et al., 2014). These results seem promising for identifying new X-encoded, disease-associated variants. Considering that the X chromosome is increasingly analyzed in GWA studies, it is not unlikely that more X-encoded variants associated with autoimmune disorders will be identified. However, a shortcoming of the abovementioned studies is that they did not take skewing of XCI into account in their analyses, which might result in under detection of X-encoded variants. To fully utilize the X-chromosomal data provided by GWA studies, skewing of XCI should be implemented in the analysis.

Skewed XCI and PCOS

Another disorder for which no X-linked locus has been identified, but which is also associated with skewed XCI is Polycystic Ovary Syndrome (PCOS). PCOS is an endocrine disorder and is one of the leading causes of subfertility in women, affecting 5-10% of the women of reproductive age (Azziz et al., 2004). It is characterized by oligo- or anovulation, hyperandrogenism and polycystic ovaries. Oligo ovulation is clinically characterized by oligomenorrhea, a menstrual cycle of more than 35 days. If ovulation is completely absent, this results in amenorrhea, the absence of menstruation. Hyperandrogenism, the increased action of male sex hormones, can clinically result in hirsutism or acne. Polycystic ovaries can be visualized using ultrasound technology and appear enlarged with a large number of small follicles. PCOS is considered a very heterogenic syndrome, and therefore women suffering from PCOS do not necessarily

experience all three of the abovementioned characteristics. According to the 2003 Rotterdam consensus criteria an individual must have two out of three of these characteristics to validate the diagnosis PCOS (Rotterdam, 2004). The heterogeneity of PCOS is further illustrated by the fact that two other diagnostic schemes exist. The 1990 National Institutes of Health (NIH) criteria uses the combination of hyperandrogenism and oligo-ovulation to diagnose PCOS, while the 2006 criteria from the Androgen Excess and PCOS Society, consider PCOS predominantly a hyperandrogenemic disorder and only use the combinations of the three characteristics that include hyperandrogenism to diagnose PCOS (Azziz et al., 2006; Azziz et al., 2009). In addition, PCOS often involves a metabolic syndrome, that is characterized by insulin resistance and obesity. While the association for autoimmunity with skewed XCI seems established, an association of skewed XCI with PCOS remains subject of debate.

The cause of PCOS is currently unknown, but there are strong indications that a genetic component is involved. Involvement XCI in the pathogenesis of PCOS has been hypothesized through the modulation of the sensitivity of the AR. The hyperandrogenemic phenotype in PCOS patients is exerted by androgens through the AR. Of all androgens, testosterone and dihydrotestosterone are the two hormones that are able to bind to the AR, with dihydrotestosterone being the more potent activator. When inactive, the AR is located in the cytoplasm, and upon binding of testosterone or dihydrotestosterone the newly formed complex translocates to the nucleus where it acts as a DNA-binding transcription factor to regulate gene expression. The sensitivity of the AR to androgens is modulated by two trinucleotide repeats, located in its first exon. These repeats are both located in the transactivation domain that is required for binding additional co-factors (Alen et al., 1999; Burd et al., 2005; Markus et al., 2002). Of these two repeats, the CAG repeat, encoding a poly-glutamine tract, is mostly studied. An inverse correlation exists between CAG repeat number and androgen sensitivity, with a shorter CAG repeat resulting in a more sensitive AR (table 2) (Beilin et al., 2000; Chamberlain et al., 1994). This increased sensitivity is the result of an increased capability to activate target genes, and not of an increase in AR transcripts. The CAG repeat is highly polymorphic in a population, with its repeat number ranging from 4 to 33 repeats with a mean of 19-22 repeats, and following a normal distribution (Ferk et al., 2008; Ibanez et al., 2003). In a female population around 80% of all female individuals are heterozygous for the CAG repeat, and as a result they probably have AR alleles with different sensitivities. Moreover, the distribution of CAG repeat length differs by ethnic background. Compared to Caucasians a Chinese population has a slightly longer CAG repeat, while an African population has a shorter CAG repeat (Edwards et al., 1992; Irvine et al., 1995; Kim et al., 2008; Liu et al., 2008; Mifsud et al., 2000; Sartor et al., 1999). Repeat length in an Indian population is comparable to Caucasians (Dasgupta et al., 2010).

Table 2
Summary of studies analyzing the association of a shorter Androgen Receptor CAG repeat with PCOS

Study	Ethnicity	number of cases	number of controls	PCOS criteria	control population	method of CAG measurement	method of analysis	biallelic mean CAG repeat length	cutoff of skewed XCI	association with skewed XCI	association with CAG repeat length after XCI correction
Mifsud, 2000	Chinese (83%) and Indian (17%)	90	112	WHO	proven fertile women	ABI	biallelic mean and separate alleles	no	-	-	-
Jaakkola, 2005	Caucasian (Finnish)	106	112	WHO	non-hirsute fertile women	PAGE		no	-	-	-
Kim, 2007	Chinese (Seoul)	114	205	WHO	healthy women and fertility patients	ABI	biallelic mean and separate alleles	no	-	-	-
Ferk, 2008	Caucasian (Slovenian)	117	110			PAGE	biallelic mean and separate alleles	no	-	-	-
Liu, 2008	Chinese (Shanghai)	148	104	Rotterdam 2003	proven fertile normal ovarian morf	ABI	biallelic mean	no	-	-	-
Van Nieuwerburgh, 2008	Caucasian (Belgian)	97 cases subgroups by CAG		Rotterdam 2003	no controls	ABI	biallelic mean and separate alleles	yes	-	-	-
Skrigatic, 2012	Caucasian (Croatian)	214	209	Rotterdam 2003	normandrogenic normal ovarian morf	PAGE	biallelic mean and separate alleles	no	-	-	-
Peng, 2014	Chinese	224 vs 223		Rotterdam 2003	population receiving IVF	PAGE	biallelic mean	no	-	-	-
Hickey, 2002	Caucasian (Australian)	171	83			ABI	biallelic mean	yes	60% and 80%	no	yes
Shah, 2008	Caucasian	330	289	NIH 1990	normandrogenic normal ovarian morf	ABI	biallelic mean	yes	60% and 80%	no	yes
Dasgupta, 2010	Caucasian and African Indian	250	299	Rotterdam 2003	eumenorroic no infertility known	ABI		no		no	no
Laisk, 2010	Caucasian (Estonian)	32	79	Rotterdam 2003	eumenorroic occlude fallopian tubes	ABI	biallelic mean and separate alleles	no		no	no
Radian, 2010	Caucasian (Romanian)	137 vs 130		Rotterdam 2003	?	?	biallelic mean	yes		no	no
Schuring, 2011	Caucasian (German)	72	179	Rotterdam 2003	eumenorroic	PAGE	biallelic mean	yes		no	yes
Rajender, 2013	Indian	169 vs 175		Rotterdam 2003	proven fertile, eumenarchic normal ovarian morf	ABI	biallelic mean	no		no	no

The other repeat region is an incomplete repeat, consisting mainly of GGC repeats but containing several GGN repeats in addition, and has therefore been termed GGN repeat. The GGN repeat encodes a poly-glycine tract, and is not as polymorphic as the poly-glutamine tract. In a Caucasian population there are two common GGN alleles that represent 85% of all alleles. This low diversity has hampered the study of the effect of the GGN repeat on androgen sensitivity. The several studies that explored the effect of the GGN repeat on androgen sensitivity have reported contradictory effects of this repeat (Brockschmidt et al., 2007; Ding et al., 2005; Werner et al., 2006). Therefore, it is still unresolved if the correlation between GGN repeat number and androgen sensitivity is a direct or an inverse correlation. The effect of GGN repeat on androgen sensitivity might not only be mediated by activating capability of the AR, but also by higher AR protein levels (Brockschmidt et al., 2007). Also for the GGN repeat, the population distribution seems to be different for different ethnic populations, as in a Chinese population one common allele was found where two are present in a Caucasian population (Kovacs et al., 2009; Sasaki et al., 2003). To really understand the effect of the GGN repeat on androgen sensitivity further studies are needed. To date, most studies have focused on the relation between CAG repeat number and hyperandrogenemic disorders.

The involvement of XCI in androgen sensitivity was first demonstrated in women with idiopathic hirsutism, where the longer AR CAG allele was preferentially inactivated (Vottero et al., 1999). Since then, a large number of studies have investigated the relationship between PCOS and CAG repeat number, but yielded contradictory results. These contradictory results might be explained by differences in study populations, as AR repeat length differs between ethnic backgrounds (Shah 2008, Platz, 2009, Edwards 1992). Alternatively, contradictory results might also be the result of the different measures that have been used to quantify the CAG repeat number of the two alleles of a single individual. Several studies used the bi-allelic mean of the CAG repeat number for each individual, while other studies used a cumulative CAG repeat number or used only the shorter AR allele to quantify AR sensitivity. In addition, a large number of studies measured CAG repeat number but did not correct for XIR, thereby disregarding the relative expression levels of the two AR alleles. Three recent meta-analyses investigated the association between CAG repeat length and PCOS, but only one of these corrected for XIR (Peng et al., 2014; Rajender et al., 2013; Zhang et al., 2013a). In this meta-analysis no association between XIR-corrected CAG repeat length and PCOS was found (Zhang et al., 2013a). Given the controversy in results it might be possible that the association between CAG repeat number and PCOS exists only in a subpopulation and not in all PCOS patients. Additionally, one might also question if peripheral blood samples that are generally used to assess CAG repeat number and XIR are representative of ovarian tissue, where differences in AR sensitivity are likely to have their effects in PCOS patients.

Escape from XCI

The clinical relevance of escape from XCI

While most genes on the Xi are silenced, not all the genes located on the Xi are subject to XCI. A subset of genes escapes from XCI and remain expressed from the Xi, both in human and in mouse. These XCI-escaping genes are of particular clinical interest for syndromes involving numerical X chromosome abnormalities, like 45, XO Turner syndrome and 47, XXY Klinefelter syndrome. The phenotype in these syndromes is unlikely to be caused by genes subject to XCI, as these genes are always expressed from a single X chromosome, despite the total number of X chromosomes present. Therefore, the genes that escape silencing are the most likely candidates to explain the phenotype in these syndromes. At first, it was hypothesized that the genes on the PAR cause the phenotype of numerical abnormalities of the X chromosome, as this region was first recognized to be not included in the XCI process (Lyon, 1962). Later it was recognized that besides the genes located in the PAR, also genes located elsewhere on the X chromosome escape the XCI process partially or completely.

Technical difficulties in defining escape from XCI

The first studies addressed escape from XCI at the level of single genes (Brown et al., 1995; Carrel and Willard, 1999; Greenfield et al., 1998). With recent technological advances in RNA-sequencing (RNA-seq) X chromosome wide analysis of allele-specific gene expression has become possible, identifying many more XCI escaping genes. The first studies employing this method analyzed XCI escape in mouse, and paved the way for studies analyzing XCI escape in human (Calabrese et al., 2012; Li et al., 2012; Yang et al., 2010). Escape from XCI is detected by RNA-seq studies using heterozygous SNPs to determine the balance in expression between two alleles of a certain gene. This method will work most robust on a sample where the parental origin of the Xi is the same in all cells, i.e. a sample that is 100% skewed. In such a sample, genes subject to XCI will have an allelic balance of 1 or 0, while genes escaping XCI will have an intermediate allelic balance. From mice or mouse cell lines, a sample that is 100% skewed can be obtained after genetic modification or enrichment of a sub-population of cells (Calabrese et al., 2012; Wu et al., 2014; Yang et al., 2010). However, in human individuals XCI is rarely a 100% skewed and several studies have dealt with this in different ways (Carrel and Willard, 2005; Cotton et al., 2013; Zhang et al., 2013b).

Escape from XCI is more common in human

When comparing the number of genes escaping from XCI between human and mouse, a larger number of genes is found to escape in humans. This suggests that XCI is much more complete in mouse compared to human. In mouse somatic tissues, the number of genes found to escape from XCI is fairly consistent among different studies ranging from 5-13 genes and represents 2-3% of the analyzed X-encoded genes (table 3) (Li et al., 2012; Wu et al., 2014; Yang et al., 2010). In human somatic tissues 94 genes were found to escape from XCI, representing 15% of all human analyzed X-linked genes (table 4) (Carrel and Willard, 2005). The lower number of XCI escaping genes in mouse corresponds with the less severe phenotype of 39X0 mice compared to 46X0 Turner women (Lynn and Davies, 2007).

In addition to a larger number of XCI escaping genes in human, the distribution of escaping genes along the X chromosome is also different between mouse and human. When considering the distribution of XCI escaping genes across the X chromosome the PAR contains the highest concentration of XCI escaping genes in both human and mouse. In both species almost all genes located in the PAR have been confirmed to escape from XCI (Carrel and Willard, 2005; Keitges and Gartler, 1986; Salido et al., 1996). When considering the escaping genes that are located outside the PAR, their distribution along the X chromosome differs between human and mouse. Where in human XCI escaping genes cluster together, while the few escaping genes in mouse do not show any clustering but appear more evenly distributed along the X chromosome (Carrel and Willard, 2005; Cotton et al., 2013; Yang et al., 2010; Zhang et al., 2013b). Interestingly, the human XCI escaping genes cluster together on the evolutionary younger regions of the human X chromosome, that contain a higher proportion of genes with a Y-encoded homolog. The human X chromosomal sequence outside the PAR can be divided in 5 evolutionary strata, with stratum 1 having the highest conservation and stratum 5 the lowest (Lahn and Page, 1999). The more ancient strata 1 and 2 contain a lower amount of escaping genes, compared to the evolutionary younger strata 3, 4 and 5 (Carrel and Willard, 2005). This is consistent with the hypothesis that the mammalian X and Y chromosome originate from the same set of ancestral autosomes, and that the ability of a gene to be X-inactivated is acquired after loss of its Y-chromosomal homolog, which occurred more frequently for genes located in the evolutionary ancient strata (Carrel and Willard, 2005).

The observations that human escapees cluster together, lead to the hypothesis that in humans escape from XCI might be regulated at the level of chromosomal domains. However, this does not exclude that escape is also regulated at the single gene level, as the human X chromosome also contains escapees that map far from other escapees and do not contain a Y-homolog (Carrel and Willard, 2005). In contrast to this hypothesis, escape from XCI in mouse is thought to be intrinsic to the DNA sequence of a gene, and independent of its chromosomal position. This hypothesis was assessed by integrating a BAC containing the X- encoded *Jarid1C*

Table 3a. RNA-seq studies of mouse XCI escape

study	material	no samples	no. genes found to		threshold for escape	genetic background	analysis of reciprocal cross		method of enrichment for monoclonality of Xi
			escape	escape			yes	no	
Calabrese et al, 2012	trophoblast stem cells	2 cell lines	35 of 262 (13,4%)	gene specific	BL6, M. Castaneus	yes	yes	imprinted XCI	
Yang et al, 2010	embryonic kidney cells	1 cell line	13 of 393 (3,3%)	10% BL6, M. Spretus	no	no	HAT selection of HPRT activity		
Li et al, 2012	neural stem cells	4 cell lines	5 of 268 (1,9%)	15% BL6, M. Molossinus JF1	yes	yes	no		
Wu et al, 2014	brain cells	2 mice	7 of 263 (2,6%)	not reported	BL6, M. Castaneus	yes	FACS for tdTomato transgene		

Table 3b. RNA-seq studies of human XCI escape

study	material	no. genes		no. Genes with heterogeneous escape
		escapin in 100% of females	escapin in 100% of females	
Cotton, 2013	LCL from CEU HapMap, fibroblast cell line from YRI HapMap	30 CEU, 31 YRI, 38 fibroblast	not reported	68 of 510 (13,3%)*
Carrel and Willard, 2005	somatic cell hybrids	9 hybrid cell lines	94 of 612 (15,1%)	60 of 612 (9,8%)
Carrel and Willard, 2005	primary fibroblast cell lines	40 fibroblast cell lines	15%	20%
Zhang, 2013	LCL from CEU HapMap, LCL from YRI HapMap	37 CEU, 40 YRI	not reported	114 of 706 (16,1%)

* Cotton and colleagues used a threshold to qualify as an XCI escaping gene where a gene should escape in 78% of individuals

gene that normally escapes XCI on different parts of the X chromosome. The generated transgenes maintained the XCI status of their original locus (Li and Carrel, 2008). Although the specific sequence and the mechanism by which *Jarid1C* escapes inactivation in a position-independent manner remains to be elucidated, but might involve recruitment of CTCF. It is also tempting to speculate that a similar mechanism might be involved in the expression of isolated single escapees on the human X chromosome.

Although one might expect XCI escaping genes to be expressed at a level comparable to their homologs located on Xa, this is surely not the case. The highest expression is found for the genes located in the human PAR1, and is at maximum 73% of the expression of their Xa homologs (Cotton et al., 2013; Zhang et al., 2013b). The expression of human escapees located outside the PAR is highly variable, and a continuum of expression is observed ranging from 10% to 73% of the levels of their Xa homologs. Genes that have a Y-chromosomal or autosomal homolog tend to have higher expression levels (Carrel and Willard, 2005; Cotton et al., 2013; Zhang et al., 2013b). Also in mouse, XCI escaping genes showed various levels of expression, with none reaching the level of their Xa homolog (Calabrese et al., 2012; Yang et al., 2010). The extent of escape is reflected by histone modifications H3K4me3, H3K27me3, H3K36me3, H3K27Ac, with stronger escaping genes showing less accumulation of inactive modifications (Cotton et al., 2013).

Human individual variation in escape from XCI

In human, escape from XCI is influenced by ethnic background for a subset of the genes that have been identified to escape. Two independent studies found differential escape between HapMap individuals with a central European (CEU) and Yoruban (YRI) background (Cotton et al., 2013; Zhang et al., 2013b). This ethnicity specific escape is further supported by comparing male to female expression levels, assuming that escaping genes will be higher expressed in females (Johnston et al., 2008). In mouse, a similar phenomenon might exist with strain specific escape. So far, this has only been demonstrated for mouse TS cells where 8 to 11 (22.9% - 31.4%) of the 35 escapers in 262 analyzed genes shows strain specific escape (Calabrese et al., 2012). If mouse somatic tissues also show strain specific escape from XCI has not been investigated yet.

Apart from ethnicity specific escape, some genes seem to exhibit tissue specific escape. Although a direct comparison of RNA-seq profiles from different tissues has not yet been performed, cell lines derived from different tissues can be compared between studies that analyzed escape from XCI. In mouse, the studied cell lines showed a significant overlap, but also displayed differences in escaping genes. These differences could be the result of differential escape between tissues, but might also be the result of technical differences between the studies. In humans, a subset of genes also seems to escape from XCI in a tissue

specific manner. Comparing lymphocyte and fibroblast derived cell lines, 35 genes (8.5%) of the analyzed 409 genes showed differential escape from XCI (Cotton et al., 2013). This differential escape is supported by studies analyzing epigenetic modifications to predict escape status. Using DNA methylation to predict XCI status for fetal muscle, kidney, brain and spinal cord 12% of the analyzed genes was found to have tissue specific escape (Cotton et al., 2011). This indicates that escape is likely tissue specific for a subset of genes.

Aim and scope of this thesis

As a result of genetic sex-determination there is a genetic imbalance for X-encoded genes between males and females. To compensate for this difference in X chromosomal gene dosage one of the two X chromosomes in every female cell is inactivated in a process called X chromosome inactivation (XCI). As a result of XCI every female individual is a mosaic of cells with an inactive paternal X chromosome or an inactive maternal X chromosome. The aim of this thesis was to further unravel the molecular mechanisms that regulate XCI and extend this knowledge to human XCI.

At the start of this thesis the stochastic model for XCI had only just been formulated. The model states that every X chromosome in a nucleus has an intrinsic probability to inactivate, which results in random X chromosome inactivation. The existence of an X-encoded *trans*-acting activator of XCI is hypothesized, but *Rnf12* has not yet been identified as such.

In [chapter 2](#) evidence is presented that supports a stochastic model for XCI. We describe the generation and analysis of triploid XXY ES cells, that have an X:autosome ratio of 2:3. The concentration of *trans*-acting activator only marginally exceeds the threshold for XCI in these cells. Computer simulation is used to show that experimental data indeed fit with a stochastic model. These simulations confirm that stochastic XCI can be determined by the sensitivity of an X chromosome for an activating stimulus and the concentration of XCI activator.

After the identification of *Rnf12* as a *trans*-acting activator of XCI, which further validated the stochastic model, the mouse *Xic* is proposed to contain a *cis*-acting part and a *trans*-acting part. In [chapter 3](#) XCI is analyzed in a female carrying a heterozygous deletion of the XIC region, demonstrating that also the human XIC can be divided in a *cis*-XIC and a *trans*-XIC. We fine-map this deletion to single nucleotide level, and redefine the maximum region that is the human *cis*-XIC. In perspective of previous X-chromosomal aberrations we define the region containing the human *trans*-acting activator to a part of the X chromosome involving *RNF12*.

In [chapter 4](#) evidence is presented that human *RNF12* functions as a *trans*-acting activator of human XCI, in a manner similar to mouse *Rnf12*. We describe three families carrying different mutations in *RNF12*. In *in vitro* studies with these *RNF12* mutants one proves to be a hypermorph, while the other two mutations are hypomorphs. Despite their opposite functional effects our results suggest that both gain and loss of RNF12 function results in delayed and skewed XCI with preferential inactivation of the mutant allele. Furthermore, our results suggest that initiation of XCI is more strictly titrated in human compared to mouse.

In [chapter 5](#) we analyze the variation of XCI between different tissues. The ratio between inactive paternal X chromosomes and inactive maternal X chromosomes can vary

considerably between tissues within an individual. These analyses indicate that while blood is most often used to determine the X-inactivation ratio, buccal swab is a better alternative. In addition, the X-inactivation ratio of ovarian stroma shows a unique association with hair follicles.

In [chapter 6](#) we analyze the potential of the iPS reprogramming technique to produce iPS cells with two active X chromosomes. Using standard reprogramming culture conditions, X chromosome reactivation is achieved but not maintained, as some cells re-initiate XCI. Using naïve human stem cell medium this continuous process of reactivation and re-initiation is stabilized, allowing expansion of clones with two active X chromosomes.

References

- Alen, P., Claessens, F., Verhoeven, G., Rombauts, W., and Peeters, B. (1999). The androgen receptor amino-terminal domain plays a key role in p160 coactivator-stimulated gene transcription. *Mol Cell Biol* 19, 6085-6097.
- Allderdice, P.W., Miller, O.J., Miller, D.A., and Klinger, H.P. (1978). Spreading of inactivation in an (X;14) translocation. *Am J Med Genet* 2, 233-240.
- Amenduni, M., De Filippis, R., Cheung, A.Y., Disciglio, V., Epistolato, M.C., Ariani, F., Mari, F., Mencarelli, M.A., Hayek, Y., Renieri, A., *et al.* (2011). iPS cells to model CDKL5-related disorders. *Eur J Hum Genet* 19, 1246-1255.
- Amir, R.E., Van den Veyver, I.B., Wan, M., Tran, C.Q., Francke, U., and Zoghbi, H.Y. (1999). Rett syndrome is caused by mutations in X-linked MECP2, encoding methyl-CpG-binding protein 2. *Nat Genet* 23, 185-188.
- Amos-Landgraf, J.M., Cottle, A., Plenge, R.M., Friez, M., Schwartz, C.E., Longshore, J., and Willard, H.F. (2006). X chromosome-inactivation patterns of 1,005 phenotypically unaffected females. *Am J Hum Genet* 79, 493-499.
- Ananiev, G., Williams, E.C., Li, H., and Chang, Q. (2011). Isogenic pairs of wild type and mutant induced pluripotent stem cell (iPSC) lines from Rett syndrome patients as in vitro disease model. *PLoS One* 6, e25255.
- Anguera, M.C., Ma, W., Clift, D., Namekawa, S., Kelleher, R.J., 3rd, and Lee, J.T. (2011). Tsx produces a long noncoding RNA and has general functions in the germline, stem cells, and brain. *PLoS Genet* 7, e1002248.
- Archer, H., Evans, J., Leonard, H., Colvin, L., Ravine, D., Christodoulou, J., Williamson, S., Charman, T., Bailey, M.E., Sampson, J., *et al.* (2007). Correlation between clinical severity in patients with Rett syndrome with a p.R168X or p.T158M MECP2 mutation, and the direction and degree of skewing of X-chromosome inactivation. *J Med Genet* 44, 148-152.
- Augui, S., Filion, G.J., Huart, S., Nora, E., Guggiari, M., Maresca, M., Stewart, A.F., and Heard, E. (2007). Sensing X chromosome pairs before X inactivation via a novel X-pairing region of the Xic. *Science* 318, 1632-1636.
- Azziz, R., Carmina, E., Dewailly, D., Diamanti-Kandarakis, E., Escobar-Morreale, H.F., Futterweit, W., Janssen, O.E., Legro, R.S., Norman, R.J., Taylor, A.E., *et al.* (2006). Positions statement: criteria for defining polycystic ovary syndrome as a predominantly hyperandrogenic syndrome: an Androgen Excess Society guideline. *J Clin Endocrinol Metab* 91, 4237-4245.
- Azziz, R., Carmina, E., Dewailly, D., Diamanti-Kandarakis, E., Escobar-Morreale, H.F., Futterweit, W., Janssen, O.E., Legro, R.S., Norman, R.J., Taylor, A.E., *et al.* (2009). The Androgen Excess and PCOS Society criteria for the polycystic ovary syndrome: the complete task force report. *Fertil Steril* 91, 456-488.
- Azziz, R., Woods, K.S., Reyna, R., Key, T.J., Knochenhauer, E.S., and Yildiz, B.O. (2004). The prevalence and features of the polycystic ovary syndrome in an unselected population. *J Clin Endocrinol Metab* 89, 2745-2749.

- Bach, I. (2000). The LIM domain: regulation by association. *Mech Dev* 91, 5-17.
- Bach, I., Rodriguez-Esteban, C., Carriere, C., Bhushan, A., Krones, A., Rose, D.W., Glass, C.K., Andersen, B., Izpisua Belmonte, J.C., and Rosenfeld, M.G. (1999). RLIM inhibits functional activity of LIM homeodomain transcription factors via recruitment of the histone deacetylase complex. *Nat Genet* 22, 394-399.
- Bacher, C.P., Guggiari, M., Brors, B., Augui, S., Clerc, P., Avner, P., Eils, R., and Heard, E. (2006). Transient colocalization of X-inactivation centres accompanies the initiation of X inactivation. *Nat Cell Biol* 8, 293-299.
- Bachtrog, D. (2013). Y-chromosome evolution: emerging insights into processes of Y-chromosome degeneration. *Nat Rev Genet* 14, 113-124.
- Bailey, J.A., Carrel, L., Chakravarti, A., and Eichler, E.E. (2000). Molecular evidence for a relationship between LINE-1 elements and X chromosome inactivation: the Lyon repeat hypothesis. *Proc Natl Acad Sci U S A* 97, 6634-6639.
- Barakat, T.S., Gunhanlar, N., Pardo, C.G., Achame, E.M., Ghazvini, M., Boers, R., Kenter, A., Rentmeester, E., Grootegoed, J.A., and Gribnau, J. (2011). RNF12 activates Xist and is essential for X chromosome inactivation. *PLoS Genet* 7, e1002001.
- Barakat, T.S., Loos, F., van Staveren, S., Myronova, E., Ghazvini, M., Grootegoed, J.A., and Gribnau, J. (2014). The trans-activator RNF12 and cis-acting elements effectuate X chromosome inactivation independent of X-pairing. *Mol Cell* 53, 965-978.
- Beilin, J., Ball, E.M., Favaloro, J.M., and Zajac, J.D. (2000). Effect of the androgen receptor CAG repeat polymorphism on transcriptional activity: specificity in prostate and non-prostate cell lines. *J Mol Endocrinol* 25, 85-96.
- Belmont, L., Mitchison, T., and Deacon, H.W. (1996). Catastrophic revelations about Op18/stathmin. *Trends Biochem Sci* 21, 197-198.
- Bhatnagar, S., Zhu, X., Ou, J., Lin, L., Chamberlain, L., Zhu, L.J., Wajapeyee, N., and Green, M.R. (2014). Genetic and pharmacological reactivation of the mammalian inactive X chromosome. *Proc Natl Acad Sci U S A* 111, 12591-12598.
- Boland, M.J., Hazen, J.L., Nazor, K.L., Rodriguez, A.R., Gifford, W., Martin, G., Kupriyanov, S., and Baldwin, K.K. (2009). Adult mice generated from induced pluripotent stem cells. *Nature* 461, 91-94.
- Bolduc, V., Chagnon, P., Provost, S., Dube, M.P., Belisle, C., Gingras, M., Mollica, L., and Busque, L. (2008). No evidence that skewing of X chromosome inactivation patterns is transmitted to offspring in humans. *J Clin Invest* 118, 333-341.
- Branco, M.R., and Pombo, A. (2006). Intermingling of chromosome territories in interphase suggests role in translocations and transcription-dependent associations. *PLoS Biol* 4, e138.
- Brockdorff, N., Ashworth, A., Kay, G.F., McCabe, V.M., Norris, D.P., Cooper, P.J., Swift, S., and Rastan, S. (1992). The product of the mouse Xist gene is a 15 kb inactive X-specific transcript containing no conserved ORF and located in the nucleus. *Cell* 71, 515-526.

- Brockschmidt, F.F., Nothen, M.M., and Hillmer, A.M. (2007). The two most common alleles of the coding GGN repeat in the androgen receptor gene cause differences in protein function. *J Mol Endocrinol* 39, 1-8.
- Brons, I.G., Smithers, L.E., Trotter, M.W., Rugg-Gunn, P., Sun, B., Chuva de Sousa Lopes, S.M., Howlett, S.K., Clarkson, A., Ahrlund-Richter, L., Pedersen, R.A., *et al.* (2007). Derivation of pluripotent epiblast stem cells from mammalian embryos. *Nature* 448, 191-195.
- Brook, F.A., and Gardner, R.L. (1997). The origin and efficient derivation of embryonic stem cells in the mouse. *Proc Natl Acad Sci U S A* 94, 5709-5712.
- Brown, C.J., Ballabio, A., Rupert, J.L., Lafreniere, R.G., Grompe, M., Tonlorenzi, R., and Willard, H.F. (1991a). A gene from the region of the human X inactivation centre is expressed exclusively from the inactive X chromosome. *Nature* 349, 38-44.
- Brown, C.J., Hendrich, B.D., Rupert, J.L., Lafreniere, R.G., Xing, Y., Lawrence, J., and Willard, H.F. (1992). The human XIST gene: analysis of a 17 kb inactive X-specific RNA that contains conserved repeats and is highly localized within the nucleus. *Cell* 71, 527-542.
- Brown, C.J., Lafreniere, R.G., Powers, V.E., Sebastio, G., Ballabio, A., Pettigrew, A.L., Ledbetter, D.H., Levy, E., Craig, I.W., and Willard, H.F. (1991b). Localization of the X inactivation centre on the human X chromosome in Xq13. *Nature* 349, 82-84.
- Brown, C.J., Miller, A.P., Carrel, L., Rupert, J.L., Davies, K.E., and Willard, H.F. (1995). The DXS423E gene in Xp11.21 escapes X chromosome inactivation. *Hum Mol Genet* 4, 251-255.
- Brown, C.J., and Willard, H.F. (1994). The human X-inactivation centre is not required for maintenance of X-chromosome inactivation. *Nature* 368, 154-156.
- Bruck, T., and Benvenisty, N. (2011). Meta-analysis of the heterogeneity of X chromosome inactivation in human pluripotent stem cells. *Stem Cell Res* 6, 187-193.
- Burd, C.J., Petre, C.E., Moghadam, H., Wilson, E.M., and Knudsen, K.E. (2005). Cyclin D1 binding to the androgen receptor (AR) NH2-terminal domain inhibits activation function 2 association and reveals dual roles for AR corepression. *Mol Endocrinol* 19, 607-620.
- Busque, L., Mio, R., Mattioli, J., Brais, E., Blais, N., Lalonde, Y., Maragh, M., and Gilliland, D.G. (1996). Nonrandom X-inactivation patterns in normal females: lyonization ratios vary with age. *Blood* 88, 59-65.
- Calabrese, J.M., Sun, W., Song, L., Mugford, J.W., Williams, L., Yee, D., Starmer, J., Mieczkowski, P., Crawford, G.E., and Magnuson, T. (2012). Site-specific silencing of regulatory elements as a mechanism of X inactivation. *Cell* 151, 951-963.
- Calaway, J.D., Lenarcic, A.B., Didion, J.P., Wang, J.R., Searle, J.B., McMillan, L., Valdar, W., and Pardo-Manuel de Villena, F. (2013). Genetic architecture of skewed X inactivation in the laboratory mouse. *PLoS Genet* 9, e1003853.
- Cantrell, M.A., Carstens, B.C., and Wichman, H.A. (2009). X chromosome inactivation and Xist evolution in a rodent lacking LINE-1 activity. *PLoS One* 4, e6252.
- Caparros, M.L., Alexiou, M., Webster, Z., and Brockdorff, N. (2002). Functional analysis of the highly conserved exon IV of XIST RNA. *Cytogenet Genome Res* 99, 99-105.

- Carmi, I., Kopczynski, J.B., and Meyer, B.J. (1998). The nuclear hormone receptor SEX-1 is an X-chromosome signal that determines nematode sex. *Nature* 396, 168-173.
- Carr, D.H. (1970). Chromosome studies in selected spontaneous abortions. 1. Conception after oral contraceptives. *Can Med Assoc J* 103, 343-348.
- Carrel, L., and Willard, H.F. (1999). Heterogeneous gene expression from the inactive X chromosome: an X-linked gene that escapes X inactivation in some human cell lines but is inactivated in others. *Proc Natl Acad Sci U S A* 96, 7364-7369.
- Carrel, L., and Willard, H.F. (2005). X-inactivation profile reveals extensive variability in X-linked gene expression in females. *Nature* 434, 400-404.
- Cattanach, B. (1991). Identification of the *Mus spretus* Xce allele. *Mouse Genome* 89, 565-566.
- Cattanach, B. (1994). Identification of the *Mus castaneus* Xce allele. *Mouse Genome*, 114.
- Cattanach, B.M. (1975). Control of chromosome inactivation. *Annu Rev Genet* 9, 1-18.
- Cattanach, B.M., and Isaacson, J.H. (1967). Controlling elements in the mouse X chromosome. *Genetics* 57, 331-346.
- Cattanach, B.M., Pollard, C.E., and Perez, J.N. (1969). Controlling elements in the mouse X-chromosome. I. Interaction with the X-linked genes. *Genet Res* 14, 223-235.
- Cattanach, B.M., and Williams, C.E. (1972). Evidence of non-random X chromosome activity in the mouse. *Genet Res* 19, 229-240.
- Cerase, A., Smeets, D., Tang, Y.A., Gdula, M., Kraus, F., Spivakov, M., Moindrot, B., Leleu, M., Tattermusch, A., Demmerle, J., *et al.* (2014). Spatial separation of Xist RNA and polycomb proteins revealed by superresolution microscopy. *Proc Natl Acad Sci U S A* 111, 2235-2240.
- Chabchoub, G., Uz, E., Maalej, A., Mustafa, C.A., Rebai, A., Mnif, M., Bahloul, Z., Farid, N.R., Ozcelik, T., and Ayadi, H. (2009). Analysis of skewed X-chromosome inactivation in females with rheumatoid arthritis and autoimmune thyroid diseases. *Arthritis Res Ther* 11, R106.
- Chadwick, B.P., and Willard, H.F. (2003). Barrng gene expression after XIST: maintaining facultative heterochromatin on the inactive X. *Semin Cell Dev Biol* 14, 359-367.
- Chadwick, L.H., Pertz, L.M., Broman, K.W., Bartolomei, M.S., and Willard, H.F. (2006). Genetic control of X chromosome inactivation in mice: definition of the Xce candidate interval. *Genetics* 173, 2103-2110.
- Chadwick, L.H., and Willard, H.F. (2005). Genetic and parent-of-origin influences on X chromosome choice in Xce heterozygous mice. *Mamm Genome* 16, 691-699.
- Chamberlain, N.L., Driver, E.D., and Miesfeld, R.L. (1994). The length and location of CAG trinucleotide repeats in the androgen receptor N-terminal domain affect transactivation function. *Nucleic Acids Res* 22, 3181-3186.
- Chang, D., Gao, F., Slavney, A., Ma, L., Waldman, Y.Y., Sams, A.J., Billing-Ross, P., Madar, A., Spritz, R., and Keinan, A. (2014). Accounting for eXentricities: analysis of the X chromosome in GWAS reveals X-linked genes implicated in autoimmune diseases. *PLoS One* 9, e113684.

- Chaumeil, J., Le Baccon, P., Wutz, A., and Heard, E. (2006). A novel role for Xist RNA in the formation of a repressive nuclear compartment into which genes are recruited when silenced. *Genes Dev* 20, 2223-2237.
- Chaumeil, J., Okamoto, I., Guggiari, M., and Heard, E. (2002). Integrated kinetics of X chromosome inactivation in differentiating embryonic stem cells. *Cytogenet Genome Res* 99, 75-84.
- Chen, X., Shen, J., Li, X., Wang, X., Long, M., Lin, F., Wei, J., Yang, L., Yang, C., Dong, K., *et al.* (2014). Rlim, an E3 ubiquitin ligase, influences the stability of Stathmin protein in human osteosarcoma cells. *Cell Signal* 26, 1532-1538.
- Cheung, A.Y., Horvath, L.M., Grafodatskaya, D., Pasceri, P., Weksberg, R., Hotta, A., Carrel, L., and Ellis, J. (2011). Isolation of MECP2-null Rett Syndrome patient hiPS cells and isogenic controls through X-chromosome inactivation. *Hum Mol Genet* 20, 2103-2115.
- Chiba, H., Hirasawa, R., Kaneda, M., Amakawa, Y., Li, E., Sado, T., and Sasaki, H. (2008). De novo DNA methylation independent establishment of maternal imprint on X chromosome in mouse oocytes. *Genesis* 46, 768-774.
- Chow, J.C., Hall, L.L., Baldry, S.E., Thorogood, N.P., Lawrence, J.B., and Brown, C.J. (2007). Inducible XIST-dependent X-chromosome inactivation in human somatic cells is reversible. *Proc Natl Acad Sci U S A* 104, 10104-10109.
- Chow, J.C., Hall, L.L., Lawrence, J.B., and Brown, C.J. (2002). Ectopic XIST transcripts in human somatic cells show variable expression and localization. *Cytogenet Genome Res* 99, 92-98.
- Chu, X., Shen, M., Xie, F., Miao, X.J., Shou, W.H., Liu, L., Yang, P.P., Bai, Y.N., Zhang, K.Y., Yang, L., *et al.* (2013). An X chromosome-wide association analysis identifies variants in GPR174 as a risk factor for Graves' disease. *J Med Genet* 50, 479-485.
- Chureau, C., Chantalat, S., Romito, A., Galvani, A., Duret, L., Avner, P., and Rougeulle, C. (2011). Ftx is a non-coding RNA which affects Xist expression and chromatin structure within the X-inactivation center region. *Hum Mol Genet* 20, 705-718.
- Chureau, C., Prissette, M., Bourdet, A., Barbe, V., Cattolico, L., Jones, L., Eggen, A., Avner, P., and Duret, L. (2002). Comparative sequence analysis of the X-inactivation center region in mouse, human, and bovine. *Genome Res* 12, 894-908.
- Clemson, C.M., Hall, L.L., Byron, M., McNeil, J., and Lawrence, J.B. (2006). The X chromosome is organized into a gene-rich outer rim and an internal core containing silenced nongenic sequences. *Proc Natl Acad Sci U S A* 103, 7688-7693.
- Clerc, P., and Avner, P. (1998). Role of the region 3' to Xist exon 6 in the counting process of X-chromosome inactivation. *Nat Genet* 19, 249-253.
- Cline, T.W. (1983). The interaction between daughterless and sex-lethal in triploids: a lethal sex-transforming maternal effect linking sex determination and dosage compensation in *Drosophila melanogaster*. *Dev Biol* 95, 260-274.
- Costanzi, C., and Pehrson, J.R. (1998). Histone macroH2A1 is concentrated in the inactive X chromosome of female mammals. *Nature* 393, 599-601.

- Cotton, A.M., Ge, B., Light, N., Adoue, V., Pastinen, T., and Brown, C.J. (2013). Analysis of expressed SNPs identifies variable extents of expression from the human inactive X chromosome. *Genome Biol* 14, R122.
- Cotton, A.M., Lam, L., Affleck, J.G., Wilson, I.M., Penaherrera, M.S., McFadden, D.E., Kobor, M.S., Lam, W.L., Robinson, W.P., and Brown, C.J. (2011). Chromosome-wide DNA methylation analysis predicts human tissue-specific X inactivation. *Hum Genet* 130, 187-201.
- Cremer, T., and Cremer, M. (2010). Chromosome territories. *Cold Spring Harb Perspect Biol* 2, a003889.
- Csankovszki, G., Panning, B., Bates, B., Pehrson, J.R., and Jaenisch, R. (1999). Conditional deletion of Xist disrupts histone macroH2A localization but not maintenance of X inactivation. *Nat Genet* 22, 323-324.
- Cunningham, D.B., Segretain, D., Arnaud, D., Rogner, U.C., and Avner, P. (1998). The mouse Tsx gene is expressed in Sertoli cells of the adult testis and transiently in premeiotic germ cells during puberty. *Dev Biol* 204, 345-360.
- Curmi, P.A., Andersen, S.S., Lachkar, S., Gavet, O., Karsenti, E., Knossow, M., and Sobel, A. (1997). The stathmin/tubulin interaction in vitro. *J Biol Chem* 272, 25029-25036.
- Dasgupta, S., Sirisha, P.V., Neelaveni, K., Anuradha, K., Reddy, A.G., Thangaraj, K., and Reddy, B.M. (2010). Androgen receptor CAG repeat polymorphism and epigenetic influence among the south Indian women with Polycystic Ovary Syndrome. *PLoS One* 5, e12401.
- de Napoles, M., Mermoud, J.E., Wakao, R., Tang, Y.A., Endoh, M., Appanah, R., Nesterova, T.B., Silva, J., Otte, A.P., Vidal, M., *et al.* (2004). Polycomb group proteins Ring1A/B link ubiquitylation of histone H2A to heritable gene silencing and X inactivation. *Dev Cell* 7, 663-676.
- Derenzini, M., Olins, A.L., and Olins, D.E. (2014). Chromatin structure in situ: the contribution of DNA ultrastructural cytochemistry. *Eur J Histochem* 58, 2307.
- Ding, D., Xu, L., Menon, M., Reddy, G.P., and Barrack, E.R. (2005). Effect of GGC (glycine) repeat length polymorphism in the human androgen receptor on androgen action. *Prostate* 62, 133-139.
- Dobson, A.T., Raja, R., Abeyta, M.J., Taylor, T., Shen, S., Haqq, C., and Pera, R.A. (2004). The unique transcriptome through day 3 of human preimplantation development. *Hum Mol Genet* 13, 1461-1470.
- Donohoe, M.E., Silva, S.S., Pinter, S.F., Xu, N., and Lee, J.T. (2009). The pluripotency factor Oct4 interacts with Ctf and also controls X-chromosome pairing and counting. *Nature* 460, 128-132.
- Duret, L., Chureau, C., Samain, S., Weissenbach, J., and Avner, P. (2006). The Xist RNA gene evolved in eutherians by pseudogenization of a protein-coding gene. *Science* 312, 1653-1655.
- Edwards, A., Hammond, H.A., Jin, L., Caskey, C.T., and Chakraborty, R. (1992). Genetic variation at five trimeric and tetrameric tandem repeat loci in four human population groups. *Genomics* 12, 241-253.
- El Kassar, N., Hetet, G., Briere, J., and Grandchamp, B. (1998). X-chromosome inactivation in healthy females: incidence of excessive lyonization with age and comparison of assays involving DNA methylation and transcript polymorphisms. *Clin Chem* 44, 61-67.
- Elisaphenko, E.A., Kolesnikov, N.N., Shevchenko, A.I., Rogozin, I.B., Nesterova, T.B., Brockdorff, N., and Zakian, S.M. (2008). A dual origin of the Xist gene from a protein-coding gene and a set of transposable elements. *PLoS One* 3, e2521.

- Ellegren, H. (2011). Sex-chromosome evolution: recent progress and the influence of male and female heterogamety. *Nat Rev Genet* 12, 157-166.
- Engreitz, J.M., Pandya-Jones, A., McDonel, P., Shishkin, A., Sirokman, K., Surka, C., Kadri, S., Xing, J., Goren, A., Lander, E.S., *et al.* (2013). The Xist lncRNA exploits three-dimensional genome architecture to spread across the X chromosome. *Science* 341, 1237973.
- Evans, M.J., and Kaufman, M.H. (1981). Establishment in culture of pluripotent cells from mouse embryos. *Nature* 292, 154-156.
- Fakan, S., and van Driel, R. (2007). The perichromatin region: a functional compartment in the nucleus that determines large-scale chromatin folding. *Semin Cell Dev Biol* 18, 676-681.
- Ferk, P., Perme, M.P., Teran, N., and Gersak, K. (2008). Androgen receptor gene (CAG)_n polymorphism in patients with polycystic ovary syndrome. *Fertil Steril* 90, 860-863.
- Fey, M.F., Liechti-Gallati, S., von Rohr, A., Borisch, B., Theilkas, L., Schneider, V., Oestreicher, M., Nagel, S., Ziemiecki, A., and Tobler, A. (1994). Clonality and X-inactivation patterns in hematopoietic cell populations detected by the highly informative M27 beta DNA probe. *Blood* 83, 931-938.
- Forrester, L.M., and Ansell, J.D. (1985). Parental influences on X chromosome expression. *Genet Res* 45, 95-100.
- Fowles, D.J., Ansell, J.D., and Micklem, H.S. (1991). Further evidence for the importance of parental source of the Xce allele in X chromosome inactivation. *Genet Res* 58, 63-65.
- Fryns, J.P., and Van den Berghe, H. (1988). Inactivation pattern of the fragile X in heterozygous carriers. *Am J Med Genet* 30, 401-406.
- Fukuda, A., Tomikawa, J., Miura, T., Hata, K., Nakabayashi, K., Eggen, K., Akutsu, H., and Umezawa, A. (2014). The role of maternal-specific H3K9me3 modification in establishing imprinted X-chromosome inactivation and embryogenesis in mice. *Nat Commun* 5, 5464.
- Gafni, O., Weinberger, L., Mansour, A.A., Manor, Y.S., Chomsky, E., Ben-Yosef, D., Kalma, Y., Viukov, S., Maza, I., Zviran, A., *et al.* (2013). Derivation of novel human ground state naive pluripotent stem cells. *Nature* 504, 282-286.
- Gartler, S.M., and Riggs, A.D. (1983). Mammalian X-chromosome inactivation. *Annu Rev Genet* 17, 155-190.
- Giorgetti, L., Galupa, R., Nora, E.P., Piolot, T., Lam, F., Dekker, J., Tiana, G., and Heard, E. (2014). Predictive polymer modeling reveals coupled fluctuations in chromosome conformation and transcription. *Cell* 157, 950-963.
- Gontan, C., Achame, E.M., Demmers, J., Barakat, T.S., Rentmeester, E., van, I.W., Grootegoed, J.A., and Gribnau, J. (2012). RNF12 initiates X-chromosome inactivation by targeting REX1 for degradation. *Nature* 485, 386-390.
- Goto, T., Wright, E., and Monk, M. (1997). Paternal X-chromosome inactivation in human trophoblastic cells. *Mol Hum Reprod* 3, 77-80.

Greenfield, A., Carrel, L., Pennisi, D., Philippe, C., Quaderi, N., Siggers, P., Steiner, K., Tam, P.P., Monaco, A.P., Willard, H.F., *et al.* (1998). The UTX gene escapes X inactivation in mice and humans. *Hum Mol Genet* 7, 737-742.

Gribnau, J., and Grootegeod, J.A. (2012). Origin and evolution of X chromosome inactivation. *Curr Opin Cell Biol* 24, 397-404.

Grumbach, M.M., Morishima, A., and Taylor, J.H. (1963). Human Sex Chromosome Abnormalities in Relation to DNA Replication and Heterochromatinization. *Proc Natl Acad Sci U S A* 49, 581-589.

Hadjantonakis, A.K., Cox, L.L., Tam, P.P., and Nagy, A. (2001). An X-linked GFP transgene reveals unexpected paternal X-chromosome activity in trophoblastic giant cells of the mouse placenta. *Genesis* 29, 133-140.

Hall, L.L., Clemson, C.M., Byron, M., Wydner, K., and Lawrence, J.B. (2002). Unbalanced X;autosome translocations provide evidence for sequence specificity in the association of XIST RNA with chromatin. *Hum Mol Genet* 11, 3157-3165.

Hanna, J., Cheng, A.W., Saha, K., Kim, J., Lengner, C.J., Soldner, F., Cassady, J.P., Muffat, J., Carey, B.W., and Jaenisch, R. (2010). Human embryonic stem cells with biological and epigenetic characteristics similar to those of mouse ESCs. *Proc Natl Acad Sci U S A* 107, 9222-9227.

Harrison, K.B. (1989). X-chromosome inactivation in the human cytotrophoblast. *Cytogenet Cell Genet* 52, 37-41.

Harrison, K.B., and Warburton, D. (1986). Preferential X-chromosome activity in human female placental tissues. *Cytogenet Cell Genet* 41, 163-168.

Hasegawa, Y., Brockdorff, N., Kawano, S., Tsutui, K., Tsutui, K., and Nakagawa, S. (2010). The matrix protein hnRNP U is required for chromosomal localization of Xist RNA. *Dev Cell* 19, 469-476.

Hatakeyama, C., Anderson, C.L., Beever, C.L., Penaherrera, M.S., Brown, C.J., and Robinson, W.P. (2004). The dynamics of X-inactivation skewing as women age. *Clin Genet* 66, 327-332.

Heard, E., Rougeulle, C., Arnaud, D., Avner, P., Allis, C.D., and Spector, D.L. (2001). Methylation of histone H3 at Lys-9 is an early mark on the X chromosome during X inactivation. *Cell* 107, 727-738.

Heine-Suner, D., Torres-Juan, L., Morla, M., Busquets, X., Barcelo, F., Pico, G., Bonilla, L., Govea, N., Bernues, M., and Rosell, J. (2003). Fragile-X syndrome and skewed X-chromosome inactivation within a family: a female member with complete inactivation of the functional X chromosome. *Am J Med Genet A* 122A, 108-114.

Hendrich, B.D., Brown, C.J., and Willard, H.F. (1993). Evolutionary conservation of possible functional domains of the human and murine XIST genes. *Hum Mol Genet* 2, 663-672.

Hendrich, B.D., Plenge, R.M., and Willard, H.F. (1997). Identification and characterization of the human XIST gene promoter: implications for models of X chromosome inactivation. *Nucleic Acids Res* 25, 2661-2671.

Her, Y.R., and Chung, I.K. (2009). Ubiquitin Ligase RLIM Modulates Telomere Length Homeostasis through a Proteolysis of TRF1. *J Biol Chem* 284, 8557-8566.

- Hernandez-Munoz, I., Lund, A.H., van der Stoop, P., Boutsma, E., Muijters, I., Verhoeven, E., Nusinow, D.A., Panning, B., Marahrens, Y., and van Lohuizen, M. (2005). Stable X chromosome inactivation involves the PRC1 Polycomb complex and requires histone MACROH2A1 and the CULLIN3/SPOP ubiquitin E3 ligase. *Proc Natl Acad Sci U S A* 102, 7635-7640.
- Holstege, H., Pfeiffer, W., Sie, D., Hulsman, M., Nicholas, T.J., Lee, C.C., Ross, T., Lin, J., Miller, M.A., Ylstra, B., *et al.* (2014). Somatic mutations found in the healthy blood compartment of a 115-yr-old woman demonstrate oligoclonal hematopoiesis. *Genome Res* 24, 733-742.
- Hong, Y.K., Ontiveros, S.D., Chen, C., and Strauss, W.M. (1999). A new structure for the murine Xist gene and its relationship to chromosome choice/counting during X-chromosome inactivation. *Proc Natl Acad Sci U S A* 96, 6829-6834.
- Hong, Y.K., Ontiveros, S.D., and Strauss, W.M. (2000). A revision of the human XIST gene organization and structural comparison with mouse Xist. *Mamm Genome* 11, 220-224.
- Howard, P.W., Jue, S.F., Ransom, D.G., and Maurer, R.A. (2010). Regulation of LIM-domain-binding 1 protein expression by ubiquitination of Lys134. *Biochem J* 429, 127-136.
- Huang, K., Maruyama, T., and Fan, G. (2014). The naive state of human pluripotent stem cells: a synthesis of stem cell and preimplantation embryo transcriptome analyses. *Cell Stem Cell* 15, 410-415.
- Huang, Y., Yang, Y., Gao, R., Yang, X., Yan, X., Wang, C., Jiang, S., and Yu, L. (2011). RLIM interacts with Smurf2 and promotes TGF-beta induced U2OS cell migration. *Biochem Biophys Res Commun* 414, 181-185.
- Huppke, P., Maier, E.M., Warnke, A., Brendel, C., Laccone, F., and Gartner, J. (2006). Very mild cases of Rett syndrome with skewed X inactivation. *J Med Genet* 43, 814-816.
- Huynh, K.D., and Lee, J.T. (2003). Inheritance of a pre-inactivated paternal X chromosome in early mouse embryos. *Nature* 426, 857-862.
- Ibanez, L., Ong, K.K., Mongan, N., Jaaskelainen, J., Marcos, M.V., Hughes, I.A., De Zegher, F., and Dunger, D.B. (2003). Androgen receptor gene CAG repeat polymorphism in the development of ovarian hyperandrogenism. *J Clin Endocrinol Metab* 88, 3333-3338.
- Irvine, R.A., Yu, M.C., Ross, R.K., and Coetzee, G.A. (1995). The CAG and GGC microsatellites of the androgen receptor gene are in linkage disequilibrium in men with prostate cancer. *Cancer Res* 55, 1937-1940.
- Jacobs, P.A., Baikie, A.G., Brown, W.M., Macgregor, T.N., Maclean, N., and Harnden, D.G. (1959). Evidence for the existence of the human "super female". *Lancet* 2, 423-425.
- Jeppesen, P., and Turner, B.M. (1993). The inactive X chromosome in female mammals is distinguished by a lack of histone H4 acetylation, a cytogenetic marker for gene expression. *Cell* 74, 281-289.
- Jiang, J., Jing, Y., Cost, G.J., Chiang, J.C., Kolpa, H.J., Cotton, A.M., Carone, D.M., Carone, B.R., Shivak, D.A., Guschin, D.Y., *et al.* (2013). Translating dosage compensation to trisomy 21. *Nature* 500, 296-300.

- Johnsen, S.A., Gungor, C., Prenzel, T., Riethdorf, S., Riethdorf, L., Taniguchi-Ishigaki, N., Rau, T., Tursun, B., Furlow, J.D., Sauter, G., *et al.* (2009). Regulation of estrogen-dependent transcription by the LIM cofactors CLIM and RLIM in breast cancer. *Cancer Res* 69, 128-136.
- Johnston, C.M., Lovell, F.L., Leongamornlert, D.A., Stranger, B.E., Dermitzakis, E.T., and Ross, M.T. (2008). Large-scale population study of human cell lines indicates that dosage compensation is virtually complete. *PLoS Genet* 4, e9.
- Johnston, C.M., Newall, A.E., Brockdorff, N., and Nesterova, T.B. (2002). Enox, a novel gene that maps 10 kb upstream of Xist and partially escapes X inactivation. *Genomics* 80, 236-244.
- Jonkers, I., Barakat, T.S., Achame, E.M., Monkhorst, K., Kenter, A., Rentmeester, E., Grosveld, F., Grootegeed, J.A., and Gribnau, J. (2009). RNF12 is an X-Encoded dose-dependent activator of X chromosome inactivation. *Cell* 139, 999-1011.
- Jonkers, I., Monkhorst, K., Rentmeester, E., Grootegeed, J.A., Grosveld, F., and Gribnau, J. (2008). Xist RNA is confined to the nuclear territory of the silenced X chromosome throughout the cell cycle. *Mol Cell Biol* 28, 5583-5594.
- Kalantry, S., Purushothaman, S., Bowen, R.B., Starmer, J., and Magnuson, T. (2009). Evidence of Xist RNA-independent initiation of mouse imprinted X-chromosome inactivation. *Nature* 460, 647-651.
- Kanellopoulou, C., Muljo, S.A., Dimitrov, S.D., Chen, X., Colin, C., Plath, K., and Livingston, D.M. (2009). X chromosome inactivation in the absence of Dicer. *Proc Natl Acad Sci U S A* 106, 1122-1127.
- Kato, T., Miyata, K., Sonobe, M., Yamashita, S., Tamano, M., Miura, K., Kanai, Y., Miyamoto, S., Sakuma, T., Yamamoto, T., *et al.* (2013). Production of Sry knockout mouse using TALEN via oocyte injection. *Sci Rep* 3, 3136.
- Kay, G.F., Barton, S.C., Surani, M.A., and Rastan, S. (1994). Imprinting and X chromosome counting mechanisms determine Xist expression in early mouse development. *Cell* 77, 639-650.
- Keitges, E., and Gartler, S.M. (1986). Dosage of the Sts gene in the mouse. *Am J Hum Genet* 39, 470-476.
- Kim, J.J., Choung, S.H., Choi, Y.M., Yoon, S.H., Kim, S.H., and Moon, S.Y. (2008). Androgen receptor gene CAG repeat polymorphism in women with polycystic ovary syndrome. *Fertil Steril* 90, 2318-2323.
- Kim, K.Y., Hysolli, E., and Park, I.H. (2011). Neuronal maturation defect in induced pluripotent stem cells from patients with Rett syndrome. *Proc Natl Acad Sci U S A* 108, 14169-14174.
- Klein, L., Klugmann, M., Nave, K.A., Tuohy, V.K., and Kyewski, B. (2000). Shaping of the autoreactive T-cell repertoire by a splice variant of self protein expressed in thymic epithelial cells. *Nat Med* 6, 56-61.
- Kovacs, D., Vassos, E., Liu, X., Sun, X., Hu, J., Breen, G., Tompa, P., Collier, D.A., and Li, T. (2009). The androgen receptor gene polyglycine repeat polymorphism is associated with memory performance in healthy Chinese individuals. *Psychoneuroendocrinology* 34, 947-952.
- Lahn, B.T., and Page, D.C. (1999). Four evolutionary strata on the human X chromosome. *Science* 286, 964-967.
- Latham, K.E., and Rambhatla, L. (1995). Expression of X-linked genes in androgenetic, gynogenetic, and normal mouse preimplantation embryos. *Dev Genet* 17, 212-222.

- Laufer, T.M., DeKoning, J., Markowitz, J.S., Lo, D., and Glimcher, L.H. (1996). Unopposed positive selection and autoreactivity in mice expressing class II MHC only on thymic cortex. *Nature* 383, 81-85.
- Lebon, J.M., Tam, P.P., Singer-Sam, J., Riggs, A.D., and Tan, S.S. (1995). Mouse endogenous X-linked genes do not show lineage-specific delayed inactivation during development. *Genet Res* 65, 223-227.
- Lee, J.T. (2005). Regulation of X-chromosome counting by Tsix and Xite sequences. *Science* 309, 768-771.
- Lee, J.T., Davidow, L.S., and Warshawsky, D. (1999). Tsix, a gene antisense to Xist at the X-inactivation centre. *Nat Genet* 21, 400-404.
- Lee, J.T., and Jaenisch, R. (1997). Long-range cis effects of ectopic X-inactivation centres on a mouse autosome. *Nature* 386, 275-279.
- Lee, J.T., and Lu, N. (1999). Targeted mutagenesis of Tsix leads to nonrandom X inactivation. *Cell* 99, 47-57.
- Lee, T.H., Perrem, K., Harper, J.W., Lu, K.P., and Zhou, X.Z. (2006). The F-box protein FBX4 targets PIN2/TRF1 for ubiquitin-mediated degradation and regulates telomere maintenance. *J Biol Chem* 281, 759-768.
- Lengner, C.J., Gimelbrant, A.A., Erwin, J.A., Cheng, A.W., Guenther, M.G., Welstead, G.G., Alagappan, R., Frampton, G.M., Xu, P., Muffat, J., *et al.* (2010). Derivation of pre-X inactivation human embryonic stem cells under physiological oxygen concentrations. *Cell* 141, 872-883.
- Leppig, K.A., Brown, C.J., Bressler, S.L., Gustashaw, K., Pagon, R.A., Willard, H.F., and Disteché, C.M. (1993). Mapping of the Distal Boundary of the X-Inactivation Center in a Rearranged X-Chromosome from a Female Expressing Xist. *Human Molecular Genetics* 2, 883-887.
- Li, L., Lee, J.Y., Gross, J., Song, S.H., Dean, A., and Love, P.E. (2010). A requirement for Lim domain binding protein 1 in erythropoiesis. *J Exp Med* 207, 2543-2550.
- Li, N., and Carrel, L. (2008). Escape from X chromosome inactivation is an intrinsic property of the Jarid1c locus. *Proc Natl Acad Sci U S A* 105, 17055-17060.
- Li, S.M., Valo, Z., Wang, J., Gao, H., Bowers, C.W., and Singer-Sam, J. (2012). Transcriptome-wide survey of mouse CNS-derived cells reveals monoallelic expression within novel gene families. *PLoS One* 7, e31751.
- Liu, Q., Hong, J., Cui, B., Zhang, Y., Gu, W., Chi, Z., Su, Y., and Ning, G. (2008). Androgen receptor gene CAG(n) trinucleotide repeats polymorphism in Chinese women with polycystic ovary syndrome. *Endocrine* 33, 165-170.
- Lock, L.F., Takagi, N., and Martin, G.R. (1987). Methylation of the Hprt gene on the inactive X occurs after chromosome inactivation. *Cell* 48, 39-46.
- Looijenga, L.H., Gillis, A.J., Verkerk, A.J., van Putten, W.L., and Oosterhuis, J.W. (1999). Heterogeneous X inactivation in trophoblastic cells of human full-term female placentas. *Am J Hum Genet* 64, 1445-1452.
- Lynn, P.M., and Davies, W. (2007). The 39,XO mouse as a model for the neurobiology of Turner syndrome and sex-biased neuropsychiatric disorders. *Behav Brain Res* 179, 173-182.
- Lyon, M.F. (1961). Gene action in the X-chromosome of the mouse (*Mus musculus* L.). *Nature* 190, 372-373.

- Lyon, M.F. (1962). Sex chromatin and gene action in the mammalian X-chromosome. *Am J Hum Genet* **14**, 135-148.
- Lyon, M.F. (1998). X-chromosome inactivation: a repeat hypothesis. *Cytogenet Cell Genet* **80**, 133-137.
- Ma, Z., Swigut, T., Valouev, A., Rada-Iglesias, A., and Wysocka, J. (2011). Sequence-specific regulator Prdm14 safeguards mouse ESCs from entering extraembryonic endoderm fates. *Nat Struct Mol Biol* **18**, 120-127.
- Maclean, N., and Mitchell, J.M. (1962). A survey of sex-chromosome abnormalities among 4514 mental defectives. *Lancet* **1**, 293-296.
- Maenner, S., Blaud, M., Fouillen, L., Savoye, A., Marchand, V., Dubois, A., Sanglier-Cianferani, S., Van Dorsselaer, A., Clerc, P., Avner, P., *et al.* (2010). 2-D structure of the A region of Xist RNA and its implication for PRC2 association. *PLoS Biol* **8**, e1000276.
- Maherali, N., Sridharan, R., Xie, W., Utikal, J., Eminli, S., Arnold, K., Stadtfeld, M., Yachechko, R., Tchieu, J., Jaenisch, R., *et al.* (2007). Directly reprogrammed fibroblasts show global epigenetic remodeling and widespread tissue contribution. *Cell Stem Cell* **1**, 55-70.
- Mak, W., Baxter, J., Silva, J., Newall, A.E., Otte, A.P., and Brockdorff, N. (2002). Mitotically stable association of polycomb group proteins *eed* and *enx1* with the inactive x chromosome in trophoblast stem cells. *Curr Biol* **12**, 1016-1020.
- Mak, W., Nesterova, T.B., de Napoles, M., Appanah, R., Yamanaka, S., Otte, A.P., and Brockdorff, N. (2004). Reactivation of the paternal X chromosome in early mouse embryos. *Science* **303**, 666-669.
- Marahrens, Y., Loring, J., and Jaenisch, R. (1998). Role of the Xist gene in X chromosome choosing. *Cell* **92**, 657-664.
- Marahrens, Y., Panning, B., Dausman, J., Strauss, W., and Jaenisch, R. (1997). Xist-deficient mice are defective in dosage compensation but not spermatogenesis. *Genes Dev* **11**, 156-166.
- Marchetto, M.C., Carromeu, C., Acab, A., Yu, D., Yeo, G.W., Mu, Y., Chen, G., Gage, F.H., and Muotri, A.R. (2010). A model for neural development and treatment of Rett syndrome using human induced pluripotent stem cells. *Cell* **143**, 527-539.
- Markaki, Y., Gunkel, M., Schermelleh, L., Beichmanis, S., Neumann, J., Heidemann, M., Leonhardt, H., Eick, D., Cremer, C., and Cremer, T. (2010). Functional nuclear organization of transcription and DNA replication: a topographical marriage between chromatin domains and the interchromatin compartment. *Cold Spring Harb Symp Quant Biol* **75**, 475-492.
- Markus, S.M., Taneja, S.S., Logan, S.K., Li, W., Ha, S., Hittelman, A.B., Rogatsky, I., and Garabedian, M.J. (2002). Identification and characterization of ART-27, a novel coactivator for the androgen receptor N terminus. *Mol Biol Cell* **13**, 670-682.
- Martinez, R., Bonilla-Henao, V., Jimenez, A., Lucas, M., Vega, C., Ramos, I., Sobrino, F., and Pintado, E. (2005). Skewed X inactivation of the normal allele in fully mutated female carriers determines the levels of FMRP in blood and the fragile X phenotype. *Mol Diagn* **9**, 157-162.

- Martorell, L., Nascimento, M.T., Colome, R., Genoves, J., Naudó, M., and Nascimento, A. (2011). Four sisters compound heterozygotes for the pre- and full mutation in fragile X syndrome and a complete inactivation of X-functional chromosome: implications for genetic counseling. *J Hum Genet* 56, 87-90.
- Masui, O., Bonnet, I., Le Baccon, P., Brito, I., Pollex, T., Murphy, N., Hupe, P., Barillot, E., Belmont, A.S., and Heard, E. (2011). Live-cell chromosome dynamics and outcome of X chromosome pairing events during ES cell differentiation. *Cell* 145, 447-458.
- Matthews, J.M., Lester, K., Joseph, S., and Curtis, D.J. (2013). LIM-domain-only proteins in cancer. *Nat Rev Cancer* 13, 111-122.
- Mifsud, A., Ramirez, S., and Yong, E.L. (2000). Androgen receptor gene CAG trinucleotide repeats in anovulatory infertility and polycystic ovaries. *J Clin Endocrinol Metab* 85, 3484-3488.
- Migeon, B.R. (2003). Is Tsix repression of Xist specific to mouse? *Nat Genet* 33, 337; author reply 337-338.
- Migeon, B.R., Axelman, J., and Jeppesen, P. (2005). Differential X reactivation in human placental cells: implications for reversal of X inactivation. *Am J Hum Genet* 77, 355-364.
- Migeon, B.R., Chowdhury, A.K., Dunston, J.A., and McIntosh, I. (2001). Identification of TSIX, encoding an RNA antisense to human XIST, reveals differences from its murine counterpart: implications for X inactivation. *Am J Hum Genet* 69, 951-960.
- Migeon, B.R., and Do, T.T. (1978). In search of nonrandom X inactivation: studies of the placenta from newborns heterozygous for glucose-6-phosphate dehydrogenase. *Basic Life Sci* 12, 379-391.
- Migeon, B.R., and Do, T.T. (1979). In search of non-random X inactivation: studies of fetal membranes heterozygous for glucose-6-phosphate dehydrogenase. *Am J Hum Genet* 31, 581-585.
- Migeon, B.R., Lee, C.H., Chowdhury, A.K., and Carpenter, H. (2002). Species differences in TSIX/Tsix reveal the roles of these genes in X-chromosome inactivation. *Am J Hum Genet* 71, 286-293.
- Migeon, B.R., Schmidt, M., Axelman, J., and Cullen, C.R. (1986). Complete reactivation of X chromosomes from human chorionic villi with a switch to early DNA replication. *Proc Natl Acad Sci U S A* 83, 2182-2186.
- Miller, L.M., Plenefisch, J.D., Casson, L.P., and Meyer, B.J. (1988). xol-1: a gene that controls the male modes of both sex determination and X chromosome dosage compensation in *C. elegans*. *Cell* 55, 167-183.
- Minkovsky, A., Barakat, T.S., Sellami, N., Chin, M.H., Gunhanlar, N., Gribnau, J., and Plath, K. (2013). The pluripotency factor-bound intron 1 of Xist is dispensable for X chromosome inactivation and reactivation in vitro and in vivo. *Cell Rep* 3, 905-918.
- Minks, J., Baldry, S.E., Yang, C., Cotton, A.M., and Brown, C.J. (2013). XIST-induced silencing of flanking genes is achieved by additive action of repeat a monomers in human somatic cells. *Epigenetics Chromatin* 6, 23.
- Mlynarczyk-Evans, S., Royce-Tolland, M., Alexander, M.K., Andersen, A.A., Kalantry, S., Gribnau, J., and Panning, B. (2006). X chromosomes alternate between two states prior to random X-inactivation. *PLoS Biol* 4, e159.

- Monkhorst, K., Jonkers, I., Rentmeester, E., Grosveld, F., and Gribnau, J. (2008). X inactivation counting and choice is a stochastic process: evidence for involvement of an X-linked activator. *Cell* **132**, 410-421.
- Moreira de Mello, J.C., de Araujo, E.S., Stabellini, R., Fraga, A.M., de Souza, J.E., Sumita, D.R., Camargo, A.A., and Pereira, L.V. (2010). Random X inactivation and extensive mosaicism in human placenta revealed by analysis of allele-specific gene expression along the X chromosome. *PLoS One* **5**, e10947.
- Mossner, M., Nolte, F., Hutter, G., Reins, J., Klaumunzer, M., Nowak, V., Oblander, J., Ackermann, K., Will, S., Rohl, H., *et al.* (2013). Skewed X-inactivation patterns in ageing healthy and myelodysplastic haematopoiesis determined by a pyrosequencing based transcriptional clonality assay. *Journal of Medical Genetics* **50**, 108-117.
- Namekawa, S.H., Park, P.J., Zhang, L.F., Shima, J.E., McCarrey, J.R., Griswold, M.D., and Lee, J.T. (2006). Postmeiotic sex chromatin in the male germline of mice. *Curr Biol* **16**, 660-667.
- Namekawa, S.H., Payer, B., Huynh, K.D., Jaenisch, R., and Lee, J.T. (2010). Two-step imprinted X inactivation: repeat versus genic silencing in the mouse. *Mol Cell Biol* **30**, 3187-3205.
- Nanda, I., Haaf, T., Scharf, M., Schmid, M., and Burt, D.W. (2002). Comparative mapping of Z-orthologous genes in vertebrates: implications for the evolution of avian sex chromosomes. *Cytogenet Genome Res* **99**, 178-184.
- Nanda, I., Shan, Z., Scharf, M., Burt, D.W., Koehler, M., Nothwang, H., Grutzner, F., Paton, I.R., Windsor, D., Dunn, I., *et al.* (1999). 300 million years of conserved synteny between chicken Z and human chromosome 9. *Nat Genet* **21**, 258-259.
- Navarro, P., Chambers, I., Karwacki-Neisius, V., Chureau, C., Morey, C., Rougeulle, C., and Avner, P. (2008). Molecular coupling of Xist regulation and pluripotency. *Science* **321**, 1693-1695.
- Navarro, P., Moffat, M., Mullin, N.P., and Chambers, I. (2011). The X-inactivation trans-activator Rnf12 is negatively regulated by pluripotency factors in embryonic stem cells. *Hum Genet* **130**, 255-264.
- Navarro, P., Oldfield, A., Legoupi, J., Festuccia, N., Dubois, A., Attia, M., Schoorlemmer, J., Rougeulle, C., Chambers, I., and Avner, P. (2010). Molecular coupling of Tsix regulation and pluripotency. *Nature* **468**, 457-460.
- Navarro, P., Page, D.R., Avner, P., and Rougeulle, C. (2006). Tsix-mediated epigenetic switch of a CTCF-flanked region of the Xist promoter determines the Xist transcription program. *Genes Dev* **20**, 2787-2792.
- Nesterova, T.B., Barton, S.C., Surani, M.A., and Brockdorff, N. (2001a). Loss of Xist imprinting in diploid parthenogenetic preimplantation embryos. *Dev Biol* **235**, 343-350.
- Nesterova, T.B., Popova, B.C., Cobb, B.S., Norton, S., Senner, C.E., Tang, Y.A., Spruce, T., Rodriguez, T.A., Sado, T., Merckenschlager, M., *et al.* (2008). Dicer regulates Xist promoter methylation in ES cells indirectly through transcriptional control of Dnmt3a. *Epigenetics Chromatin* **1**, 2.
- Nesterova, T.B., Senner, C.E., Schneider, J., Alcayna-Stevens, T., Tattermusch, A., Hemberger, M., and Brockdorff, N. (2011). Pluripotency factor binding and Tsix expression act synergistically to repress Xist in undifferentiated embryonic stem cells. *Epigenetics Chromatin* **4**, 17.

- Nesterova, T.B., Slobodyanyuk, S.Y., Elisaphenko, E.A., Shevchenko, A.I., Johnston, C., Pavlova, M.E., Rogozin, I.B., Kolesnikov, N.N., Brockdorff, N., and Zakian, S.M. (2001b). Characterization of the genomic Xist locus in rodents reveals conservation of overall gene structure and tandem repeats but rapid evolution of unique sequence. *Genome Res* 11, 833-849.
- Nicodemi, M., and Prisco, A. (2007). Symmetry-breaking model for X-chromosome inactivation. *Phys Rev Lett* 98, 108104.
- Nora, E.P., Lajoie, B.R., Schulz, E.G., Giorgetti, L., Okamoto, I., Servant, N., Piolot, T., van Berkum, N.L., Meisig, J., Sedat, J., *et al.* (2012). Spatial partitioning of the regulatory landscape of the X-inactivation centre. *Nature* 485, 381-385.
- Ogawa, Y., and Lee, J.T. (2003). Xite, X-inactivation intergenic transcription elements that regulate the probability of choice. *Mol Cell* 11, 731-743.
- Ogawa, Y., Sun, B.K., and Lee, J.T. (2008). Intersection of the RNA interference and X-inactivation pathways. *Science* 320, 1336-1341.
- Ohhata, T., Hoki, Y., Sasaki, H., and Sado, T. (2008). Crucial role of antisense transcription across the Xist promoter in Tsix-mediated Xist chromatin modification. *Development* 135, 227-235.
- Ohhata, T., Senner, C.E., Hemberger, M., and Wutz, A. (2011). Lineage-specific function of the noncoding Tsix RNA for Xist repression and Xi reactivation in mice. *Genes Dev* 25, 1702-1715.
- Ohno, S. (1967). Sex chromosomes and sex-linked genes (Berlin, Springer-Verlag).
- Oikawa, M., Inoue, K., Shiura, H., Matoba, S., Kamimura, S., Hirose, M., Mekada, K., Yoshiki, A., Tanaka, S., Abe, K., *et al.* (2014). Understanding the X chromosome inactivation cycle in mice: a comprehensive view provided by nuclear transfer. *Epigenetics* 9, 204-211.
- Okamoto, I., Otte, A.P., Allis, C.D., Reinberg, D., and Heard, E. (2004). Epigenetic dynamics of imprinted X inactivation during early mouse development. *Science* 303, 644-649.
- Okamoto, I., Patrat, C., Thepot, D., Peynot, N., Fauque, P., Daniel, N., Diabangouaya, P., Wolf, J.P., Renard, J.P., Duranthon, V., *et al.* (2011). Eutherian mammals use diverse strategies to initiate X-chromosome inactivation during development. *Nature* 472, 370-374.
- Okita, K., Ichisaka, T., and Yamanaka, S. (2007). Generation of germline-competent induced pluripotent stem cells. *Nature* 448, 313-317.
- Osborne, C.S., Chakalova, L., Mitchell, J.A., Horton, A., Wood, A.L., Bolland, D.J., Corcoran, A.E., and Fraser, P. (2007). Myc dynamically and preferentially relocates to a transcription factory occupied by Igh. *PLoS Biol* 5, e192.
- Ostendorff, H.P., Peirano, R.I., Peters, M.A., Schluter, A., Bossenz, M., Scheffner, M., and Bach, I. (2002). Ubiquitination-dependent cofactor exchange on LIM homeodomain transcription factors. *Nature* 416, 99-103.
- Ozbalkan, Z., Bagislar, S., Kiraz, S., Akyerli, C.B., Ozer, H.T., Yavuz, S., Birlik, A.M., Calguneri, M., and Ozelik, T. (2005). Skewed X chromosome inactivation in blood cells of women with scleroderma. *Arthritis Rheum* 52, 1564-1570.

- Pace, H.C., and Brenner, C. (2003). Feminizing chicks: a model for avian sex determination based on titration of Hint enzyme activity and the predicted structure of an Asw-Hint heterodimer. *Genome Biol* 4, R18.
- Palmer, A.C., Egan, J.B., and Shearwin, K.E. (2011). Transcriptional interference by RNA polymerase pausing and dislodgement of transcription factors. *Transcription* 2, 9-14.
- Panning, B., Dausman, J., and Jaenisch, R. (1997). X chromosome inactivation is mediated by Xist RNA stabilization. *Cell* 90, 907-916.
- Pasque, V., Tchieu, J., Karnik, R., Uyeda, M., Sadhu Dimashkie, A., Case, D., Papp, B., Bonora, G., Patel, S., Ho, R., *et al.* (2014). X chromosome reactivation dynamics reveal stages of reprogramming to pluripotency. *Cell* 159, 1681-1697.
- Patrat, C., Okamoto, I., Diabangouaya, P., Vialon, V., Le Baccon, P., Chow, J., and Heard, E. (2009). Dynamic changes in paternal X-chromosome activity during imprinted X-chromosome inactivation in mice. *Proc Natl Acad Sci U S A* 106, 5198-5203.
- Payer, B., Rosenberg, M., Yamaji, M., Yabuta, Y., Koyanagi-Aoi, M., Hayashi, K., Yamanaka, S., Saitou, M., and Lee, J.T. (2013). Tsix RNA and the germline factor, PRDM14, link X reactivation and stem cell reprogramming. *Mol Cell* 52, 805-818.
- Pehrson, J.R., Changolkar, L.N., Costanzi, C., and Leu, N.A. (2014). Mice without macroH2A histone variants. *Mol Cell Biol* 34, 4523-4533.
- Peng, C.Y., Xie, H.J., Guo, Z.F., Nie, Y.L., Chen, J., Zhou, J.M., and Yin, J. (2014). The association between androgen receptor gene CAG polymorphism and polycystic ovary syndrome: a case-control study and meta-analysis. *J Assist Reprod Genet* 31, 1211-1219.
- Penny, G.D., Kay, G.F., Sheardown, S.A., Rastan, S., and Brockdorff, N. (1996). Requirement for Xist in X chromosome inactivation. *Nature* 379, 131-137.
- Pettigrew, A.L., McCabe, E.R., Elder, F.F., and Ledbetter, D.H. (1991). Isodicentric X chromosome in a patient with Turner syndrome--implications for localization of the X-inactivation center. *Hum Genet* 87, 498-502.
- Plath, K., Fang, J., Mlynarczyk-Evans, S.K., Cao, R., Worringer, K.A., Wang, H.B., de la Cruz, C.C., Otte, A.P., Panning, B., and Zhang, Y. (2003). Role of histone H3 lysine 27 methylation in X inactivation. *Science* 300, 131-135.
- Plenge, R.M., Hendrich, B.D., Schwartz, C., Arena, J.F., Naumova, A., Sapienza, C., Winter, R.M., and Willard, H.F. (1997). A promoter mutation in the XIST gene in two unrelated families with skewed X-chromosome inactivation. *Nat Genet* 17, 353-356.
- Puck, J.M., Stewart, C.C., and Nussbaum, R.L. (1992). Maximum-likelihood analysis of human T-cell X chromosome inactivation patterns: normal women versus carriers of X-linked severe combined immunodeficiency. *Am J Hum Genet* 50, 742-748.
- Pugacheva, E.M., Tiwari, V.K., Abdullaev, Z., Vostrov, A.A., Flanagan, P.T., Quitschke, W.W., Loukinov, D.I., Ohlsson, R., and Lobanenko, V.V. (2005). Familial cases of point mutations in the XIST promoter reveal a

correlation between CTCF binding and pre-emptive choices of X chromosome inactivation. *Hum Mol Genet* **14**, 953-965.

Pullirsch, D., Hartel, R., Kishimoto, H., Leeb, M., Steiner, G., and Wutz, A. (2010). The Trithorax group protein Ash2l and Saf-A are recruited to the inactive X chromosome at the onset of stable X inactivation. *Development* **137**, 935-943.

Rajender, S., Carlus, S.J., Bansal, S.K., Negi, M.P., Sadasivam, N., Sadasivam, M.N., and Thangaraj, K. (2013). Androgen receptor CAG repeats length polymorphism and the risk of polycystic ovarian syndrome (PCOS). *PLoS One* **8**, e75709.

Rastan, S. (1983). Non-random X-chromosome inactivation in mouse X-autosome translocation embryos--location of the inactivation centre. *J Embryol Exp Morphol* **78**, 1-22.

Rastan, S., and Robertson, E.J. (1985). X-chromosome deletions in embryo-derived (EK) cell lines associated with lack of X-chromosome inactivation. *J Embryol Exp Morphol* **90**, 379-388.

Reed, K.J., and Sinclair, A.H. (2002). FET-1: a novel W-linked, female specific gene up-regulated in the embryonic chicken ovary. *Mech Dev* **119 Suppl 1**, S87-90.

Rice, W.R. (1987). Genetic hitchhiking and the evolution of reduced genetic activity of the Y sex chromosome. *Genetics* **116**, 161-167.

Ropers, H.H., Wolff, G., and Hitzeroth, H.W. (1978). Preferential X inactivation in human placenta membranes: is the paternal X inactive in early embryonic development of female mammals? *Hum Genet* **43**, 265-273.

Ross, M.T., Grafham, D.V., Coffey, A.J., Scherer, S., McLay, K., Muzny, D., Platzer, M., Howell, G.R., Burrows, C., Bird, C.P., *et al.* (2005). The DNA sequence of the human X chromosome. *Nature* **434**, 325-337.

Rotterdam, E.A.-S.P.C.W.G. (2004). Revised 2003 consensus on diagnostic criteria and long-term health risks related to polycystic ovary syndrome. *Fertil Steril* **81**, 19-25.

Russell, L.B., and Montgomery, C.S. (1970). Comparative studies on X-autosome translocations in the mouse. II. Inactivation of autosomal loci, segregation, and mapping of autosomal breakpoints in five T (X;1) S. *Genetics* **64**, 281-312.

Sado, T., Fenner, M.H., Tan, S.S., Tam, P., Shioda, T., and Li, E. (2000). X inactivation in the mouse embryo deficient for Dnmt1: distinct effect of hypomethylation on imprinted and random X inactivation. *Dev Biol* **225**, 294-303.

Sado, T., Hoki, Y., and Sasaki, H. (2005). Tsix silences Xist through modification of chromatin structure. *Dev Cell* **9**, 159-165.

Sado, T., Hoki, Y., and Sasaki, H. (2006). Tsix defective in splicing is competent to establish Xist silencing. *Development* **133**, 4925-4931.

Sado, T., Wang, Z., Sasaki, H., and Li, E. (2001). Regulation of imprinted X-chromosome inactivation in mice by Tsix. *Development* **128**, 1275-1286.

- Salido, E.C., Li, X.M., Yen, P.H., Martin, N., Mohandas, T.K., and Shapiro, L.J. (1996). Cloning and expression of the mouse pseudoautosomal steroid sulphatase gene (Sts). *Nat Genet* **13**, 83-86.
- Salz, H.K., Maine, E.M., Keyes, L.N., Samuels, M.E., Cline, T.W., and Schedl, P. (1989). The *Drosophila* female-specific sex-determination gene, *Sex-lethal*, has stage-, tissue-, and sex-specific RNAs suggesting multiple modes of regulation. *Genes Dev* **3**, 708-719.
- Sandovici, I., Naumova, A.K., Leppert, M., Linares, Y., and Sapienza, C. (2004). A longitudinal study of X-inactivation ratio in human females. *Hum Genet* **115**, 387-392.
- Sartor, O., Zheng, Q., and Eastham, J.A. (1999). Androgen receptor gene CAG repeat length varies in a race-specific fashion in men without prostate cancer. *Urology* **53**, 378-380.
- Sasaki, M., Kaneuchi, M., Sakuragi, N., Fujimoto, S., Carroll, P.R., and Dahiya, R. (2003). The polyglycine and polyglutamine repeats in the androgen receptor gene in Japanese and Caucasian populations. *Biochem Biophys Res Commun* **312**, 1244-1247.
- Schmidt, M., Certoma, A., Du Sart, D., Kalitsis, P., Leversha, M., Fowler, K., Sheffield, L., Jack, I., and Danks, D.M. (1990). Unusual X chromosome inactivation in a mentally retarded girl with an interstitial deletion Xq27: implications for the fragile X syndrome. *Hum Genet* **84**, 347-352.
- Schultz, G.A., and Heyner, S. (1992). Gene expression in pre-implantation mammalian embryos. *Mutat Res* **296**, 17-31.
- Schulz, E.G., Meisig, J., Nakamura, T., Okamoto, I., Sieber, A., Picard, C., Borensztein, M., Saitou, M., Bluthgen, N., and Heard, E. (2014). The two active X chromosomes in female ESCs block exit from the pluripotent state by modulating the ESC signaling network. *Cell Stem Cell* **14**, 203-216.
- Senner, C.E., Nesterova, T.B., Norton, S., Dewchand, H., Godwin, J., Mak, W., and Brockdorff, N. (2011). Disruption of a conserved region of Xist exon 1 impairs Xist RNA localisation and X-linked gene silencing during random and imprinted X chromosome inactivation. *Development* **138**, 1541-1550.
- Sharp, A., Robinson, D., and Jacobs, P. (2000). Age- and tissue-specific variation of X chromosome inactivation ratios in normal women. *Hum Genet* **107**, 343-349.
- Sheardown, S.A., Duthie, S.M., Johnston, C.M., Newall, A.E., Formstone, E.J., Arkell, R.M., Nesterova, T.B., Alghisi, G.C., Rastan, S., and Brockdorff, N. (1997). Stabilization of Xist RNA mediates initiation of X chromosome inactivation. *Cell* **91**, 99-107.
- Shibata, S., and Lee, J.T. (2003). Characterization and quantitation of differential Tsix transcripts: implications for Tsix function. *Hum Mol Genet* **12**, 125-136.
- Shibata, S., and Lee, J.T. (2004). Tsix transcription- versus RNA-based mechanisms in Xist repression and epigenetic choice. *Curr Biol* **14**, 1747-1754.
- Shin, J., Bossenz, M., Chung, Y., Ma, H., Byron, M., Taniguchi-Ishigaki, N., Zhu, X., Jiao, B., Hall, L.L., Green, M.R., *et al.* (2010). Maternal Rnf12/RLIM is required for imprinted X-chromosome inactivation in mice. *Nature* **467**, 977-981.

Shin, J., Wallingford, M.C., Gallant, J., Marcho, C., Jiao, B., Byron, M., Bossenz, M., Lawrence, J.B., Jones, S.N., Mager, J., *et al.* (2014). RLIM is dispensable for X-chromosome inactivation in the mouse embryonic epiblast. *Nature* **511**, 86-89.

Silva, J., Mak, W., Zvetkova, I., Appanah, R., Nesterova, T.B., Webster, Z., Peters, A.H.F.M., Jenuwein, T., Otte, A.P., and Brockdorff, N. (2003). Establishment of histone H3 methylation on the inactive X chromosome requires transient recruitment of Eed-Enx1 Polycomb group complexes. *Developmental Cell* **4**, 481-495.

Silva, S.S., Rowntree, R.K., Mekhoubad, S., and Lee, J.T. (2008). X-chromosome inactivation and epigenetic fluidity in human embryonic stem cells. *Proc Natl Acad Sci U S A* **105**, 4820-4825.

Simmler, M.C., Cunningham, D.B., Clerc, P., Verma, T., Caudron, B., Cruaud, C., Pawlak, A., Szpirer, C., Weissenbach, J., Claverie, J.M., *et al.* (1996). A 94 kb genomic sequence 3' to the murine Xist gene reveals an AT rich region containing a new testis specific gene Tsx. *Hum Mol Genet* **5**, 1713-1726.

Simon, M.D., Pinter, S.F., Fang, R., Sarma, K., Rutenberg-Schoenberg, M., Bowman, S.K., Kesner, B.A., Maier, V.K., Kingston, R.E., and Lee, J.T. (2013). High-resolution Xist binding maps reveal two-step spreading during X-chromosome inactivation. *Nature* **504**, 465-469.

Simonis, M., Klous, P., Homminga, I., Galjaard, R.J., Rijkers, E.J., Grosveld, F., Meijerink, J.P., and de Laat, W. (2009). High-resolution identification of balanced and complex chromosomal rearrangements by 4C technology. *Nat Methods* **6**, 837-842.

Singer-Sam, J., Chapman, V., LeBon, J.M., and Riggs, A.D. (1992). Parental imprinting studied by allele-specific primer extension after PCR: paternal X chromosome-linked genes are transcribed prior to preferential paternal X chromosome inactivation. *Proc Natl Acad Sci U S A* **89**, 10469-10473.

Skaletsky, H., Kuroda-Kawaguchi, T., Minx, P.J., Cordum, H.S., Hillier, L., Brown, L.G., Repping, S., Pyntikova, T., Ali, J., Bieri, T., *et al.* (2003). The male-specific region of the human Y chromosome is a mosaic of discrete sequence classes. *Nature* **423**, 825-837.

Smahi, A., Courtois, G., Vabres, P., Yamaoka, S., Heuertz, S., Munnich, A., Israel, A., Heiss, N.S., Klauck, S.M., Kioschis, P., *et al.* (2000). Genomic rearrangement in NEMO impairs NF-kappaB activation and is a cause of incontinentia pigmenti. The International Incontinentia Pigmenti (IP) Consortium. *Nature* **405**, 466-472.

Smeets, D., Markaki, Y., Schmid, V.J., Kraus, F., Tattermusch, A., Cerase, A., Sterr, M., Fiedler, S., Demmerle, J., Popken, J., *et al.* (2014). Three-dimensional super-resolution microscopy of the inactive X chromosome territory reveals a collapse of its active nuclear compartment harboring distinct Xist RNA foci. *Epigenetics Chromatin* **7**, 8.

Smith, A.G., Heath, J.K., Donaldson, D.D., Wong, G.G., Moreau, J., Stahl, M., and Rogers, D. (1988). Inhibition of pluripotential embryonic stem cell differentiation by purified polypeptides. *Nature* **336**, 688-690.

Smith, K.P., Byron, M., Clemson, C.M., and Lawrence, J.B. (2004). Ubiquitinated proteins including uH2A on the human and mouse inactive X chromosome: enrichment in gene rich bands. *Chromosoma* **113**, 324-335.

- Spencer, R.J., del Rosario, B.C., Pinter, S.F., Lessing, D., Sadreyev, R.I., and Lee, J.T. (2011). A boundary element between Tsix and Xist binds the chromatin insulator Ctf and contributes to initiation of X-chromosome inactivation. *Genetics* 189, 441-454.
- Splinter, E., de Wit, E., Nora, E.P., Klous, P., van de Werken, H.J., Zhu, Y., Kaaij, L.J., van Ijcken, W., Gribnau, J., Heard, E., *et al.* (2011). The inactive X chromosome adopts a unique three-dimensional conformation that is dependent on Xist RNA. *Genes Dev* 25, 1371-1383.
- Stadtfield, M., Maherali, N., Breault, D.T., and Hochedlinger, K. (2008). Defining molecular cornerstones during fibroblast to iPS cell reprogramming in mouse. *Cell Stem Cell* 2, 230-240.
- Stavropoulos, N., Rowntree, R.K., and Lee, J.T. (2005). Identification of developmentally specific enhancers for Tsix in the regulation of X chromosome inactivation. *Mol Cell Biol* 25, 2757-2769.
- Stolfi, C., De Simone, V., Colantoni, A., Franze, E., Ribichini, E., Fantini, M.C., Caruso, R., Monteleone, I., Sica, G.S., Sileri, P., *et al.* (2014). A functional role for Smad7 in sustaining colon cancer cell growth and survival. *Cell Death Dis* 5, e1073.
- Strahl, B.D., and Allis, C.D. (2000). The language of covalent histone modifications. *Nature* 403, 41-45.
- Sun, B.K., Deaton, A.M., and Lee, J.T. (2006). A transient heterochromatic state in Xist preempts X inactivation choice without RNA stabilization. *Mol Cell* 21, 617-628.
- Sun, S., Del Rosario, B.C., Szanto, A., Ogawa, Y., Jeon, Y., and Lee, J.T. (2013). Jpx RNA activates Xist by evicting CTCF. *Cell* 153, 1537-1551.
- Swierczek, S.I., Agarwal, N., Nussenzveig, R.H., Rothstein, G., Wilson, A., Artz, A., and Prchal, J.T. (2008). Hematopoiesis is not clonal in healthy elderly women. *Blood* 112, 3186-3193.
- Szymanski, K., Miskiewicz, P., Pirko, K., Jurecka-Lubieniecka, B., Kula, D., Hasse-Lazar, K., Krajewski, P., Bednarczuk, T., and Ploski, R. (2014). rs3827440, a nonsynonymous single nucleotide polymorphism within GPR174 gene in X chromosome, is associated with Graves' disease in Polish Caucasian population. *Tissue Antigens* 83, 41-44.
- Takagi, N., and Sasaki, M. (1975). Preferential inactivation of the paternally derived X chromosome in the extraembryonic membranes of the mouse. *Nature* 256, 640-642.
- Takahashi, K., Tanabe, K., Ohnuki, M., Narita, M., Ichisaka, T., Tomoda, K., and Yamanaka, S. (2007). Induction of pluripotent stem cells from adult human fibroblasts by defined factors. *Cell* 131, 861-872.
- Takahashi, K., and Yamanaka, S. (2006). Induction of pluripotent stem cells from mouse embryonic and adult fibroblast cultures by defined factors. *Cell* 126, 663-676.
- Tchieu, J., Kuoy, E., Chin, M.H., Trinh, H., Patterson, M., Sherman, S.P., Aimiwu, O., Lindgren, A., Hakimian, S., Zack, J.A., *et al.* (2010). Female human iPSCs retain an inactive X chromosome. *Cell Stem Cell* 7, 329-342.
- Teklenburg, G., Weimar, C.H., Fauser, B.C., Macklon, N., Geijsen, N., Heijnen, C.J., Chuva de Sousa Lopes, S.M., and Kuijk, E.W. (2012). Cell lineage specific distribution of H3K27 trimethylation accumulation in an in vitro model for human implantation. *PLoS One* 7, e32701.

- Tesar, P.J., Chenoweth, J.G., Brook, F.A., Davies, T.J., Evans, E.P., Mack, D.L., Gardner, R.L., and McKay, R.D. (2007). New cell lines from mouse epiblast share defining features with human embryonic stem cells. *Nature* *448*, 196-199.
- Tian, D., Sun, S., and Lee, J.T. (2010). The long noncoding RNA, *Jpx*, is a molecular switch for X chromosome inactivation. *Cell* *143*, 390-403.
- Tonon, L., Bergamaschi, G., Dellavecchia, C., Rosti, V., Lucotti, C., Malabarba, L., Novella, A., Vercesi, E., Frassoni, F., and Cazzola, M. (1998). Unbalanced X-chromosome inactivation in haemopoietic cells from normal women. *Br J Haematol* *102*, 996-1003.
- Tsai, C.L., Rowntree, R.K., Cohen, D.E., and Lee, J.T. (2008). Higher order chromatin structure at the X-inactivation center via looping DNA. *Dev Biol* *319*, 416-425.
- Uz, E., Loubiere, L.S., Gadi, V.K., Ozbalkan, Z., Stewart, J., Nelson, J.L., and Ozcelik, T. (2008). Skewed X-chromosome inactivation in scleroderma. *Clin Rev Allergy Immunol* *34*, 352-355.
- van den Berg, I.M., Laven, J.S., Stevens, M., Jonkers, I., Galjaard, R.J., Gribnau, J., and van Doorninck, J.H. (2009). X chromosome inactivation is initiated in human preimplantation embryos. *Am J Hum Genet* *84*, 771-779.
- Vottero, A., Stratakis, C.A., Ghizzoni, L., Longui, C.A., Karl, M., and Chrousos, G.P. (1999). Androgen receptor-mediated hypersensitivity to androgens in women with nonhyperandrogenic hirsutism: skewing of X-chromosome inactivation. *J Clin Endocrinol Metab* *84*, 1091-1095.
- Ware, C.B., Wang, L., Mecham, B.H., Shen, L., Nelson, A.M., Bar, M., Lamba, D.A., Dauphin, D.S., Buckingham, B., Askari, B., *et al.* (2009). Histone deacetylase inhibition elicits an evolutionarily conserved self-renewal program in embryonic stem cells. *Cell Stem Cell* *4*, 359-369.
- Weaving, L.S., Williamson, S.L., Bennetts, B., Davis, M., Ellaway, C.J., Leonard, H., Thong, M.K., Delatycki, M., Thompson, E.M., Laing, N., *et al.* (2003). Effects of MECP2 mutation type, location and X-inactivation in modulating Rett syndrome phenotype. *Am J Med Genet A* *118A*, 103-114.
- Webb, S., de Vries, T.J., and Kaufman, M.H. (1992). The differential staining pattern of the X chromosome in the embryonic and extraembryonic tissues of postimplantation homozygous tetraploid mouse embryos. *Genet Res* *59*, 205-214.
- Werner, R., Holterhus, P.M., Binder, G., Schwarz, H.P., Morlot, M., Struve, D., Marschke, C., and Hiort, O. (2006). The A645D mutation in the hinge region of the human androgen receptor (AR) gene modulates AR activity, depending on the context of the polymorphic glutamine and glycine repeats. *J Clin Endocrinol Metab* *91*, 3515-3520.
- Wernig, M., Meissner, A., Foreman, R., Brambrink, T., Ku, M., Hochedlinger, K., Bernstein, B.E., and Jaenisch, R. (2007). In vitro reprogramming of fibroblasts into a pluripotent ES-cell-like state. *Nature* *448*, 318-324.
- West, J.D., Frels, W.I., Chapman, V.M., and Papaioannou, V.E. (1977). Preferential expression of the maternally derived X chromosome in the mouse yolk sac. *Cell* *12*, 873-882.
- Whitacre, C.C. (2001). Sex differences in autoimmune disease. *Nat Immunol* *2*, 777-780.

- Wise, A.L., Gyi, L., and Manolio, T.A. (2013). eXclusion: toward integrating the X chromosome in genome-wide association analyses. *Am J Hum Genet* 92, 643-647.
- Wu, H., Luo, J., Yu, H., Rattner, A., Mo, A., Wang, Y., Smallwood, P.M., Erlanger, B., Wheelan, S.J., and Nathans, J. (2014). Cellular resolution maps of X chromosome inactivation: implications for neural development, function, and disease. *Neuron* 81, 103-119.
- Wutz, A., and Jaenisch, R. (2000). A shift from reversible to irreversible X inactivation is triggered during ES cell differentiation. *Mol Cell* 5, 695-705.
- Wutz, A., Rasmussen, T.P., and Jaenisch, R. (2002). Chromosomal silencing and localization are mediated by different domains of Xist RNA. *Nat Genet* 30, 167-174.
- Xu, N., Tsai, C.L., and Lee, J.T. (2006). Transient homologous chromosome pairing marks the onset of X inactivation. *Science* 311, 1149-1152.
- Yang, F., Babak, T., Shendure, J., and Distech, C.M. (2010). Global survey of escape from X inactivation by RNA-sequencing in mouse. *Genome Res* 20, 614-622.
- Yildirim, E., Kirby, J.E., Brown, D.E., Mercier, F.E., Sadreyev, R.I., Scadden, D.T., and Lee, J.T. (2013). Xist RNA is a potent suppressor of hematologic cancer in mice. *Cell* 152, 727-742.
- Zeng, S.M., and Yankowitz, J. (2003). X-inactivation patterns in human embryonic and extra-embryonic tissues. *Placenta* 24, 270-275.
- Zhang, L., Huang, H., Zhou, F., Schimmel, J., Pardo, C.G., Zhang, T., Barakat, T.S., Sheppard, K.A., Mickanin, C., Porter, J.A., *et al.* (2012). RNF12 controls embryonic stem cell fate and morphogenesis in zebrafish embryos by targeting Smad7 for degradation. *Mol Cell* 46, 650-661.
- Zhang, T., Liang, W., Fang, M., Yu, J., Ni, Y., and Li, Z. (2013a). Association of the CAG repeat polymorphisms in androgen receptor gene with polycystic ovary syndrome: a systemic review and meta-analysis. *Gene* 524, 161-167.
- Zhang, Y., Castillo-Morales, A., Jiang, M., Zhu, Y., Hu, L., Urrutia, A.O., Kong, X., and Hurst, L.D. (2013b). Genes that escape X-inactivation in humans have high intraspecific variability in expression, are associated with mental impairment but are not slow evolving. *Mol Biol Evol* 30, 2588-2601.
- Zhao, J., Sun, B.K., Erwin, J.A., Song, J.J., and Lee, J.T. (2008). Polycomb proteins targeted by a short repeat RNA to the mouse X chromosome. *Science* 322, 750-756.
- Zhao, X.Y., Li, W., Lv, Z., Liu, L., Tong, M., Hai, T., Hao, J., Guo, C.L., Ma, Q.W., Wang, L., *et al.* (2009). iPS cells produce viable mice through tetraploid complementation. *Nature* 461, 86-90.
- Zhao, Y., Flandin, P., Vogt, D., Blood, A., Hermesz, E., Westphal, H., and Rubenstein, J.L. (2014). Ldb1 is essential for development of Nkx2.1 lineage derived GABAergic and cholinergic neurons in the telencephalon. *Dev Biol* 385, 94-106.

CHAPTER 2



The probability to initiate X chromosome inactivation is determined by the X to autosomal ratio and X chromosome specific allelic properties

Kim Monkhorst* , Bas de Hoon*, Iris Jonkers, Eskeatnaf Mulugeta Achame, Wouter Monkhorst, Jos Hoogerbrugge, Eveline Rentmeester, Hans V. Westerhoff, Frank Grosveld, J. Anton Grootegoed, and Joost Gribnau

*authors contributed equally

Published in:
Plos One, 2009, volume 4, issue 5: e5616



Abstract

Background

In female mammalian cells, random X chromosome inactivation (XCI) equalizes the dosage of X-encoded gene products to that in male cells. XCI is a stochastic process, in which each X chromosome has a probability to be inactivated. To obtain more insight in the factors setting up this probability, we studied the role of the X to autosome (X:A) ratio in initiation of XCI, and have used the experimental data in a computer simulation model to study the cellular population dynamics of XCI.

Methods and results

To obtain more insight in the role of the X:A ratio in initiation of XCI, we generated triploid mouse ES cells by fusion of haploid round spermatids with diploid female and male ES cells. These fusion experiments resulted in only XXY triploid ES cells. XYY and XXX ES lines were absent, suggesting cell death related either to insufficient X-chromosomal gene dosage (XYY) or to inheritance of an epigenetically modified X chromosome (XXX). Analysis of active (Xa) and inactive (Xi) X chromosomes in the obtained triploid XXY lines indicated that the initiation frequency of XCI is low, resulting in a mixed population of XaXiY and XaXaY cells, in which the XaXiY cells have a small proliferative advantage. This result, and findings on XCI in diploid and tetraploid ES cell lines with different X:A ratios, provides evidence that the X:A ratio determines the probability for a given X chromosome to be inactivated. Furthermore, we found that the kinetics of the XCI process can be simulated using a probability for an X chromosome to be inactivated that is proportional to the X:A ratio. These simulation studies re-emphasize our hypothesis that the probability is a function of the concentration of an X-encoded activator of XCI, and of X chromosome specific allelic properties determining the threshold for this activator.

Conclusions

The present findings reveal that the probability for an X chromosome to be inactivated is proportional to the X:A ratio. This finding supports the presence of an X-encoded activator of the XCI process.

Introduction

In placental mammals, dosage compensation of X-encoded gene products is achieved by inactivation of either of the two X chromosomes in female cells (Lyon, 1961). Random X chromosome inactivation (XCI) is initiated early during female embryonic development, and results in a transcriptionally inactive X chromosome (Xi). The inactive state of the Xi is clonally propagated through many cell divisions. At the onset of XCI the X-linked non-coding *Xist* gene is transcriptionally up-regulated on the future Xi, and *Xist* RNA coats the Xi in *cis* (Borsani et al., 1991; Brockdorff et al., 1992; Brown et al., 1991; Brown et al., 1992). *Xist* RNA is required for XCI and most likely attracts chromatin modifying enzymes involved in the silencing process (Marahrens et al., 1997; Penny et al., 1996). The *Tsix* and *Xite* genes play a crucial role in the early stages of XCI by suppression of *Xist* transcription and *Xist* RNA accumulation. Both *Tsix* and *Xite* also are non-coding genes that overlap with *Xist*, but are transcribed in anti-sense direction (Lee and Lu, 1999; Ogawa and Lee, 2003).

The first phase of XCI comprises a counting process, followed by initiation of XCI when more than one X chromosome is present per diploid nucleus. We have recently shown that initiation of XCI is directed by a stochastic mechanism, in which all X chromosomes in a nucleus have an independent probability to initiate XCI within a certain time-span (Monkhorst et al., 2008). We proposed that this probability is proportional to the X to autosome ratio (X:A), and most likely depends on at least two factors that act through *Xist* and *Tsix*: an X-encoded XCI-activator that stimulates *Xist* expression, and itself is transcriptionally inactivated by the XCI process, and an autosomally encoded XCI-inhibitor that suppresses *Xist* by activating *Tsix*. Although the action of *Tsix* is still not understood, *Tsix* transcription and chromatin modifications in the *Xist* promoter (possibly mediated by *Tsix*) provide a threshold that has to be overcome by the XCI-activator, allowing accumulation of sufficient *Xist* molecules to silence *Tsix* and spread in *cis*. Early in mouse development or upon differentiation of embryonic stem (ES) cells, the XCI-activator concentration in a cell will increase, and in female cells this will drive the initiation of XCI with a specific probability. This probability is the consequence of stochastic transcriptional activation of both *Xist* and *Tsix*. In male cells, the XCI-activator concentration will be too low; therefore, these cells induce XCI only sporadically (Monkhorst et al., 2008).

Several findings support the presence of an X-linked XCI-activator. Tetraploid XXXX ES cells initiate XCI significantly faster than XXXY cells (Monkhorst et al., 2008). In addition, female ES cells with a heterozygous deletion including *Xist*, *Tsix* and *Xite* (Δ XTX), still show initiation of XCI on the wild type X chromosome. XCI is not initiated in male cells with one copy of *Xist*, *Tsix* and *Xite* indicating a novel *trans* acting activator, encoded by a gene located outside the deleted area (Monkhorst et al., 2008). Also, studies in differentiating ES cell lines with stably

integrated *Xist* promoter transgenes show significantly more expression of a linked reporter in female cells compared to male cells (Sun et al., 2006). The genomic location of the XCI-activator is unknown so far. However, previous studies which analyzed XCI in male cell lines with multi-copy YAC transgenes ranging in size from 320 to 460 kb, encompassing *Xist* and flanking regions, revealed initiation of XCI on the single X chromosome (Heard et al., 1999; Lee et al., 1996). Interestingly, a BAC sequence covering a region upstream of *Xist*, not including *Xist* itself, also induced ectopic XCI in transgenic male and female cells (Augui et al., 2007). These studies indicate that the sequence encoding the XCI-activator is likely to be located within the sequence covered by these transgenes. Smaller transgenes, only including *Xist* and flanking sequences, have also been reported to induce ectopic XCI in male cells, when present as multiple tandemly inserted transgenes (Herzing et al., 1997; Lee et al., 1999). Our finding that XCI is still initiated in female cells with a Δ XTX deletion, however, indicates that the overlapping region covered by the Δ XTX deletion and these transgenes (Herzing et al., 1997; Lee et al., 1999) is not required for the counting process. Some of the reported observations may also be attributed to the presence of *Tsix* transcription, which was not yet discovered, and hence not taken into consideration, at the time these studies were performed.

In diploid and tetraploid cells, one X chromosome will remain active per diploid genome. However, in triploid cells this ratio of one active X chromosome per diploid autosomal set cannot be achieved. Therefore, triploid cells provide a unique situation for studying the mechanism of XCI counting and choice and gene dosage related cell selection. Several studies have been conducted with human and mouse XXY and XXX triploid embryos and embryo-derived cell lines, to try to determine the pattern of X inactivation. In these experiments cultured differentiated cells were examined which had completed the XCI process (Gartler et al., 2006), and indicated that the majority of cell lines derived from human live born XXX triploids predominantly show two active X chromosomes (Hendriksson et al., 1974; Leisti et al., 1970; Willard and Breg, 1977). In contrast, analysis of 10-day-old XXY and XXX mouse triploid embryos showed that most cells had one active X chromosome (Speirs et al., 1990). Unfortunately, both studies did not discriminate between primary choice in XCI and the effect of cell selection processes on XCI.

To explore the mechanism determining the probability of an X chromosome to be inactivated, we have generated XXY triploid mouse ES cells. Analysis of XCI in these cells allowed us to determine the influence of the X:A ratio on the initiation of XCI, and to discriminate between the effects of XCI initiation and cell selection. In addition, we have used stochastic and mathematical simulation studies to follow the kinetics of XCI in a population of developing or differentiating cells.

Results

Generation of triploid ES cells

Our previous studies with tetraploid XXXX, XXXY and XYY mouse ES cell lines have indicated that the probability for an X chromosome to be inactivated is directly related to the X:A ratio (Monkhorst et al., 2008). To further explore this finding we aimed to generate triploid ES cell lines with XYY and XXY karyotypes, having an X:A ratio of 1:3 and 2:3, respectively, for which XCI has not been studied before. To generate triploid ES cell lines we decided to fuse puromycin resistant female and male ES cells with round spermatids or spermatozoa containing a *neomycin resistance (neo)* gene targeted to either the autosomal *Ube2b* gene or the X-chromosomal *Ube2a* gene. Both *Ube2a* and *Ube2b* encode ubiquitin-conjugating enzymes involved in DNA replicative damage bypass (Ulrich, 2005). The encoded proteins have at least partially overlapping functions, and two functional alleles of either *Ube2a* or *Ube2b* per cell are sufficient to generate viable diploid mice. Also, spermatogenesis is not dysregulated in *Ube2a* knockout and *Ube2b* heterozygous mutant mice (Roest et al., 2004; Roest et al., 1996). Therefore, it was expected that loss-of-function of one targeted *Ube2a* or *Ube2b* allele, in the *Ube2b*^{+/-} and *Ube2a*^{+/-} mice, respectively, will not have an effect on the viability of hybrid fusion products. In the present study, the targeted mutant alleles serve the function of selection for fused cells.

All PEG mediated fusion experiments were conducted twice. Fusion of the neomycin resistant *Ube2a-neo* round spermatids and spermatozoa with female or male ES cells did not result in double resistant colonies (Fig. 1a). In addition, fusions of *Ube2b-neo* round spermatids with male ES cells, and fusions of *Ube2b-neo* spermatozoa with either female or male ES cells, also did not result in double resistant colonies. In contrast, double resistant colonies were obtained by fusion of *Ube2b-neo* round spermatids with female ES cells, and these colonies were picked and expanded for further analysis. PCR analysis of genomic DNA indicated the presence of the *Ube2b-neo* allele in all the ES clones picked, confirming the fusion of a round spermatid containing the *Ube2b-neo* allele (Fig. 1b). FACS analysis, using propidium iodide to determine the DNA content, indicated that all our cell lines were triploid (Fig. 1c). The small 2n population we attribute to contamination of the triploid cells with diploid male feeders that we used to grow the ES cells on. Karyotyping also indicated that, in all cell lines, the majority of cells had 60 chromosomes, which are stably maintained through many passages (Fig. 1d, and data not shown). Interestingly, X and Y chromosome paint analysis showed that all cell lines had an XXY 3n karyotype (N=18) although the haploid round spermatids that were used for fusion can be expected to contain either an X chromosome or a Y chromosome in a 50/50 ratio (Fig. 1e and 1f).

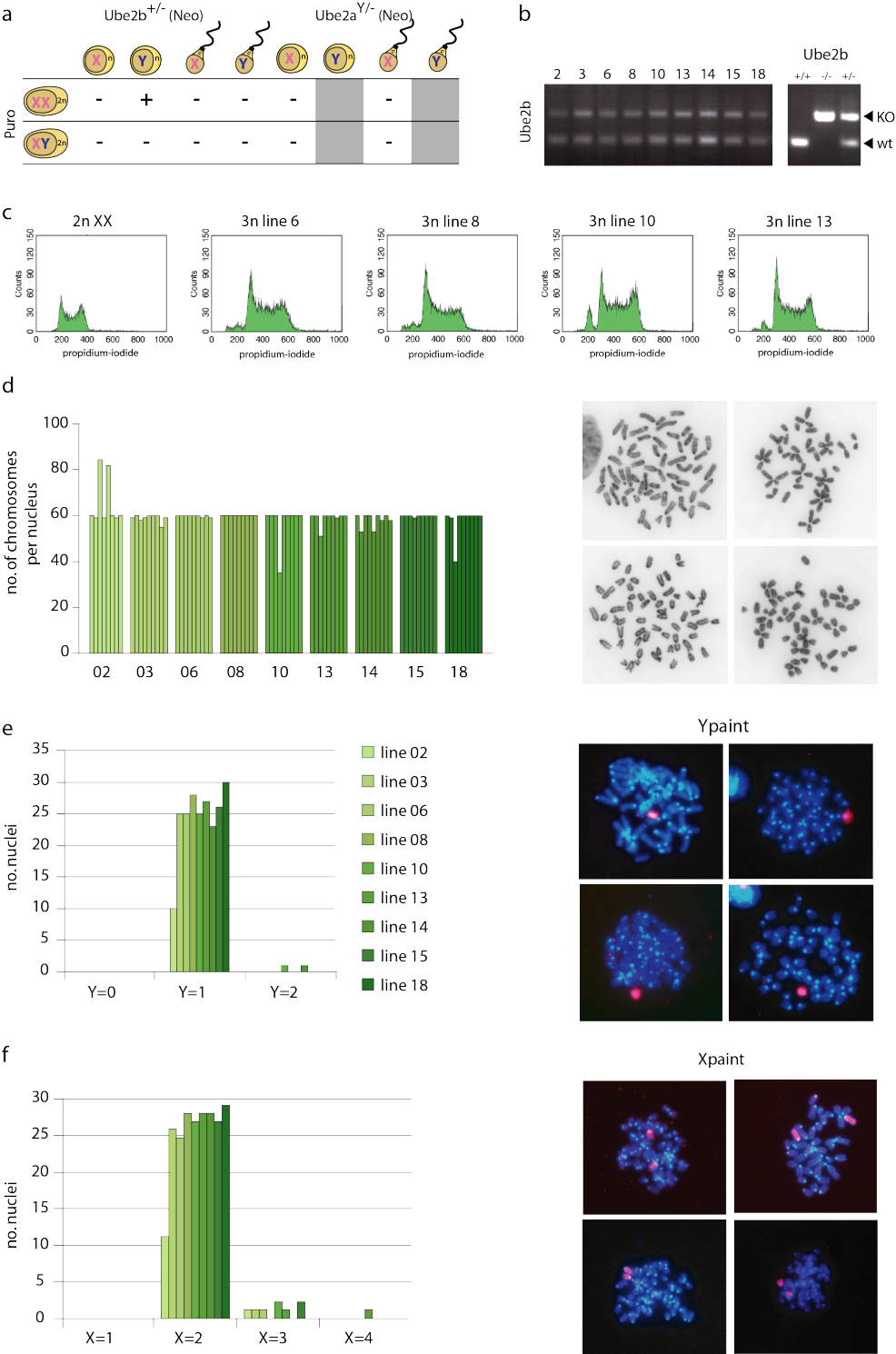


Figure 1.

Generation of triploid ES cells

- a. The different fusion experiments performed; (-) no clones present, (+) clones present which could be picked and expanded. Fusion of Y-bearing spermatids and spermatozoa for *Ube2a* knockout mice was not examined, since the neo selection marker localizes to the X (gray boxes).
- b. PCR with genomic DNA detecting the wild type and mutated *Ube2b-neo* allele. Clone numbers are indicated, and control DNA was isolated from wild type, *Ube2b*^{-/-} and +/- mice.
- c. FACS analysis detecting the DNA content of diploid ES cells, and four different triploid ES cell lines analyzed in (B).
- d. Karyotyping of 9 triploid ES cell lines, shown in (B); indicated are chromosome counts of individual metaphase spreads. Right panels show representative examples of metaphase spreads.
- e. Y chromosome paint analysis; shown is the number of metaphase spreads with 0, 1, and 2 Y chromosomes. Right panels show representative examples of metaphase spreads subjected to DNA FISH using a Y paint probe (red, DNA is blue).
- f. X chromosome paint analysis, shown is the number of metaphase spreads with 1, 2, 3, and 4 X chromosomes. Right panels show representative examples of metaphase spreads subjected to DNA FISH using an X paint probe (Red, DNA is blue).

These results suggest that triploid XYY cells are absent due to an insufficient dosage of X-encoded genes. In addition, the lack of XXX 3n karyotypes suggests that introduction of an X chromosome through a round spermatid leads to a non-viable triploid ES cell. The absence of triploid XXX ES cell lines (X:A ratio of 1) cannot be explained by a dosage problem, but might be due to the presence of an epigenetically modified X chromosome present in spermatids. During spermatogenesis, the largely unpaired X and Y chromosomes are transcriptionally inactivated, forming the XY body or sex body in a process called meiotic sex chromosome inactivation (MSCI) (Turner, 2007). Chromatin modifications present on the XY body may be partly maintained in post-meiotic round spermatids. Such modifications, particularly relevant for the X chromosome with a large gene content, may explain lethality of the triploid XXX ES cells.

To test whether the spermatid derived X was reactivated after cell fusion, we fused round spermatids of males containing an X-linked *GFP* transgene (Hadjantonakis et al., 2001) with male and female ES cells. Analysis of diploid ES cells containing the X-linked *GFP* transgene shows robust GFP expression, indicating that the transgene is properly expressed in ES cells. In contrast, after fusion of *GFP* round spermatids with ES cells, we did not see reactivation of the transgene (data not shown). Selection for reactivation of the transgene by applying puromycin selection, at days 0, 3 and 5 after fusion, did not result in clones resistant to both selection reagents. Therefore, we conclude that ES cells are incapable of reactivating the X from

spermatids. This is in contrast to ES fusions with female somatic cells, which lead to reactivation of the Xi (Takagi et al., 1983).

XCI in triploid XXY ES cells

To study XCI in the obtained XXY triploid ES cells, we differentiated 9 of these cell lines into embryoid bodies (EB). Cells were fixed and subjected to RNA-FISH after 3, 5, 7, and 10 days of differentiation, using an *Xist* specific probe to stain the *Xist* coated Xi's. After a three-day differentiation period, we mainly found cells with zero or one Xi, indicating that the triploid XXY cells are capable to initiate XCI (Fig. 2a). At this time point only ~2.5% of cells had one Xi (XiXiY) and we sporadically (<0.1%) found cells with two Xi's (XiXiY). During the differentiation process, the relative number of cells with one Xi increased, to ~40% at day 10 of differentiation (Fig. 2b).

To exclude the possibility that our triploid XXY ES cells lost or gained X chromosomes over the differentiation process, we performed DNA-FISH with an X chromosome specific BAC probe on cells differentiated for seven days. To obtain a reliable measurement, at least 100 nuclei were scored for every cell line. We found that over 93% of the XXY cells still contained two X chromosomes, and only 3% of the cells were found to have three X chromosomes, suggesting that the karyotype of these triploid XXY ES cells is stable throughout the differentiation period that we assayed (Fig. 2c).

We further examined whether the increase in time of the percentage of XiXiY cells (Fig. 2b) might be caused by cell selection. We therefore added BrdU 24 hours prior to cell fixation of day 7 differentiated ES cells, and performed immuno/RNA-FISH, detecting BrdU positive cells and *Xist* RNA. Comparison of BrdU positive cells with one or no *Xist* cloud(s) shows that there are significantly more cells with one cloud, indicating that XiXiY cells indeed have a small but significant proliferative advantage ($p < 0.001$; Fig. 2d and 2e).

Previously, we have proposed that the probability for an X chromosome to be inactivated is proportional to the X:A ratio (Monkhorst et al., 2008). To further explore this finding we compared the percentage of cells that had initiated XCI at day 3 of differentiation between cell lines with various X:A ratios, notably our XXY triploid ES cell lines (with an X:A ratio of 0.67) and tetraploid and diploid cells (4n XXXX cells with X:A=1; 4n XXXY cells with X:A=0.75; 4n XXYY cells with X:A=0.5; 2n XX cells with X:A=1; and 2n XY cells with X:A=0.5). ES cell lines were differentiated through EB differentiation and subjected to RNA-FISH to detect *Xist* RNA. For each line with a different X:A ratio or a different ploidy number, we performed three independent differentiation experiments.

The results (Fig. 2f) confirm our previous findings (Monkhorst et al., 2008) that, at day 3 of differentiation, XXXX cells have initiated XCI in significantly more cells (58%) than XXXY cells have (20%). Furthermore, tetraploid XXYY and diploid XY cells initiated XCI in less than 0.3% of

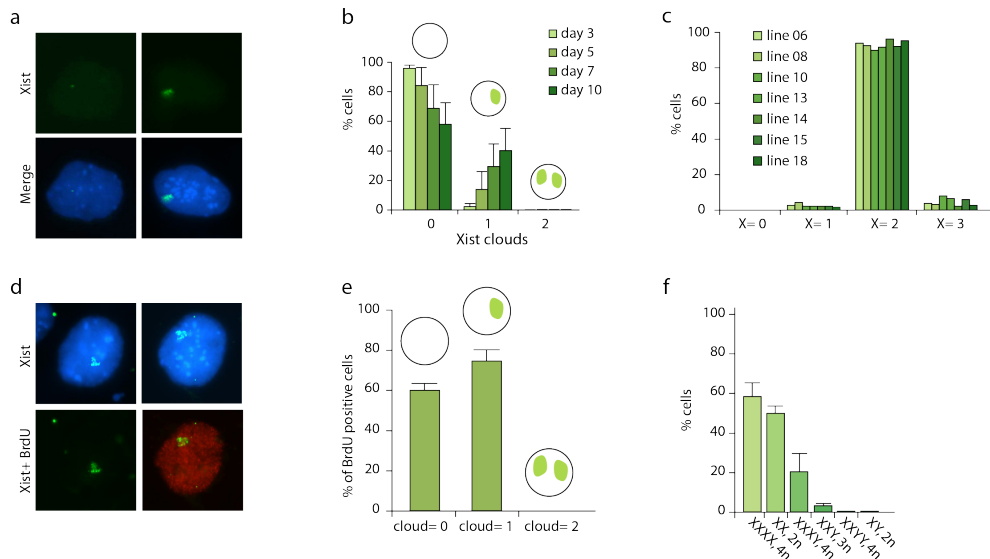


Figure 2.

Analysis of XCI in differentiating triploid XXY ES cells

- RNA-FISH analysis with an *Xist* probe (FITC, DNA in blue) on day 3 differentiated triploid ES cells, shows cells with no (left panels) or one (right panels) *Xist* cloud.
- The average distribution and standard deviation of cells with different numbers of *Xist* clouds throughout differentiation.
- DNA FISH analysis on day 7 differentiated triploid ES cells. Shown is the relative number of cells with 0, 1, 2 and 3 X chromosomes.
- Combined *Xist* RNA-BrdU detection (*Xist* in FITC, BrdU in Rhodamine red, DNA in DAPI blue), indicating the presence of cells with negative and positive BrdU staining (from left to right).
- Quantification of the *Xist* RNA-BrdU detection, shown are the relative number and standard deviation of BrdU positive cells with 0, 1 and 2 *Xist* clouds.
- The relative number and standard deviation of cells that have initiated XCI (at least one Xi), per cell line at day 3 of differentiation.

the cells, whereas diploid XX ES cells initiated XCI in 50% of the cells (Fig. 2f). At day 3, triploid XXY cells had initiated XCI in 3-4% of the cells (Fig. 2f). This percentage falls between that found for XXXY and XXYY cells. From these results, we conclude that the probability to initiate XCI depends on the X:A ratio and that this relationship appears not to be linear (Fig. 2f).

Parameters required for computer simulated XCI

To better understand the kinetics of XCI in a developing female embryo or a differentiating population of female ES cells we decided to simulate the XCI process. There are four important parameters required to simulate XCI, based on a stochastic model for XCI: 1) the probability for an X to initiate XCI, 2) the time window required for one choice round, 3) the rate of cell division, and 4) cell selection.

As indicated by our findings, the probability for an X to initiate XCI is proportional to the X:A ratio, and XCI is most likely triggered by a threshold nuclear concentration of an X-encoded XCI activator. Although the nuclear concentration of XCI activator will be the same for both X chromosomes present in a female cell, specific allelic properties of the individual X chromosomes can result in different probabilities because of effects *in cis*. Previous studies with female ES cell lines harboring deletions of either *Xist*, *Tsix* or *Xite* have indicated that the probability to initiate XCI positively correlates with the *Xist* transcription rate and negatively with the transcription rate of *Tsix* and *Xite* (Lee and Lu, 1999; Marahrens et al., 1997; Nesterova et al., 2003; Ogawa and Lee, 2003; Penny et al., 1996). Based on their anti-sense nature, transcription initiated by the *Tsix* and *Xite* promoters may constitute a threshold for *Xist* to accumulate *in cis*. Also, *Xist* promoter related modifications could restrict the action of the XCI activator and may therefore be involved in setting up the threshold. Only when sufficient XCI activator is present in the nucleus enough *Xist* transcription is initiated to overcome *Tsix* mediated repression, thereby effectuating a probability to initiate XCI. *Xist* transcription initiation is a stochastic process itself, and depending on the nuclear XCI activator concentration, bursts of *Xist* transcription will generate a continuum of small probabilities to initiate XCI in time. This probability will drop after inactivation of an X chromosome with the decline in the XCI activator concentration that depends on the nuclear half-life of the XCI activator. In our simulations we have used a time window with a specified probability, which represents the integrated probability within that time window.

To test whether XCI is dependent on cell division, we first analyzed the number of cell divisions during a 10 day period of embryoid body (EB) differentiation, for ES cells with different X:A ratios. To determine the increase in cell number we differentiated 10^5 cells, and isolated DNA before and after differentiation. OD measurements of two independent differentiation experiments indicated that the different ES lines divided between 4 and 7 times in the 10 day differentiation period (Fig. 3a). Next, female diploid ES cells were EB differentiated for one or two days, and then subjected to γ -irradiation-, mimosine- or colcemid-mediated cell cycle arrests for one day. Initiation of XCI in treated and untreated cells was compared by counting the number of cells with or without an Xi, using RNA-FISH with an *Xist* probe. We found no significant increase or decrease in the number of cells with an Xi after

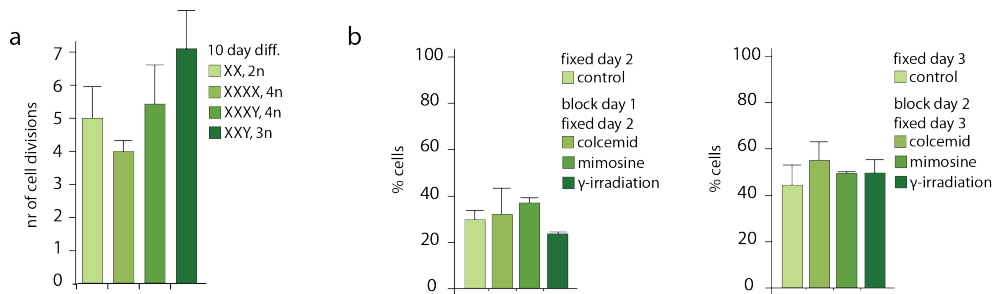


Figure 3

Initiation of XCI independent of cell division

- Determination of the number of cell divisions during a 10 day EB differentiation period. Shown are the average and standard deviation of two separate experiments with two different ES lines per X:A ratio or ploidy number.
- Analysis of initiation of XCI after a cell cycle block. Diploid female ES cells were EB differentiated for one day (left graph) or two days (right graph), and treated with colcemid or mimosine, or cells were lethally γ -irradiated, and allowed to differentiate for one more day before fixation. Control samples were allowed to differentiate for two or three days. The percentage of cells that initiated XCI was determined by *Xist* RNA FISH, followed by the quantification of the number of cells with *Xist* clouds.

cell cycle arrest, although the cells that had been γ -irradiated at day 1 showed a slight decrease in cells that initiated XCI (Fig. 3b). This result suggests that cell division is not required, or perhaps plays a minor role in the initiation of XCI. Nevertheless, cell division characteristics are important in the XCI process, because previous studies have shown that cells that inactivate too many X chromosomes stop dividing or slow down the cell division rate, which allows the cycling population of cells to outgrow the cells that inactivated too many X chromosomes (Monkhorst et al., 2008; Wutz et al., 2002).

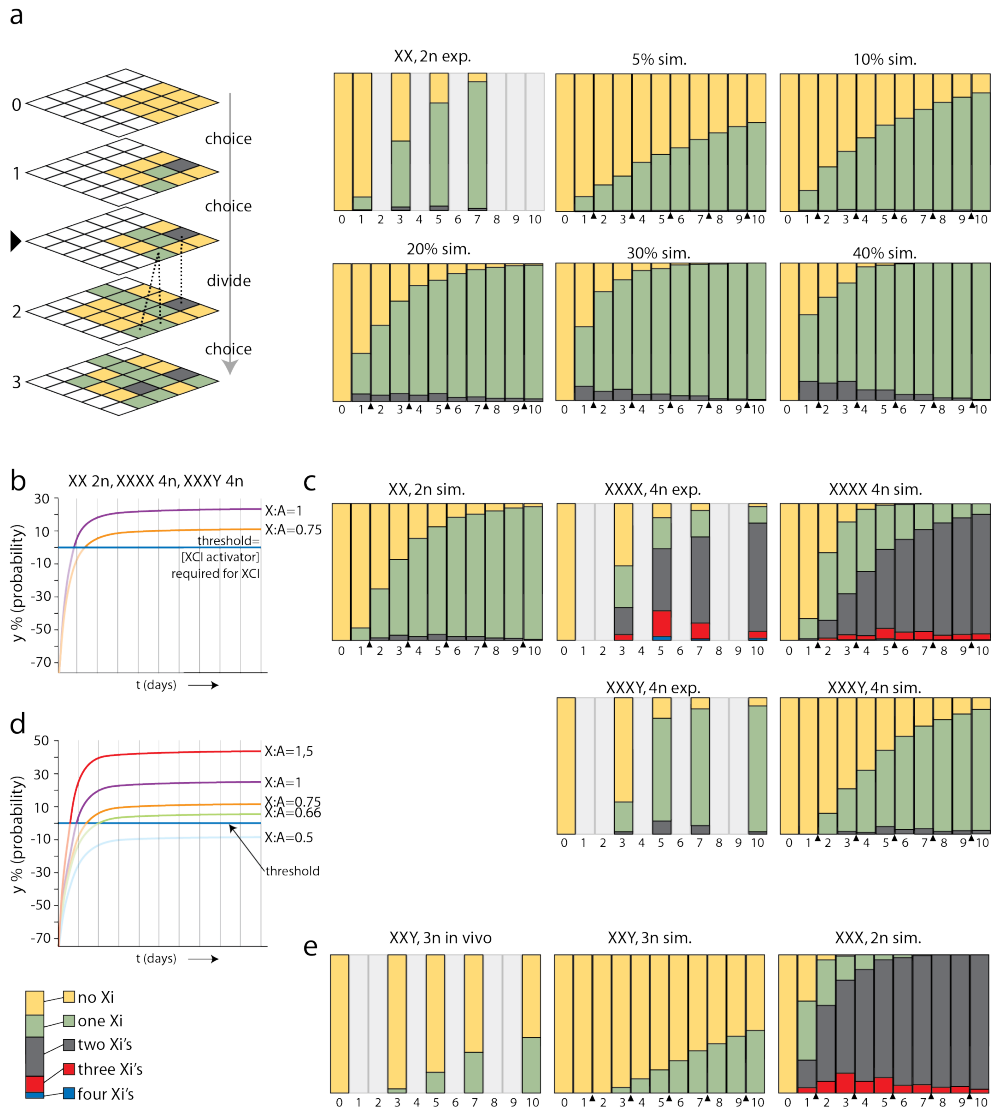
Cell selection also plays an important role in the XCI process, as male cells that inactivate their single X chromosome will die. Studies with inducible *Xist* cDNA transgenes integrated on the single X chromosome in male cells showed that *Xist* mediated silencing manifests within 24 hours, and that cell death becomes imminent within three days of *Xist* induction (Wutz et al., 2002). Also, diploid female cells inactivating two X chromosomes or incapable of initiating XCI are prone to die (Lee, 2005; Marahrens et al., 1997).

Computer simulated XCI

To comprehend the kinetics of XCI, we have developed a stochastic simulation model to determine the populations of cells with a different number of Xa's and Xi's. In this approach, the distribution of different cell populations is derived using a simulation program with a random number generator, thereby mimicking the choice process. With a small starting population of cells, as present in the female mouse embryo around the time XCI is induced, the stochasticity resulted in different outcomes of the choice process for every new calculation. This phenomenon deviates from what would be obtained in deterministic mathematical models, but corresponds to experimental reality. Our stochastic simulation of the XCI process used a three-dimensional matrix in which each Z stack represented one choice round (Fig. 4a). For our simulations we used a fixed or changing probability per choice round per X chromosome, and specific cell cycle characteristics depending on the X:A ratio.

different bar-graphs show the relative distribution of the three different cell types (XaXa = yellow, XiXa = green, XiXi = gray). Numbers below the bar graphs indicate days of differentiation (1-10), and cell division is indicated with a triangle. For time points represented by light gray bars no data is available.

- b. Probability curves representing the increase of the probability y in time based on equation [6], with $m=1$, for XX 2n and XXXX 4n cells (purple), and $m=0,75$ for XXXY 4n cells (orange). The probability at a given time point is the integrated probability over a time frame of one day. A negative value for y results in a probability of 0, and is represented by a faint line.
- c. Upper left panel shows simulation of XCI in XX diploid cells based on probabilities determined using different probabilities in time indicated in the curve, shown in Fig. 4b. Upper middle panel shows the experimental percentages of 4n XXXX cells with a different number of Xi's throughout EB differentiation. The upper right panel shows the simulation of XCI using the same parameters as used for the XX diploid simulation (XaXaXaXa = yellow, XaXaXaXi = green, XaXaXiXi = grey, XiXiXiXi = red, XiXiXiXi, blue). Bottom left panel shows the experimentally determined percentages of 4n XXXY cells with a different number of Xi's throughout EB differentiation. Bottom right panel shows the XCI simulation of 4n XXXY cells using the different probabilities in time indicated in the curve presented in (B) (XaXaXaY = yellow, XaXaXiY = green, XaXiXiY = grey, XiXiXiY = red).
- d. Curves representing the probability y in time using equation [6] for cells with a different X:A ratio, ranging from 0,5 to 1,5.
- e. Left panel shows the experimentally determined percentages of 3n XXY cells with a different number of Xi's throughout EB differentiation. Middle panel shows the XCI simulation of 3n XXY cells using different probabilities indicated in the curve presented in Fig. 4d (XaXaY = yellow, XaXiY = green, XiXiY = grey). Right panel shows the simulation of XCI in XXX 2n cells (XaXaXa = yellow, XaXaXi = green, XiXiXi = grey, XiXiXi, red).



We started by simulating the XCI process in XX diploid female ES cells throughout a 10 day differentiation period, using a fixed probability in time to run the simulations, and compared the resulting distributions with experimental data obtained with differentiating XX female ES cells. For cells with an X:A ratio ≥ 0.5 we used a cell division rate of once every two days, based on our cell division analysis (described above). In addition, the simulation assumed that cells with all X chromosomes inactivated stop dividing, which is based on previous studies (Wutz and Jaenisch, 2000). To be able to compare the simulations with available experimental data, we set the time window to 1 day, representing the integrated probability for cells choosing the X to be inactivated over 1 day. In the calculations we have excluded the option that, in XaXi cells that just have inactivated an X chromosome, the active second X chromosome may still have a probability to be inactivated. We performed the simulations with 100 cells, which mimics the number of cells present in the female mouse embryo around the time XCI is initiated. A number of 5 independent stochastic simulations generated the data for statistical analysis of the average and standard deviation. The graphs in the figures only show the average value for each time point. Comparison of the simulations, using an increasing range of fixed probabilities from 5% to 40% for both X-chromosomes, with previously obtained experimental results for differentiated XX female ES cells indicated that a fixed probability between 10% and 20% fits our experimental data best (Fig. 4a; Supplemental Fig. 2a, b and c and Supplemental Fig. 3a, b and c) (Monkhorst et al., 2008). To validate the simulation results we also compared these with data obtained using a mathematical approach where fixed probabilities were used to calculate the different XaXa, XaXi and XiXi populations, which showed similar population dynamics (Supplemental Text 1 and Supplemental Fig. 1). The fluctuation in the percentage of XiXi cells in time is the consequence of applying two choice rounds (1 per day) within one cell division (once every two days for XaXa and XaXi cells). Because cell division is synchronized in the simulations, XiXi cells are diluted out after every cell division.

From previous experimental data it appears that the probability to initiate XCI is lower in the beginning than later during the XCI process, and our experimental findings indicate that the probability is dependent on the concentration of XCI activator in the nucleus. In our model, the labile XCI activator is produced at a rate ($v_{a.synthesis}$) that is proportional to the number of active X chromosomes. This leads to the following differential equation for the concentration of the XCI activator:

$$[1] \quad \frac{d[XCI - activator]}{dt} = v_{a.synthesis}(t) - k_d \cdot [XCI - activator]$$

with:

$$[2] V_{a.synthesis}(t) = k_s [m_{active}(t)]$$

Here, k_s is the rate constant for synthesis (in $\mu\text{Molar per second per active promoter}$), and m_{active} is the number of active X chromosomes per haploid genome, which can be substituted by the X:A ratio by renormalizing the rate constant k_s . Before XCI, i.e. at the start of the simulation, all X chromosomes are active, and whenever the number of active X chromosomes remains (approximately) constant in time, the above equation integrates as:

$$[3] [XCI - activator](m, t) = \frac{m_{active} \cdot k_s}{k_d} \cdot (1 - e^{-k_d \cdot t}) = \frac{m_{active} \cdot k_s}{k_d} \cdot (1 - (1/2)^{t/t_{1/2}})$$

where:

$$[4] t_{1/2} = \frac{k_d}{\ln(2)} = 1.44 \cdot k_d$$

We expect that the decision probability for X inactivation in any very short time period, is proportional to the concentration $[y]$ of a number of molecules (or chromosome modifications) y that effectuate *Xist* promoter activation. These molecules are being synthesized through an enzymatic activity that depends on the concentration of the allosteric XCI activator through a Hill relationship, with V_{ys} and K_a , representing rate at maximum activator concentration and activation constants, respectively. Y is degraded by another enzymatic process, depending on the concentration y through a Michaelis Menten relationship, with V_{yd} and K_{My} and maximum rate and Michaelis constants, respectively. We anticipate that K_{My} is very small, whereby this degradation process of Y effectively always has the same rate. Also, we expect that y has a certain constant lability, through a first order process, with first order rate constant k_{dy} :

$$[5] \frac{dy}{dt} = \frac{[XCI - activator](t) \cdot V_{ys}}{K_a + [XCI - activator](t)} - \frac{y \cdot V_{yd}}{K_{My} + y} - k_{dy} \cdot y$$

These molecular processes will reach a quasi-steady state. Equating dy/dt to zero, and assuming that K_{My} is much smaller than any relevant concentration of y , the concentration of y is given by:

$$[6] \quad y = \left(\frac{[XCI - activator](t)}{K_a + [XCI - activator](t)} \cdot \frac{V_{ys}}{k_{dy}} - \frac{V_{yd}}{k_{dy}} \right),$$

or y will be zero if this yields a negative number. At the threshold level, y will be zero, resulting in:

$$[7] \quad [XCI - activator](t) = K_a \cdot \frac{V_{yd}}{V_{ys} - V_{yd}}$$

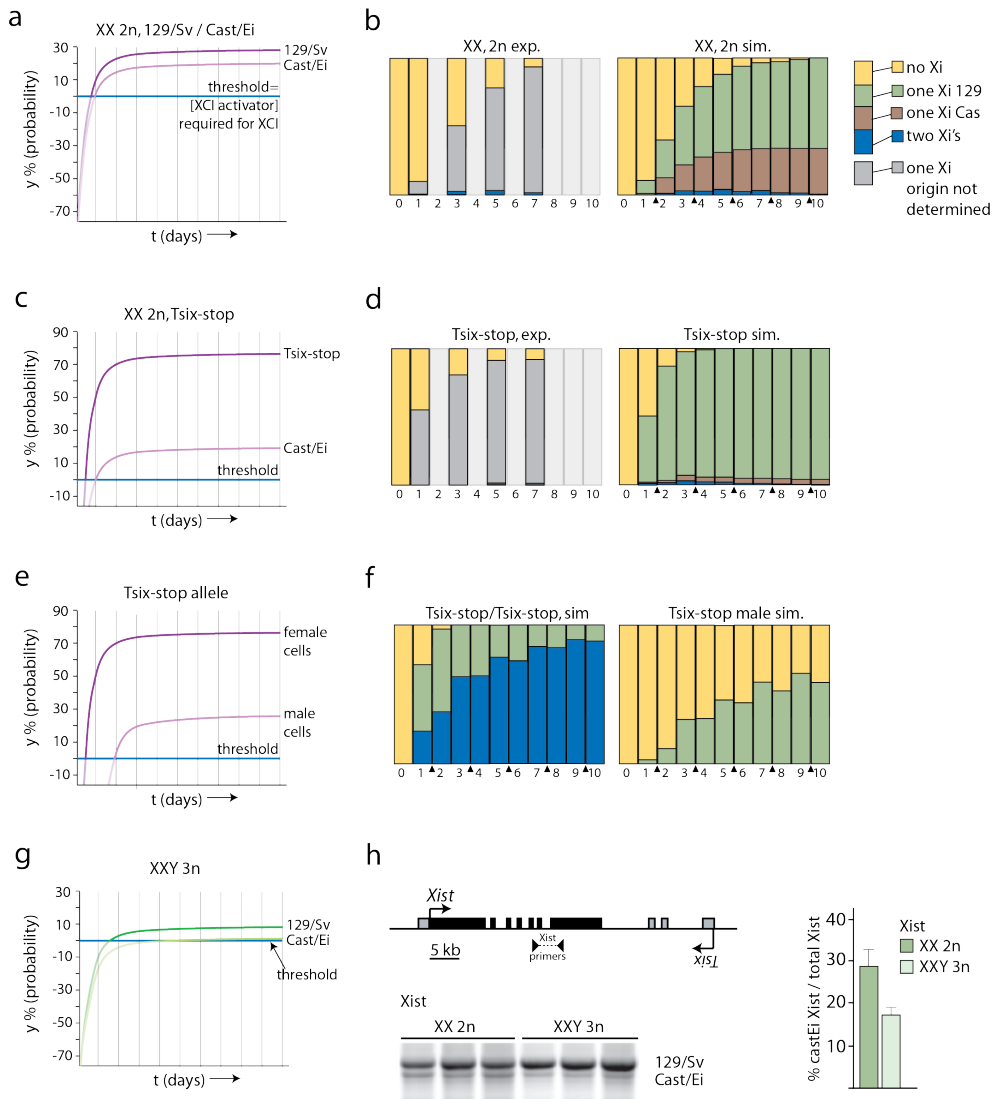
Above the threshold level its value will increase with an increase in $[XCI \text{ activator}]$ towards a maximum. By plotting y in time we generated a probability curve, which in the simulations represents the integrated probability over a time frame of 1 day. The values for y at different days from 0-10 were imported in the simulation program to assign the different X_i 's with a specific probability per choice round. After XCI has started on one or more X chromosomes, the concentration of the XCI activator will drop fairly quickly, according to the half-life of the XCI activator protein (Supplemental Text 1). For cells that started XCI in one choice round, the probability will drop according to the m value reached after that choice round.

Using graded preset values for the parameters, the outcome of simulations using the above model, was compared with experimental data sets that were obtained by differentiation of diploid XX ($m=1$) and tetraploid XXXX ($m=1$) and XXXY ($m=0.75$) cells (Monkhorst et al., 2008). This approach enabled us to obtain best-fit values for the parameters (independent variables). Probability curves for $m=1$ (2n XX and 4n XXXX) and $m=0.75$ (4n XXXY) were derived (Supplemental Fig. 4a, b and c, and Fig. 4b) with a K_a of 3.3 μM , equal to the maximum XCI activator concentration in diploid XX and tetraploid XXXX cells, and values for k_s , k_d , k_{dy} , V_{ys} and V_{yd} of 2 μM , 0.6 μM , 1.5 μM , 3 μM and 1.15 μM , respectively. These curves resulted in simulated populations with different X_a 's and X_i 's in time that matched our experimental data with diploid XX and tetraploid XXXX, XXXY cells (Fig. 4c, and Supplemental Fig. 5a and b and Supplemental Fig. 6). In a different approach, we used the same probabilities in time for diploid female XX cells in a mathematical model, and obtained distributions of different cell populations that supported our findings with the stochastic simulations (Supplemental Text 1, and Supplemental Fig. 1b).

To validate the findings, we introduced two different m values of 0.67 found in XXY triploid cells, and 0.5 found in diploid XY and tetraploid XXYY cells, keeping all other parameter values constant. The probability curves obtained with these m values resulted in a negative probability (is equal to 0) for diploid XY and tetraploid XXYY cells, as expected (Fig. 4d). For XXY cells with an $m=0.67$ we obtained a positive value for y , predicting initiation of XCI, albeit at an even lower level than found in XXXY tetraploid cells (Fig. 4d). Using the probabilities derived with $m=0.67$ we obtained simulated distributions that match well with our experimental data (Fig. 4e, and Supplemental Figure 7a). Raising m to 1.5, as found in females with an 47,XXX aneuploid karyotype, increases the probability to a maximum of 44% (Supplemental Fig. 4c and Fig. 4d). Simulations using this probability curve result in a majority of cells that inactivate two X chromosomes (Fig. 4e, and Supplemental Fig. 7b), as reported for 47,XXX human individuals. Interestingly, simulation of XXX diploid (aneuploid) cells only resulted in a 26% cell loss. This percentage is well below the 50% cell loss obtained for human individuals and viable mice with X:autosome translocations (Du Sart et al., 1992; McMahon and Monk, 1983), and does explain why mice and humans with one or more additional X chromosomes are viable. Taken together, the results show that the XCI process can be simulated using a probability curve representing the effective XCI activator concentration in combination with a threshold level required to initiate XCI.

Allele specific activation levels for the XCI activator

A stochastic model implies that different X chromosomes within one nucleus can have different probabilities to be inactivated, because X chromosome specific thresholds are determined independently. In inbred mice, the X chromosomes are genetically identical and XCI will therefore result in two evenly distributed populations of XiXa cells with one of the parental X chromosomes inactivated. However, in several F1 hybrid mice, XCI has been reported to be skewed towards one of the parental alleles. For mouse, skewing of XCI has been attributed to differences in the X controlling element (Xce), a region overlapping and extending 3' of *Xist* (Cattanach and Isaacson, 1967; Chadwick et al., 2006). In cells where two X chromosomes are present with different Xce alleles, a strong Xce is associated with a lower probability to initiate XCI compared to the X chromosome harboring the weaker Xce. These reported differences in probabilities could be explained as allele specific thresholds for the XCI activator. A more sensitive allele (weak Xce) for the XCI activator will result in a higher probability for XCI at a certain XCI activator concentration than a less sensitive allele (strong Xce). As a consequence, one XCI activator concentration can result in different probabilities for different alleles in the same nucleus. *Mus musculus castaneus* (Cast/Ei) mice harbor a strong Xce in contrast to *Mus musculus* 129/SV (129/Sv) mice, which harbor a weak Xce, and in somatic tissues of

**Figure 5****Implementing allele specific thresholds**

- a,b XCI skewing can be simulated by attributing different probabilities to the two X chromosomes in female XX cells. To simulate the 30%:70% skewing of XCI observed in Cast/Ei – 129/Sv F1 mice and differentiating F1 ES cells different allele specific probabilities were applied. b. The experimentally obtained XCI data (left panel) with differentiating XX Cast/Ei – 129/Sv F1 ES cells does not discriminate between inactivation of the Cast/Ei or 129/Sv X chromosome. Right panel shows simulations with allele specific probability curves presented in Fig. 5a.
- c. Almost complete skewing of XCI towards the *Tsix*-stop containing 129/Sv X chromosome was simulated using allele specific probabilities for the Cast/Ei and mutated 129/Sv X chromosomes.

- d. Left panel shows the experimentally obtained XCI data with 2n XX heterozygous *Tsix*-stop female cells. In this experiment no discrimination was made between inactivation of the Cast/Ei and 129/Sv X chromosomes. The right panel shows simulated XCI experiments using the probability γ presented in Fig. 5c.
- e. Predicted probabilities in time for a *Tsix*-stop X chromosome in male and female ES cells.
- f. Left panel shows simulation experiments with homozygous female *Tsix*-stop cells. Right panel shows initiation of XCI occurring in simulation experiments with *Tsix*-stop male cells.
- g. Predicted probability curves for Cast/Ei and 129/Sv X chromosomes in 3n XXY ES cells.
- h. Schematic presentation of the *Xist* locus and the localization of the PCR primers used to determine skewing of *Xist* expression. RT PCR was performed with cDNA of 7 day differentiated 2n XX cells and 3n XXY cells, with *Xist* primers spanning intron 6, amplifying a length polymorphism present in exon 7. The average percentage, and standard deviation, of *Xist* emanating from the Cast/Ei X chromosomes relative to the total amount of *Xist* is shown in the right graph.

Cast/Ei -129/Sv F1 female mice and differentiated F1 female ES cells, the 129/Sv X chromosome is inactivated in ~70% of the cells (Fig. 5h). Allele specific sequence differences in *Xist*, *Tsix*, and *Xite* will lead to different values for V_{ys} and/or V_{yd} .

As indicated above, γ may represent activated XCI activator molecules or chromatin modifications (as targets for activated XCI activator), for which V_{ys} and V_{yd} reflect the composition and breakdown, respectively, of the complex involved in *Xist* transcriptional activation and/or *Xist* RNA mediated silencing. The values for V_{ys} and V_{yd} will depend on allelic properties of different X chromosomes, such as SNPs in the Xce region associated with allelic threshold levels to initiate XCI. We have investigated both options, using different allele specific values for V_{ys} or V_{yd} . By training the stochastic simulation program, we found best-fit allele specific V_{ys} values for the 129/Sv X and Cast/Ei X alleles of 3.19 and 2.87, respectively, or V_{yd} values for the 129/Sv X and Cast/Ei X alleles of 1.05 and 1.20, respectively (Figure S4D and E). Keeping all other variables constant, these obtained values resulted in probability curves that, in stochastic simulations of XCI, generated a relative distribution of 129/Sv : Cast/Ei of 70% : 30% (Fig. 5a and 5b, and Supplemental Fig. 8a).

Completely skewed XCI has been reported in female mice and ES cells, in which *Tsix* transcription is abrogated by deletion of *Tsix* regulatory elements or a block of *Tsix* transcription through insertion of poly-adenylation sequences. These mice and ES cells show almost completely skewed XCI towards inactivation of the *Tsix* mutant X chromosome. We have recently shown that XCI starts earlier in differentiating *Tsix* mutant ES cells compared to wild type female cells, and that by day one of differentiation already 50% of the mutant cells

have initiated XCI, compared to ~10% of the wild type cells. In the stochastic simulation, a raise in the probability for the 129/Sv X chromosome harboring the *Tsix* stop by increasing V_{ys} to 4.60 μ M, results in an outcome that matched the experimental findings (Fig. 5c and 5d, and Supplemental Fig. 4f and Supplemental Fig. 8b). This simulation also shows that in this case only few cells inactivate both X chromosomes, as we previously reported (Monkhorst et al., 2008), because early during differentiation the mutant X chromosome is subject to a high probability to undergo XCI compared to the wild type X, meaning that the XCI activator level will drop well before the second X might become a target. Using the same parameters in a simulation of homozygous female *Tsix*-stop cells we found a very high number of cells inactivating both X chromosomes (Fig. 5f and Supplemental Fig. 9a), as was reported for differentiating female ES cells with a homozygous mutation of *Tsix* (Lee, 2005). Interestingly, in *Tsix*-stop male cells with $m=0.5$ we still find that y can eventually, over a period of time, reach a value above zero (Supplemental Fig. 4f), suggesting that the single X in these male cells will still have a probability to undergo initiation of XCI upon differentiation or development (Supplemental Fig. 9b). Indeed this has been reported in differentiating male ES cells with this *Tsix*-stop mutation and other mutations that abrogate *Tsix* function (Clerc and Avner, 1998; Luikenhuis et al., 2001; Morey et al., 2004; Vigneau et al., 2006).

Although the thresholds for both Cast/Ei and 129/Sv X chromosomes are similar in F1 2-1 diploid XX cells and the triploid XXY cells that we generated for this study, the putative X-encoded XCI activator concentration in the nucleus will be different. In the 3n XXY cells, the XCI activator concentration will be lower than in 2n XX cells, related to the larger volume of the nucleus of triploid cells as compared to diploid cells. Hence, the allele specific threshold for the strong Xce of the Cast/Ei X chromosome in 3n XXY cells may be too high to generate a probability to start XCI (Fig. 5g). To test whether this is true, we differentiated 2n XX and 3n XXY lines for 7 days (in triplo), and performed RT-PCR analysis with an *Xist* specific primer set. As predicted, we found that skewing of XCI is enhanced towards the weak Xce of the 129/Sv X chromosome in the 3n XXY cell lines (Fig. 5h). We conclude that the stochastic simulation studies show that our hypothesis that the probability for an X chromosome to undergo initiation of XCI is effectuated by an X-encoded activator of XCI, above a nuclear threshold level, is feasible, at least when considered in the light of the experimental information. They also demonstrated that the probability to initiate XCI may well depend on the number of X chromosomes per nucleus, the nuclear volume related to ploidy and different thresholds for specific Xce alleles.

Discussion

We have analyzed XCI in differentiating triploid mouse ES cells, and found that XXY cells with an X:A ratio of 0.67 initiate XCI less frequently compared to cells with a higher X:A ratio. Cells that do initiate XCI (XaXiY) proliferate slightly faster than XaXaY cells, and slowly accumulate in time. Simulation studies of XCI, based on a stochastic principle, indicate that XCI counting and choice can be mimicked when using a probability for an X chromosome to be inactivated, in which the probability is dependent on a nuclear XCI activator concentration acting at differential threshold levels for X chromosomes with specific Xce alleles.

Triploid ES cells and the need for speed

In this study, we have generated triploid mouse ES cells by PEG mediated fusion of diploid ES cells with haploid round spermatids. Interestingly, we could only generate triploid ES cells with a XXY karyotype, in which the Y chromosome was donated by the round spermatid. The fact that we could not generate an ES cell line with the same XXY karyotype by fusion of a male ES cell with a round spermatid donating an X chromosome indicates that the presence of a spermatid derived X chromosome results in a triploid cell that is not viable. This difference could be the consequence of epigenetic interference with transcription of the X chromosome from spermatids, which hampered the viability of our triploid cells. However, such an effect has never been reported in mice (Kaufman et al., 1989). Epigenetic modification of the X in spermatids might be a consequence of meiotic sex chromosome inactivation (MSCI) (Turner, 2007), that is overcome in normal sperm development and fertilization, but cannot be reversed by the ES cell. Indeed, fusion experiments with round spermatids harboring an X-linked *GFP* transgene indicate that the spermatidal X chromosome is not reactivated by the ES cell. In contrast, fusion of ES cells with somatic XaXi diploid cells results in proper reactivation of the inactive X chromosome (Takagi et al., 1983). Therefore, the apparent absence of spermatidal X reactivation in our triploid XXY and XXX ES cells indicates the presence of epigenetic differences laid down on an Xi during the MSCI and the XCI processes. The Y chromosome is also subject to MSCI, but fusion of XX diploid ES cells with a round spermatid containing a Y chromosome does result in viable 3n ES cell lines. This shows that the spermatidal autosomes do not affect the viability. The Y chromosome has little gene content, compared to the large X chromosome, such that possible epigenetic modification of the Y chromosomes by MSCI may not impact on the outcome of the fusion process.

The absence of triploid XYY ES cells can be attributed to these cells having an X:A ratio of 0.33, which is probably lower than required for normal viability and growth for ES cells. Lethality due to an elevated level of Y chromosome transcripts is not likely, in view of the viability of 47,XYY aneuploid male individuals. Although XYY triploid embryos have been

observed to occur in mouse and human, the observed frequencies are much lower than expected (Iliopoulos et al., 2005; Uchida and Freeman, 1985). Interestingly, for differentiating mouse triploid XXY ES cells we find many cells with a single Xa, indicating that an X chromosome under-dosage problem, of one active X per triploid genome, plays a role in particular in undifferentiated ES cells or during early embryonic development. Moreover, after 10 days of EB differentiation of these XXY triploid ES cells, we found an increase in the relative number of XaXiY cells, making up 41% of the total cell population. This indicates that XaXiY is the inactivation pattern that results in a cell with the preferred dosage of X-linked genes. This observation is supported by previous *in vivo* experiments, examining XCI in mouse XXY and XXX triploid 10 dpc (days *post coitum*) embryos, which showed that 83% of the cells were XaXiY, and 92% of the cells were XaXiXi, respectively (Speirs et al., 1990). Therefore, we conclude that mouse triploid cells preferably keep only one of their X chromosomes active.

The present observation, that after three days of ES cell differentiation 3-4% of XXY triploid ES cells have started XCI, provides additional evidence for the hypothesis that the X:A ratio indeed determines the probability to initiate XCI. Our studies also show that the XCI initiation rate for the differentiating XXY triploid ES cells is too low to allow all cells to inactivate one X chromosome within the time span where XCI can be initiated. These cells cannot meet the need for speed.

XCI counting and initiation

The finding that the probability to initiate XCI is proportional to the X:A ratio suggests the presence of an X-linked gene encoding an XCI activator, which itself is transcriptionally inactivated during the XCI process. During differentiation or development, the nuclear concentration of this XCI activator will increase and reach a threshold level required to generate a probability to initiate XCI. In cells with a relatively high X:A ratio, the XCI activator concentration will reach the threshold level at an earlier time point and will plateau at a higher level, and therefore generate a higher probability, compared to cells with a lower X:A.

Silencing of one of the XCI activator genes in female cells will lead to a drop in the XCI activator level equal to that found in male cells, which is not sufficient to initiate XCI on the remaining X. Nevertheless, *Xist* remains expressed on the Xi because its negative regulator *Tsix* is also silenced in *cis*, allowing a lower XCI activator concentration to maintain *Xist* expression. Persistent expression of *Tsix* on the Xa results in silencing of *Xist* on that chromosome. In female mice and cell lines with only one functional copy of *Xist*, XCI will only be initiated on the wild type X chromosome. If *Tsix* is intact on the other X chromosome the non functional *Xist* gene is silenced in *cis* (Sado et al., 2006). However, in female cell lines heterozygous for a single allelic region containing both a non-functional *Xist* and *Tsix* gene, the *Xist* promoter of the mutated allele will not be silenced. This explains the reported persistent expression of non-

functional *Xist* from the *Xa*, and the finding that this mutant *Xist* promoter adopts the same chromatin configuration as found for the wild type *Xist* promoter on the *Xi* (Ohhata et al., 2008).

A stochastic model for XCI, involving an X-encoded XCI activator, assumes that the nuclear volume is directly proportional to the ploidy, which in mice is indeed the case (Henery and Kaufman, 1992, 1993). We found that triploid XXY ES cells, and tetraploid XXXY and XXXX ES cells showed a significant difference in the number of cells that initiated XCI after three days of differentiation, supporting the presence of an XCI activator. Moreover, tetraploid XXXX cells have initiated XCI after three days of differentiation more effectively than diploid XX cells, despite a similar XCI activator concentration (number of X chromosomes per nuclear volume). We attribute this difference to the different number of X chromosomes, that each have a probability to initiate XCI. This is supported by our simulations, that also show a faster increase of tetraploid XXXX cells with one or more *Xi*'s than the rate of appearance of diploid XX cells with an *Xi*.

The counting and initiation phase of XCI has also been explained by the presence of an autosomally encoded blocking factor or nuclear entity, of which one dose or one functional unit is present in the diploid nucleus, preventing inactivation of one X chromosome. We advocate that our current and previous findings do not support a blocking factor model for the XCI counting and initiation process. Examination of XCI after a 3-day differentiation period of the different tetraploid cell lines showed that XCI counting works properly in XYY tetraploid cells, which only sporadically initiate XCI. Nevertheless, for the XXXY and XXXX tetraploid cell lines, we found many cells that initiated XCI on the wrong number of X chromosomes, more than one in XXXY and more than two in XXXX tetraploid cells (Monkhorst et al., 2008). A blocking factor model cannot explain these results because the two functional units of blocking factor (present in tetraploid cells) that properly block XCI on both X chromosomes in XYY cells should have done the same in XXXY and XXXX cells, which is not the case. Nevertheless, the actual results could be explained if the blocking factor is assembled out of a limiting amount of molecules as predicted by the symmetry-breaking model (Nicodemi and Prisco, 2007), which is used up with an increasing number of X chromosomes, but a comparison of our results of diploid XX cells with triploid XXY cells argues against this possibility. We found a much lower number of triploid XXY cells compared to diploid XX cells that initiated XCI at day 3, despite the fact that the concentration of the molecules making up the blocking factor would be the same in both cell lines.

Cellular population dynamics of XCI

The present simulation studies of XCI indicate that the XCI counting and initiation process can be simulated by inclusion of relatively few variable parameters. First, there is a probability to initiate XCI for any individual X chromosome. Second, specific Xce alleles respond to different nuclear threshold levels of an XCI activator. This is all that is required to explain the initiation of XCI. The simulations only tested whether a stochastic model for XCI could explain the available and new experimental data. Other models explaining the initiation phase of XCI, including the blocking factor, symmetry breaking, and transvection models, hypothesize that XCI is directed by a mutual exclusive choice process (Wutz and Gribnau, 2007). Unfortunately, this situation could not be simulated in our program. Nevertheless, the simulations based on a stochastic model make predictions, some of which we have thoroughly tested and other predictions that await further analysis.

In the computer simulations, we have used ten XCI choice rounds over a 10 day differentiation period. However, *in vivo* the number of choice rounds may be less than ten, resulting in more cells with too many Xa's, which would be selected against. This is supported by observations made in female embryos that show a significant number of cells with two Xa's after completion of the X inactivation process (Speirs et al., 1990; Webb et al., 1992). Our simulations also predict less cells with too many Xi's than we detected *in vivo*, especially for the 4n XXXX and XXXY cells. This can be explained, if initiation of XCI on the right number of X chromosomes does not result in an immediate drop of the XCI activator level below the threshold, so that XCI can still be initiated on additional chromosomes until turnover of the XCI activator has resulted in a drop below the threshold level. We have not incorporated this possibility in our simulation program.

With regard to embryo development, it is interesting that simulations with 2n XX ES cells indicate that the cell number in female diploid XX embryos will be significantly reduced by about 12% when compared to male diploid XY embryos (Figure S5, blue box). This is in the range of reported size differences between female and male embryos around the time XCI has been completed, and before hormonal cues start to influence growth of the embryo (Burgoyne et al., 1995). Therefore, this reported *in vivo* size difference could be explained by female specific cell loss as a by-product of the X inactivation process. Furthermore, for female homozygous *Tsix*-stop cells, our simulation showed that almost all the cells are lost during the XCI process. In male ES cells the reduction in expected cell number is 88%. This may explain the reported sex-ratio distortion in homozygous Δ CpG *Tsix* knockout mice (Lee, 2002). However, the high loss of cells in our simulations of male and female embryos with a homo/hemizygous *Tsix*-stop mutation indicates that these mice will most likely not be viable. Interestingly, viable mice, albeit at a lower mendelian ratio, have been reported with a homo/hemizygous Δ CpG *Tsix* knockout allele suggesting that the probability to initiate XCI for this allele is lower than for

the *Tsix*-stop allele used in our simulations (Lee, 2002). This indicates that the Δ CpG *Tsix* allele is a partial knockout of *Tsix*, which is supported by *in vivo* studies showing that a hemizygous *Tsix*-stop allele results in a non-viable phenotype, in contrast to the hemizygous Δ CpG *Tsix* mice that are viable and breed (Lee, 2002; Sado et al., 2001). Also, other mutations of *Tsix* result in activation of *Xist* in male cells upon ES cell differentiation, in contrast to male cells with a Δ CpG *Tsix* mutation that do not show initiation of XCI (Clerc and Avner, 1998; Luikenhuis et al., 2001; Morey et al., 2004; Vigneau et al., 2006).

The XCI activator has not been identified yet. However, several lines of evidence indicate that it acts through *Xist*, and could be a protein or RNA involved in activation and/or stabilization of *Xist* (Monkhorst et al., 2008). Studies with different *Tsix* mutant cell lines suggest that, in mice, *Tsix* plays a crucial role in determining the XCI activator level required for generating a probability to initiate XCI by suppression of *Xist*. In addition, chromatin modifications of the *Xist* promoter may also play a role in determining the threshold, which might be even more relevant in human were the presence and function of *TSIX* are still speculative. Identification and characterization of the XCI activator, and factors involved in setting up the threshold, will be of crucial importance for a better understanding of the initiation phase of XCI.

Materials and Methods

Culture and differentiation of ES cells

ES cells were cultured in DMEM supplemented with 15% heat inactivated foetal calf serum, 100 U ml⁻¹ penicillin, 100 mg ml⁻¹ streptomycin, non-essential amino acids, 1000 U/ml leukaemia inhibitory factor (LIF) and 0,1 mM β -mercaptoethanol. ES cells were grown on a layer of male mouse embryonic fibroblast (MEF) feeder cells. To induce differentiation into EBs, ES cells were pre-plated for 60 minutes and non-adherent ES cells were transferred to non-gelatinized bacterial culture dishes without feeder cells in differentiation medium, IMDM Glutamax, 15% heat inactivated foetal calf serum, 50 μ g/ml ascorbic acid, 100 U ml⁻¹ penicillin, 100 mg ml⁻¹ streptomycin, 37.8 μ l/l monothioglycerol.

Mice and staput isolation of round spermatids

All animals were treated in accordance with guidelines of the Erasmus MC, Rotterdam, the Netherlands. Testes from two *Ube2a* homozygous mutant mice and two *Ube2b* heterozygous mutant mice were excised and decapsulated to remove the tunica albuginea. Decapsulated testes were pooled in 20 ml PBS (140 mM NaCl, 3 mM KCl, 1.5 mM KH₂PO₄, 8 mM NaH₂PO₄) /

1.1 mM Ca^{2+} / 0.5 mM Mg^{2+} / 12 mM lactate (Sigma-Aldrich) of 34°C, containing 10mg hyaluronidase (from ovine testes, Roche-Diagnostics), 20mg trypsin (from bovine pancreas, Roche-Diagnostics) and 20 mg collagenase A (Roche-Diagnostics). Testes were shaken for 20 minutes at 90 rpm with 10 mm amplitude to release seminiferous tubuli from interstitial cells. Tubuli were collected by centrifugation for 3 minutes at 2000 rpm and resuspended in 34°C PBS/ 12 mM lactate. After shaking 10 minutes at 120 rpm with 10 mm amplitude to release germinal cells from the tubuli, tubuli remnants were removed. Germinal cells were collected by centrifugation and resuspended in 34°C PBS/ 1.1 mM Ca^{2+} / 0.5 mM Mg^{2+} / 12 mM lactate. The cell suspension was filtrated using a 60 μm filtration cloth. Germinal cells were collected by centrifugation and resuspended in 50 ml PBS/ 1.1 mM Ca^{2+} / 0.5 mM Mg^{2+} / 12 mM lactate/ 0.5% w/v BSA. Cells were separated by sedimentation velocity at unit gravity in a 1-4% w/v BSA gradient at room temperature. First 20 ml PBS/ 1.1 mM Ca^{2+} / 0.5 mM Mg^{2+} / 12 mM lactate was bottom-loaded in a chamber, followed by 50 ml cell suspension. A BSA gradient was created by loading a total of 500 ml of 1%, 2% and 4% w/v BSA in PBS. Cells were allowed to sediment for 2 hours. The chamber was emptied in 8 ml fractions using a fraction collector, and fractions containing peak amounts of cells were identified using a 340 nm UV light source. Fractions containing round spermatids were pooled, collected by centrifugation and resuspended in PBS/ 1.1 mM Ca^{2+} / 0.5 mM Mg^{2+} / 12 mM lactate. Purity of round spermatid preparations derived by this procedure were shown to be >90%, as determined by microscopic analysis of an aliquot of purified cells fixed in Bouins' fixative on glass slides (Baarends et al., 2003).

Fusion experiments

Mus musculus castaneus/ 129/Sv F1 (F1-2 1) female and C57Bl6/ 129/Sv (V6.5) male ES cell-lines were separated from MEF feeder cells by trypsinizing and preplating for 45 minutes on uncoated culture dishes. PEG1500 fusion was performed according to the manufacturer's instructions (Invitrogen). Briefly, $4 \cdot 10^6$ cells were combined with $4 \cdot 10^6$ round spermatids in DMEM. After centrifugation, cells were resuspended in 300 μl 50% v/v PEG1500 and incubated for 2 minutes at 37°C under continuous stirring. The mixture was gradually diluted with serum containing medium and plated on drug-resistant MEF feeder cells. After 24 hours medium was replaced with medium containing 0.3 $\mu\text{g}/\text{ml}$ neomycin and 2 $\mu\text{g}/\text{ml}$ puromycin. After nine days, individual ES cell colonies were picked, trypsinized and plated on individual culture dishes in neomycin and puromycin containing medium.

Cell cycle block

ES cells were EB differentiated for one or two days and then blocked in the cell cycle by adding 0.75 mM mimosine, 12 $\mu\text{l}/\text{ml}$ colcemid (KaryoMax, Gibco) or 2100centiGray γ -irradiation. Cells were fixed one day after applying the cell cycle block.

Karyotyping

ES cells were blocked in metaphase by incubation in medium containing 0.12 µg/ml colcemid for 1 hour. Cells were trypsinized and resuspended in 5 ml 0.075 M KCl at 37°C, collected and resuspended in 0.0625M KCl/ 12.5% methanol/ 4.17% acetic acid. Cells were fixed by washing three times in 75% methanol/ 25% acetic acid and stored in 200µl at 4°C. The fixed cell suspension was spotted on ethanol cleaned slides and air dried. For determining the total number of chromosomes slides were mounted with 20 µl Dapi vectashield.

To determine the number of X chromosomes, slides were denatured by a three minute incubation at 80°C in 100 µl 50% formamide/ 2x SSC/ 10 mM phosphate buffer. Subsequently slides were dehydrated, and hybridized overnight at 37°C with a Cy3 labelled X-paint probe (Cambio). After hybridization, slides were washed once with 2xSSC at 45°C, three times with 2xSSC/ 50% formamide at 45°C and two times with PBS. Slides were dehydrated through ethanol steps (70%, 90% and 100%) air-dried and mounted with 20 µl dapi vectashield. For determining the number of Y chromosomes, Y-chromosome paint (Cambio) was applied, following the same protocol as for the X chromosome paint.

RNA-FISH analysis

One day prior to fixation, non-adherent EBs were trypsinized and differentiated ES cells were grown on gelatin-coated cover slips. Cells were rinsed once with PBS and permeabilized by successive incubation in cytoskeletal buffer (100 mM NaCl, 300 mM sucrose, 3 µM MgCl₂, 10 mM PIPES pH 6.8 in H₂O) for 30 seconds, cytoskeletal buffer containing detergent (0.5% triton X-100, 100 mM NaCl, 300 mM sucrose, 3 µM MgCl₂, 10 mM PIPES pH 6.8 in H₂O) for 2 minutes and cytoskeletal buffer for 30 seconds. Cells were fixed in 4% paraformaldehyde/PBS for 10 minutes, rinsed three times with 70% ethanol and stored in 70% ethanol at 4°C.

The *Xist* probe was a digoxigenin labelled 5.5 kb cDNA sequence (Monkhorst et al., 2008). To suppress repetitive sequences 25 µg/ml mouse Cot1 DNA was added and probe mixture was incubated at 95°C for 5 minutes and at 37°C for 45 minutes. After overnight hybridization at 37°C, slides were washed in 2xSSC at 37°C for 5 minutes, and three times in 50% formamide/ 2xSSC at 37°C for 10 minutes. Probe detection was performed at room temperature. Detection was with a sheep anti-digoxigenin antibody (Roche diagnostics), followed by a FITC labelled rabbit anti-sheep antibody (Jackson labs) and a FITC labelled goat anti-rabbit antibody (Jackson labs), each for 30 minutes, in 100 mM Tris pH 7.5/ saline/ Tween, BSA. After detection cover slips were dehydrated and mounted on a slide in Vectashield and DAPI to counter stain DNA. To determine the number of inactive X chromosomes in a cell, a non-overlapped intact nucleus was selected, and the number of *Xist* clouds were scored.

BrdU analysis

For BrdU analysis, differentiated ES cells of trypsinized non-adherent EBs were grown on gelatin-coated cover slips in the presence of 20 μ M BrdU, and fixed as described in the RNA-FISH section. Cover slips were dehydrated, air-dried and denatured in 70% formamid/ 2x SSC/ 50 mM phosphate for 3 minutes at 85°C. Coverslips were washed in ice cold 70% ethanol and through 70%, 90% and 100% ethanol washes and air dried after which the *Xist* probe was applied. Detection of *Xist* RNA was as described in the previous section, detection of BrdU was performed with a mouse monoclonal BrdU antibody (DAKO), followed by a rhodamin labelled donkey anti-mouse antibody (Jackson labs), 30 minutes incubation each.

To determine the number of BrdU labelled cells for the XaXaY and XaXiY cell populations, first a microscope field was selected, containing one or more intact nuclei with an *Xist* cloud. Within this field, the number of cells containing an *Xist* cloud with negative or positive BrdU staining was determined. Subsequently this was also done for all cells without an *Xist* cloud in the same microscopic field.

DNA-FISH analysis

For DNA-FISH, cells were fixed as for RNA-FISH, and pretreated for 4 min with 0.5% pepsin in 10mM HCl at 37°C, post fixed for 5 minutes in 4% paraformaldehyde/PBS, washed twice with PBS, and dehydrated prior to denaturation. Denaturation of target sequences was as described in the BrdU analysis section. Cover slips were incubated with a combination of two biotin-labelled BACs (CT7-155J2 and CT7-474E4) at 37°C overnight. BACs were detected using mouse anti-biotin (Roche diagnostics) and donkey anti-mouse antibodies (Jackson labs) as described for RNA FISH. To determine the number of X chromosomes, non-overlapping nuclei were selected and the number of signals per nucleus was determined.

Genotyping and RT PCR analysis

For genotyping the mutant *Ube2b* allele was amplified with primers CTTTACGGTATCGCCGCTCCCGAT, TTGAAATCCGCATGAGC, and CGGAGGGAGACGTCATTG. For RT-PCR RNA was isolated with Trizol reagent, treated with RNase free DNase and reverse transcribed (all Invitrogen). *Xist* RNA was amplified with primers ACTGGGTCTTCAGCGTGA, and GGGAATAGGTAAGACAACTG spanning intron 6, which amplify a length polymorphism in exon 7 (129/Sv fragment is 888 bp, Cast/Ei fragment is 845 bp).

Stochastic simulations

Stochastic simulations were performed in a SQL based program (the source code can be found in Supplemental Text 1), using 10 Z-stacks, and 100 starting cells. The program allows the use

of different probabilities in time, a different number of X chromosomes per cell, and a different rate of cell division depending on the number of Xi's.

Acknowledgements

We would like to thank Willy Baarends and all other department members for helpful discussions.

References

- Augui, S., Filion, G.J., Huart, S., Nora, E., Guggiari, M., Maresca, M., Stewart, A.F., and Heard, E. (2007). Sensing X chromosome pairs before X inactivation via a novel X-pairing region of the Xic. *Science* 318, 1632-1636.
- Baarends, W.M., Wassenaar, E., Hoogerbrugge, J.W., van Cappellen, G., Roest, H.P., Vreeburg, J., Ooms, M., Hoeijmakers, J.H., and Grootegoed, J.A. (2003). Loss of HR6B ubiquitin-conjugating activity results in damaged synaptonemal complex structure and increased crossing-over frequency during the male meiotic prophase. *Mol Cell Biol* 23, 1151-1162.
- Borsani, G., Tonlorenzi, R., Simmler, M.C., Dandolo, L., Arnaud, D., Capra, V., Grompe, M., Pizzuti, A., Muzny, D., Lawrence, C., *et al.* (1991). Characterization of a murine gene expressed from the inactive X chromosome. *Nature* 351, 325-329.
- Brockdorff, N., Ashworth, A., Kay, G.F., McCabe, V.M., Norris, D.P., Cooper, P.J., Swift, S., and Rastan, S. (1992). The product of the mouse Xist gene is a 15 kb inactive X-specific transcript containing no conserved ORF and located in the nucleus. *Cell* 71, 515-526.
- Brown, C.J., Ballabio, A., Rupert, J.L., Lafreniere, R.G., Grompe, M., Tonlorenzi, R., and Willard, H.F. (1991). A gene from the region of the human X inactivation centre is expressed exclusively from the inactive X chromosome. *Nature* 349, 38-44.
- Brown, C.J., Hendrich, B.D., Rupert, J.L., Lafreniere, R.G., Xing, Y., Lawrence, J., and Willard, H.F. (1992). The human XIST gene: analysis of a 17 kb inactive X-specific RNA that contains conserved repeats and is highly localized within the nucleus. *Cell* 71, 527-542.
- Burgoyne, P.S., Thornhill, A.R., Boudreau, S.K., Darling, S.M., Bishop, C.E., and Evans, E.P. (1995). The genetic basis of XX-XY differences present before gonadal sex differentiation in the mouse. *Philos Trans R Soc Lond B Biol Sci* 350, 253-260 discussion 260-251.
- Cattanach, B.M., and Isaacson, J.H. (1967). Controlling elements in the mouse X chromosome. *Genetics* 57, 331-346.

- Chadwick, L.H., Pertz, L.M., Broman, K.W., Bartolomei, M.S., and Willard, H.F. (2006). Genetic control of X chromosome inactivation in mice: definition of the Xce candidate interval. *Genetics* 173, 2103-2110.
- Clerc, P., and Avner, P. (1998). Role of the region 3' to Xist exon 6 in the counting process of X-chromosome inactivation. *Nat Genet* 19, 249-253.
- Du Sart, D., Kalitsis, P., and Schmidt, M. (1992). Noninactivation of a portion of Xq28 in a balanced X-autosome translocation. *American journal of medical genetics* 42, 156-160.
- Gartler, S.M., Varadarajan, K.R., Luo, P., Norwood, T.H., Canfield, T.K., and Hansen, R.S. (2006). Abnormal X: autosome ratio, but normal X chromosome inactivation in human triploid cultures. *BMC Genet* 7, 41.
- Hadjantonakis, A.K., Cox, L.L., Tam, P.P., and Nagy, A. (2001). An X-linked GFP transgene reveals unexpected paternal X-chromosome activity in trophoblastic giant cells of the mouse placenta. *Genesis* 29, 133-140.
- Heard, E., Mongelard, F., Arnaud, D., and Avner, P. (1999). Xist yeast artificial chromosome transgenes function as X-inactivation centers only in multicopy arrays and not as single copies. *Mol Cell Biol* 19, 3156-3166.
- Hendriksson, P., Hakansson, L., and Sandahl, B. (1974). A live-born triploid infant. *Acta Paediatr Scand*, 447-449.
- Henery, C.C., and Kaufman, M.H. (1992). Relationship between cell size and nuclear volume in nucleated red blood cells of developmentally matched diploid and tetraploid mouse embryos. *The Journal of experimental zoology* 261, 472-478.
- Henery, C.C., and Kaufman, M.H. (1993). Cellular and nuclear volume of primitive red blood cells in digynic and diandric triploid and control diploid mouse embryos. *European journal of morphology* 31, 237-249.
- Herzing, L.B., Romer, J.T., Horn, J.M., and Ashworth, A. (1997). Xist has properties of the X-chromosome inactivation centre. *Nature* 386, 272-275.
- Iliopoulos, D., Vassiliou, G., Sekerli, E., Sidiropoulou, V., Tsigas, A., Dimopoulou, D., and Voyiatzis, N. (2005). Long survival in a 69,XXX triploid infant in Greece. *Genet Mol Res* 4, 755-759.
- Kaufman, M.H., Speirs, S., and Lee, K.K. (1989). The sex-chromosome constitution and early postimplantation development of diandric triploid mouse embryos. *Cytogenetics and cell genetics* 50, 98-101.
- Lee, J.T. (2002). Homozygous Tsix mutant mice reveal a sex-ratio distortion and revert to random X-inactivation. *Nat Genet* 32, 195-200.
- Lee, J.T. (2005). Regulation of X-chromosome counting by Tsix and Xite sequences. *Science* 309, 768-771.
- Lee, J.T., and Lu, N. (1999). Targeted mutagenesis of Tsix leads to nonrandom X inactivation. *Cell* 99, 47-57.
- Lee, J.T., Lu, N., and Han, Y. (1999). Genetic analysis of the mouse X inactivation center defines an 80-kb multifunction domain. *Proc Natl Acad Sci U S A* 96, 3836-3841.
- Lee, J.T., Strauss, W.M., Dausman, J.A., and Jaenisch, R. (1996). A 450 kb transgene displays properties of the mammalian X-inactivation center. *Cell* 86, 83-94.
- Leisti, J., Raivo, K.O., Rapola, J., Saksela, E., and Aula, P. (1970). Triploidy (69, XXY) in a newborn infant: a new syndrome in man? *Scand J Clin Lab Invest* 25, 60.
- Luikenhuis, S., Wutz, A., and Jaenisch, R. (2001). Antisense transcription through the Xist locus mediates Tsix function in embryonic stem cells. *Mol Cell Biol* 21, 8512-8520.
- Lyon, M.F. (1961). Gene action in the X-chromosome of the mouse (*Mus musculus* L.). *Nature* 190, 372-373.

- Marahrens, Y., Panning, B., Dausman, J., Strauss, W., and Jaenisch, R. (1997). Xist-deficient mice are defective in dosage compensation but not spermatogenesis. *Genes Dev* 11, 156-166.
- McMahon, A., and Monk, M. (1983). X-chromosome activity in female mouse embryos heterozygous for Pgk-1 and Searle's translocation, T(X; 16) 16H. *Genet Res* 41, 69-83.
- Monkhorst, K., Jonkers, I., Rentmeester, E., Grosveld, F., and Gribnau, J. (2008). X inactivation counting and choice is a stochastic process: evidence for involvement of an X-linked activator. *Cell* 132, 410-421.
- Morey, C., Navarro, P., Debrand, E., Avner, P., Rougeulle, C., and Clerc, P. (2004). The region 3' to Xist mediates X chromosome counting and H3 Lys-4 dimethylation within the Xist gene. *The EMBO journal* 23, 594-604.
- Nesterova, T.B., Johnston, C.M., Appanah, R., Newall, A.E., Godwin, J., Alexiou, M., and Brockdorff, N. (2003). Skewing X chromosome choice by modulating sense transcription across the Xist locus. *Genes Dev* 17, 2177-2190.
- Nicodemi, M., and Prisco, A. (2007). Symmetry-breaking model for X-chromosome inactivation. *Phys Rev Lett* 98, 108104.
- Ogawa, Y., and Lee, J.T. (2003). Xite, X-inactivation intergenic transcription elements that regulate the probability of choice. *Mol Cell* 11, 731-743.
- Ohhata, T., Hoki, Y., Sasaki, H., and Sado, T. (2008). Crucial role of antisense transcription across the Xist promoter in Tsix-mediated Xist chromatin modification. *Development* 135, 227-235.
- Penny, G.D., Kay, G.F., Sheardown, S.A., Rastan, S., and Brockdorff, N. (1996). Requirement for Xist in X chromosome inactivation. *Nature* 379, 131-137.
- Roest, H.P., Baarends, W.M., de Wit, J., van Klaveren, J.W., Wassenaar, E., Hoogerbrugge, J.W., van Cappellen, W.A., Hoeijmakers, J.H., and Grootegoed, J.A. (2004). The ubiquitin-conjugating DNA repair enzyme HR6A is a maternal factor essential for early embryonic development in mice. *Mol Cell Biol* 24, 5485-5495.
- Roest, H.P., van Klaveren, J., de Wit, J., van Gurp, C.G., Koken, M.H., Vermey, M., van Roijen, J.H., Hoogerbrugge, J.W., Vreeburg, J.T., Baarends, W.M., *et al.* (1996). Inactivation of the HR6B ubiquitin-conjugating DNA repair enzyme in mice causes male sterility associated with chromatin modification. *Cell* 86, 799-810.
- Sado, T., Hoki, Y., and Sasaki, H. (2006). Tsix defective in splicing is competent to establish Xist silencing. *Development* 133, 4925-4931.
- Sado, T., Wang, Z., Sasaki, H., and Li, E. (2001). Regulation of imprinted X-chromosome inactivation in mice by Tsix. *Development* 128, 1275-1286.
- Speirs, S., Cross, J.M., and Kaufman, M.H. (1990). The pattern of X-chromosome inactivation in the embryonic and extra-embryonic tissues of post-implantation digynic triploid LT/Sv strain mouse embryos. *Genet Res* 56, 107-114.
- Sun, B.K., Deaton, A.M., and Lee, J.T. (2006). A transient heterochromatic state in Xist preempts X inactivation choice without RNA stabilization. *Mol Cell* 21, 617-628.
- Takagi, N., Yoshida, M.A., Sugawara, O., and Sasaki, M. (1983). Reversal of X-inactivation in female mouse somatic cells hybridized with murine teratocarcinoma stem cells in vitro. *Cell* 34, 1053-1062.
- Turner, J.M. (2007). Meiotic sex chromosome inactivation. *Development* 134, 1823-1831.
- Uchida, I.A., and Freeman, V.C. (1985). Triploidy and chromosomes. *Am J Obstet Gynecol* 151, 65-69.

Ulrich, H.D. (2005). The RAD6 pathway: control of DNA damage bypass and mutagenesis by ubiquitin and SUMO. *Chembiochem* 6, 1735-1743.

Vigneau, S., Augui, S., Navarro, P., Avner, P., and Clerc, P. (2006). An essential role for the DXPas34 tandem repeat and Tsix transcription in the counting process of X chromosome inactivation. *Proc Natl Acad Sci U S A* 103, 7390-7395.

Webb, S., de Vries, T.J., and Kaufman, M.H. (1992). The differential staining pattern of the X chromosome in the embryonic and extraembryonic tissues of postimplantation homozygous tetraploid mouse embryos. *Genet Res* 59, 205-214.

Willard, H.F., and Breg, W.R. (1977). Two highly synchronous, early-replicating X chromosomes in fibroblasts from a live-born 69, XXY triploid infant. *Am J Hum Genet* 29.

Wutz, A., and Gribnau, J. (2007). X inactivation Xplained. *Curr Opin Genet Dev* 17, 387-393.

Wutz, A., and Jaenisch, R. (2000). A shift from reversible to irreversible X inactivation is triggered during ES cell differentiation. *Mol Cell* 5, 695-705.

Wutz, A., Rasmussen, T.P., and Jaenisch, R. (2002). Chromosomal silencing and localization are mediated by different domains of Xist RNA. *Nat Genet* 30, 167-174.

The probability to initiate X chromosome inactivation is determined by | 117
the X to autosomal ratio and X chromosome specific allelic properties

CHAPTER 3



X chromosome inactivation in a female carrier of a 1.28 Mb deletion encompassing the human X inactivation center

Bas de Hoon, Erik Splinter, Bert Eussen, Hannie Douben, Eveline Rentmeester, Monique van de Heijning, Annelies de Klein, Joop Laven, Jan Liebelt and Joost Gribnau

Submitted



Abstract

Background

X chromosome inactivation (XCI) is a mechanism specifically initiated in female cells to silence one of their X chromosomes, thereby equalizing the dose of X-linked gene products between male and female cells. XCI is regulated by a locus on the X chromosome termed the X-inactivation center (XIC). Located within the XIC is *XIST*, which acts as a master regulator of XCI. During XCI, *XIST* is up-regulated on the inactive X chromosome and chromosome-wide *cis* spreading of *XIST* leads to inactivation. In mouse, the Xic comprises *Xist* and all *cis*-regulatory elements and genes involved in *Xist* regulation. The activity of the Xic is regulated by *trans*-acting factors located elsewhere in the genome: X-encoded XCI activators positively regulating XCI, and autosomally encoded XCI inhibitors providing the threshold for XCI initiation.

Methods and results

Whether human XCI is regulated through a similar mechanism, involving *trans*-regulatory factors acting on the XIC has remained elusive so far. Here, we describe a female individual with ovarian dysgenesis and a small X chromosomal deletion of the XIC. SNP-array and Targeted Locus Amplification (TLA) analyses define the deletion to a 1.28 megabase region, including *XIST* and all elements and genes that perform *cis*-regulatory functions in mouse XCI. Cells carrying this deletion still initiate XCI on the unaffected X chromosome, indicating that XCI can be initiated in the absence of two XICs.

Conclusions

Our results indicate that the *trans*-acting factors required for XCI initiation are located outside the deletion, providing evidence that the regulatory mechanisms of XCI are conserved between mouse and human.

Introduction

In all XX female somatic cells one X chromosome is inactivated, to balance X-chromosomal gene activity to XY males (Lyon, 1961). X chromosome inactivation (XCI) is initiated early during embryogenesis, where all cells of the female embryo proper randomly initiate inactivation of either the paternal or the maternal X chromosome. After the inactive state is established, the inactive X (Xi) is clonally passed on to all daughter cells. As a result, all females are a mosaic of cells with an active paternal X chromosome and cells with an active maternal X chromosome.

Genetic studies identified a region on the X chromosome to be required for XCI. In human, this X inactivation center (XIC) has been mapped to a 680-1200 kb region at chromosome Xq13 (Allderdice et al., 1978; Lafreniere et al., 1993; Leppig et al., 1993). In mouse, the Xic is less well defined and has been mapped to a 10-20 Mb region on the X chromosome (Rastan and Robertson, 1985; Russell, 1963). The genes that constitute the XIC/Xic are conserved in eutherians, and many of them are long non-coding RNA (lncRNA) genes. The lncRNA gene *XIST/Xist* is located within the XIC/Xic and plays a key role in XCI in human and mouse (Brockdorff et al., 1991; Brown et al., 1991a). Initiation of XCI is characterized by *XIST/Xist* up-regulation on the future Xi, resulting in *cis* spreading of *XIST/Xist* RNA, which recruits chromatin remodeling complexes that silence the X chromosome (Brockdorff et al., 1992). In mouse, several other lncRNA genes located within the Xic are involved in the regulation of XCI, through co-activation and -repression mechanisms that predominantly act *in-cis* to regulate *Xist* (Barakat et al., 2014; Chureau et al., 2011; Lee et al., 1999; Nora et al., 2012; Tian et al., 2010). Female exclusive initiation of XCI is regulated by X-encoded *trans*-acting XCI activators (Monkhorst et al., 2008). To date the only known XCI activator is RING finger protein 12 (*Rnf12*, also known as RING finger LIM domain interacting protein *Rlim*) (Jonkers et al., 2009; Shin et al., 2010). *Rnf12* encodes an E3-ubiquitin ligase that targets REX1, a repressor of *Xist*, for proteasomal degradation (Gontan et al., 2012). Only in cells with more than one X chromosome present in the nucleus the XCI activator concentration is high enough to initiate XCI.

In human, the regulation of XCI is less clear. Although the XIC has been localized, the requirement for *trans*-regulatory mechanisms has not been studied. To examine whether in human XCI is also regulated by *trans*-regulatory cues acting on the XIC, harboring all the *cis*-regulatory information to direct *XIST* expression, we have identified and studied a female carrier with a deletion of the XIC.

Results

A 26 year old, intellectually normal, non-dysmorphic woman presented with primary amenorrhea, and was diagnosed with hypergonadotropic ovarian failure due to ovarian dysgenesis, also known as premature ovarian insufficiency (POI). Blood examination showed increased FSH levels (> 40 IU/l), with decreased estrogen (< 60 pmol/l). Height was between the 75th-90th centile and no stigmata of Turner syndrome were evident on examination. External genitalia were unambiguously female. Breast development, pubic and axillary hair distribution were normal female at the time of examination following several years on oral contraceptive hormone treatment. On transvaginal ultrasound examination a small uterus was visible, measuring 1,9 x 0,9 x 1,4 cm, with hypoplastic endometrium of 0,1 mm thick. No clear ovarian tissue was identified, however an area of thickening without antral follicles 0.6cm in length was seen in the left ovarian fossa and a similar region 1cm in length, in the right ovarian fossa. Karyotype analysis of blood cells showed a normal 46XX karyotype. DNA was isolated from peripheral blood and was used for molecular SNP karyotyping, using the Human OmniExpress-24 SNP-array from Illumina. Several copy number changes were identified, with the largest being a 1.08-1.24 Mb deletion on chromosome Xq13, encompassing the XIC (Fig. 1a and supplemental table 1). The centromeric breakpoint was located in a 148 kb long segment between SNPs rs6650032 and rs6650032. This region is characterized by a large inverted segmental duplication, including *DMRTC1* and *DMRTC1b*, complicating the precise mapping of this breakpoint (Fig. 1b). The location of this breakpoint determines if the duplication is intact and present as two copies of *DMRTC1* and *DMRTC1b*, or partially deleted and consequently present as a single copy of *DMRTC1* on the affected X. The telomeric breakpoint of this region was located in a 17 kb region, delineated by SNPs rs12688161 and rs5981589.

A deletion encompassing the XIC and as small as this, has not been reported before, which prompted us to study this deletion in detail. We therefore characterized the breakpoint regions by qPCR to determine the copy number at consecutive positions along the breakpoint regions. As a control, DNA from a healthy female and a healthy male was used. Primer sets and their chromosomal locations are listed in supplemental methods 1. QPCR analysis along the inverted duplication of the centromeric breakpoint region, detected two copies centromeric of the duplication, and one copy telomeric of *DMRTC1*. Three qPCR amplicons within the duplication all indicated the presence of 1.5 copies, suggesting the breakpoint is located in the middle of the duplication (Fig. 1b). Through performing qPCR along the telomeric breakpoint region, the deletion was found to extend approximately 40 kb beyond the region identified by SNP-array analysis (Fig. 1b). To map the deletion at the single nucleotide level, Targeted Locus Amplification (TLA) was performed on frozen lymphoblastoid cells. The TLA technology enables results in the sequencing of all sequences that occur in physical proximity to a primer pair used



Figure 1.

XIC deletion identified by SNP-array and qPCR.

- The XIC deletion as identified by CGH. At the top a schematic representation of the X chromosome is shown, with the deleted region marked in red. Below, a magnification of chromosome Xq13 and SNP-array results for this region is shown. In the upper graph the signal intensity of each probe is plotted against its chromosomal position. The deleted region is marked in red. The green line depicts the average intensity. The lower graph displays B allele frequency for each probe.
- Comparison of qPCR results to CGH. A magnification is shown of the regions containing the breakpoints. The top panel shows qPCR results along the breakpoint regions, with copy number plotted against chromosomal position. In the map of the chromosomal region below, the inverted duplication in the centromeric breakpoint region is marked in blue. The two panels at the bottom show the CGH results for the breakpoint regions.

for targeted amplification. Using this technology we found an increase in coverage in the center of the inverted duplication, indicating the position of the centromeric breakpoint (Fig. 2a,b).

Among the obtained reads the break-spanning read was also identified (Fig. 2c). The flanking sequence of the centromeric breakpoint maps to both duplicons of the inverted duplication, but the orientation of the sequence corresponds to the telomeric duplicon. This maps the deletion to ChrX: 72.080.568-73.367.054 (hg19), a region of 1,28 Mb and among the genes involved in the deletion are *XIST*, *TSIX* and other *cis*-regulatory sequences (Supplemental table 2).

The deletion was confirmed by DNA-FISH, using several BACs mapping to different regions of the X chromosome. DNA-FISH using BACs containing *PHKA2* or *RNF12* confirmed the presence of two X chromosomes in all nuclei, while DNA-FISH using BACS covering *XIST* or *JPX* showed the presence of these regions on only one X chromosome in all cells (Fig. 3a).

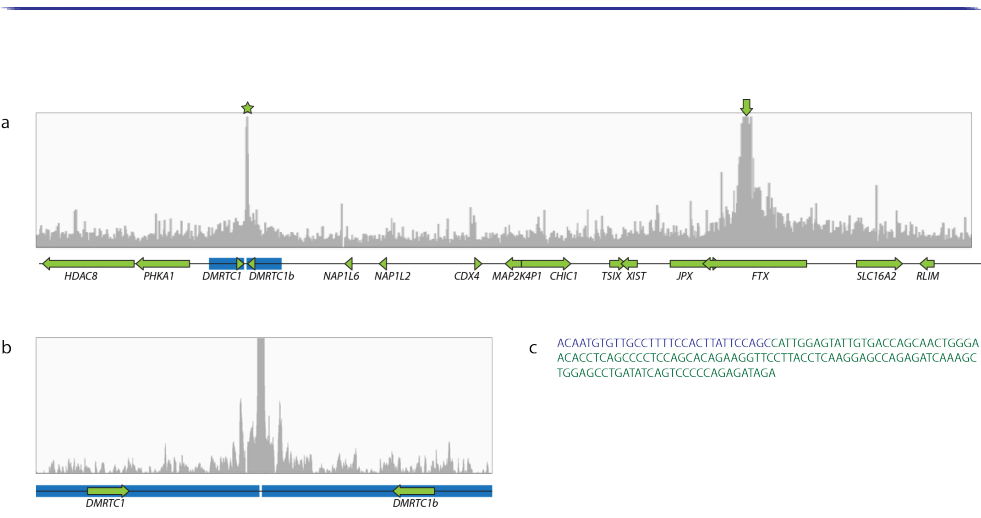


Figure 2.
XIC deletion identified by TLA

- TLA coverage is plotted against chromosomal position. Arrow indicates the location of the primer sets. Star indicates the increase in coverage on the other side of the deleted region. A genetic map of the region is shown below, with the inverted duplication in blue.
- Magnification of the centromeric breakpoint region.
- The break-spanning read, with sequence centromeric of the breakpoint marked in blue and the sequence telomeric of the breakpoint marked in green.

X chromosome inactivation in a female carrier of a 1.28 Mb deletion | 125
encompassing the human X inactivation center

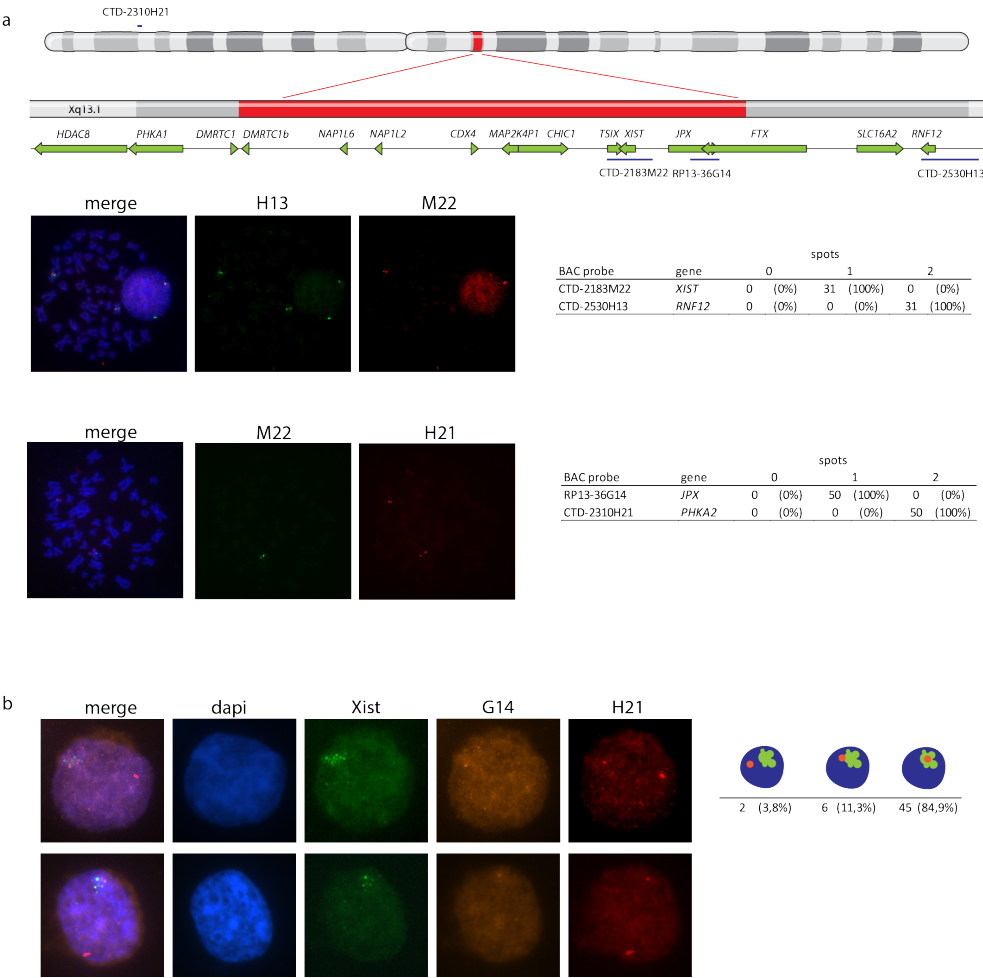


Figure 3.
The X chromosome carrying the deletion is preferentially active

- a. Shown is a map of the X chromosome with the location of the BAC probes indicated in blue (top). The location of the deletion identified by SNP-array and TLA is marked in red. Below, representative images of DNA-FISH for regions located inside or outside the deleted region are shown. BACs CTD-2310H21, CTD-2183M22, RP13-36G14, and CTD 2530H13, cover *PHKA2*, *XIST*, *JPX*, and *RNF12*, respectively. At least 30 metaphases were analyzed.
- b. Representative pictures of sequential RNA-DNA-FISH experiments. Two representative nuclei are shown with RNA-FISH results for *XIST* RNA (green), and DNA-FISH results for BAC RP13-36G14 in blue and BACs CTD-2310H21 in red. The table shows the percentage of nuclei with overlapping signals of *XIST* RNA and BAC RP13-36G14 DNA.

XCI was analyzed by *XIST* RNA-FISH on cells from a lymphoblastoid cell line of the patient. All examined cells contained an *XIST* RNA cloud, indicating XCI is initiated in with the presence of the 1,28 Mb deletion (Fig 3b). Allele specific methylation analysis of FMR, on DNA isolated of peripheral blood, showed predominant inactivation of one allele (93:7%), indicating that XCI is severely skewed in the patient. To determine which X chromosome was inactivated sequential DNA-RNA FISH was performed for *XIST* RNA and the *JPX* locus, included in the deletion. *XIST* RNA domains co-localized with the *JPX* locus of the unaffected X chromosome in most cells, indicating the preferential inactivation of the unaffected X chromosome (Fig. 3b).

Discussion

Our results indicate complete skewing of XCI, with the affected X chromosome remaining active. Therefore this deletion could possibly be involved in the ovarian dysgenesis of the female individual described here. Prior work has implicated chromosome Xq13, harboring the XIC, in amenorrhea, as several cases have been described with a breakpoint in this region and primary amenorrhea and various signs of Turner syndrome (Therman and Susman, 1990). Even though the XIC deletion was the most likely candidate region, all copy number changes were assessed for candidate genes possibly causing the ovarian phenotype. All genes affected by copy number changes were screened by Gene Ontology (GO) analysis using the AmiGO 2 browser. GO terms involved in gonadal functioning or gonadal development, revealed one candidate gene: DMRT-like family C1 (*DMRTC1*), implicated in sex differentiation, and included in the 1.28Mb deletion studied here. Little is known about *DMRTC1* itself. It is part of the Doublesex and Mab-3 Related Transcription factor (*DMRT*) gene family, involved in sex-determination in vertebrates. *DMRT1*, has been extensively studied, and loss of one copy of human *DMRT1* results in defective testicular development and XY male-to-female sex reversal. No studies regarding *DMRTC1* functioning in human are published. However, of the three mouse homologs of *DMRTC1*, *Dmrt8.3* is expressed in XX germ cells of the embryonic ovary, from embryonic day 13,5 onwards, suggesting involvement in meiosis (Chen et al., 2012). Taken together, a role for *DMRTC1* in ovarian development is likely, and it can be hypothesized that the deletion of one of the two copies present on the X chromosome causes ovarian dysgenesis in the individual described here. XCI is 100% skewed and as a result cells carrying the XIC deletion will contain only one active copy of *DMRTC1/DMRTC1b* instead of two, which might result in a dosage deficiency for *DMRTC1/DMRTC1b* (Fig. 4), leading to ovarian dysgenesis.

Our results demonstrate that in the presence of the 1.28Mb deletion, XCI can still occur on the unaffected X chromosome. Therefore, the deletion extending from *FTX* to the first duplicon of *DMRTC1*, does not affect the *trans*-regulation of XCI, but most likely covers most elements and genes involved in *cis*-regulation of human XCI. The identified deletion, and the absence of an X-inactivation phenotype resemble the Δ XTX and Δ (Xite-Dxmit171) deletions that were studied in mouse ES cells (Barakat et al., 2014; Monkhorst et al., 2008). The Δ XTX deletion involves only *Xist*, *Tsix* and *Xite*, whereas the Δ (Xite-Dxmit171) deletion also includes the neighboring regulators *Jpx* and *Ftx*. ES cells carrying heterozygous Δ XTX and Δ (Xite-Dxmit171) deletions, inactivate the wildtype X chromosome, at a rate comparable to wildtype ES cells, indicating all *trans*-acting factors are present. These results and the present human deletion indicate that *JPX*, and other sequences including *TSIX*, previously implicated in *trans*-regulation of XCI, through X-pairing and RNA mediated recruitment mechanisms, are not required to properly initiate the human XCI process (Tian et al., 2010; Xu et al., 2006). Whether the deletion described here, represents the entire *cis*-acting XIC remains elusive. This human

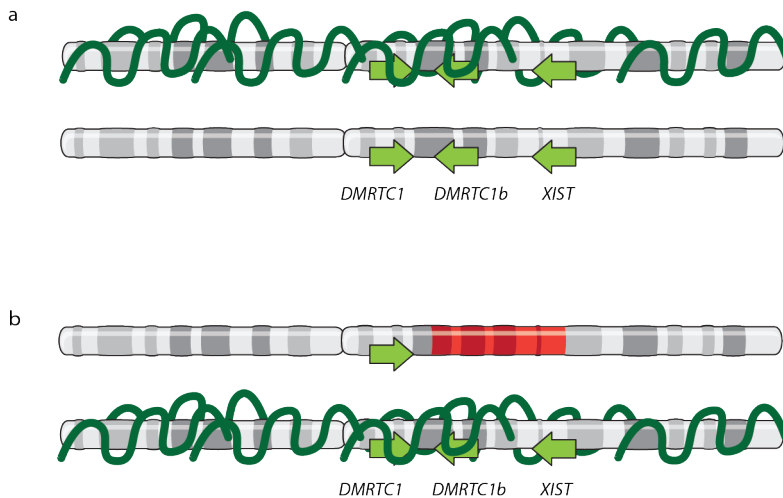


Figure 4.

***In-cis* deletion of the *cis*-XIC and *DMRTC1* results in *DMRTC1* dose deficiency.**

- Normal situation: A schematic representation of two X chromosomes after X-inactivation is shown. Two copies of *DMRTC1* remain active.
- In-cis* deletion of the XIC and *DMRTC1*: As a result of the deletion the unaffected X chromosome is preferentially inactivated, and only one copy of *DMRTC1* remains active.

cis-XIC is most likely delineated by the Topologically Associating Domain(s) (TAD) XIST, and its regulatory elements are embedded in. TADs were identified by studies examining the higher order chromatin structure, which indicated limitation of special interactions in *cis* domains of ~1Mb in size (Dixon et al., 2012; Nora et al., 2012). Analysis of available data on TADs in human H1 male ES cells and IMR90 female fibroblasts, indicates that the human XIC of H1 ES cells is included in a single large TAD, ranging from *DMRTC1* to *RNF12*, not including *RNF12* (Dixon et al., 2012). In human IMR90 fibroblasts containing an Xi, this putative *cis*-XIC is divided in two smaller TADS with the boundary at the *XIST/TSIX* locus which now includes *RNF12*, similar to mouse (Fig. 5). This change in higher order topology might be instructive in XCI and considering these data, the human XIC might extend beyond the studied deletion from *DMRTC1* to *FTX*, and might include *RNF12*.

In the female individual described here *RNF12* is not included in the deletion and still present on both X chromosomes, in support of a role for *RNF12* as *trans*-acting activator of human XCI (Fig. 3a). Such a role is further supported by a recent finding that female carriers of a mutation in *RNF12*, show exclusive XCI of the mutated X (Tonne et al., 2015). These results are concordant with mouse studies that show that one functional copy of *Rnf12* is required for establishment of the inactive X chromosome (Barakat et al., 2014).

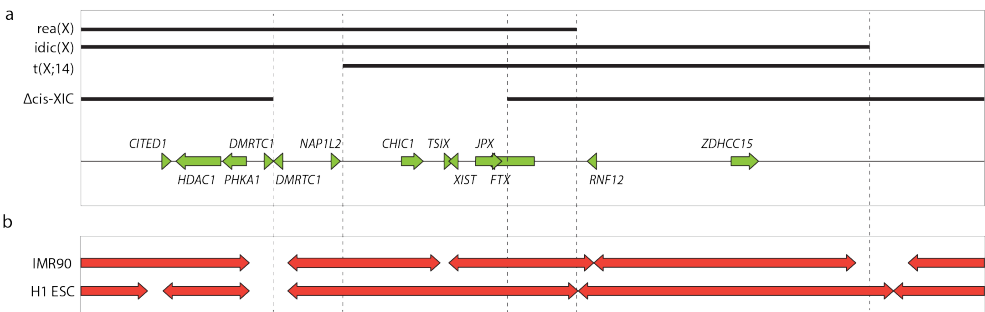


Figure 5.
Deletions delineating the human XIC

- a. Graph of the chromosomal abnormalities used to define the XIC. Black bars indicate the sequence present on the abnormal X chromosome. From top to bottom: the *rea*(X) of female S.A., the *idic*(Xp) of female A.G., the X;14 translocation chromosome from a 47XXY male, and the *cis*-XIC deletion reported here. Below, a map of the X chromosomal region Xq13.
- b. The topological domains as identified in female IMR90 fibroblasts and male H1 human ES cells.

Mouse studies also hinted at the presence of additional XCI activators besides *Rnf12*, as ES cells carrying a heterozygous *Rnf12* deletion still initiate XCI, although at a reduced frequency (Barakat et al., 2011; Shin et al., 2010). Interestingly, also in humans a hint towards the presence and location of multiple human *trans*-acting factors is provided by previous studies involving the identification of the XIC. The human XIC was defined by genetic studies involving large X chromosomal abnormalities resulting from truncations and translocations. At first the XIC was delineated by an X;14 translocation in an XXY male and the breakpoint of an idic(X) (Allderdice et al., 1978; Brown et al., 1991b; Lafreniere et al., 1993). Based on these rearrangements the XIC was estimated to measure at least 0.8 Mb in size with a maximum of 2.89 Mb (Fig. 5). Later the telomeric boundary was redefined by the rea(X), reducing the estimated size of the XIC to 0.68-1.2 Mb (Leppig et al., 1993). In all these individuals XCI is still initiated, leading to inactivation of the X;14 translocation product, or the mutated idic(X) and rea(X) X chromosomes, demonstrating the presence of sufficient levels of XCI activators for initiation of XCI. Interestingly, the rea(X) does not contain an intact copy of *RNF12*. This suggests that a single copy of *RNF12* is sufficient to initiate XCI, as is found in mouse ES cells, and that other human *trans*-acting activators exist and are located on the proportion of the X chromosome not deleted from rea(X).

In summary, our study indicates that XCI is normally initiated in a female carrier with a 1.28 Mb deletion of the XIC. Our findings also show that the *trans*-acting information required for female specific initiation of XCI is located outside the reported deletion, and highlight the evolutionary conservation of pathways and mechanisms involved in regulation of XCI in eutherians.

Material and Methods

Targeted Locus Amplification

Cross-linked chromatin, was fragmented and re-ligated, and two sets of primer pairs were designed for the sequence telomeric of the deletion, and used in individual TLA amplifications according to (de Vree et al., 2014). PCR products were purified and pooled, prepared for sequencing using the Illumina NexteraXT protocol, and sequenced on an Illumina Miseq sequencer. Reads were mapped using a BWA-SW algorithm allowing partial mapping. In case of a deletion existing interactions with the deleted region are abolished and new interactions with the new neighboring sequence are produced.

DNA-FISH

Cells were arrested in metaphase using Colcemid for 2 hours, treated with 0,075M KCl, and fixed with methanol/ acetic acid. Slides were dehydrated, denatured and incubated with probe mixture as described in (Jonkers et al., 2009). Probes, indicated in Fig 3a, were detected with a FITC conjugated mouse-anti-digoxigenin antibody or Alexa 594 conjugated Streptavidin. Metaphase spreads were first identified in DAPI and subsequently the number of red and green foci were counted.

DNA-RNA-FISH

Cytospin preparations were prepared and cells were fixed with 4% PFA, and RNA-FISH was performed as described before (Monkhorst et al., 2008). Cells were analyzed for presence of an *XIST* RNA cloud and photographs were taken. Subsequently slides were subject to DNA-FISH. Cells were denatured and incubated with probe mixture and detected with a FITC conjugated mouse-anti-digoxigenin antibody or Alexa 594 conjugated Streptavidin. Cells analyzed for RNA-FISH were re-analyzed for a DNA-FISH signal. Pictures from DNA-FISH and RNA-FISH were overlaid and scored for co-localization of signals.

RT-PCR

Quantitative RT-PCR was performed using Platinum Taq DNA polymerase (Life technologies), SYBR green (Sigma Aldrich) according to manufacturer's instructions, using primers listed in the Supplemental methods 1.

References

- Allderdice, P.W., Miller, O.J., Miller, D.A., and Klinger, H.P. (1978). Spreading of inactivation in an (X;14) translocation. *Am J Med Genet* 2, 233-240.
- Barakat, T.S., Gunhanlar, N., Pardo, C.G., Achame, E.M., Ghazvini, M., Boers, R., Kenter, A., Rentmeester, E., Grootegoed, J.A., and Gribnau, J. (2011). RNF12 activates Xist and is essential for X chromosome inactivation. *PLoS Genet* 7, e1002001.
- Barakat, T.S., Loos, F., van Staveren, S., Myronova, E., Ghazvini, M., Grootegoed, J.A., and Gribnau, J. (2014). The trans-activator RNF12 and cis-acting elements effectuate X chromosome inactivation independent of X-pairing. *Mol Cell* 53, 965-978.
- Brockdorff, N., Ashworth, A., Kay, G.F., Cooper, P., Smith, S., McCabe, V.M., Norris, D.P., Penny, G.D., Patel, D., and Rastan, S. (1991). Conservation of position and exclusive expression of mouse Xist from the inactive X chromosome. *Nature* 351, 329-331.

- Brockdorff, N., Ashworth, A., Kay, G.F., McCabe, V.M., Norris, D.P., Cooper, P.J., Swift, S., and Rastan, S. (1992). The product of the mouse *Xist* gene is a 15 kb inactive X-specific transcript containing no conserved ORF and located in the nucleus. *Cell* **71**, 515-526.
- Brown, C.J., Ballabio, A., Rupert, J.L., Lafreniere, R.G., Grompe, M., Tonlorenzi, R., and Willard, H.F. (1991a). A gene from the region of the human X inactivation centre is expressed exclusively from the inactive X chromosome. *Nature* **349**, 38-44.
- Brown, C.J., Lafreniere, R.G., Powers, V.E., Sebastio, G., Ballabio, A., Pettigrew, A.L., Ledbetter, D.H., Levy, E., Craig, I.W., and Willard, H.F. (1991b). Localization of the X inactivation centre on the human X chromosome in Xq13. *Nature* **349**, 82-84.
- Chen, H.J., Palmer, J.S., Thiagarajan, R.D., Dinger, M.E., Lesieur, E., Chiu, H.S., Schulz, A., Spiller, C., Grimmond, S.M., Little, M.H., *et al.* (2012). Identification of Novel Markers of Mouse Fetal Ovary Development. *PLoS One* **7**.
- Chureau, C., Chantalat, S., Romito, A., Galvani, A., Duret, L., Avner, P., and Rougeulle, C. (2011). *Ftx* is a non-coding RNA which affects *Xist* expression and chromatin structure within the X-inactivation center region. *Hum Mol Genet* **20**, 705-718.
- de Vree, P.J., de Wit, E., Yilmaz, M., van de Heijning, M., Klous, P., Verstegen, M.J., Wan, Y., Teunissen, H., Krijger, P.H., Geeven, G., *et al.* (2014). Targeted sequencing by proximity ligation for comprehensive variant detection and local haplotyping. *Nat Biotechnol* **32**, 1019-1025.
- Dixon, J.R., Selvaraj, S., Yue, F., Kim, A., Li, Y., Shen, Y., Hu, M., Liu, J.S., and Ren, B. (2012). Topological domains in mammalian genomes identified by analysis of chromatin interactions. *Nature* **485**, 376-380.
- Gontan, C., Achame, E.M., Demmers, J., Barakat, T.S., Rentmeester, E., van, I.W., Grootegoed, J.A., and Gribnau, J. (2012). RNF12 initiates X-chromosome inactivation by targeting REX1 for degradation. *Nature* **485**, 386-390.
- Jonkers, I., Barakat, T.S., Achame, E.M., Monkhorst, K., Kenter, A., Rentmeester, E., Grosveld, F., Grootegoed, J.A., and Gribnau, J. (2009). RNF12 is an X-Encoded dose-dependent activator of X chromosome inactivation. *Cell* **139**, 999-1011.
- Lafreniere, R.G., Brown, C.J., Rider, S., Chelly, J., Taillon-Miller, P., Chinault, A.C., Monaco, A.P., and Willard, H.F. (1993). 2.6 Mb YAC contig of the human X inactivation center region in Xq13: physical linkage of the RPS4X, PHKA1, XIST and DXS128E genes. *Hum Mol Genet* **2**, 1105-1115.
- Lee, J.T., Davidow, L.S., and Warshawsky, D. (1999). *Tsix*, a gene antisense to *Xist* at the X-inactivation centre. *Nat Genet* **21**, 400-404.
- Leppig, K.A., Brown, C.J., Bressler, S.L., Gustashaw, K., Pagon, R.A., Willard, H.F., and Distèche, C.M. (1993). Mapping of the Distal Boundary of the X-Inactivation Center in a Rearranged X-Chromosome from a Female Expressing *Xist*. *Human Molecular Genetics* **2**, 883-887.
- Lyon, M.F. (1961). Gene action in the X-chromosome of the mouse (*Mus musculus* L.). *Nature* **190**, 372-373.

Monkhorst, K., Jonkers, I., Rentmeester, E., Grosveld, F., and Gribnau, J. (2008). X inactivation counting and choice is a stochastic process: evidence for involvement of an X-linked activator. *Cell* **132**, 410-421.

Nora, E.P., Lajoie, B.R., Schulz, E.G., Giorgetti, L., Okamoto, I., Servant, N., Piolot, T., van Berkum, N.L., Meisig, J., Sedat, J., *et al.* (2012). Spatial partitioning of the regulatory landscape of the X-inactivation centre. *Nature* **485**, 381-385.

Rastan, S., and Robertson, E.J. (1985). X-chromosome deletions in embryo-derived (EK) cell lines associated with lack of X-chromosome inactivation. *Journal of Embryology & Experimental Morphology* **90**, 379-388.

Russell, L.B. (1963). Mammalian X-chromosome action: inactivation limited in spread and region of origin. *Science* **140**, 976-978.

Shin, J., Bossenz, M., Chung, Y., Ma, H., Byron, M., Taniguchi-Ishigaki, N., Zhu, X., Jiao, B., Hall, L.L., Green, M.R., *et al.* (2010). Maternal Rnf12/RLIM is required for imprinted X-chromosome inactivation in mice. *Nature* **467**, 977-981.

Therman, E., and Susman, B. (1990). The similarity of phenotypic effects caused by Xp and Xq deletions in the human female: a hypothesis. *Hum Genet* **85**, 175-183.

Tian, D., Sun, S., and Lee, J.T. (2010). The long noncoding RNA, Jpx, is a molecular switch for X chromosome inactivation. *Cell* **143**, 390-403.

Tonne, E., Holdhus, R., Stansberg, C., Stray-Pedersen, A., Petersen, K., Brunner, H.G., Gilissen, C., Hoischen, A., Prescott, T., Steen, V.M., *et al.* (2015). Syndromic X-linked intellectual disability segregating with a missense variant in RLIM. *Eur J Hum Genet*.

Xu, N., Tsai, C.L., and Lee, J.T. (2006). Transient homologous chromosome pairing marks the onset of X inactivation. *Science* **311**, 1149-1152.

CHAPTER 4



Mutations in *RNF12* segregate with X-linked intellectual disability and result in hypomorphic alleles

Suzanna Frints*, Bas de Hoon*, Cristina Gontan*, Eveline Rentmeester,
Jozef Gecz and Joost Gribnau
**authors contributed equally*

Work in progress



Abstract

Background

X-linked intellectual disability (XLID) affects 1-2% of the general population, but the genetic defect causing XLID is unknown for a large number of families. Several recent publications reported the co-segregation of XLID with mutations in *RNF12*, accompanied by skewed X chromosome inactivation (XCI) ratios in carrier females. However, a functional effect of these mutations has not been shown yet. RNF12 is a E3 ubiquitin-ligase with several known targets.

Methods and results

Here, we present three families with mutations in *RNF12* that segregate with XLID and skewed XCI. The identified mutations lead to altered ubiquitination activities and substrate binding capacities. Despite these changes in functional characteristics, changes in protein levels of its target REX1 could not be detected.

Conclusions

Our findings indicate that the three different mutations result in hypomorphic alleles. This might explain the observed XLID phenotype and skewed XCI.

Introduction

Intellectual disability (ID) is a neurodevelopmental disorder that is characterized by impaired intellectual functioning (generally defined as an IQ < 70) and by impaired adaptive behavior. Its onset during childhood or adolescence discriminates ID from adult neurodegenerative disorders like Alzheimer's disease. ID is estimated to affect 1-2% of the general population (Ellison et al., 2013; Leonard and Wen, 2002). X-linked intellectual disabilities (XLID) are forms of intellectual disability, characterized by a pattern of X-linked inheritance and thought to account for 10-12% of all male IDs (Ropers and Hamel, 2005). The attention for XLID was originally raised by the observations that ID is more prevalent among men than women and by reports of large pedigrees showing X-linked inheritance of ID. Over the last decades the number of identified X-encoded genes that cause XLID when mutated has grown substantially, and momentarily over 100 XLID genes have been identified (Piton et al., 2013). However, the potential number of XLID is estimated much higher given that around 40% of the protein-coding genes of the X chromosome are expressed in brain (Ropers, 2006). Indeed, in a large number of XLID families the molecular cause remains unidentified, and to identify new genetic causes of XLID a recent study performed exome-sequencing in probands of 405 families with unresolved XLID (Hu et al., 2015). In two families mutations in *RNF12* were identified, that co-segregate with XLID. This observation was confirmed by two other studies also describing the segregation of *RNF12* mutations with an XLID phenotype (Rodriguez Criado, 2012; Tonne et al., 2015). However, while all studies observed co-segregation of *RNF12* mutations with XLID, they did not show any functional effect of the observed mutations.

RNF12 is an E3 ubiquitin ligase, targeting other proteins for proteasomal degradation through poly-ubiquitination. The function of *Rnf12* has been thoroughly studied in mice, and was originally identified as a negative regulator of the LIM-homeodomain transcription factors, as it was shown to target co-factors LDB1 and LDB2 for proteasomal degradation (Bach et al., 1999; Ostendorff et al., 2002). Later studies implicated a role for *RNF12* in many other processes, including telomere length homeostasis, through the ubiquitination-mediated degradation of TRF1, and cell proliferation through the targeted degradation of Stathmin (Chen et al., 2014; Her and Chung, 2009). *RNF12* also affects TGF- β family signaling by targeting SMAD7 and SMURF2 for proteasomal degradation. Furthermore, *RNF12* affects expression of Estrogen responsive genes through the ubiquitination of Estrogen Receptor alpha (ER α) (Huang et al., 2011; Johnsen et al., 2009; Zhang et al., 2012). In addition, *RNF12* has been identified as an important activator of X chromosome inactivation (XCI) in mouse (Gontan et al., 2012; Jonkers et al., 2009).

XCI is an epigenetic process that compensates the genetic imbalance between XX females and XY males by inactivation of one X chromosome in every female cell (Lyon, 1961).

XCI is initiated around gastrulation in the early female embryo, and is random with respect to the parental origin of the X chromosomes. After the inactive X chromosome (Xi) is established, this inactive state is clonally passed on to all daughter cells. As a result of XCI, every female individual is a mosaic of two cell populations that carry either an inactive paternal X chromosome or an inactive maternal X chromosome (Beutler et al., 1962). In most females the ratio between cells with an inactive paternal X chromosome and an inactive maternal X chromosome is 50:50, but skewed XCI where more than 80% of the cells have inactivated the same X chromosome is common (Amos-Landgraf et al., 2006). It is thought that skewed XCI can ameliorate disease phenotypes in female carriers of X-encoded mutations by preferentially inactivating the X chromosome carrying the affected allele (Archer et al., 2007; Martorell et al., 2011).

RNF12 was identified as an activator of XCI in mouse, with most studies of the genetic elements involved in XCI being performed in mice and mouse embryonic stem cells. In mouse, XCI is regulated from a locus on the X chromosome termed the X-inactivation center (Xic) (Rastan, 1983; Rastan and Robertson, 1985). The mouse Xic can be divided in a *cis*-acting part required for *cis* inactivation of the X chromosome, and a *trans*-acting part that ensures inactivation of the correct number of X chromosomes in a cell (Gribnau and Grootegoed, 2012). The *cis*-Xic harbors the two antisense non-coding genes *Xist* and *Tsix*. *Xist* produces a non-coding RNA that accumulates on the future Xi *in-cis* and is required for inactivation, while *Tsix* acts as a repressor of *Xist* (Brockdorff et al., 1992; Lee et al., 1999; Lee and Lu, 1999; Penny et al., 1996). The *trans*-Xic contains inhibitors of XCI and *trans*-acting activators that ensure proper counting of the number of X chromosomes in relation to the ploidy of a cell and the inactivation of the correct amount of X chromosomes. To date, RNF12 is the only *trans*-acting activator that has been identified (Jonkers et al., 2009). RNF12 activates XCI by targeting the XCI inhibitor REX1 for proteasomal degradation via poly-ubiquitination, resulting in the upregulation of *Xist* (Gontan et al., 2012). Intact *Rnf12* is essential for counting the number of active X chromosomes as the introduction of additional copies of *Rnf12* coding sequences in mouse ES cells results in ectopic XCI (Jonkers et al., 2009). In addition, *Rnf12* provides feedback of XCI via its own inactivation, which lowers the concentration of RNF12 and prevents inactivation of the second X chromosome (Gontan et al., 2012). One allele of *Rnf12* needs to remain active to establish the Xi (Barakat et al., 2014).

The elements of the mouse Xic, including *Xist*, *Tsix* and *Rnf12* are conserved from mouse to human, and human *XIST* has been shown to function in a similar way to mouse *Xist*. In addition, extra copies of human *RNF12* coding sequence also lead to ectopic XCI in transgenic male and female mouse cells. However, whether RNF12 also functions as an XCI activator in human has not been shown. In a previous report we have shown that like the mouse Xic, the human XIC can be divided in a *cis*-acting part and a *trans*-acting part. Cells

carrying a deletion of the *cis-Xic* are still able to inactivate the unaffected X chromosome, indicating that a *trans*-acting activator is located outside the deletion (Chapter 3 of this thesis). Other X-chromosomal truncations and translocations limit the region where this *trans*-acting activator is located to a region telomeric of the *cis-Xic*, encompassing *RNF12* (Allderdice et al., 1978; Brown et al., 1991; Lafreniere and Willard, 1993). Interestingly, another rearrangement involving the X chromosome suggests the presence of additional *trans*-acting activators centromeric of the *cis-Xic* (Leppig et al., 1993).

Here, we report three families where mutations in *RNF12* are accompanied by XLID in males and skewed XCI in carrier females. Two of these mutations have recently been reported as newly identified associations with XLID (Hu et al., 2015). However, neither effect on *RNF12* functions have been shown yet for these mutations, nor for the other mutations that have been reported in *RNF12*. Therefore, we investigated the effect of three different mutations on the interaction of *RNF12* with REX1 and the subsequent ubiquitination and degradation of REX1. As the XLID phenotype segregating with the different *RNF12* mutations has been described elsewhere, we will not focus on the XLID phenotype. Finally, we hypothesize that functional effects of *RNF12* mutations induce skewed XCI through altered REX1 degradation.

Results

RNF12 has recently been associated with XLID in a large study performing exome sequencing in 405 families with unresolved XLID (Hu et al., 2015). In two of the analyzed families mutations in *RNF12* were identified, and subsequently a third family with XLID was also diagnosed with a mutation in *RNF12*. In all three families the mutation in *RNF12* segregates with XLID, with males being exclusively affected, while females carrying the mutation appear unaffected (Fig 1. a,b,c). Affected males show mild to profound ID, with variable behavior problems. As no other mutations segregating with the ID phenotype were identified in these families the identified *RNF12* mutations are likely to cause the phenotype. Furthermore, the three identified mutations are located in functional domains of the *RNF12* protein. All three mutations are missense mutations resulting in amino-acid substitutions. The c.1093C>T mutation identified in family 1 results in a p.Arg365Cys substitution and is located in the central region of the *RNF12* protein. This region has not been functionally characterized for human *RNF12*, but is highly conserved to the homologous region in mouse *RNF12*, which is essential for the interaction with its target proteins LDB1 and LDB2 (Fig. 1d) (Ostendorff et al., 2002). The other two mutations, c.1795C>T resulting in a p.Arg599Cys in family 2 and c.1760C>G resulting in a p.Arg578Cys in family 3, are located in the RING domain of *RNF12*, which is essential for

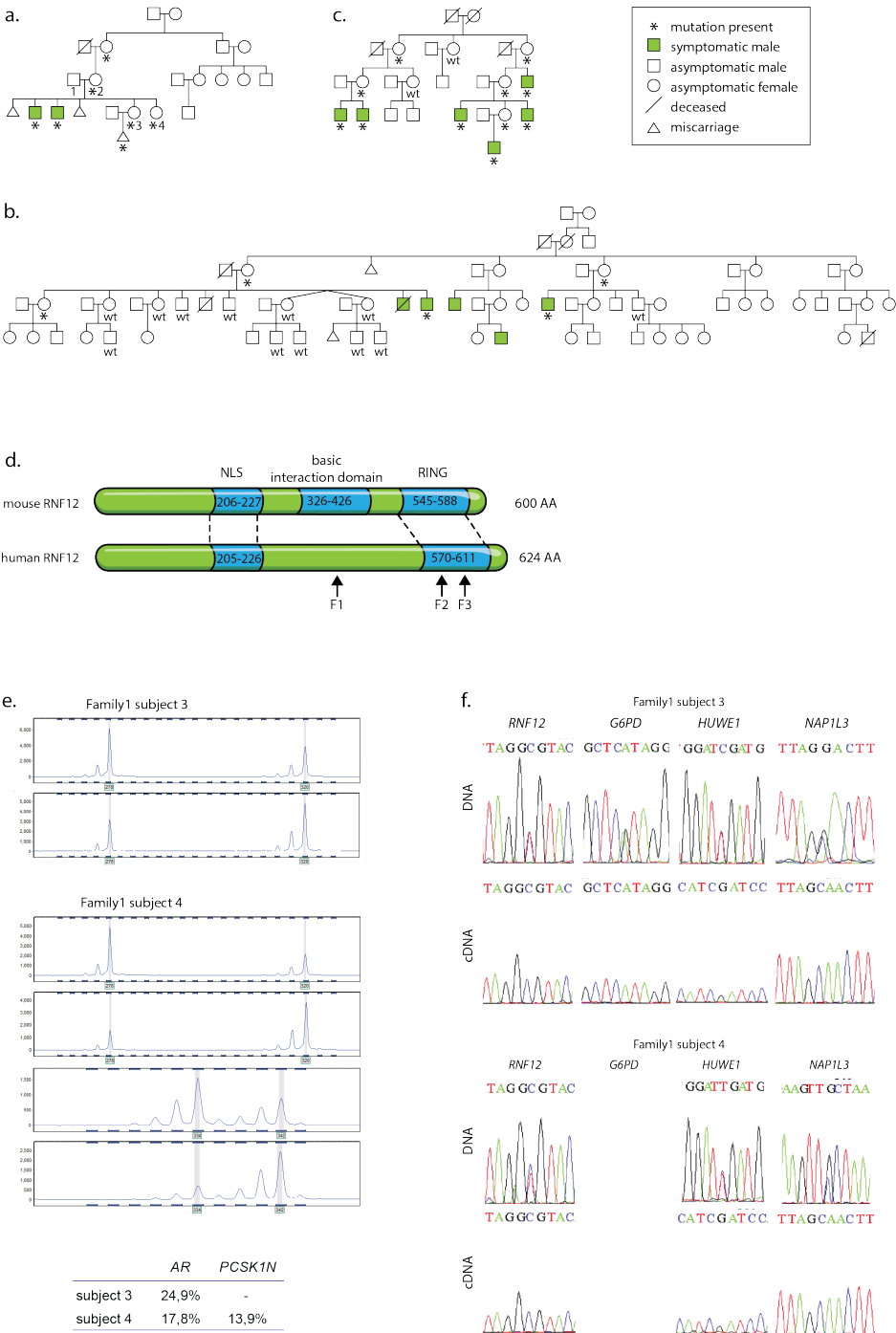


Figure 1.

Three families in which different mutations in *RNF12* co-segregate with skewed XCI.

Pedigrees of the three families carrying different mutations in *RNF12*, all segregating with XLID. The pedigrees of families 2 and 3 have been published in Hu, et al. 2015.

- a. Pedigree of family 1 with the amino-acid substitution Arg 365Cys. Subjects 1, 3 and 4 experience color blindness. Individuals 2, 3 and 4 suffer from POI.
 - b. Pedigree of family 2 with the amino-acid substitution Arg 599Cys.
 - c. Pedigree of family 3 with the amino-acid substitution Pro587Arg.
 - d. Comparison of mouse and human *RNF12* protein, with the relevant functional domains and identified mutations indicated.
 - e. Methylation-based analysis of X-inactivation ratio in skin fibroblasts from individuals 3 and 4 of family 1. Top panels show analysis for the *AR* locus, without methyl-sensitive *HpaII* digestion and with *HpaII* digestion. Bottom panels show analysis for the *PCSK1N* locus, which was informative only in individual 4, without and with *HpaII* digestion. Table indicates XIR.
 - f. Expression analysis of skin fibroblasts from subjects 3 and 4 of family 1. Sequences are shown for DNA and cDNA. Note that for *HUWE1* cDNA was sequenced in the opposite direction.
-

ubiquitination of its substrate. HOPE analysis predicts all three mutations to be damaging as they are located in functional domains or highly conserved regions (Venselaar et al., 2010).

In all three families females carrying a mutated *RNF12* allele appeared unaffected and analysis of X chromosome Inactivation Ratio's (XIR) of peripheral blood leukocytes using methylation-based analyses of the Androgen Receptor (*AR*) and Fragile X Mental Retardation 1 (*FMR1*) loci revealed highly skewed XCI in all carrier females. Considering that females carrying the mutation appear unaffected it is likely that the X chromosome harboring the mutant *RNF12* allele is exclusively inactivated. Further evidence hereto was provided by a phenotype of color vision deficiency occurring alongside the *RNF12* mutation in two female individuals from family 1 (Fig. 1b). These two female individuals inherited color vision deficiency through their father, and inherited the mutated *RNF12* allele through their mother, indicating the maternal X chromosome carrying the *RNF12* mutation is inactive while the paternal X chromosome responsible for color vision deficiency is active. To confirm that the *RNF12* mutation was located on the Xi detailed analysis of skin fibroblasts from individuals 3 and 4 was performed. Methylation based XIR analyses confirmed skewed XCI in their fibroblasts (75,1% and 84,1%), although this was less extreme than the XIR observed in peripheral blood leukocytes (91% and 100%)(Fig. 1e). This difference is likely caused by acquired changes in methylation patterns in fibroblasts during culture, as transcriptional analysis for the X-encoded genes *G6PD*, *HUWE1* and *NAP1L3* confirmed that XCI in skin fibroblasts was highly skewed, corresponding to the XIR

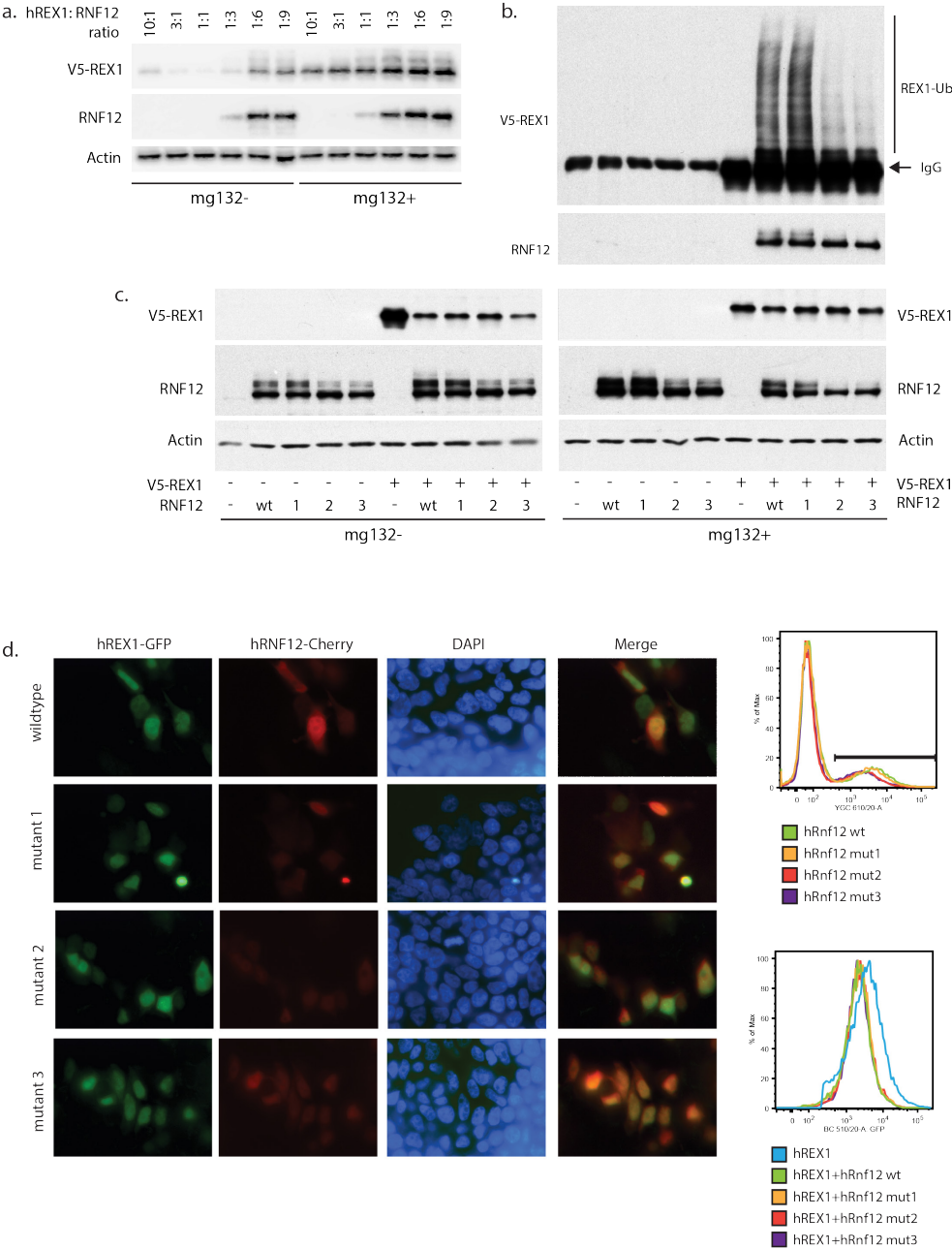
observed in peripheral blood leukocytes (Fig. 1f). Transcriptional analysis of *RNF12* revealed that the mutated allele was indeed silenced in the majority of skin fibroblasts (Fig. 1f).

To test whether the identified mutations altered RNF12 functioning, the effect of the different mutants was tested in vitro on REX1, the single known target of RNF12 during XCI. First, the proteasomal-dependent degradation of human REX1 was tested in HEK293 by co-transfecting constructs expressing *FLAG-RNF12* and *V5-REX1* in HEK293 cells. A clear increase in V5-tagged REX1 was observed upon proteasomal inhibition with mg132, indicating human REX1 is degraded by the ubiquitin proteasome, like mouse REX1 (fig. 2a). When testing different ratios of REX1: RNF12, the amount of nuclear REX1 is most completely degraded in a ratio of 3:1 to 1:3 (fig. 2a). To test the effect of the identified mutations in *RNF12* on ubiquitination of REX1, HEK293 cells were co-transfected with *FLAG-RNF12* and *V5-REX* expressing constructs. After proteasomal inhibition to allow accumulation of ubiquitinated REX1, immunoprecipitation for V5-REX1 was performed. A clear difference in REX 1

Figure 2.

RNF12 mutations result in different ubiquitination efficiencies, but not in altered target protein levels

- a. Immunoblot of nuclear protein extracts from HEK293 cells co-transfected with different ratios of *FLAG-RNF12* and *V5-REX1* expressing constructs. HEK293 cells were treated with proteasome inhibitor mg132 for 3 hours prior to protein isolation. REX1 was detected using a V5 antibody. RNF12 was detected using an RNF12 antibody.
- b. Immunoblot of immunoprecipitates for V5-tagged human REX1 from nuclear protein extracts of HEK293 cells that were transfected with human wt RNF12 or mutant RNF12 alone, or in combination with V5-tagged human REX1. HEK293 cells were treated with proteasome inhibitor mg132 for 3 hours prior to protein isolation. Immunoprecipitates were generated from nuclear extracts shown below in figure 2c.
- c. Immunoblot analysis of nuclear protein extracts from co-transfections using human REX1 and human wildtype or mutant RNF12. Left panels shows nuclear protein extracts of HEK293 cells not treated with mg132. Right panels show nuclear protein extracts of HEK293 cells cultured in the presence of mg132 for 3 hours.
- d. FACS analysis of hREX1 levels in HEK293 cells co-transfected with constructs expressing hREX1-GFP and hRNF12-Cherry. Top panel shows representative images of HEK293 cells co-transfected with different combinations of hREX1-GFP and wildtype or mutant hRNF12-Cherry. The left plot shows the GFP intensity plotted against the number of cells for cells transfected with hREX1 alone, and hREX1 co-transfected with wildtype or mutant hRNF12. Only cells expressing hRNF12-Cherry were included. The right plot shows the Cherry intensity plotted against the number of cells for wildtype and mutant hRNF12.



ubiquitination was observed between wildtype RNF12 and all three RNF12 mutants (Fig. 2b). Interestingly, RNF12 mutant 1 with a mutation in the putative interaction domain showed increased REX1 ubiquitination, while RNF12 mutants 2 and 3 containing a mutation in the RING domain showed decreased REX1 ubiquitination. In addition, the amount of RNF12 that co-immunoprecipitated with REX1, was slightly increased for mutant 1, while it was decreased for mutant 2 and 3, arguing that the three mutants have altered binding affinities. Despite the change in REX1 ubiquitination, no obvious differences in REX1 protein levels were observed between wildtype and mutant Rnf12 when nuclear extracts were analyzed by immunoblot (Fig. 2b). Also, when HEK293 cells were co-transfected with GFP-tagged REX1 and Cherry-tagged RNF12 and REX1 levels were measured by flow cytometry for GFP, no difference in REX1 levels could be detected. When co-transfected cells were treated with the proteasome inhibitor mg132 an increased level of REX1 was observed in nuclear extracts, indicating REX1 is subject to proteasomal degradation (Fig. 2b). However, no difference in REX1 accumulation was apparent between wildtype and mutant RNF12 upon proteasomal inhibition.

RNF12 levels did not differ between wildtype and mutants, whether they were transfected alone or co-transfected with *REX1* (Fig. 2b). Interestingly, an upper band representing phosphorylated RNF12 and possibly auto-ubiquitinated RNF12, was present and stronger in wildtype and mutant 1 compared to mutant 2 and 3, further confirming a functional effect of the three mutations. When Cherry-tagged RNF12 was transfected alone and levels were analyzed by flow cytometry, a slight decrease in RNF12 levels was detected for mutants 2 and 3, which is consistent with immunoblot results (Fig. 2c). In summary, the identified mutations in *RNF12* result in altered phosphorylation susceptibilities, and different capacities to ubiquitinate REX1, but do not lead to changes in REX1 protein levels in co-transfection experiments.

To test if differences in ubiquitination of REX1 resulted in an altered half-life of REX1 protein, the decay of REX1 was measured in co-transfected HEK293 cells after translational inhibition with cycloheximide. In the presence of RNF12 REX1 has a half-life of 1,7-2,0 hours. Small differences in REX1 decay were observed after two hours of cyclohexamide treatment, which shifted the half-life in the expected direction for the relative ubiquitination capacities of the three RNF12 mutants, with a shorter REX1 half-life correlating with increased ubiquitination by RNF12 mutant 1, and a longer REX1 half-life correlating with decreased ubiquitination by RNF12 mutants 2 and 3 (Fig. 3). However, these differences are not significant, as there is a large variation between experiments. Although the obtained results show that the identified mutations affect RNF12 binding and ubiquitination capacities, RNF12 functioning is not completely abolished. To confirm that the identified mutations result in hypomorphic proteins, their ability to degrade mouse REX1 was compared to mouse wildtype RNF12 and an inactive RNF12 mutant. The catalytic inactive mutant of mouse RNF12 carries

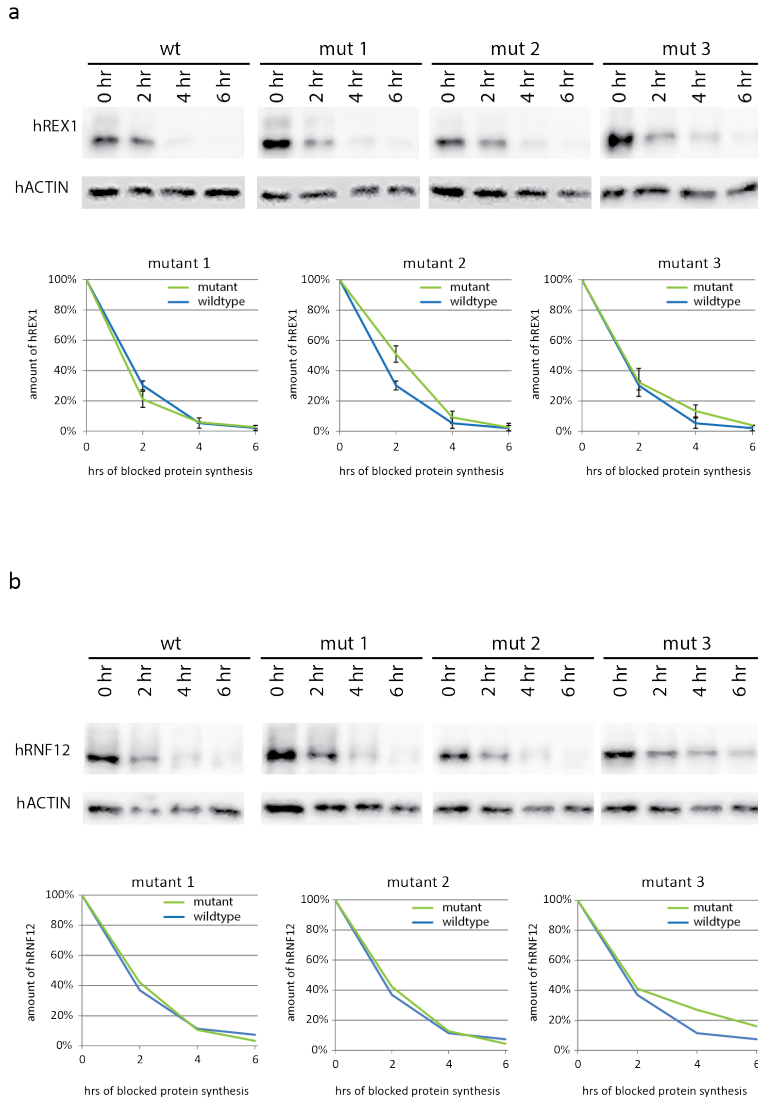


Figure 3.

hREX1 degradation is not affected by RNF12 mutation

Half-life analysis of hREX1 and hRNF12 in HEK293 cells co-transfected with constructs expressing V5-hREX1 and wildtype or mutant hRNF12. HEK293 cells were treated with to block protein synthesis for 0,2,4 and 6 hours.

- Human V5-REX1 was detected using a V5 antibody. REX1 decay curves are based on three separate Western Blots
- Human FLAG-RNF12 was detected using a FLAG antibody. RNF12 decay curves are based on one Western Blot. Decay curves were plotted using the 0 hour measurement as reference.

two mutations in the RING domain (H569A, C572A) that completely abolish its capacity to ubiquitinate REX1. Where both mouse and human wildtype RNF12 completely degrade REX1, the catalytic inactive version of mouse RNF12 is unable to degrade REX1. In comparison, the identified RNF12 mutants are able to degrade mouse REX1 to an extent almost comparable to wildtype RNF12. These results suggest that the identified mutants in RNF12 indeed result in hypomorphic alleles.

Discussion

We present three families with different mutations in *RNF12* segregating with XLID in males and skewed XCI in females. The identified mutations in *RNF12* are most likely causing the XLID phenotype, as XLID phenotype segregates with the XLID phenotype in all three families. Using exome sequencing, no other mutations segregating with the XLID phenotype were identified. The association of *RNF12* mutations with XLID is further supported by two other recently published families where other mutations in *RNF12* co-segregate with a XLID phenotype, similar to that described here (Rodríguez Criado, 2012; Tonne et al., 2015). While the association of XLID with mutations in *RNF12* has been described before, none of these reports have shown a functional effect of the identified mutations on RNF12 functioning. Here, we show that the identified mutations affect the ubiquitination capacity and substrate binding capacity of RNF12. The mutation of family 1, located in the putative substrate binding domain, results in increased substrate ubiquitination and increased binding affinity. In contrast, the mutations identified in families 2 and 3 which are located in the RING domain of RNF12 result in a reduced ubiquitination capacity.

Interestingly, while our results showed a clear effect of the identified mutations on the ubiquitination capacity of RNF12, our results did not reveal a change in REX1 protein levels or REX1 half-life. Although this might be a consequence of the used experimental setup involving transient expression of *RNF12* and its substrate *REX1* in HEK293 cells, it could also be that ubiquitination of human REX1 might not result in targeted degradation, but instead in altered cellular localization or different DNA-binding capacities. However, this contrasts with the observed proteasomal degradation that is suggested by the accumulation of ubiquitinated REX1 upon proteasomal inhibition (Fig. 2a). This discrepancy in results could be a consequence of transient overexpression of *REX1* and *RNF12*. In addition, the used co-transfection assay might not be sensitive enough to detect changes in REX1 protein levels.

Regardless of an effect of the identified *RNF12* mutations on REX1 protein levels, it is unlikely that the XLID phenotype is caused by altered REX1 levels. REX1 is not expressed in

brain, the tissue that would be expected to be primarily affected in XLID. Instead, REX1 is a pluripotency marker, that is expressed in stem cells and which expression is lost upon differentiation. Therefore, it seems more likely that mutations in *RNF12* result in XLID by altering protein levels of a substrate other than REX1. Several substrates have been identified and have been shown to be degraded after poly-ubiquitination by *RNF12* (Bach et al., 1999; Chen et al., 2014; Her and Chung, 2009; Huang et al., 2011; Ostendorff et al., 2002; Zhang et al., 2012). Of these substrates, several are involved in signaling cascades involved in embryonic development, and can therefore be considered interesting candidates as intermediates in causing the XLID phenotype.

In all three families reported here, females carrying the mutation exhibit skewed XCI in which the X chromosome carrying the mutant *RNF12* allele is inactivated. This skewed XIR could be the result of primary skewed XCI, in which the cells of the early female embryo undergoing XCI all inactivate the X chromosome carrying the mutation, or post-XCI secondary cell selection, where a selective pressure favors cells carrying an active wildtype X chromosome. Given the function of mouse *Rnf12* as a *trans*-acting activator of XCI, it is not unlikely that the identified mutations in human *RNF12* result in primary skewed XCI. However, the involvement of human *RNF12* and *REX1* in XCI has not been demonstrated yet. As the identified *RNF12* mutations clearly affect REX1 ubiquitination, a functional effect of REX1 protein levels on *XIST* expression should be demonstrated to confirm that human *RNF12* also functions as a *trans*-acting activator of XCI. Although a function as a *trans*-acting activator has not been shown yet for human *RNF12*, observations from individuals carrying X-chromosomal aberrations make *RNF12* a likely candidate for this function.

Although a human *trans*-acting activator of XCI has not been identified yet, observations from individuals carrying X-chromosomal aberrations make *RNF12* a likely candidate for this function. In a previous report we described a female individual carrying a 1,28 Mb deletion encompassing *XIST* and *TSIX*, but leaving *RNF12* intact (De Hoon et al, unpublished). As XCI was still present in cells heterozygous for this deletion a *trans*-acting activator must be located outside this deletion. Other X chromosomal truncations and translocations limit the region where this *trans*-acting activator is located to a region telomeric of the *cis*-XIC, encompassing *RNF12* (Allderdice et al., 1978; Brown et al., 1991; Lafreniere and Willard, 1993). It is interesting to note that one X-chromosomal rearrangement lacking *RNF12* suggests the presence of additional *trans*-acting activators centromeric of the *cis*-XIC (Leppig et al., 1993). In addition, a strong conservation of *RNF12* between mouse and human, with 89% protein sequence similarity, suggests that *RNF12* performs a comparable function in humans and mice (Ostendorff et al., 2000). It should also be noted that in mouse, *Rnf12* is the only *trans*-acting activator of XCI identified to date, and that in human no alternative *trans*-acting activator has been identified.

If indeed, human *RNF12* functions as a *trans*-acting activator of XCI, it can be hypothesized that the observed mutations in *RNF12* result in primary skewed XCI, as mouse cells carrying a heterozygous deletion of *Rnf12* show primary skewed XCI in which the mutant X chromosome is preferentially inactivated (Barakat et al., 2014; Jonkers et al., 2009; Shin et al., 2010). This hypothesis is supported by the observation that two female carriers of family 1 show skewed XCI in multiple tissues of different embryonic origin.

In summary, we present three families with XLID segregating with different mutations in *RNF12*. We provide evidence that the identified mutations alter the capacity of *RNF12* to bind and ubiquitinate target proteins. A function of *RNF12* as a *trans*-acting activator of XCI can be hypothesized based on other studies involving chromosomal deletions, and on the skewed XIR that is observed in multiple tissues of two carrier females of family 1, and therefore is likely to be primary. To demonstrate that *RNF12* acts as a *trans*-acting activator of human XCI, it should be shown that its target *REX1* regulates *XIST* expression.

Methods

Skewing analysis

Genomic DNA was isolated using phenol/chloroform extraction and subjected to digestion with and *EcoRI* and methylation sensitive *HpaII*, or *EcoRI* alone over night at 37°C. Restriction enzymes were inactivated by incubating at 80°C for 25 minutes. The CAG repeat of the Androgen Receptor gene was amplified using primers TGCAGTTAGGGCTGGGAAGG and CTGTGGGGCCTCTACGATGG. The AC repeat in the *SLITRK4* gene was amplified using primers GCACACAAGCAGTCCTTCCT and TGGCTTCTTGTTGCTCTCT. The tandem CA and AG repeat of *PCSK1N* was amplified using primers ATGCGAAGACCATTCCTCT and GTGCGTGTGATGTGAGGAGA. The amplified products were analyzed separately on an ABI3130 genetic analyzer.

Expression analysis

The presence of informative SNPs was analyzed on genomic DNA using primers TCCGTGACTCTGCCCTTCC and GCTGCCAGTGGTGAATCTACAGG for *RNF12*, GCTGGGTAGAATTAAAGCTCTGC and GGGCAAATACACAACACATAGAAAACG for *HUWE1*, primers TGCAGAGTTGGTGGGACAGG and CCCTCGCTGCTGCTACTACCC for *G6PDX*, and primers TCAGGGTTGCCTCCATACAG and CAGCAGTGATGAGGAGGTGCA for *HUWE1*. PCR products were analyzed using Sanger sequencing. CDNA was generated using Superscript® II First Strand Synthesis kit and DNase I from Life Technologies, according to the manufacturer's instructions.

Expression of *RNF12* mutation was analyzed by PCR using primers CCGATTGGATCGAGAAGAAGC and TTCTACGAATGGGAATTCTGATGG. Expression of SNPs was analyzed for G6PDX using primers CCGTGTACACCAAGATGATGACC and CCAGGAATGTGCAGCTGAGG, for HUWE1 using primers TGCTACCCGTGAAGTCCTTGG and CTTGGGGGAGGAGCAGTGG, and for NAP1L3 using primers AAGAAGAATGTGAATGGAATTCAGAGG and CAATCAGCCAATAGTCAGGAATGC.

Generation of RNF12 and REX1 encoding constructs

The coding sequences from human *RNF12* and *REX1* were amplified from human cDNA and cloned into the TOPO Blunt II vector from Invitrogen. Mutations in *RNF12* were generated using site-directed mutagenesis. *RNF12* coding sequences were subcloned in pCAG-Flag, a CAG-driven expression vector containing a Flag-tag (gift from D. van den Berg) and a modified pCherry-C1 vector (gift from H. Lans). *REX1* coding sequence was cloned into pCAG-Flag-V5 (gift from H. Lans) and pEGFP-N3 (Clontech).

Cell culture and transfection

HEK 293 cells were cultured under standard conditions with 50% DMEM/ 50% Ham's F10, supplemented with 15% heat inactivated fetal calf serum, 100 U ml⁻¹ penicillin, 100 mg ml⁻¹ streptomycin, non-essential amino acids. Cells were transiently transfected using polyethylenimine (Polysciences) for 48 h with 2 µg wild-type or mutant *Rnf12* expression vectors, in the absence or presence of 2 µg V5-tagged Rex1 expression vector. Where indicated, cells were treated with 15 µM proteasome inhibitor MG132 for 3 h (Sigma). For half-life analysis cells were incubated with 50 µg/ml Cyclohexamid, 24 hours after being transfected.

Nuclear extract preparation

Cells were collected by scraping in ice-cold PBS. To isolate nuclear extracts cells were incubated with 400 µl buffer containing 10 mM Hepes, 1.5 mM MgCl₂, 10 mM KCl, 0.5 mM DTT, protease inhibitor, and 15 uM MG132 for 10 minutes on ice. After vortexing briefly, nuclei were resuspended in buffer containing 20 mM Hepes, 25% glycerol, 420 mM NaCl, 1.5 mM MgCl₂, 0.2 mM EDTA, 0.5 mM DTT, protease inhibitor and 15 uM MG132 and incubated for 20 minutes, on ice. After centrifugation, the supernatant was used as nuclear extract. For immunoblotting 20 µg of nuclear extract was used and detected with antibodies against REX1, RNF12, V5-tag, and actin was used as a loading control.

To recover V5-tagged REX1 15 µl of V5 antibody-agarose beads (Sigma) were added to nuclear extracts and the mixture was centrifugated for 10 minutes at 4 °C. Beads were washed with buffer containing 20 mM Hepes, 10% glycerol, 150 mM KCl, 1.5 mM MgCl₂, 0.2 mM EDTA, 0.02% NP40, 0.5 mM DTT, protease inhibitors and 15 µM mg132. Bound proteins were eluted

with sample buffer and visualized by immunoblotting. Co-immunoprecipitated RNF12 was detected with RNF12 antibody, and poly-ubiquitinated REX1 with a V5 antibody.

References

- Allderdice, P.W., Miller, O.J., Miller, D.A., and Klinger, H.P. (1978). Spreading of inactivation in an (X;14) translocation. *Am J Med Genet* 2, 233-240.
- Amos-Landgraf, J.M., Cottle, A., Plenge, R.M., Friez, M., Schwartz, C.E., Longshore, J., and Willard, H.F. (2006). X chromosome-inactivation patterns of 1,005 phenotypically unaffected females. *Am J Hum Genet* 79, 493-499.
- Archer, H., Evans, J., Leonard, H., Colvin, L., Ravine, D., Christodoulou, J., Williamson, S., Charman, T., Bailey, M.E., Sampson, J., *et al.* (2007). Correlation between clinical severity in patients with Rett syndrome with a p.R168X or p.T158M MECP2 mutation, and the direction and degree of skewing of X-chromosome inactivation. *J Med Genet* 44, 148-152.
- Bach, I., Rodriguez-Esteban, C., Carriere, C., Bhushan, A., Krones, A., Rose, D.W., Glass, C.K., Andersen, B., Izpisua Belmonte, J.C., and Rosenfeld, M.G. (1999). RLIM inhibits functional activity of LIM homeodomain transcription factors via recruitment of the histone deacetylase complex. *Nat Genet* 22, 394-399.
- Barakat, T.S., Gunhanlar, N., Pardo, C.G., Achame, E.M., Ghazvini, M., Boers, R., Kenter, A., Rentmeester, E., Grootegoed, J.A., and Gribnau, J. (2011). RNF12 activates Xist and is essential for X chromosome inactivation. *PLoS Genet* 7, e1002001.
- Barakat, T.S., Loos, F., van Staveren, S., Myronova, E., Ghazvini, M., Grootegoed, J.A., and Gribnau, J. (2014). The trans-activator RNF12 and cis-acting elements effectuate X chromosome inactivation independent of X-pairing. *Mol Cell* 53, 965-978.
- Beutler, E., Yeh, M., and Fairbanks, V.F. (1962). The normal human female as a mosaic of X-chromosome activity: studies using the gene for C-6-PD-deficiency as a marker. *Proc Natl Acad Sci U S A* 48, 9-16.
- Brockdorff, N., Ashworth, A., Kay, G.F., McCabe, V.M., Norris, D.P., Cooper, P.J., Swift, S., and Rastan, S. (1992). The product of the mouse Xist gene is a 15 kb inactive X-specific transcript containing no conserved ORF and located in the nucleus. *Cell* 71, 515-526.
- Brown, C.J., Lafreniere, R.G., Powers, V.E., Sebastio, G., Ballabio, A., Pettigrew, A.L., Ledbetter, D.H., Levy, E., Craig, I.W., and Willard, H.F. (1991). Localization of the X inactivation centre on the human X chromosome in Xq13. *Nature* 349, 82-84.
- Chen, X., Shen, J., Li, X., Wang, X., Long, M., Lin, F., Wei, J., Yang, L., Yang, C., Dong, K., *et al.* (2014). Rlim, an E3 ubiquitin ligase, influences the stability of Stathmin protein in human osteosarcoma cells. *Cell Signal* 26, 1532-1538.

- Ellison, J.W., Rosenfeld, J.A., and Shaffer, L.G. (2013). Genetic basis of intellectual disability. *Annu Rev Med* 64, 441-450.
- Gontan, C., Achame, E.M., Demmers, J., Barakat, T.S., Rentmeester, E., van, I.W., Grootegoed, J.A., and Gribnau, J. (2012). RNF12 initiates X-chromosome inactivation by targeting REX1 for degradation. *Nature* 485, 386-390.
- Gribnau, J., and Grootegoed, J.A. (2012). Origin and evolution of X chromosome inactivation. *Curr Opin Cell Biol* 24, 397-404.
- Her, Y.R., and Chung, I.K. (2009). Ubiquitin Ligase RLIM Modulates Telomere Length Homeostasis through a Proteolysis of TRF1. *J Biol Chem* 284, 8557-8566.
- Hu, H., Haas, S.A., Chelly, J., Van Esch, H., Raynaud, M., de Brouwer, A.P., Weinert, S., Froyen, G., Frants, S.G., Laumonnier, F., *et al.* (2015). X-exome sequencing of 405 unresolved families identifies seven novel intellectual disability genes. *Mol Psychiatry*.
- Huang, Y., Yang, Y., Gao, R., Yang, X., Yan, X., Wang, C., Jiang, S., and Yu, L. (2011). RLIM interacts with Smurf2 and promotes TGF-beta induced U2OS cell migration. *Biochem Biophys Res Commun* 414, 181-185.
- Johnsen, S.A., Gungor, C., Prenzel, T., Riethdorf, S., Riethdorf, L., Taniguchi-Ishigaki, N., Rau, T., Tursun, B., Furlow, J.D., Sauter, G., *et al.* (2009). Regulation of estrogen-dependent transcription by the LIM cofactors CLIM and RLIM in breast cancer. *Cancer Res* 69, 128-136.
- Jonkers, I., Barakat, T.S., Achame, E.M., Monkhorst, K., Kenter, A., Rentmeester, E., Grosveld, F., Grootegoed, J.A., and Gribnau, J. (2009). RNF12 is an X-Encoded dose-dependent activator of X chromosome inactivation. *Cell* 139, 999-1011.
- Lafreniere, R.G., and Willard, H.F. (1993). Pulsed-field map of Xq13 in the region of the human X inactivation center. *Genomics* 17, 502-506.
- Lee, J.T., Davidow, L.S., and Warshawsky, D. (1999). Tsix, a gene antisense to Xist at the X-inactivation centre. *Nat Genet* 21, 400-404.
- Lee, J.T., and Lu, N. (1999). Targeted mutagenesis of Tsix leads to nonrandom X inactivation. *Cell* 99, 47-57.
- Leonard, H., and Wen, X. (2002). The epidemiology of mental retardation: challenges and opportunities in the new millennium. *Ment Retard Dev Disabil Res Rev* 8, 117-134.
- Leppig, K.A., Brown, C.J., Bressler, S.L., Gustashaw, K., Pagon, R.A., Willard, H.F., and Distèche, C.M. (1993). Mapping of the Distal Boundary of the X-Inactivation Center in a Rearranged X-Chromosome from a Female Expressing Xist. *Human Molecular Genetics* 2, 883-887.
- Lyon, M.F. (1961). Gene action in the X-chromosome of the mouse (*Mus musculus* L.). *Nature* 190, 372-373.
- Martorell, L., Nascimento, M.T., Colome, R., Genoves, J., Naudó, M., and Nascimento, A. (2011). Four sisters compound heterozygotes for the pre- and full mutation in fragile X syndrome and a complete inactivation of X-functional chromosome: implications for genetic counseling. *J Hum Genet* 56, 87-90.

- Ostendorff, H.P., Bossenz, M., Mincheva, A., Copeland, N.G., Gilbert, D.J., Jenkins, N.A., Lichter, P., and Bach, I. (2000). Functional characterization of the gene encoding RLIM, the corepressor of LIM homeodomain factors. *Genomics* 69, 120-130.
- Ostendorff, H.P., Peirano, R.I., Peters, M.A., Schluter, A., Bossenz, M., Scheffner, M., and Bach, I. (2002). Ubiquitination-dependent cofactor exchange on LIM homeodomain transcription factors. *Nature* 416, 99-103.
- Penny, G.D., Kay, G.F., Sheardown, S.A., Rastan, S., and Brockdorff, N. (1996). Requirement for Xist in X chromosome inactivation. *Nature* 379, 131-137.
- Piton, A., Redin, C., and Mandel, J.L. (2013). XLID-causing mutations and associated genes challenged in light of data from large-scale human exome sequencing. *Am J Hum Genet* 93, 368-383.
- Rastan, S. (1983). Non-random X-chromosome inactivation in mouse X-autosome translocation embryos--location of the inactivation centre. *J Embryol Exp Morphol* 78, 1-22.
- Rastan, S., and Robertson, E.J. (1985). X-chromosome deletions in embryo-derived (EK) cell lines associated with lack of X-chromosome inactivation. *J Embryol Exp Morphol* 90, 379-388.
- Rodriguez Criado, G. (2012). [New X linked mental retardation syndrome]
Nuevo síndrome de retraso mental ligado a X. *An Pediatr (Barc)* 76, 184-191.
- Ropers, H.H. (2006). X-linked mental retardation: many genes for a complex disorder. *Curr Opin Genet Dev* 16, 260-269.
- Ropers, H.H., and Hamel, B.C. (2005). X-linked mental retardation. *Nat Rev Genet* 6, 46-57.
- Shin, J., Bossenz, M., Chung, Y., Ma, H., Byron, M., Taniguchi-Ishigaki, N., Zhu, X., Jiao, B., Hall, L.L., Green, M.R., *et al.* (2010). Maternal Rnf12/RLIM is required for imprinted X-chromosome inactivation in mice. *Nature* 467, 977-981.
- Tonne, E., Holdhus, R., Stansberg, C., Stray-Pedersen, A., Petersen, K., Brunner, H.G., Gilissen, C., Hoischen, A., Prescott, T., Steen, V.M., *et al.* (2015). Syndromic X-linked intellectual disability segregating with a missense variant in RLIM. *Eur J Hum Genet*.
- Venselaar, H., Te Beek, T.A., Kuipers, R.K., Hekkelman, M.L., and Vriend, G. (2010). Protein structure analysis of mutations causing inheritable diseases. An e-Science approach with life scientist friendly interfaces. *BMC Bioinformatics* 11, 548.
- Zhang, L., Huang, H., Zhou, F., Schimmel, J., Pardo, C.G., Zhang, T., Barakat, T.S., Sheppard, K.A., Mickanin, C., Porter, J.A., *et al.* (2012). RNF12 controls embryonic stem cell fate and morphogenesis in zebrafish embryos by targeting Smad7 for degradation. *Mol Cell* 46, 650-661.

CHAPTER 5



Buccal swab as a reliable predictor for X inactivation ratio in inaccessible tissues

Bas de Hoon, Kim Monkhorst, Peter Riegman, Joop Laven, and Joost Gribnau

Published in:
Journal of Medical Genetics, 28 July 2015



Abstract

Background

As a result of the epigenetic phenomenon of X chromosome inactivation (XCI) every woman is a mosaic of cells with either an inactive paternal X chromosome or an inactive maternal X chromosome. The ratio between inactive paternal and maternal X chromosomes is different for every female individual, and can influence an X-encoded trait or disease. A multitude of X linked conditions is known, and for many of them it is recognised that the phenotype in affected female carriers of the causative mutation is modulated by the XCI ratio. To predict disease severity an XCI ratio is usually determined in peripheral blood samples. However, the correlation between XCI ratios in peripheral blood and disease affected tissues, that are often inaccessible, is poorly understood. Here, we tested several tissues obtained from autopsies of 12 female individuals for patch size and XCI ratio.

Methods and results

XCI ratios were analysed using methyl-sensitive PCR-based assays for the AR, PCSK1N and SLITRK4 loci. XCI patch size was analysed by testing the XCI ratio of tissue samples with decreasing size. XCI patch size was analysed for liver, muscle, ovary and brain samples and was found too small to confound testing for XCI ratio in these tissues. XCI ratios were determined in the easily accessible tissues, blood, buccal epithelium and hair follicle, and compared with ratios in several inaccessible tissues.

Conclusions

Buccal epithelium is preferable over peripheral blood for predicting XCI ratios of inaccessible tissues. Ovary is the only inaccessible tissue showing a poor correlation to blood and buccal epithelium, but has a good correlation to hair follicle instead.

Introduction

Female XX mammals equalize their X-chromosomal gene dosage to XY males by inactivating one of their two X chromosomes in a process called X chromosome inactivation (XCI)(Lyon, 1961) . XCI is initiated early during embryonic development, and once the inactive X chromosome (Xi) is established the Xi is propagated through a near infinite number of cell divisions. As a result every female is a mosaic of cells with an inactive paternal X chromosome (Xp) and cells with an inactive maternal X chromosome (Xm)(Beutler et al., 1962). XCI mosaicism will be organized in clones of cells that have the same inactive X chromosome. The size of these clones, or XCI patches, might differ between tissues and depends on the number of cells present at the moment of XCI, and the extent of cell migration. To assess XCI mosaicism most studies use the ratio between cells with a different active X chromosome in a population of cells largely exceeding the patch size. This X-inactivation ratio (XIR) will be approximately 50:50 in most women, but deviations from this 50:50 XIR are common. When 80% of cells has the same inactive X chromosome this is termed skewed XCI, while for extremely skewed XCI over 90% of cells should have the same inactive X chromosome (Amos-Landgraf et al., 2006; El Kassar et al., 1998).

A skewed XIR can be caused by conditions that influence the XCI process itself, resulting in primary skewed XCI, or as a result of secondary cell selection. Primary skewed XCI occurs around gastrulation of the early embryo, when XCI is initiated. Initiation of XCI is a stochastic process, resulting in a cell autonomous random choice of which X chromosome will be inactivated. After establishing an inactive X chromosome, the silent state of this X chromosome will be clonally passed on to all daughter cells. The random nature of this choice makes most female embryos end up with a ratio of 50:50. By coincidence, the majority of cells can inactivate the same X chromosome, resulting in primary skewed XCI. The chance of this happening increases if the cell population undergoing XCI is smaller in size (Sandovici et al., 2004; Tan et al., 1993). Primary skewed XCI can also be caused genetically driven by mutations or variations in the genes involved in the inactivating process (Plenge et al., 1997; Pugacheva et al., 2005). Secondary skewed XCI is the result of post-inactivation cell selection that occurs when there is a selective pressure for a heterozygous X-linked gene. Such a selection can occur at any age, in all tissues or might be tissue specific. Secondary skewed XCI might also be the result of a decreasing stem cell pool during life, increasing the chance that most stem cells have the same inactive X chromosome (Holstege et al., 2014a).

A skewed XIR is clinically important whenever an X-chromosomally encoded trait or disease is involved. By inactivating predominantly the healthy or the mutated allele, skewing of XCI can modulate the severity of an X-linked disease . This has been established for Fragile X syndrome, where the full mutation does not affect cell viability, but only cell functioning.

Conversely, an X-encoded mutation can also induce secondary skewed XCI. This can be clearly seen in Incontinentia Pigmenti, where cells with an active *IKBKG* mutation are more prone to undergo apoptosis. For some conditions females carrying the mutation might even appear to be unaffected, because they display completely skewed XCI. Despite the correlation between disease severity and skewed XCI, the mechanism through which this selection is achieved remains unclear for some diseases (Archer et al., 2007; Knudsen et al., 2006; Orstavik et al., 1998). Currently, clinical analysis of the XIR is widely used to explain disease severity in female carriers of X-linked diseases, or to predict disease severity in females with a heterozygous X-linked recessive disease, like Fragile X syndrome, Barth syndrome or Rett syndrome.

Interestingly, there are also several clinical conditions for which no causative X-linked locus has been identified, but that have been associated with skewed XCI. This association has for example been shown for autoimmune thyroiditis, where it is thought that female individuals with extremely skewed XIR can develop autoimmunity to self-antigens encoded by the X chromosome that is inactive in the majority of cells (Ozcelik et al., 2006; Simmonds et al., 2014). Also for polycystic ovary syndrome (PCOS) skewed XCI is thought to play a role in its etiology, by preferentially inactivating the less sensitive androgen receptor gene and thereby contribution to the hyperandrogenaemic phenotype. However, both these associations are still under discussion.

When analyzing the XIR to assess or predict the severity of an X-linked disease, the tissue being tested should have a high degree of correlation with the affected tissue. A complicating factor is that secondary skewed XCI might occur mainly in the disease affected tissue without affecting other tissues. Peripheral blood is most commonly used for testing the XIR, but its correspondence to other tissues has been investigated only infrequently. Other easily accessible tissues, such as buccal epithelium and hair follicles have scarcely been evaluated. One previous study performed an elaborate comparison between several tissues using autopsy samples. However, a direct comparison to blood was not performed, because blood samples were only available in a limited number of individuals, and instead XCI patterns from spleen were also used to represent blood (Bittel et al., 2008). In the present study, we test the correlation between the easily accessible tissues, blood, buccal swab and hair follicles, and a number of inaccessible tissues (thyroid, heart, liver, kidney, muscle and ovary), using samples collected during autopsy of 12 female individuals.

Results

Before testing the XIR of several tissues, we verified that our analysis is not confounded by the XCI patch size. If a sample taken for XIR analysis consists largely of a single clone, or patch, the observed XIR does not represent the XIR of that tissue, but rather the contribution of the patch to the analyzed sample. To exclude an influence of patch size on XIR analysis, we attempted to identify the patch size for different tissues by determining the XIR for tissue samples with decreasing size. A sample composed entirely of a single patch will have the same X chromosome inactive in all cells, instead of a mixture of both X chromosomes. Liver and muscle were used first to determine patch size, because these organs have a homogeneous structure. Liver is mainly comprised of hepatocytes and muscle mainly of myocytes, and both tissues have relatively little contamination of other cell types that could possibly affect the XIR. An organ specific XIR, to which the test samples could be compared, was determined by taking the average of three samples of approximately 6mm^3 from different sites of each tissue fragment. Liver samples used to determine patch size were obtained from four individuals and were 0.008mm^3 to 0.064mm^3 in size, containing 17,000 to 100,000 cells. Sensitivity tests of the Human Androgen Receptor Assay (HumARA) on samples of equal size, using male DNA and female DNA with a known XIR of 10%, confirmed that the assay provides a reliable XIR in this range of cell number (data not shown). When using the threshold for extremely skewed XCI (below 10% and above 90%) to identify an XCI patch, no sample encompassing a patch could be detected (Fig. 1a). Muscle samples contained a lower number of cells, ranging from 700 to 46,000 cells. Since striated muscle consists of multinucleated cells, the calculated cell number does not represent the actual number of cells, but instead represents the number of nuclei in a sample. The amount of nuclei reflects the number of cells that have fused to one or more multinucleated cells. Although the term “nuclei” might be more appropriate, for convenience we will use the term “cells” instead. Although no was observed, several samples showed a clear deviation from the tissue specific XIR in one individual. This deviation occurred in the range of 4,000 up to 6,000 cells (Fig. 1b), possibly indicating that these samples approach the patch size in muscle.

Next, patch size analysis was performed for brain and ovary, because of the clinical relevance of these tissues. The X chromosome inactivation patterns in brain are of particular clinical relevance, because the X chromosome is relatively enriched for genes involved in neuronal functioning (Graves et al., 2002). Samples obtained from cerebral cortex contained 3,000 to 100,000 cells, but did not display an extremely skewed XIR, nor a clear deviation from the tissue-specific XIR (Fig. 1c). Ovarian patch size is of clinical importance for ovarian phenotypes involving hyperandrogensim, such as PCOS. Ovarian samples for patch size analysis were isolated from the cortical region using laser microdissection to ensure they did not

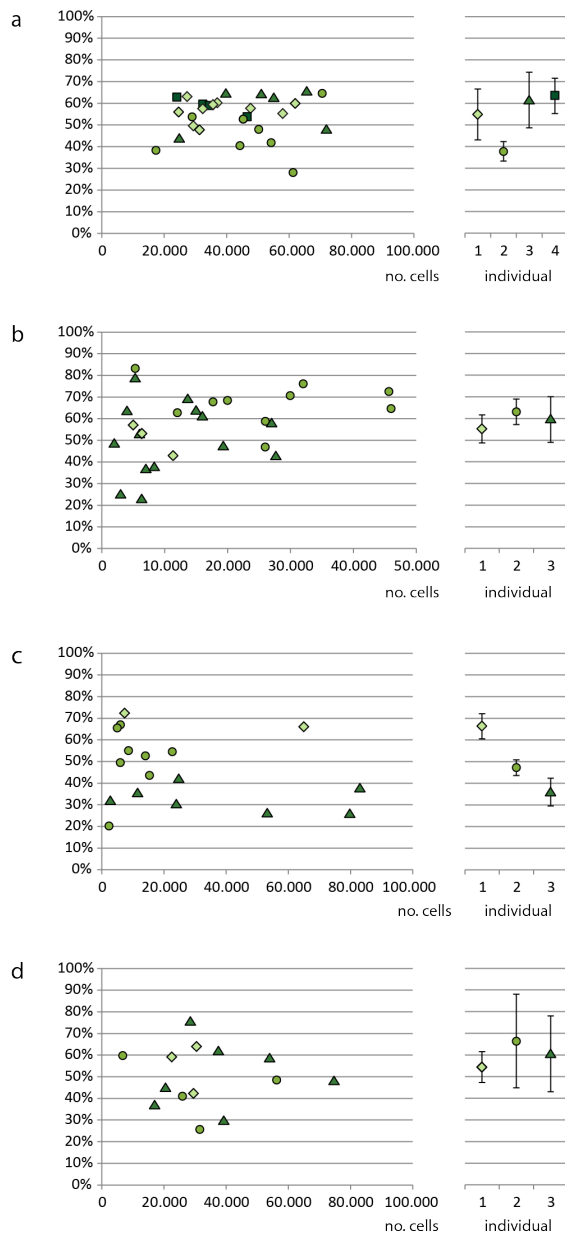


Figure 1.
X-inactivation ratios compared to number of cells
Patch size analysis for:
a. liver of four different individuals.
b. muscles from three individuals.
c. brain samples of three individuals.
d. ovary from three individuals.
The left part of the graph shows the X-inactivation ratio plotted against the number of cells. Different symbols represent different individuals. The right part of the graph shows the tissue-specific X-inactivation ratio determined for each individual, as determined from three larger samples. Error bars show 2 standard deviations from the tissue specific average.

contain any follicles or vascular structures with possible oligoclonal expansion. The obtained samples were 0.001mm^3 to 0.002mm^3 in size and contained 7,000 to 75,000 cells. No skewed XCI was observed in these samples, indicating that the patch size in ovarian cortex is less than 7,000 cells (Fig. 1d). These results show that the patch sizes for liver, muscle, brain and ovary are smaller than 17,000, 6,000, 3,000, and 7,000 cells respectively. A sample of 1mm^3 will therefore be large enough to measure XIR, without being biased by patch size.

After validating that patch size does not affect skewing analyses, we compared XIR's between different human tissues. We obtained tissues from 12 female individuals, with a median age of 58 (table 1). Cause of death varied from blood loss, to infection or sepsis and complications of an organ transplantation. Of the 12 individuals for which tissue samples were collected, 9 were informative for the Androgen Receptor (AR) locus. To analyze XCI in all 12 individuals we used the assays designed by Bertelsen and colleagues, that are based on a technique similar to the AR assay, but use a methyl-sensitive HpaII site in proximity of a dinucleotide repeat in the *PCSK1N* and *SLITRK4* genes (Bertelsen et al., 2011). The *PCSK1N* and *SLITRK4* assays were informative in 7 of 12 and 8 of 12 individuals, respectively, which is a slightly lower frequency of heterozygosity than the 75% and 80% observed by Bertelsen and colleagues (Bertelsen et al., 2011). After performing the three assays on all informative tissue samples, we tested the correlation between the three assays in our samples. For the AR and *PCSK1N* assays we found a Pearson correlation coefficient of 0,80, for the AR and *SLITRK4* assays 0,64, and for the *PCSK1N* and *SLITRK4* assays 0,81, indicating a good correlation between the three assays (Fig. 2).

For testing the XIR between different tissue samples, we used the average XIR from all informative assays. When comparing XIR's between tissues of an individual they cluster together, although there is considerable variation between tissues (Fig. 3). The largest observed difference between two tissues of the same individual was 58.8% between blood and thyroid of individual 4. The average difference between all tissues within one individual ranged from 6.9% in individual 7 to 17.2% in individual 4. Information regarding infection and blood transfusion was documented, because theoretically these conditions could be accompanied by proliferation of a subpopulation of lymphocytes, possibly resulting in a secondary skewed XCI in blood. Also occurrence of monoclonal diseases and administration of cytostatic drugs was documented, since also these conditions could theoretically result in the selective increase of a subpopulation of cells in any tissue. No clear pattern was observed between these conditions and the occurrence of skewed XCI >90% in a single or multiple tissues.

The correlation of the easily accessible tissues to the inaccessible tissues was tested using Pearson's correlation coefficient. Using blood as easily accessible tissue, a good correlation was found with liver ($r=0.58$, $p=0.078$), kidney ($r=0.50$, $p=0.097$) and buccal epithelium ($r=0.70$, $p=0.016$) (Table 2 and Supplemental Fig. 1). When buccal epithelium was

Table 1.
Characteristics of individuals from which autopsy samples were obtained

patient	age (years)	time between death and dna sampling (hours)	cause of death	erythrocyte transfusion	monoclonal diseases	cytostatic therapy	sepsis	tissues not in analysis	AR	PCSKIN	SLTRK4
1	57	3	blood loss	on day of death	squamous cell carcinoma of oesophagus	yes, until 4 months before death	no		I	I	I
2	67	50	mesenteric ischemia	4 days before death	no	no	no		I	I	I
3	45	25	meningitis	no	no	no	no		I	I	I
4	85	33	myocardial infarction	no	no	no	no		I	I	NI
5	63	51	complications of lung transplantation	10 days before death	no	no	yes		I	I	NI
6	44	56	cardiac failure	no	no	no	no		I	NI	I
7	1	22	pneumonia	on day of death	no	no	yes		I	NI	I
8	59	28	mult organ failure, sepsis	1 day before death	no	no	yes		NI	I	I
9	51	66	myocardial infarction	on day of death	no	no	no	liver, transplant	NI	I	I
10	66	24	metastatic monoclonal disease	18 days before death	squamous cell carcinoma of the bladder	no	no		I	NI	NI
11	46	20	complications of liver transplantation	1 day before death	no	no	yes	liver, transplant	I	NI	NI
12	62	19	myocardial infarction	no	no	no	no	heart	NI	NI	I

In columns AR, PCSKIN and SLTRK4, 'I' denotes if an individual was informative for the respective assay, 'NI' means the individual was not informative.

used as easily accessible tissue a much stronger correlation ($r > 0.68$) was found with all tissues, except for ovary and hair, and for several tissues this correlation was significant. Surprisingly, blood and buccal epithelium both have a weak correlation with the ovarian XIR ($r = 0.18$ and $r = 0.23$ respectively). Instead, hair follicles show a strong correlation to ovarian XIR ($r = 0.77$, $p = 0.005$), while for all other inaccessible tissue there is a weak correlation ($r < 0.40$) with hair follicles.

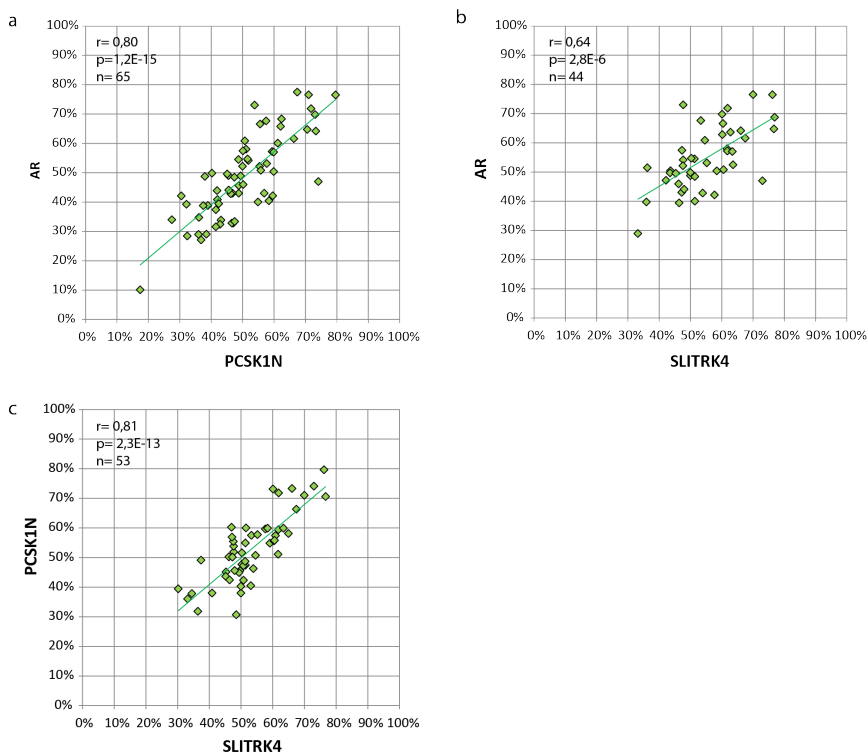


Figure 2.

Correlation between the three assays used for analyzing XCI: AR, PCSK1N and SLITRK4

- Plot showing the correlation between the XIR obtained by analyzing the AR and PCSK1N loci for each tissue of all informative individuals using a Pearson correlation coefficient.
- Plot showing the correlation between the XIR obtained by analyzing the AR and SLITRK4 loci for each tissue of all informative individuals using a Pearson correlation coefficient.
- Plot showing the correlation between the XIR obtained by analyzing the PCSK1N and SLITRK4 loci for each tissue of all informative individuals using a Pearson correlation coefficient.

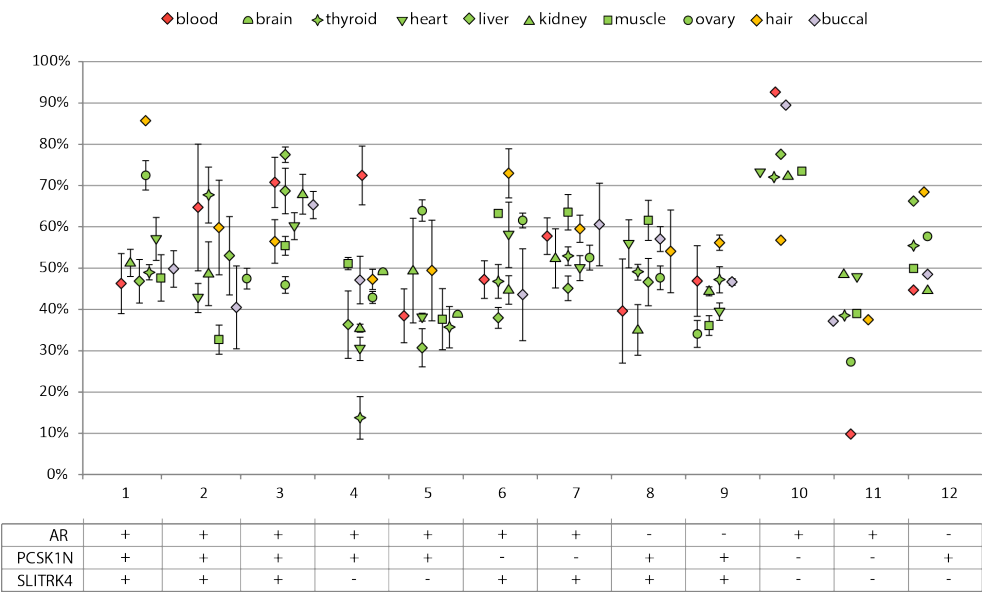


Figure 3.
X inactivation ratio (XIR) analysis in all accessible and inaccessible tissues of female individuals.
Each data point represents the average XIR value from the assays informative in an individual. For every assay PCRs were performed in triplicate. Error bars represent the SD from the assays that were used. Different tissues are represented by different symbols. The table below shows which assays were informative for each individual

Since long it has been described that there is an age-related increase of skewing in blood, occurring above the age of 60 (Amos-Landgraf et al., 2006; Busque et al., 1996; Sharp et al., 2000). This has been attributed to oligoclonal expansion from a limited number of stem cells, an effect that might be increased by a possible decrease of the number of stem cells in older women (Amos-Landgraf et al., 2006; Holstege et al., 2014a). If this is true, it can be expected that within a female individual the XIR's of different tissues initially cluster together around the same value, but diverge at later ages. To test if tissue specific XIR's within an individual diverge with increasing age, the average XIR difference was calculated from the XIR differences for every tissue combination within an individual. The average XIR difference is the smallest in the youngest individual and the largest in the oldest individual and showed a significant correlation with age ($r=0.72$, $p=0.008$) (Supplemental Fig. 2). These data suggest that XIR's of different tissues within an individual diverge with increasing age, although a larger number of individuals will be required to confirm this hypothesis.

Table 2
Pearson product moment correlation between XIR's of
easily accessible tissues and inaccessible tissues.

	blood	buccal	hair
blood	x	0,70 *	0,16
buccal	0,70 *	x	0,02
hair	0,16	0,02	x
thyroid	0,39	0,52	0,32
heart	0,30	0,71 *	0,40
liver	0,58	0,68 *	0,05
kidney	0,50	0,72 *	0,07
muscle	0,48	0,76 **	0,21
ovary	0,18	0,23	0,77 **

*p<0.05; ** p<0.01.

Discussion

We performed a XIR-based patch size analysis for several inaccessible tissues, to avoid XIR analyses being confounded by XCI patch size. The obtained results show that the patch size for liver, muscle, brain and ovary is smaller than 17,000, 6,000, 3,000, and 7,000 cells respectively. These results are consistent with results from previous studies, that have all been performed on epithelial layers. Most of these studies used a mutation in the glucose-6-phosphate dehydrogenase (G6PD) gene, to stain tissue sections for the presence of G6PD activity. These studies estimated the patch size of endothelium in the arterial wall to be 50 cells, of the epidermis to be smaller than 30mm², and smaller than 1 mm² in hair follicles (Benditt and Gown, 1980; Gartler et al., 1971; Linder and Gartler, 1965). Another study employed the HumARA to assess patch size in bladder urothelium and estimated the patch size to be 120mm² (Tsai et al., 1995). Unlike in some of the abovementioned studies we did not identify a XCI patch in our samples, although our sample sizes were in the same range or smaller. A possible explanation is that epithelium has a larger patch size, compared to tissues that contain a mixture of parenchyma and stromal cells, as parenchyma and stromal cells might already originate from different embryonic germ layers with different XIR's.

While the HumARA assay is probably the most widely used assay to determine the XIR, the AR locus is not informative for every individual. To analyze the XIR in all individuals, we used recently published assays for the *SLITRK4* and *PCSK1N* loci alongside the HumARA. Like the HumARA, these assays determine XCI by assessing the methylation status of a locus

neighboring a polymorphic repeat. A methylation sensitive restriction enzyme is used to digest unmethylated DNA, leaving methylated templates intact, which are subsequently amplified by PCR. The amplified polymorphic repeat is used to discriminate between the two alleles. Although a strong correlation was found between all three assays, the three assays do not always perfectly agree. The average difference between two assays was 6.4% for the AR and PCSK1N assays, 6.2% for AR and SLITRK4 and 4.8% for PCSK1N and SLITRK4. The largest observed difference comparing all three assays was 27.1%, in blood of patient 2. This difference in XIR between the assays might be explained by the low number of methylation sites that are analyzed. When using only one (PCSK1N and SLITRK4) or two (AR) methylation sites, this might not always reflect the methylation status of the complete locus. Indeed, it was shown for the HumARA that DNA methylation not always corresponds to relative expression of the two alleles (Swierczek et al., 2012). Expression of the *PCSK1N* and *SLITRK4* loci has not been compared to methylation status, but instead to AR methylation (Bertelsen et al., 2011). Theoretically, the three assays may also differ because of tissue specific gene silencing, independent of X-inactivation status. Altogether, this difference shows that analyzing a single methylation site might not be representative for the inactive status of an entire X chromosome, and using three loci increases reliability.

The tissues that were used in this study were collected during autopsies of females that died of various causes, and theoretically several clinical conditions might affect the XIR of different tissues. In case of cancer or cytostatic therapy the XIR of all analyzed tissues could theoretically be affected. Any tissue could be affected by cancer, altering the XIR through monoclonal expansion of the primary tumor or metastases. In addition, cytostatic therapy could also affect any tissue by dramatically reducing the number of stem cells, resulting in oligoclonal expansion and a secondary skewed XIR. In both conditions the expected result would be a shift of the XIR towards extremely skewed XCI, which was not observed. In several other individuals, the T-lymphocyte composition in peripheral blood, that was used to assess XIR, could have been altered. First, the occurrence of infection and sepsis is likely to alter T lymphocyte composition in the peripheral blood samples analyzed. However, this is not likely to skew the XIR, as this would require an oligoclonal expansion of thymocytes and during an immune response a larger number of thymocytes will be activated. Therefore, it can be considered unlikely that infection or sepsis will affect the XIR. Secondly, after major blood loss the peripheral T-lymphocyte population is largely lost and needs to be replaced. However, as the peripheral T-lymphocyte population is a reflection of the stem cell population, it is not likely that the population of newly circulating T-lymphocytes will have a different XIR. An erythrocyte transfusion will not affect the XIR of a peripheral blood sample, as erythrocytes are enucleated cells. In none of the individuals suffering from any of the conditions that could alter the peripheral T-lymphocyte population extremely skewed XCI was observed. Although this

argues against an oligoclonal expansion, we cannot exclude that these conditions have affected the XIR of peripheral blood in a small degree.

The comparison of tissue-specific XIR's yielded an interesting correlation pattern for hair follicle, as hair follicles display a weak correlation with all inaccessible tissues, except ovary. Contradictory to our results, a previous study analyzed XIR in hair follicles of 21 individuals and found a significant correlation to blood XIR ($r=0.67$; $p=0.009$) (Kaupert et al., 2010). One possible explanation for this difference is the number of hair follicles used to assay XCI. We used 20 hair follicles, where Kaupert and colleagues used 3-4 follicles to assay XCI. Hair follicles originate from a small number of precursor cells, and the chance that a hair follicle is monoclonal regarding XCI status has been estimated around 50% (Goldstein et al., 1971). Consequently, using a smaller number of hair follicles, increases the chance that patch size confounds XIR analysis. Given the strong correlation between hair follicles and ovary, we conclude that when interested in the XIR of an ovary, of use in for instance PCOS patients, testing XCI in hair follicles should be preferred over testing peripheral blood samples or buccal swabs.

The comparison of XIR's between easily accessible tissues blood and buccal swap and inaccessible tissues demonstrated that buccal epithelium has a better correlation to inaccessible tissues compared to blood. To date most studies analyzing skewing of XCI in single patients or patient populations use peripheral blood samples for analysis. A good correlation between XCI in blood and buccal epithelium has been reported before by two studies, and is confirmed by our results (Bolduc et al., 2008; Sharp et al., 2000). However, given the stronger correlation of buccal epithelium to all examined tissues we conclude that when testing for XCI skewing, buccal swab should be the method of choice.

Many studies have reported an age-related increase of skewing in blood, occurring above the age of 60, which has been attributed to a decreasing number of stem cells in older women (Amos-Landgraf et al., 2006; Busque et al., 1996; Holstege et al., 2014b; Sharp et al., 2000). Given the small number of individuals we were unable to test for an age-related increase in skewed XCI. However, the obtained XIR's from different tissues presented an unique opportunity to test if an age-related increase in skewed XCI might be caused by a decreasing stem cell number. Indeed we find that tissue specific XIR's within an individual diverge, although a larger number of individuals will be required to confirm this hypothesis.

In conclusion, we show that the patch size of XCI in liver, muscle, brain and ovary is small enough not to confound XIR analysis of 1mm^3 biopsies. When comparing blood, buccal epithelium and hair follicle as easily accessible tissues for assaying XIR, hair follicles show the best correlation with ovary. For all other inaccessible tissues buccal epithelium shows the best correlation. Moreover, buccal swap is non-invasive, and should therefore be considered the best and most convenient method for determining XIR.

Materials and Methods

All samples used in this study were obtained from the Erasmus MC Tissue Bank, in accordance with the Dutch Law on Medical Research and autopsy materials were only used for research after permission was obtained through signed informed consent from the next of kin. This research was approved by the local medical ethical committee (MEC-2011-145). Tissue samples for comparison of tissue specific XIR were collected during autopsies performed in the Erasmus Medical Centre in Rotterdam, between June 2012 and August 2014. Tissue samples were snap frozen and DNA was extracted using phenol-chloroform purification. Blood samples could not be extracted by peripheral vein puncture and were therefore obtained through cardiac puncture. Ovarian samples for XIR analysis were cut by hand from the ovarian cortex, only selecting regions that did not contain any visible follicles.

Samples for patch size analysis were obtained by cutting cryosections of 8µm thick, from which final samples were cut by hand measuring 1mm² to 8mm². DNA was isolated using phenol-chloroform extraction. The number of cells in each sample was calculated back from the total amount of DNA present, assuming a single cell contains 6pg DNA. Ovarian samples for patch size analysis were obtained during autopsies of three female individuals of premenopausal age. Samples were 0.10mm² to 0.16mm² were isolated from 14µm cryosections using a PALM laser dissection.

XIRs were analyzed using the Human Androgen Receptor Assay (HumARA). DNA samples were digested with the methyl-sensitive restriction enzyme HpaII and EcoRI, or EcoRI alone for 24 hours at 37°C. After inactivating the enzyme by incubating at 80°C for 25 minutes, the Androgen Receptor locus was amplified using primers TGCAGTTAGGGCTGGGAAGG and CTGTGGGGCCTCTACGATGG. The AC repeat in the *SLITRK4* gene was amplified using primers GCACACAAGCAGTCCTTCCT and TGGCTTCTGGTTGCTCTCT. The tandem CA and AG repeat of *PCSK1N* was amplified using primers ATGCGAAGACCATTCCCTCT and GTGCGTGTGATGTGAGGAGA. The amplified products were analyzed separately on an ABI3130 genetic analyzer. Correlations of XIRs between different tissues were calculated using Pearson's correlation coefficient. All individuals were pooled in a single group, regardless of their age and menopausal status.

Acknowledgements

We thank Ruben Boers for helping with sample collection and Guido Breedveld, Bianca de Graaf and Marialuisa Quadri for technical assistance. We also thank all department members for helpful discussions.

References

- Amos-Landgraf, J.M., Cottle, A., Plenge, R.M., Friez, M., Schwartz, C.E., Longshore, J., and Willard, H.F. (2006). X chromosome-inactivation patterns of 1,005 phenotypically unaffected females. *Am J Hum Genet* 79, 493-499.
- Archer, H., Evans, J., Leonard, H., Colvin, L., Ravine, D., Christodoulou, J., Williamson, S., Charman, T., Bailey, M.E., Sampson, J., *et al.* (2007). Correlation between clinical severity in patients with Rett syndrome with a p.R168X or p.T158M MECP2 mutation, and the direction and degree of skewing of X-chromosome inactivation. *J Med Genet* 44, 148-152.
- Benditt, E.P., and Gown, A.M. (1980). Atheroma: the artery wall and the environment. *Int Rev Exp Pathol* 21, 55-118.
- Bertelsen, B., Tumer, Z., and Ravn, K. (2011). Three new loci for determining x chromosome inactivation patterns. *J Mol Diagn* 13, 537-540.
- Beutler, E., Yeh, M., and Fairbanks, V.F. (1962). The normal human female as a mosaic of X-chromosome activity: studies using the gene for C-6-PD-deficiency as a marker. *Proc Natl Acad Sci U S A* 48, 9-16.
- Bittel, D.C., Theodoro, M.F., Kibiryeva, N., Fischer, W., Talebizadeh, Z., and Butler, M.G. (2008). Comparison of X-chromosome inactivation patterns in multiple tissues from human females. *J Med Genet* 45, 309-313.
- Bolduc, V., Chagnon, P., Provost, S., Dube, M.P., Belisle, C., Gingras, M., Mollica, L., and Busque, L. (2008). No evidence that skewing of X chromosome inactivation patterns is transmitted to offspring in humans. *J Clin Invest* 118, 333-341.
- Busque, L., Mio, R., Mattioli, J., Brais, E., Blais, N., Lalonde, Y., Maragh, M., and Gilliland, D.G. (1996). Nonrandom X-inactivation patterns in normal females: lyonization ratios vary with age. *Blood* 88, 59-65.
- El Kassar, N., Hetet, G., Briere, J., and Grandchamp, B. (1998). X-chromosome inactivation in healthy females: incidence of excessive lyonization with age and comparison of assays involving DNA methylation and transcript polymorphisms. *Clin Chem* 44, 61-67.
- Gartler, S.M., Gansini, E., Hutchison, H.T., Campbell, B., and Zechhi, G. (1971). Glucose-6-phosphate dehydrogenase mosaicism: its study of hair follicle variegation. *Ann Hum Genet* 35, 1-7.
- Goldstein, J.L., Marks, J.F., and Gartler, S.M. (1971). Expression of two X-linked genes in human hair follicles of double heterozygotes. *Proc Natl Acad Sci U S A* 68, 1425-1427.
- Graves, J.A., Gecz, J., and Hameister, H. (2002). Evolution of the human X—a smart and sexy chromosome that controls speciation and development. *Cytogenet Genome Res* 99, 141-145.

Holstege, H., Pfeiffer, W., Sie, D., Hulsman, M., Nicholas, T.J., Lee, C., Ross, T., Lin, J., Miller, M.A., Ylstra, B., *et al.* (2014a). Somatic mutations found in the healthy blood compartment of a 115-yr-old woman demonstrate oligoclonal hematopoiesis. *Genome Res* 24, 733–742.

Holstege, H., Pfeiffer, W., Sie, D., Hulsman, M., Nicholas, T.J., Lee, C.C., Ross, T., Lin, J., Miller, M.A., Ylstra, B., *et al.* (2014b). Somatic mutations found in the healthy blood compartment of a 115-yr-old woman demonstrate oligoclonal hematopoiesis. *Genome Res* 24, 733–742.

Kaupert, L.C., Billerbeck, A.E., Brito, V.N., Mendonca, B.B., and Bachega, T.A. (2010). Could the leukocyte x chromosome inactivation pattern be extrapolated to hair bulbs? *Horm Res Paediatr* 73, 238–243.

Knudsen, G.P., Neilson, T.C., Pedersen, J., Kerr, A., Schwartz, M., Hulten, M., Bailey, M.E., and Orstavik, K.H. (2006). Increased skewing of X chromosome inactivation in Rett syndrome patients and their mothers. *Eur J Hum Genet* 14, 1189–1194.

Linder, D., and Gartler, S.M. (1965). Distribution of Glucose-6-Phosphate Dehydrogenase Electrophoretic Variants in Different Tissues of Heterozygotes. *Am J Hum Genet* 17, 212–220.

Lyon, M.F. (1961). Gene action in the X-chromosome of the mouse (*Mus musculus* L.). *Nature* 190, 372–373.

Orstavik, K.H., Orstavik, R.E., Naumova, A.K., D'Adamo, P., Gedeon, A., Bolhuis, P.A., Barth, P.G., and Toniolo, D. (1998). X chromosome inactivation in carriers of Barth syndrome. *Am J Hum Genet* 63, 1457–1463.

Ozelik, T., Uz, E., Akyerli, C.B., Bagislar, S., Mustafa, C.A., Gursoy, A., Akarsu, N., Toruner, G., Kamel, N., and Gullu, S. (2006). Evidence from autoimmune thyroiditis of skewed X-chromosome inactivation in female predisposition to autoimmunity. *Eur J Hum Genet* 14, 791–797.

Plenge, R.M., Hendrich, B.D., Schwartz, C., Arena, J.F., Naumova, A., Sapienza, C., Winter, R.M., and Willard, H.F. (1997). A promoter mutation in the XIST gene in two unrelated families with skewed X-chromosome inactivation. *Nat Genet* 17, 353–356.

Pugacheva, E.M., Tiwari, V.K., Abdullaev, Z., Vostrov, A.A., Flanagan, P.T., Quitschke, W.W., Loukinov, D.I., Ohlsson, R., and Lobanenko, V.V. (2005). Familial cases of point mutations in the XIST promoter reveal a correlation between CTCF binding and pre-emptive choices of X chromosome inactivation. *Hum Mol Genet* 14, 953–965.

Sandovici, I., Naumova, A.K., Leppert, M., Linares, Y., and Sapienza, C. (2004). A longitudinal study of X-inactivation ratio in human females. *Hum Genet* 115, 387–392.

Sharp, A., Robinson, D., and Jacobs, P. (2000). Age- and tissue-specific variation of X chromosome inactivation ratios in normal women. *Hum Genet* 107, 343–349.

Simmonds, M.J., Kavvoura, F.K., Brand, O.J., Newby, P.R., Jackson, L.E., Hargreaves, C.E., Franklyn, J.A., and Gough, S.C. (2014). Skewed X chromosome inactivation and female preponderance in autoimmune thyroid disease: an association study and meta-analysis. *J Clin Endocrinol Metab* 99, E127–131.

Swierczek, S.I., Piterkova, L., Jelinek, J., Agarwal, N., Hammoud, S., Wilson, A., Hickman, K., Parker, C.J., Cairns, B.R., and Prchal, J.T. (2012). Methylation of AR locus does not always reflect X chromosome inactivation state. *Blood* 119, e100-109.

Tan, S.S., Williams, E.A., and Tam, P.P. (1993). X-chromosome inactivation occurs at different times in different tissues of the post-implantation mouse embryo. *Nat Genet* 3, 170-174.

Tsai, Y.C., Simoneau, A.R., Spruck, C.H., 3rd, Nichols, P.W., Steven, K., Buckley, J.D., and Jones, P.A. (1995). Mosaicism in human epithelium: macroscopic monoclonal patches cover the urothelium. *J Urol* 153, 1697-1700.

CHAPTER 6



Stable X chromosome reactivation in female human induced pluripotent stem cells

Tahsin Stefan Barakat*, Mehrnaz Ghazvini*, Bas de Hoon, Tracy Li,
Bert Eussen, Hannie Douben, Reinier van de Linden, Nathalie van der Stap,
Marjan Boter, Joop Laven, Robert-Jan Galjaard, J. Anton Grootegoed,
Annelies de Klein, and Joost Gribnau

*authors contributed equally

Published in:

Stem Cell Reports, 10 Feb 2015, Volume 4, Issue 2, page 199-208



Abstract

Background

In placental mammals balanced expression of X-linked genes is accomplished by X chromosome inactivation (XCI) in female cells. In human rXCI is initiated early during embryonic development. To investigate whether reprogramming of female human fibroblasts into induced pluripotent stem cells (iPSCs) leads to reactivation of the inactive X chromosome (Xi), we have generated iPSC lines from fibroblasts heterozygous for large X-chromosomal deletions.

Methods and results

These fibroblasts show completely skewed XCI of the mutated X chromosome, enabling monitoring of X chromosome reactivation (XCR) and XCI using allele-specific single cell expression analysis.

Conclusions

This approach revealed that XCR is robust under standard culture conditions, but does not prevent re-initiation of XCI, resulting in a mixed population of cells with either two active X chromosomes (Xa's) or one Xa and one Xi. This mixed population of XaXa and XaXi cells is stabilized in naïve human stem cell medium allowing expansion of clones with two Xa's.

Introduction

Inactivation of one of the two X chromosomes in eutherian female cells by XCI is an epigenetic process, which compensates for potential dosage differences of X-linked genes between female XX and male XY cells (Lyon, 1961). Mechanistic and regulatory aspects of XCI have been extensively studied during mouse development and for mouse embryonic stem cells (mESCs). These mESCs are derived from the inner cell mass (ICM) of the blastocyst and contain two active X chromosomes (Xa), but will undergo XCI upon *in vitro* differentiation. The non-coding *Xist* RNA is crucial for XCI and becomes up-regulated upon differentiation of mESCs. *Xist* coats the future Xi, attracting chromatin remodelling enzymes which infer the transcriptional shutdown of the Xi (reviewed in: (Barakat and Gribnau, 2012; Pollex and Heard, 2012)). Several components of the regulatory network driving XCI are conserved between mouse and man, but many questions regarding human XCI remain unanswered. Contrary to undifferentiated mESCs, most human ESC lines (hESCs) are in a post-XCI state, and are prone to epigenetic fluidity (Silva et al., 2008). This variation in regulation and stability of the XCI state between these eutherian species might reflect suboptimal culture conditions for the human cells, resulting in a gradual progression towards a more differentiated state, including initiation of XCI. Alternatively, the XCI process itself may have reached a more advanced state in the human ICM compared to the mouse, so that XCI in the hESCs derived from the ICM has occurred already prior to or during ESC derivation.

The derivation of human induced pluripotent stem cells (hiPSCs) from fibroblasts (Takahashi et al., 2007) offers an opportunity to study XCI in human cells. For mouse fibroblasts, it has been shown that the Xi becomes reactivated during the reprogramming process, followed by random XCI (rXCI) upon differentiation of these miPSCs (Maherali et al., 2007; Stadtfeld et al., 2008). Similar to studies involving hESC lines, previous studies of XCI in hiPSCs have provided varying results. Systematic analysis of multiple female hiPSC lines derived from several fibroblast populations under different reprogramming strategies indicated that all hiPSC lines retained the Xi inherited from the starting fibroblasts (Amenduni et al., 2011; Ananiev et al., 2011; Cheung et al., 2011; Tchieu et al., 2010). In another study it was found that in all hiPSC lines derived from one fibroblast population with established rXCI, one and the same X chromosome had become the Xi in all lines, indicating involvement of cell selection processes (Pomp et al., 2011). In contrast, other studies showed reactivation of the Xi, an apparent reversal of XCI which is herein referred to as X chromosome reactivation (XCR), in all or a limited number of hiPSC lines, but XCI was reinitiated upon differentiation of these hiPSC lines (Bruck and Benvenisty, 2011; Kim et al., 2011; Marchetto et al., 2010). XCR followed by reinitiation of XCI and stable establishment of the Xi upon hiPSC differentiation, are crucial steps that need to take place for hiPSCs to be applied for various purposes. If hiPSC lines do not

pass through this series of events, they show signs of stochastic reactivation of the Xi inherited from the founder fibroblasts (Mekhoubad et al., 2012). This erosion of XCI is detrimental for studies involving cell types generated from female hiPSC, as it can be expected that many of these cell types will be prone to gene dosage inequalities. Therefore the availability of such hiPSC lines with stable XCR, having two active X chromosomes as in mESCs, would greatly advance research on modelling of X-linked human diseases and studies on regulatory mechanisms of human XCI.

The varying results regarding XCR and XCI obtained for hiPSCs may be explained by different reprogramming techniques and the growth conditions in which hiPSCs are generated and maintained. In a recent study it was found that growth of hESCs and hiPSCs in defined conditions (naïve human stem cell medium; NHSM) results in more naïve iPSCs, and leads to efficient loss of Xi specific markers including XIST RNA and Xi specific histone modifications, which are re-established upon differentiation (Gafni et al., 2013). Although these NHSM-cultured hESCs and hiPSCs resemble mESCs and miPSCs in several aspects, it is unclear if the described loss of Xi specific markers under these growth conditions has resulted in XCR, as expression of X-linked loci was not assessed (Gafni et al., 2013).

Skewed rXCI is obtained in cells which carry a large X chromosomal deletion on either one of the two X chromosomes outside the X inactivation center (XIC), based on selection against cells which inactivate the intact X chromosome. Here, we have generated and analysed hiPSC lines derived from female carriers with such heterozygous large X chromosomal deletions, which were expanded under different growth conditions (standard versus NHSM). These hiPSCs provide a powerful model system to study XCR and XCI, facilitated by allele specific expression analysis. Single cell expression analysis of these hiPSC lines, when generated under standard culture conditions, revealed robust XCR, which was followed by XCI. Hence, the presence of two active X chromosomes in these hiPSCs is not a stable condition, as it is in undifferentiated mESCs. However, growth of the present hiPSC lines in NHSM conditions did stabilize the equilibrium between XCR and XCI over several passages, and allowed rapid expansion of hiPSC clones with two active X chromosomes.

Results

Cell lines with non-rXCI for hiPSC formation

To generate novel hiPSC lines to investigate XCR and XCI during reprogramming at a single cell level, we screened cell repositories for female cell lines harbouring large deletions on one of the X chromosomes. Due to secondary selection, an X chromosome with a large deletion is preferentially inactivated in female carriers providing a sensitive assay to identify hiPSC lines which have reactivated the Xi inherited from the founder fibroblasts, because this results in bi-allelic expression of polymorphic informative genes.

Cell lines were collected through different sources, and the gene content was further characterized by MLPA, SNP array, and DNA-FISH analysis (Fig. 1a,b, Supplemental Table 1, Supplemental Fig. 1). The fibroblast lines X12, X14, and X15 containing informative large deletions of Xq, were selected for further studies examining XCR and XCI. The respective deletions concern regions outside the XIC. Deletions including the XIC would block XCI of the X chromosome carrying the deletion, whereas large deletions which do not include the XIC will lead to clonal selection of the cells which have inactivated the mutant X chromosome, keeping the intact X chromosome as the Xa. In addition, 46,XX fibroblasts not carrying an X-chromosomal deletion, and 47,XXX fibroblasts derived from a patient with triple X syndrome, were included as controls (Brosens et al., 2014). RNA-FISH analysis indicated that in fibroblast cell lines X12, X14, and X15, 99% of the cells showed one *XIST* cloud per nucleus (Fig. 1c, n=200 cells analysed per cell line). In the 47,XXX fibroblasts, two *XIST* clouds marking two inactive X chromosomes were found in almost every cell (Fig. 1c), in agreement with the rule that all but one X chromosome becomes inactivated per diploid genome (Harnden, 1961). HUMARA analysis amplifies a polymorphic region in the *androgen receptor* (*Ar*) gene after digestion with a methylation sensitive enzyme, and is used to detect the methylated *Ar* allele marking the Xi (Allen et al., 1994). This analysis indicated that rXCI is completely skewed towards inactivation of one of the two X chromosomes, for all three X12, X14, and X15 fibroblast cell lines (Supplemental Table 1). Both in the 46,XX and the 47,XXX fibroblast cell lines, rXCI without such skewing was observed (Supplemental Table 1) (Brosens et al., 2014). Preferential inactivation of one specific X chromosome in fibroblast line X12 was confirmed by RFLP RT-PCR analysis of a SNP in *XIST* (Fig. 1d). Although no informative SNPs were available for *XIST* in the X14 and X15 fibroblast cell lines, analysis of X-linked genes showed completely skewed XCI in both cell lines (Supplemental Fig. 1d). We conclude that the X12, X14, and X15 fibroblast cell lines show highly skewed rXCI, most likely silencing the X carrying the deletion.

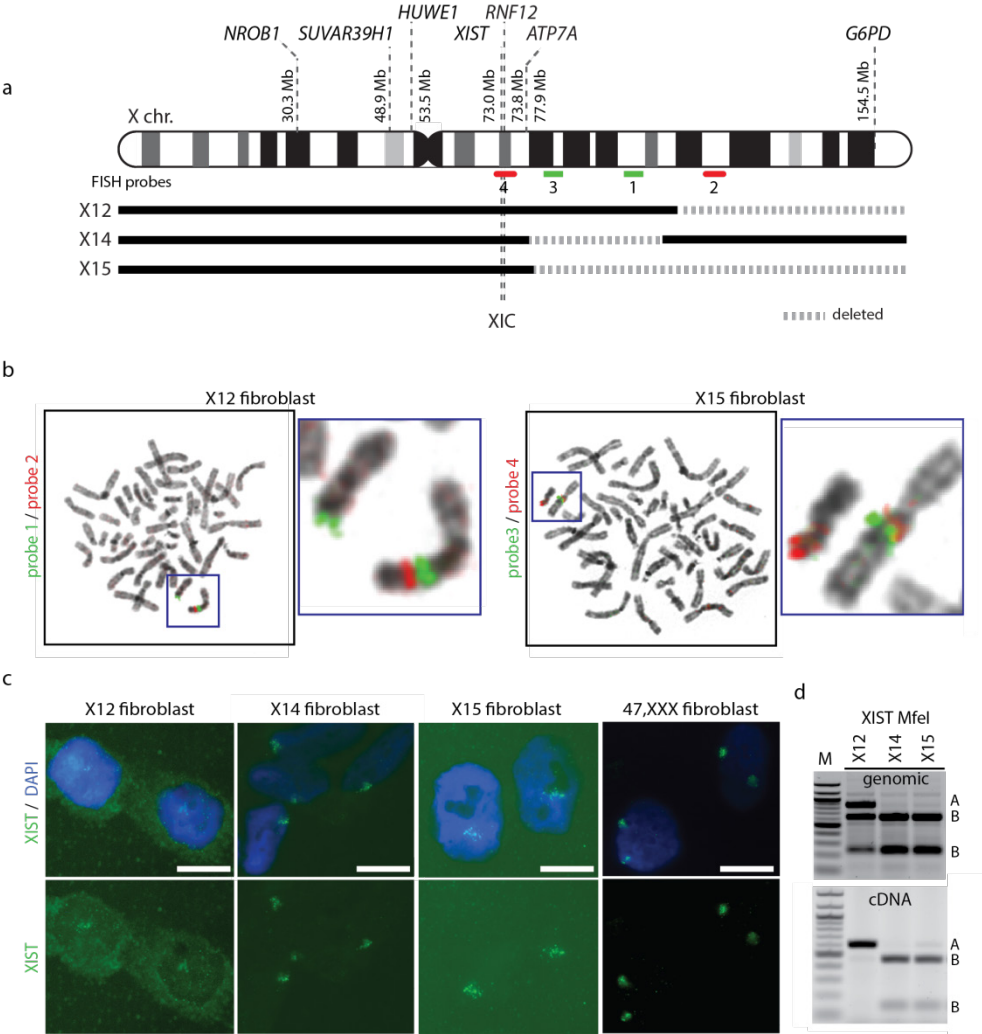
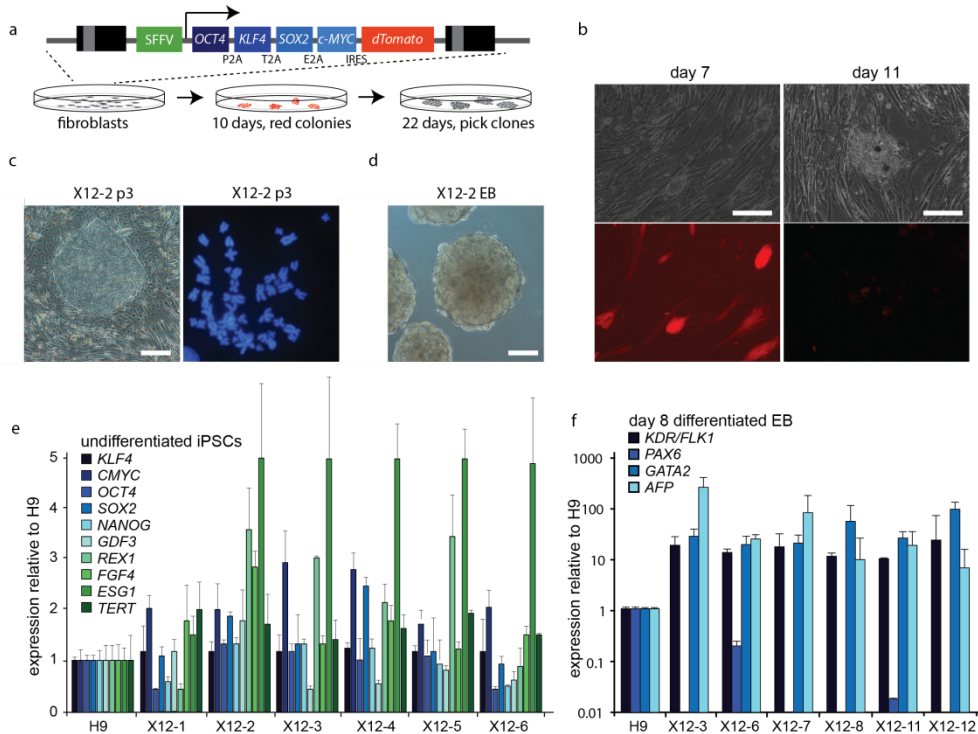


Figure 1.
Fibroblast cell lines with skewed rXCI

a. Schematic representation of the human X chromosome. Location of genes analyzed in this study is indicated. The dashed lines indicate the deletions in the X12, X14, and X15 fibroblast cell lines. Also DNA-FISH probes are indicated.

b. DNA-FISH on metaphase chromosomes of X12 and X15 fibroblasts, using probes 1, 2, 3, and 4. Magnification of X chromosomes is shown in the insets.

c. RNA-FISH detecting *XIST* RNA (FITC) in X12, X14, X15, and 47,XXX fibroblasts. DNA is counterstained with DAPI (blue, bar=10µm). D) PCR and RT-PCR analysis with DNA and cDNA from X12, X14, and X15 fibroblast cell lines, amplifying an RFLP in *XIST*. PCR products were digested with *MfeI*, to discriminate between both alleles.

**Figure 2.****Generation of hiPSC lines from fibroblasts**

- Schematic overview of the lentiviral reprogramming cassette (Warlich et al., 2011), and the procedure to establish the present hiPSC lines.
- Transduced fibroblasts express dTomato (left panel), which is silenced upon proper reprogramming (right panel, bar=100µm).
- Representative picture of a hiPSC colony (p3 denotes passage 3) from iPSC line X12-2 (left panel, bar=100µm), and karyogram of iPSC X12-2, revealing a 46,XX karyotype (right panel).
- Representative picture of EBs derived from iPSC line X12-2 after 8 days of differentiation (bar=100µm).
- qRT-PCR analysis of pluripotency factors in X12 hiPSC lines (1-6). Expression of the same factors in an hESC line (H9) served as a control, and was set at 100%.
- qRT-PCR analysis of differentiation associated markers in day 8 (d8) EBs from X12 hiPSC lines. Gene expression was normalized to a differentiated hESC line H9.

Generation of hiPSC lines

To generate hiPSC lines, X12, X14, X15, 46,XX, and 47,XXX fibroblasts were transduced with a polycistronic lentiviral vector expressing *OCT4*, *SOX2*, *KLF4*, and *MYC*, and a dTomato reporter, under the control of a retroviral promoter (SFFV) that is rapidly silenced during the reprogramming process (Warlich et al., 2011) (Fig. 2a, b). These fibroblasts were plated on MEFs, and cultured in the presence of standard human ESC medium. After approximately 10 days, small clusters of cells appeared which started to develop a human ESC cell morphology. These clusters gradually lost the expression of the dTomato reporter (Fig. 2b and Supplemental Fig. 2a), which indicated proper silencing of the lentiviral transgene, required to establish fully reprogrammed hiPSCs. For each one of the different genotypes, we obtained several iPSC lines, of which the X12, X15, 46,XX, and 47,XXX iPSC lines were subjected to further analysis. All these iPSC lines showed morphology resembling hESCs, with a stable 46,XX karyotype (or 47,XXX in case of lines derived from the 47,XXX fibroblasts) and expression of key endogenous pluripotency factors including *NANOG* and *REX1*, at different passages (p) after establishment (Fig. 2c, d, e, Supplementary Fig. 2c, d, and data not shown). Also, SNP arrays of various hiPSC lines confirmed an identical genome content compared to the founder fibroblasts (Supplementary Fig. 2d). Upon embryoid body (EB) differentiation, qPCR analysis indicated that most hiPSC lines showed expression of endodermal (*FLK1*, *AFP*), mesodermal (*GATA2*), and ectodermal (*PAX6*) marker genes (Fig. 2g, only X12 clones are shown). This was confirmed by immunocytochemistry analysis on EB differentiated iPSCs plated on slides, revealing *GFAP* (ectoderm), *Vimentin* (mesoderm) and *AFP* positive cells for all iPSC lines, which supports our conclusion that all iPSC clones were completely reprogrammed and acquired full differentiation potential (Supplementary Fig. 2b, results of one representative X12 clone is shown).

Early passage female hiPSCs show reactivation of the Xi

The X12, X15, and 47,XXX iPSCs were subjected to immuno-RNA-FISH analysis at passages 3-5, to investigate the XCI status of these cell lines. This analysis showed that in several iPSC lines generated from the X12 and X15 fibroblasts only 30% of the nuclei displayed *XIST*-coated X chromosomes (Fig. 3a, d). In hiPSC lines generated from the 47,XXX fibroblasts, many cells did not show Xi markers, or showed signs of only one Xi (Fig. 3a,e). In all cell lines, analysis of heterochromatin markers associated with the Xi, including enrichment of H3K27me3, indicated variable staining, with many cells not displaying all characteristic Xi features (Fig. 3a and data not shown). Also, Barr bodies (e.g. DAPI-dense, heterochromatic regions covering the Xi) were detected in a minority of cells. Strikingly, in many colonies, cells with all Xi hallmarks, including depletion of H3K9ac, were most often found at the edges or in the centre of the colonies, where most of the differentiated cells are found. In contrast, cells without *XIST* and associated Xi markers were found in a donut shaped region surrounding the middle of the colonies (Fig.

3b,c). These results could be explained by: 1) loss of X chromosome(s), 2) loss of *XIST* expression and Xi markers during hiPSC cell culture and colony formation, similar to findings for hESC lines (Bruck and Benvenisty, 2011), or 3) XCR in a pluripotent subpopulation of hiPSCs, possibly followed by XCI. Option 1 was excluded, as karyotyping and SNP array analysis did not reveal a significant population of cells with X chromosome aneuploidies at different passages after establishment of the iPSC lines. To distinguish between options 2 and 3, we first analysed the methylation pattern of the Xi by HUMARA analysis, focussing on the hiPSC lines derived from the X12 and X15 fibroblasts. If the Xi in the hiPSCs is the same X chromosome as the Xi inherited from the founder fibroblasts, HUMARA analysis will detect completely skewed methylation of the *Ar* gene. Furthermore, using this analysis, XCR in all cells would lead to an absence of methylation at the *Ar* gene, whereas XCR followed by rXCI which might also involve the intact X chromosome would result in methylation of the previously unmethylated *Ar* allele. HUMARA analysis for genomic DNA of undifferentiated X15 hiPSC lines showed the initial 100:0 skewing ratio (Fig. 3f), which was also observed for the founder fibroblast cell line, compatible with either an absence of XCR, or XCR in a small subpopulation of cells which cannot be detected by this method. In undifferentiated X12 p3 hiPSC lines, we observed methylation, in some clones up to 12%, also of the second *Ar* allele located on the intact X chromosome (Fig. 3f). This finding indicates that XCR in the X12 p3 hiPSCs is unstable, and that these cells have started rXCI also on the intact X chromosome in a subpopulation of cells. We next performed allele specific expression analysis of *XIST* using RFLP RT-PCR analysis on RNA from X12 hiPSCs, the only hiPSC line with an informative *XIST* SNP. On the whole cell population level we detected *XIST* expression from both X chromosomes (Fig. 3g). This supported the findings with the HUMARA analysis, indicating that *XIST* upregulation and initiation of XCI have occurred following XCR, in X12 hiPSC lines. In the day 8 differentiated progeny of X12 hiPSC lines, we detected mono-allelic *XIST* expression (Fig. 3h), comparable to that in the original X12 fibroblasts. This is explained by survival, at later passages, of cells which have silenced the mutant X chromosome and loss of cells which have initiated XCI on the intact X chromosome

Bi-allelic expression of X-linked loci, and reversal of *XIST* expression

The observed presence of *XIST* negative cells within colonies at early passages of the X12 hiPSC lines is in agreement with the present findings for the whole cell populations with the HUMARA assay and *XIST* expression analysis. Taken together, the results provide evidence that the hiPSCs, cultured under the above standard conditions, engage in both XCR and subsequent initiation of XCI.

To precisely evaluate the dynamics of XCR we performed allele specific single cell RT-PCR analysis, amplifying RFLPs in the X-linked genes *XIST*, *SUVAR39H1*, and *G6PD* at different time points after reprogramming. X12 iPSC and 47,XXX iPSC lines were FACS sorted in 96-well

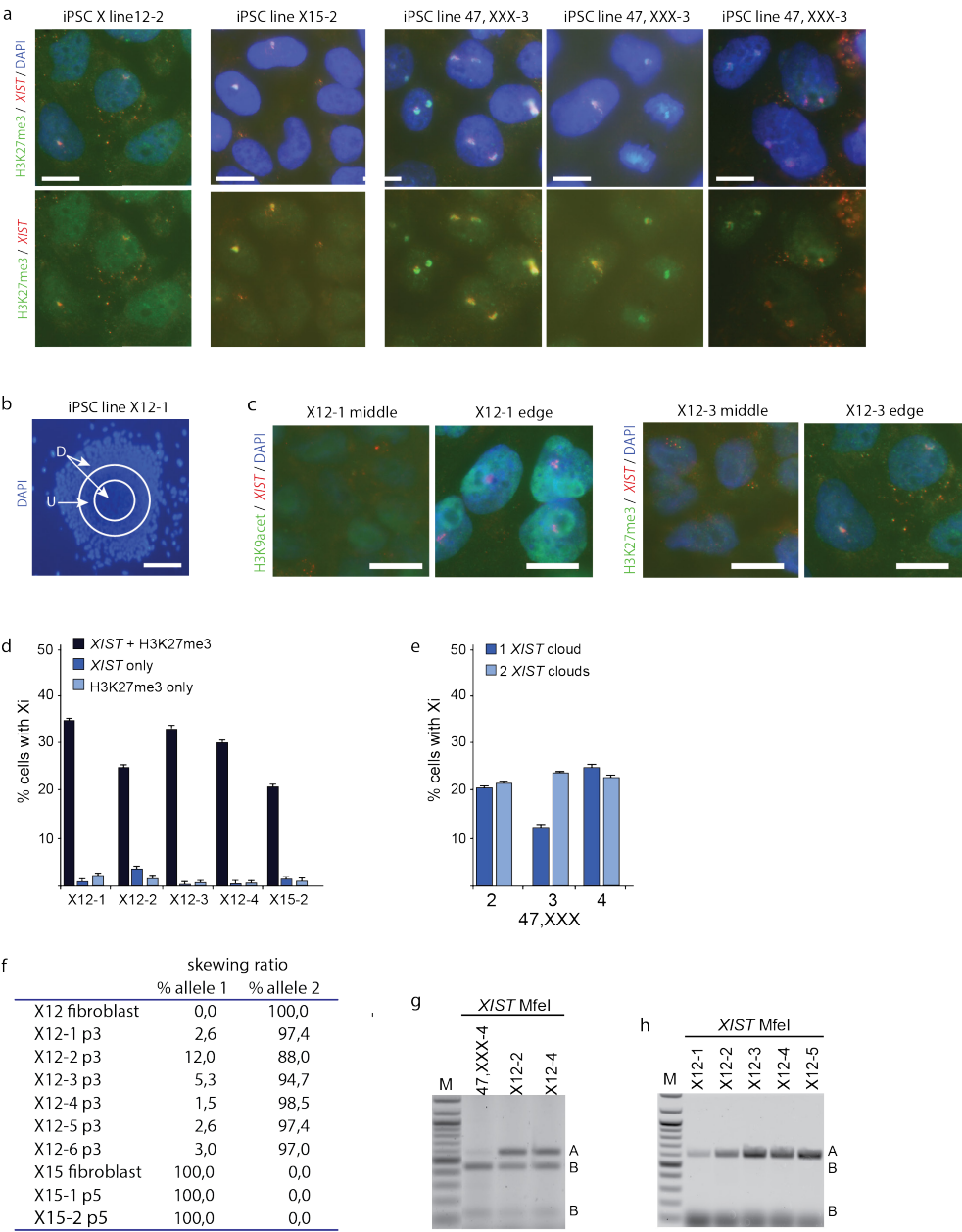


Figure 3.**XCI analysis of hiPSCs**

- a. Immuno-RNA-FISH analysis on hiPSC lines X12-2, X15-2, and 47,XXX-3 (all cells in a-e and g, passage 3), detecting *XIST* (Rhodamine Red) and H3K27me3 (FITC). In the upper panels, the nuclei are counterstained with DAPI (bar=10µm).
- b. Example of an X12-1 hiPSC clone, at lower magnification. Center part and edge of colony are indicated with D, the undifferentiated middle part of the colony with an U (bar=100µm).
- c. Immuno-RNA-FISH detecting *XIST* (Rhodamine Red) and H3K9ac (FITC, top panels), and detecting *XIST* (Rhodamine Red) and H3K27me3 (FITC, bottom panels) on cells found in U (left panels) and in d (right panels) (bar=10µm).
- d. Quantification of immuno-RNA-FISH analysis of representative hiPSC lines X12 (1-4) and X15-2. Percentages of cells with both an *XIST* cloud and H3K27me3 accumulation, only an *XIST* cloud, or only H3K27me3 accumulation are shown (mean±SD, n=3 experiments, >100 cells were counted per experiment).
- e. Quantification of immuno-RNA-FISH analysis of representative hiPSC lines 47,XXX (2-4). Percentage of cells with either one or two *XIST* clouds is plotted (mean±SD, n=3 experiments, >100 cells were counted per experiment).
- f. Quantification of all HUMARA analyses performed with different fibroblast and hiPSC lines, passages 3 and 5 (p3 and p5).
- g. Allele-specific RT-PCR analysis of *XIST*. PCR products were digested using MfeI to distinguish between both parental alleles. The hiPSC lines X12-2 and X12-4 show bi-allelic *XIST* expression, which was not found in the original fibroblast line (compare to Fig. 1d).
- h. As for Fig. 3g, but here day 8 differentiated X12 hiPSC lines are assessed.

plates, using antibodies against the pluripotency associated surface markers SSEA4 and Tra1-81, at p0, p3/4 and p25 after establishment. All sorted cells were tdTomato negative. Passage 0 cells were isolated 20 days after the start of the reprogramming procedure, prior to picking. For all time points, the SSEA4 and Tra1-81 double positive fraction represented more than 40% of the total viable cell fraction (Fig. 4a, and data not shown), and qPCR analysis showed increased expression of the pluripotency markers in pooled double positive SSEA4⁺/Tra1-81⁺ and GCTM2⁺/CD9⁺ sorted cells (Fig. 4b). SSEA4⁺/Tra1-81⁺ double positive (tdTomato negative) cells were sorted in lysis buffer, and single cell nested RT-PCR was performed, followed by restriction digestion to distinguish between expression from the different alleles. Analysis of *XIST* in X12 hiPSCs revealed a high percentage of cells not expressing *XIST*, and cells displaying expression of *XIST* emanating from the Xa (allele B) at all stages after reprogramming (Fig 4d,e). Also, allele specific expression analysis of X-linked *SUVAR39H1* revealed a high percentage of cells displaying expression of the previously inactive allele B (Supplemental Fig. 3).

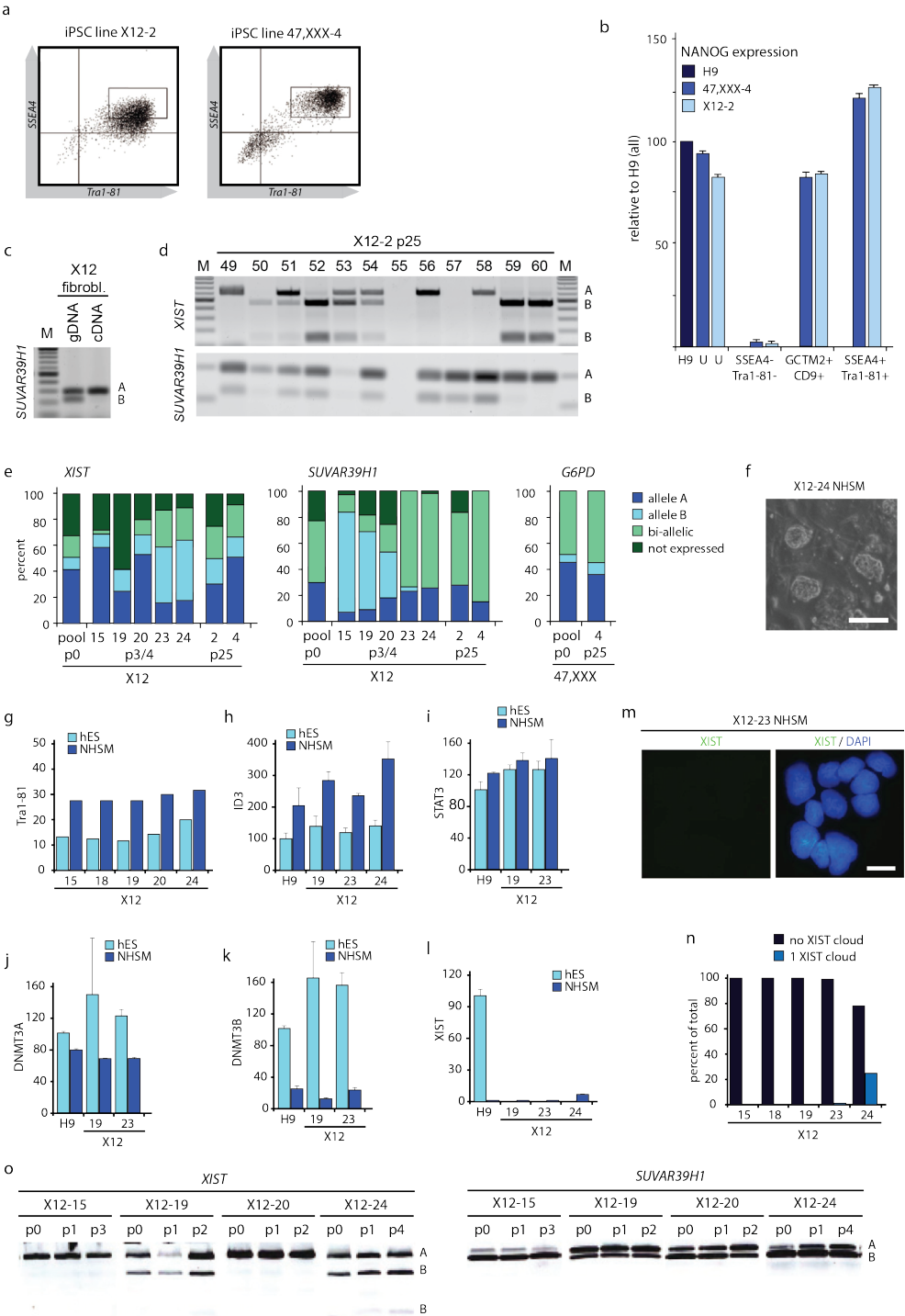


Figure 4

Single cell RT-PCR analysis of sorted hiPSCs

- a. FACS analysis of hiPSCs stained for the pluripotency associated surface markers SSEA4 and TRA1-81 (gate used to sort hiPSCs is shown).
- b. qRT-PCR analysis of NANOG in living sorted H9 ESCs, and X12-2 and 47,XXX-4 hiPSCs, comparing: unsorted cells (U), SSEA4-/TRA1-81- double negative cells, CD9+/GCTM2+ double positive cells, and SSEA4+/TRA1-81+ double positive cells. Results are normalized for GAPDH. NANOG expression in unsorted H9, the positive control, was set at 100.
- c. Allele specific expression analysis of SUVAR39H1 on gDNA and cDNA isolated from X12 fibroblasts.
- d. Single cell RT-PCR analysis of SSEA1+/TRA1-81+ sorted cells from hiPSC line X12-2 (passage 25, p25). Shown are the cells numbered 49-60. Allele-specific expression of *XIST* and *SUVAR39H1* was assessed by digestion with MfeI and MspI, distinguishing the parental alleles (indicated with A and B).
- e. Quantification of (Fig. 4d) for *XIST* (left graph) and *SUVAR39H1* (middle graph) on X12 iPSC lines (X12-2 up to X12-24, and the pooled lines) at different passages (p0 up to p25) after reprogramming. The right graph shows the quantification of allele specific expression analysis of *G6PD* on SSEA4+/Tra1-81+ sorted 47,XXX iPSCs (for all experiments N=96 cells per cell line)
- f. Dome shaped morphology of NHSM cultured hiPSCs (bar=100µm).
- g-k TRA1-81 (Fig. 4g), ID3 (Fig. 4h) and STAT3 (Fig. 4i) expression is increased, and DNMT3A (Fig. 4j) and DNMT3B (Fig. 4k) expression is decreased in NHSM cultured iPSC lines. Shown is mean intensity of TRA1-81 determined by FACS analysis. For ID3, STAT3, DNMT3A and DNMT3B expression per iPSC line is shown relative to H9 hESCs cultured in human ES medium.
- l. *XIST* expression analysis as in (Fig. 4h-k).
- m. *XIST* RNA-FISH analysis on X12-23 iPSCs grown in NHSM, passage 6 (>100 cells were counted per experiment, bar=10µm).
- n. Quantification of cells with XIST-coated X chromosomes in different X12 iPSC lines (p6).
- o. Allele specific expression analysis of *XIST* and *SUVAR39H1* at different passages (p0 – p4) of X12 hiPSC lines growing in NHSM (alleles A and B, as in Fig. 4d).

Interestingly, only a small percentage of cells displayed *XIST* and *SUVAR39H1* expression both exclusively from the alleles A, as was found for the founder fibroblasts used to generate the iPSCs (Fig. 4c, d, e, and Supplemental Fig. 3). In addition, the percentage of cells expressing only the *XIST* and *SUVAR39H1* alleles A did not markedly drop after establishment of the iPSC line. Similar results were obtained with iPSCs generated from 47,XXX fibroblasts analysed at p0 and p25, revealing a considerable amount of cells which showed bi-allelic expression of *G6PD*, indicating reactivation of the Xi (Fig 4e). These results indicate robust reactivation of the Xi during the early stages of the reprogramming process. In addition, the results of the RNA-FISH analysis on iPSC clones X12-2 and X12-4 suggest that in most cells expressing *XIST*, this RNA is detected only at very low levels (Fig. 3d and Fig. 4e). To test whether XCR involved multiple genes on the X chromosome we performed allele specific expression analysis of three additional informative genes located at different positions on the X. RNA was isolated from pooled cells of different X12 clones. In two out of the three tested iPSC clones (X12-23 and X12-24) we found bi-allelic expression of *HUWE1*, *ATP7A* and *NROB1*, whereas in iPS clone X12-19 only *NROB1* expression was bi-allelic (Supplemental Fig. 4, indicating that the robustness of XCR is variable between clones.

Recently, hESCs and hiPSCs have been generated with more naïve characteristics closely resembling the mouse mESCs (Gafni et al., 2013). Naïve hiPSC lines were established by reprogramming human fibroblasts in NHSM medium, but could also be generated by culturing hiPSCs established in standard hESC medium in NHSM. To test whether NHSM medium would enhance XCR in our iPSCs, we passaged (p3/4) five different hiPSC lines in NHSM medium, which already at passage one resulted in morphologically mouse-like hiPSCs that could be passaged through trypsinization (Fig. 4f). FACS and quantitative RT-PCR analysis indicated that expression of *TRA1-81*, *ID3* and *STAT3* was up-regulated, and that expression of *DNMT3A* and *DNMT3B* was down-regulated, in NHSM culture conditions as described (Gafni et al., 2013) (Fig. 4g, h, i, j, k). Other tested markers, including *TEAD4* and *DUSP10*, did not show consistent changes. *XIST* RNA-FISH and quantitative-RT-PCR analysis on these hiPSC lines, fixed after six passages in NHSM, indicated a near loss of *XIST* clouds and *XIST* expression in most lines (Fig. 4l, m, n), consistent with reported findings (Gafni et al., 2013). Allele specific RT-PCR analysis indicated no change in the allelic expression ratio of *XIST* after culturing the hiPSCs in NHSM, with different clones showing either bi- or mono-allelic expression of *XIST* (Figure 4O). For most clones, the allele specific expression ratio of *SUVAR39H1* was stable throughout several passages in NHSM. Also, allele specific expression analysis of *HUWE1*, *ATP7A* and *NROB1*, on three different X12 iPSC lines, indicated no change in the expression status before and after transfer to NHSM. These findings indicate that culture of the hiPSC lines in NHSM does not have an effect on XCR, but reduces *XIST* expression. This indicates that indeed a further shift towards stable XCR in hiPSCs can be obtained by culturing iPSCs in NHSM.

Discussion

Here, we have investigated the dynamics of X chromosome inactivation in hiPSCs derived from human female fibroblast cultures with completely skewed rXCI. This approach allowed us to include analysis of X chromosome reactivation (XCR) and X chromosome inactivation (XCI) at the single cell level. The present results show that, at the single cell level, reprogramming of human cells into hiPSCs results in XCR, even at early passages. Bi-allelic expression of different X-linked loci indicates that the Xi is reactivated in a large part of the cell population of our hiPSC lines, but is variable between iPSC lines. In several hiPSC lines we also detected *XIST* expression and expression of several X-linked genes from the allele which was not active in the starting fibroblast culture. Human iPSC lines share a clonal origin, and therefore this switch in expression from one allele to the other, or bi-allelic expression, indicates that during the reprogramming process XCR must have occurred in a high proportion of cells. Differentiation of hiPSCs was found to result in completely skewed rXCI, similar to that of the starting fibroblast population, indicating a high selective pressure against cells which have inactivated the intact X chromosome.

A recent study indicated that *XIST* expression can be lost upon prolonged passaging of female hiPSCs, referred to as “erosion of XCI” (Mekhoubad et al., 2012). This epigenetic erosion was found to be irreversible, and correlated with a loss of differentiation characteristics, and is very relevant for disease modelling procedures. Erosion of XCI in hiPSC lines can be effectively prevented by XCR followed by XCI upon differentiation. Several studies have been published assessing XCR during the reprogramming process. Derepression attributed to XCR of genes located on the Xi has been observed in hESC lines (Lengner et al., 2010), and has been reported in studies involving gene expression profile comparison of multiple female hESC and hiPSC lines (Bruck and Benvenisty, 2011). Very recently, XCR was shown to happen efficiently early during reprogramming of human cells, but that this was quickly followed by initiation of XCI upon generation of nascent hiPSC lines, leading to XaXi cells only (Kim et al., 2014). These authors concluded that XCR was the result of over-expression of the exogenous reprogramming factors, and that shut-down of the reprogramming cassette leads to XCI initiation. In contrast, our study indicates that in the present reprogramming and culture conditions hiPSCs maintain the XaXa state in a high percentage of cells in the absence of ectopic expression of the reprogramming factors. The present single cell allele specific expression analysis revealed expression of the *SUVAR39H1*, *HUWE1*, *ATP7A*, *NROB1* and *G6PD* alleles located at different positions on the X chromosome that was the Xi in the starting fibroblasts, in a high (>50%) proportion of cells of X12 and 47,XXX hiPSC lines. This effect was already present 20 days post-transduction, arguing against erosion of XCI in our hiPSC lines, and favouring XCR of the silenced Xi upon reprogramming. Our studies also showed that XaXa cells represent the major

population of cells at all stages after reprogramming, indicating that the present experimental conditions prevented robust precocious initiation of XCI, but allowed cells to maintain either the XaXa or the XaXi situation. Our findings would be in agreement with the suggestion that culturing hiPSCs in naïve growth conditions facilitates XCR, which was not addressed in this initial report (Gafni et al., 2013). Indeed, our studies indicate that NHSM growth conditions effectuate a reduction in the percentage of cells with *XIST*-coated X chromosomes. However, this does not lead to changes in the allele specific expression ratio of *SUVAR39H1*, *HUWE1*, *ATP7A* and *NROB1* in most hiPSC lines, and although we only analysed our cells at an early stage after changing to the NHSM condition (passage 4), these findings suggest that XCR and XCI characteristics are hiPSC line specific and established during reprogramming, and cannot be changed afterwards. Recently, two other protocols have been described to revert primed into naïve hESCs (Takashima et al., 2014; Theunissen et al., 2014). Surprisingly, one study reports initiation of XCI after induction of the naïve state (Theunissen et al., 2014), whereas another study indicates loss of *XIST* and H3K27me3 accumulation after a reset of primed to naïve ESCs (Takashima et al., 2014). These findings emphasize that knowledge about the transcriptional status of the X chromosomes in the ICM of the female pre-implantation human embryo will be crucial to conclude which of these conditions result in hESCs that resemble ICM cells most.

The results presented herein strongly suggest that XCR of the Xi is an important first step in reprogramming of human female fibroblasts, and demonstrate that rXCI is often *de novo* initiated during the culture of the generated hiPSC lines, most likely triggered by partial differentiation of the hiPSCs. In addition we found that XCR appears to occur remarkably efficient under standard reprogramming conditions, and that subsequent NHSM culture conditions stabilize this XaXa state. This facilitates rapid expansion and genetic manipulation of established female hiPSC lines with two active X chromosomes, to be used for various applications, in particular disease modelling, offering differentiated cell types that have newly established an Xi, thereby avoiding effects related to erosion of XCI. Furthermore, this provides us with a powerful model system to study human XCI, allowing us to examine the effects of a wide spectrum of X-linked mutations and deletions on XCI.

Experimental Procedures

Cell lines

GM07148 (X12), GM03923 (X14) and GM03827 (X15) fibroblast were obtained from the Corriel cell repository, and 47,XXX fibroblasts established from a skin biopsy of a triple X patient (Brosens et al., 2014). All fibroblast were cultured in standard fibroblast medium.

hiPS cell generation and culture

To generate iPSC, human fibroblasts from lines X12 (p12), X15 (p4), and 47,XXX (p14) were reprogrammed according to Warlich et al., with minor modifications (Warlich et al., 2011). NHSM medium and culture conditions were as described by Gafni et al., 2013. Detailed information is provided in the supplementary experimental procedures.

Immuno-RNA-FISH analysis

Detailed protocols and probes for RNA-FISH and immuno-RNA-FISH have been described (Barakat and Gribnau, 2014; Barakat et al., 2011; Jonkers et al., 2009). For immunostainings, the following antibodies were used: anti-Nanog (1:100, Abcam), anti-KLF4 (1:250, Abcam), anti-H3K27me3 (1:500, Diagenode), anti-H3K4me3 (1:1000, Upstate), anti-H3K9ac (1:1000, Sigma), anti-CD9 (Invitrogen), anti-GCTM2 (BD), anti-SSEA4 (BD) and anti-TRA1-80 (BD).

RT-PCR and single cell RT-PCR

All primers used are described in Supplementary Table 2. For single cell RT-PCR, *SSEA1+*/*TRA1-81+* double positive cells were FACS sorted in 96-well plates containing 9 µl lysis buffer using a BD FACSAria apparatus. Lysis buffer consisted of 8 µl 2xReaction mix (SuperScript One-Step RT-PCR kit, Invitrogen), 10U RNaseOut (Invitrogen), and 0.15% IGEPAL CA-630 (Sigma). cDNA was prepared with gene specific outer primers, and further processed as described in the supplementary experimental procedures. PCR products were precipitated, and digested with the indicated restriction enzymes (New England Biolabs) to distinguish expression from the different alleles. RFLPs in *XIST*, *SUVAR39H1*, *G6PD*, and SNPs in *HUWE1*, *NROB1* and *ATP7A* were identified by PCR amplification and Sanger sequencing, followed by allele specific expression analysis using cDNA specific primer sets described in Supplementary Table 2.

SNP array and HUMARA analysis

To map the deletions in our fibroblast cell lines, SNP array was performed using Human CYTO SNP 12 version 1 arrays (Illumina®, San Diego, CA, USA), aligned to human genome build 18. A detailed description of the HUMARA assay applied to determine skewing of XCI is provided in the supplementary experimental procedures.

DNA-FISH analysis

To visualize the deletion in cell lines, DNA-FISH was performed according to standard procedures. Probes used were BAC CTD-3076O23 (BAC1FITC, Xq23, 108,9 Mb, HG19), RP11-799O20 (BAC2, A595, Xq25, 123 Mb) RP11-75N13 (BAC3, FITC, Xq21.1, 84,5 Mb), and RP1-279N11 (BAC4, A595, Xq13.3, 75,8 Mb).

Statistics qRT-PCR analysis

For qRT-PCR expression analysis the average and standard deviation of three biological replicates is shown.

Acknowledgements

We thank dr. Axel Schambach for providing the reprogramming vector. We thank dr. Dorota Kurek and dr. Derk ten Berge for providing anti-GCTM2 antibody. Dr. Sabrina Roth is acknowledged for advice on single cell RT-PCR.

References

- Allen, R.C., Nachtman, R.G., Rosenblatt, H.M., and Belmont, J.W. (1994). Application of carrier testing to genetic counseling for X-linked agammaglobulinemia. *Am J Hum Genet* 54, 25-35.
- Amenduni, M., De Filippis, R., Cheung, A.Y., Disciglio, V., Epistolato, M.C., Ariani, F., Mari, F., Mencarelli, M.A., Hayek, Y., Renieri, A., *et al.* (2011). iPS cells to model CDKL5-related disorders. *Eur J Hum Genet* 19, 1246-1255.
- Ananiev, G., Williams, E.C., Li, H., and Chang, Q. (2011). Isogenic pairs of wild type and mutant induced pluripotent stem cell (iPSC) lines from Rett syndrome patients as in vitro disease model. *PLoS One* 6, e25255.
- Barakat, T.S., and Gribnau, J. (2012). X chromosome inactivation in the cycle of life. *Development* 139, 2085-2089.
- Barakat, T.S., and Gribnau, J. (2014). Combined DNA-RNA fluorescent in situ hybridization (FISH) to study X chromosome inactivation in differentiated female mouse embryonic stem cells. *J Vis Exp*.

- Barakat, T.S., Gunhanlar, N., Pardo, C.G., Achame, E.M., Ghazvini, M., Boers, R., Kenter, A., Rentmeester, E., Grootegoed, J.A., and Gribnau, J. (2011). RNF12 activates Xist and is essential for X chromosome inactivation. *PLoS Genet* 7, e1002001.
- Brosens, E., de Jong, E.M., Barakat, T.S., Eussen, B.H., D'Haene, B., De Baere, E., Verdin, H., Poddighe, P.J., Galjaard, R.J., Gribnau, J., *et al.* (2014). Structural and numerical changes of chromosome X in patients with esophageal atresia. *Eur J Hum Genet*.
- Bruck, T., and Benvenisty, N. (2011). Meta-analysis of the heterogeneity of X chromosome inactivation in human pluripotent stem cells. *Stem Cell Res* 6, 187-193.
- Cheung, A.Y., Horvath, L.M., Grafodatskaya, D., Pasceri, P., Weksberg, R., Hotta, A., Carrel, L., and Ellis, J. (2011). Isolation of MECP2-null Rett Syndrome patient hiPS cells and isogenic controls through X-chromosome inactivation. *Hum Mol Genet* 20, 2103-2115.
- Gafni, O., Weinberger, L., Mansour, A.A., Manor, Y.S., Chomsky, E., Ben-Yosef, D., Kalma, Y., Viukov, S., Maza, I., Zviran, A., *et al.* (2013). Derivation of novel human ground state naive pluripotent stem cells. *Nature* 504, 282-286.
- Harnden, D.G. (1961). Nuclear sex in triploid XXY human cells. *Lancet* 2, 488.
- Jonkers, I., Barakat, T.S., Achame, E.M., Monkhorst, K., Kenter, A., Rentmeester, E., Grosveld, F., Grootegoed, J.A., and Gribnau, J. (2009). RNF12 is an X-Encoded dose-dependent activator of X chromosome inactivation. *Cell* 139, 999-1011.
- Kim, K.Y., Hysolli, E., and Park, I.H. (2011). Neuronal maturation defect in induced pluripotent stem cells from patients with Rett syndrome. *Proc Natl Acad Sci U S A* 108, 14169-14174.
- Lengner, C.J., Gimelbrant, A.A., Erwin, J.A., Cheng, A.W., Guenther, M.G., Welstead, G.G., Alagappan, R., Frampton, G.M., Xu, P., Muffat, J., *et al.* (2010). Derivation of pre-X inactivation human embryonic stem cells under physiological oxygen concentrations. *Cell* 141, 872-883.
- Lyon, M.F. (1961). Gene action in the X-chromosome of the mouse (*Mus musculus* L.). *Nature* 190, 372-373.
- Maherali, N., Sridharan, R., Xie, W., Utikal, J., Eminli, S., Arnold, K., Stadtfeld, M., Yachechko, R., Tchieu, J., Jaenisch, R., *et al.* (2007). Directly reprogrammed fibroblasts show global epigenetic remodeling and widespread tissue contribution. *Cell stem cell* 1, 55-70.
- Marchetto, M.C., Carromeu, C., Acab, A., Yu, D., Yeo, G.W., Mu, Y., Chen, G., Gage, F.H., and Muotri, A.R. (2010). A model for neural development and treatment of Rett syndrome using human induced pluripotent stem cells. *Cell* 143, 527-539.
- Mekhoubad, S., Bock, C., de Boer, A.S., Kiskinis, E., Meissner, A., and Eggan, K. (2012). Erosion of dosage compensation impacts human iPSC disease modeling. *Cell Stem Cell* 10, 595-609.
- Pollex, T., and Heard, E. (2012). Recent advances in X-chromosome inactivation research. *Curr Opin Cell Biol* 24, 825-832.

- Pomp, O., Dreesen, O., Leong, D.F., Meller-Pomp, O., Tan, T.T., Zhou, F., and Colman, A. (2011). Unexpected X chromosome skewing during culture and reprogramming of human somatic cells can be alleviated by exogenous telomerase. *Cell Stem Cell* 9, 156-165.
- Silva, S.S., Rowntree, R.K., Mekhoubad, S., and Lee, J.T. (2008). X-chromosome inactivation and epigenetic fluidity in human embryonic stem cells. *Proc Natl Acad Sci U S A* 105, 4820-4825.
- Stadtfield, M., Maherali, N., Breault, D.T., and Hochedlinger, K. (2008). Defining molecular cornerstones during fibroblast to iPS cell reprogramming in mouse. *Cell Stem Cell* 2, 230-240.
- Takahashi, K., Tanabe, K., Ohnuki, M., Narita, M., Ichisaka, T., Tomoda, K., and Yamanaka, S. (2007). Induction of pluripotent stem cells from adult human fibroblasts by defined factors. *Cell* 131, 861-872.
- Takashima, Y., Guo, G., Loos, R., Nichols, J., Ficz, G., Krueger, F., Oxley, D., Santos, F., Clarke, J., Mansfield, W., *et al.* (2014). Resetting transcription factor control circuitry toward ground-state pluripotency in human. *Cell* 158, 1254-1269.
- Tchieu, J., Kuoy, E., Chin, M.H., Trinh, H., Patterson, M., Sherman, S.P., Aimiwu, O., Lindgren, A., Hakimian, S., Zack, J.A., *et al.* (2010). Female human iPSCs retain an inactive X chromosome. *Cell Stem Cell* 7, 329-342.
- Theunissen, T.W., Powell, B.E., Wang, H., Mitalipova, M., Faddah, D.A., Reddy, J., Fan, Z.P., Maetzel, D., Ganz, K., Shi, L., *et al.* (2014). Systematic identification of culture conditions for induction and maintenance of naive human pluripotency. *Cell Stem Cell* 15, 471-487.
- Warlich, E., Kuehle, J., Cantz, T., Brugman, M.H., Maetzig, T., Galla, M., Filipczyk, A.A., Halle, S., Klump, H., Scholer, H.R., *et al.* (2011). Lentiviral vector design and imaging approaches to visualize the early stages of cellular reprogramming. *Mol Ther* 19, 782-789.

CHAPTER 7



Discussion



Human iPS cells as a model system for XCI

At this moment there is no efficient model system at hand for studying the mechanisms of human XCI. In addition, studying human XCI as it occurs during female embryonic development would require the study of human embryos, which is difficult and ethically objectionable. With the generation of human iPS cells, a model system for studying human XCI may be within reach. Human iPS cells were first generated by S. Yamanaka's lab in 2007 (Takahashi et al., 2007). By introducing four pluripotency-associated transcription factors in adult somatic cells they were able to reprogram these cells into pluripotent stem cells. This technology circumvents the need for human embryos in generating pluripotent stem cells, and holds great promise for the field of regenerative medicine. In addition, human iPS cell technology has been very useful to model human disease and to study human embryonic development. Furthermore, as iPS cells can be maintained indefinitely, and hold the potential to maintain two Xa's, they also seem a promising model system for studying the mechanisms of XCI. However, several studies that analyzed the status of X chromosomes in iPS cells have reported contradictory outcomes regarding reactivation of the Xi (Amenduni et al., 2011; Ananiev et al., 2011; Cheung et al., 2011; Kim et al., 2011; Marchetto et al., 2010; Pomp et al., 2011; Tchieu et al., 2010).

In chapter 6 we studied reactivation of the Xi during reprogramming of human fibroblasts towards iPS cells, using fibroblasts that are 100% skewed. Using fibroblasts with 100% skewed XCI will increase the sensitivity to detect expression from the Xi. We found that only one of the three fibroblast lines that were used, had reactivated the Xi during iPSC reprogramming. The inability to generate iPSC clones with two Xa's from the other two cell lines, illustrates the inefficiency of the reactivation process during the reprogramming from adult somatic cells towards iPS cells. In addition, it is also possible that we obtained iPSC clones with two Xa's for only one of the three cell lines purely by chance. The reprogramming process is highly variable, and only a few iPSC clones reach a state that is naïve enough to facilitate reactivation of the Xi. Therefore, the large variability in reprogramming efficiency will probably result in a stochastic outcome of the Xi reactivation process. The outcome of only one of the three cell lines managing to reach a state with two reactivated X chromosomes, might also be subject to coincidence during the analysis. As only six iPSC clones were analyzed per cell line, clones with an Xi could by coincidence have been selected. Although unlikely, this option cannot be ruled out. Another, intriguing, hypothesis explaining why only one of the three cell lines yielded iPSC clones with two Xa's is that the X chromosome aberration of this cell line is implicated in the reactivation process of the Xi. The fibroblast cell line for which we could generate iPSC clones with two Xa's carries an abnormal X chromosome, involving a truncation of the long arm of the Xi. Loss of genetic material from the Xi might facilitate its reactivation

during reprogramming. One explanation how loss of genetic material might facilitate reactivation, is if the region involved in the truncation contains a trans-acting activator of XCI. Genetic loss of a trans-acting activator is likely to result in a larger probability for reactivation of the Xi. This hypothesis is contradicted by the observation that one of the other fibroblast cell lines that was used in this experiment did not show any Xi reactivation, while it carried an Xi with a deletion involving the same region that is deleted in the X12 fibroblasts. This line, X15, carries an Xi with a larger truncation of the long arm, encompassing the truncation of the X12 line. Therefore, involvement of the deleted region of the X12 fibroblast line in successful Xi reactivation, should be considered with caution.

The reactivation of the Xi which was observed, was found to be instable. Instead of a stable reactivation, the Xi seems to be subject to a continuous process of reactivation and inactivation in conventional culture medium. When cultured in naïve medium, expansion of clones containing two Xa's is possible. This observation illustrates the difficulties in obtaining and maintaining iPSC clones carrying two Xa's, and indicates that Xi reactivation in iPSC cells should be considered with care.

Another argument to consider Xi reactivation in iPSC cells with caution is provided by a rather unusual reactivation pattern that was observed in an iPSC clone generated from fibroblasts of a female carrying an *RNF12* mutation on the Xi (unpublished results). This female carried the *RNF12* hypermorph mutation of family 1, described in chapter 4. Two fibroblast cell lines were obtained from siblings that are carriers of this mutation, and were subjected to iPSC reprogramming. Six iPSC clones were obtained in total, with only one of these clones showing Xi reactivation. Transcriptional analysis of the Xi showed reactivation of the X-encoded genes *G6PD*, *HUWE1* and *NAP1L3* in this iPSC clone. However, the mutant *RNF12* allele was not expressed in these iPSC cells, suggesting that most of the X chromosome, if not all, was reactivated except for *RNF12*. This observation might be explained by the *RNF12* mutation itself, although we consider this option unlikely, as the point mutation of the mutant allele would have to result in either complete transcriptional inhibition or transcript instability. This is something we did not observe in HEK293 cells or mouse ES cells transfected with this mutant allele. A more likely explanation would be that while most of the X chromosome is reactivated, a small region surrounding the XIC is not, and *Xist* is still expressed from the reactivated Xi. The continued expression of *Xist* after reactivation of the Xi, provides an explanation why the region surrounding the Xic is not reactivated, as *Xist* RNA still accumulates locally in the Xic region. Furthermore, this hypothesis might explain why human iPSC cells preferentially inactivate the reactivated Xi upon iPSC differentiation, as *Xist* might already have locally accumulated on this chromosome prior to differentiation. Lastly, the continued expression of *Xist* from the reactivated X might explain why the Xi of iPSC cells in conventional medium seems to be subject to continuous reactivation and inactivation. Unfortunately, the described

reactivation pattern of reactivation along the X chromosome, except for a region surrounding the *Xic*, was observed only in a single iPSC clone. So far we could not confirm these results for other iPSC clones, as allele specific *RNF12* expression analysis could only been performed for one other iPSC line.

In conclusion, it seems possible to obtain iPSC clones that contain two active X chromosomes, at a low efficiency and with questionable stability. In addition, it could be that reactivation does not involve the entire X chromosome, and *XIST* continues to be expressed from the partially reactivated X chromosome. Altogether, it appears unlikely that iPSC technology will be suitable as a standard model for studying the mechanisms of human XCI at this moment. Perhaps that with the inclusion of additional reprogramming factors, new culture media and increasing knowledge of the reprogramming process, iPSC reprogramming will be more efficient and can be accompanied by stable reactivation of the Xi. Future experiments should be aimed at understanding the difference between human and mouse ES and iPS cells, as mouse ES and iPSC cells are characterized by two Xa's, where human ES cells and iPS cells mostly carry an Xi. The differences between mouse and human systems might be explained by the developmental stage represented by these cells. In addition, studies with human embryos will be crucial to understand how XCI precedes during normal human peri-implantation development, providing a benchmark what to expect with respect to human iPS cells.

The stochastic model for counting and choice

In chapter 2 we provided additional evidence that XCI in mouse ES cells is stochastic, with both X chromosomes having an individual probability to inactivate. The previously postulated models are deterministic in nature and propose that prior to actual inactivation, a cell determines which X chromosome will be inactivated. However, a deterministic model cannot explain the observation of diploid female cells that have initiated XCI on both X chromosomes. In a stochastic model initiation of XCI on both X chromosomes is possible, as both X chromosomes have an intrinsic probability to inactivate, independent of each other.

Although a stochastic model of XCI is most fitting with *in vitro* and *in vivo* observations, debate has continued on whether a stochastic model should be supplemented or replaced by the transvection model. In the transvection model, inactivation of one of the two X chromosomes present in female cells is accomplished by a transient co-localization of the two X chromosomes, before initiation of XCI. Co-localization of the *Xic*'s of the two X-chromosomes regulates monoallelic *Xist* upregulation, resulting in the inactivation of only one X chromosome (Augui et al., 2007; Bacher et al., 2006; Donohoe et al., 2009; Masui et al., 2011; Xu et al.,

2006). Indeed, in a recent publication it is argued that the frequency at which biallelic *Xist* upregulation is observed is too low to be explained by stochastic gene expression alone, and other mechanisms need to exist to ensure monoallelic expression (Masui et al., 2011). Therefore, the authors propose the transvection model as an alternative model to stochastic initiation of XCI. The hypothesis of transvection in XCI is based on the observations that the two Xic's co-localize for 45 minutes during initiation of XCI, and that during co-localization *Tsix* expression is often monoallelic. The observed monoallelic expression of *Tsix* is proposed to be the consequence of an asymmetric distribution of regulatory factors, and will result in monoallelic *Xist* expression. Although *Tsix* expression is restored to biallelic expression after one hour, *Xist* continues to be monoallelic expressed, resulting in XCI.

Although transvection is an intriguing hypothesis, the observed frequency of Xic-Xic pairing is too low to explain *in vitro* observations, with XCI initiating at a much higher frequency. Instead, the observed Xic-Xic pairing could also be explained by a more general mechanism of transcriptional regulation. Gene transcription occurs at nuclear foci enriched for RNA pol II, termed transcription factories. Genes are transcribed in bursts, separated by pauses of gene silence. During their transcriptional bursts genes tend to co-localize in transcription factories, and multiple genes, located *in-cis* or *in-trans* can therefore share the same transcription factory (Osborne et al., 2007). Given these observations, it seems more likely that the co-localization of the two Xic's during initiation of XCI is a reflection of their change from transcriptional silence to transcriptional activity, during which they will co-localize with increased frequency at the same transcription factory.

In addition, several *in vitro* experiments suggest that transvection of the two X chromosomes is not required for proper initiation of XCI. The elements that were proposed to be required for transvection are the *Xite*, *Tsix* and *Xpr* regions. However, studies with mouse ES cells carrying deletions of these genetic elements, separately or together, showed proper initiation of XCI in absence of these elements (Barakat et al., 2014). This indicates that transvection is not required for initiation of XCI, or can still occur in absence of these elements.

In addition, transvection seems relatively easy when two X chromosomes are involved, but can be envisioned as highly problematic when more than two X chromosomes are present. If in such a situation the co-localization of more than two X chromosomes occurs sequentially or parallel was never specified. Nevertheless, XCI takes place in situations where more than two X chromosomes are present. In human female 47XXX individuals two of the X chromosomes are inactivated (Grumbach et al., 1963). Also in mouse tetraploid XXXX and XXXY embryos and ES cells, XCI occurs and the majority of cells maintains two Xa's (Webb et al., 1992). Although co-localization of more than two X chromosomes would be a complicated process none of these experiments measured co-localization of the two X chromosomes during XCI, and can therefore conclude that it does not occur. Therefore, the most convincing

evidence that transvection is not required for proper initiation of XCI comes from experiments where XX and XY ES cells were fused to form XX-XY heterokaryons. Upon differentiation, these cells still initiate XCI on the single X chromosome present in the male nucleus, a situation that is incompatible with transvection. Taken together, these results indicate that X-pairing or transvection is not required for determining the number of X chromosomes and proper initiation of XCI. Therefore, we conclude that a stochastic model for XCI counting and choice is the only model compatible with all observed outcomes of the XCI process.

Trans-acting activators of XCI

Rnf12 is likely not the only trans-acting activator of XCI in mouse

Correct regulation of XCI is probably subject to a sensitive titration between XCI activators and XCI inhibitors. The XCI activators are responsible for counting the number of X chromosomes in a nucleus and together with autosomal XCI inhibitors determine how many X chromosomes will be inactivated. The major representative of the XCI activators in the mouse is *Rnf12*, as it is the only XCI activator identified to date (Gontan et al., 2012; Jonkers et al., 2009). Despite being the only identified *trans*-acting activator of XCI, the involvement of other XCI activators in mouse is indicated by experiments with female *Rnf12*^{-/-} ES cells. Such ES cells should with regard to XCI, be similar to male ES cells that have only one allele of *Rnf12*. However, where male ES cells do not initiate XCI, female *Rnf12*^{-/-} ES cells can initiate XCI, although at a lower rate compared to wildtype cells (Barakat et al., 2014).

When speculating on the genomic location of other XCI activators, one should consider the evidence that hinted at the genomic location of *Rnf12*. *Rnf12* was identified as an activator of XCI by screening transgenic ES lines carrying BACs covering two regions of 5 Mb, located centromeric and telomeric of the Xic. The presence of an XCI activator in these regions was indicated by experiments analyzing XCI in mice carrying the HD3 truncation and the T(16;X) Searle's translocation (Fig 1). Cells carrying an X chromosome with the HD3 truncation were still able to inactivate both the wildtype X chromosome and the X chromosome with the HD3 truncation, indicating the presence of an XCI activator on this X chromosome. On the other hand, cells carrying the X¹⁶ product of Searle's translocation never showed inactivation of the X¹⁶ product, indicating the XCI activator is missing from this chromosome. In addition, deletion of the Xic from one of the X chromosomes in female ES cells did not result in an XCI phenotype, indicating that this region not contains an XCI activator (Monkhorst et al., 2008). From these observations it followed that an XCI activator had to be located in between the breakpoints of these two X-chromosomal aberrations, leading to the identification of *Rnf12*.

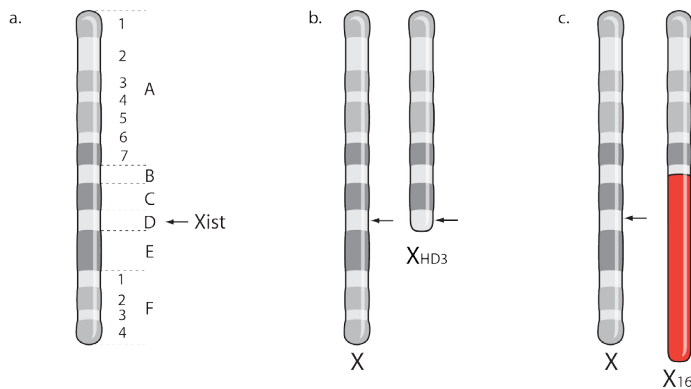


Figure 1.

Mouse X chromosome abnormalities defining the region harboring a trans-acting activator

- Ideogram of a mouse X chromosome depicting the chromosome bands
- The HD3 truncation has its breakpoint in the middle of chromosome band D.
- Searle's translocation involves the exchange of genetic material between the X chromosome and chromosome 16. The X-chromosomal breakpoint is located in chromosome band B.

As *Rnf12* is the first XCI activator identified in the region delineated by the HD3 truncation and Searle's translocation, it is likely to be the most important. The location of other XCI activators can also be hypothesized between the breakpoints of the HD3 truncation and Searle's translocation (Rastan, 1983; Rastan and Robertson, 1985; Takagi, 1980). However, the presence of XCI activators outside this region should certainly not be excluded. The breakpoints delineating this region were described and examined in the early 80's. The breakpoint of the HD3 truncation, was mapped to the middle of the X-D band using karyotyping (Robertson et al., 1983). However, a later study examined hybrid cell lines from the HD3 ES cell line, and found 7 classes of HD3 breakpoints. Only one of these breakpoints retained an *Xist* allele, as is compatible with the observed XCI from this truncated X chromosome. Using PCR this breakpoint was not mapped to the X-D band, but instead to the interval between *DXMit4* and *Plp1* in band X-F1 (Arnaud et al., 1993). Based on this study the telomeric interval harboring the XCI activators is not 5 Mb but 36 Mb instead. Given that these early studies analyzed XCI using chromosome staining techniques (like the Kanda method) to identify the inactive X chromosome, it is not unlikely that they were unable to detect early initiation of XCI in the analyzed cells and embryos (Kanda, 1973). As *Rnf12* is the major XCI

activator, the effect of less important activators might have been missed using these less sensitive methods. Taken together, the location of the breakpoints delineating the region harboring the XCI activators can be questioned, as well as the sensitivity of XCI analysis. Therefore the location of additional XCI activators with less potential than *Rnf12* should best be approached in an unbiased, hypothesis-free way.

Human RNF12 as a trans-acting activator of XCI

While *Rnf12* is identified as an activator of murine XCI, it is uncertain whether *RNF12* also acts as an activator for human XCI. In chapter 3 and 4 several observations suggest that *RNF12* might act as an activator of human XCI as well, although definite proof still needs to be provided. In chapter 3 genetic evidence is provided that *RNF12* might act as a *trans*-acting activator of human XCI. We describe a female individual, with a 1.2 Mb deletion of the *Xic*, involving *XIST*, *TSIX* and their *cis*-regulatory elements, but not *RNF12*. Cells heterozygous for this deletion are able to undergo XCI, which is in agreement with our observations in the mouse, and indicate that also in human the XCI activator(s) is located outside the deleted region. Comparing this deletion to other X-chromosomal aberrations narrows down the location of a *trans*-acting activator to a region telomeric of the *cis*-XIC, encompassing *RNF12* (Allderdice et al., 1978; Brown et al., 1991; Lafreniere and Willard, 1993).

Other lines of genetic evidence suggesting that *RNF12* might act as a *trans*-acting activator of XCI are provided by ring X chromosomes. Ring X chromosomes are truncated X chromosomes that retain a centromere and are fused at their truncated telomeres, resulting in a ring-shaped chromosome. They can be detected in Turner syndrome patients, that show mosaicism with the majority of their cells having a 45X0 karyotype and a small proportion containing an additional ring X chromosome. The active state of these ring X chromosomes is associated with a more severe phenotype. Some of these ring X chromosomes contain different regions of the XIC and adjacent regions and could provide a clue to the location of *trans*-acting activators. Quite a number of X chromosomes contain a breakpoint nearby *RNF12*, but unfortunately they are not characterized with enough precision to assess involvement of *RNF12*. Therefore, more precise characterization of the breakpoints of these ring X chromosomes is mandatory before conclusions can be made with respect to involvement of *RNF12* in XCI. Nevertheless, XCI phenotypes of cell lines containing ring X chromosomes need to be interpreted with caution, as the ring X chromosome could have arisen after XCI had occurred and the *trans*-acting activator might have been deleted after onset of XCI. An example of an abnormal X chromosome not undergoing XCI because it had arisen after XCI is described in a female individual with Turner syndrome and chromosomal mosaicism involving three abnormal cell lines (Migeon et al., 1996). One of these cell lines retained a truncated X chromosome involving a deletion of the long arm, but leaving the *cis*-XIC and *RNF12* intact.

Despite the presence of two copies of *RNF12* and two XIC's this cell line did not show XCI. The relative proportions of the three cell lines in this individual, and the absence of XCI in the cell line containing the truncated X chromosome led the researchers to believe that the truncated X chromosome had been formed through duplication of a monosomic X chromosome and subsequent degeneration of the duplicated X chromosome. This report illustrates that the XCI phenotype might not always be related to the observed X chromosomal abnormalities found in Turner syndrome patients. However, when iPS cell reprogramming can reliably generate cells with two active X chromosomes, iPS cells generated from cell lines containing well characterized ring X chromosomes will be very interesting for genetic dissection of the human XCI machinery. Alternatively, human XCI activators could be identified by introducing large deletions in the X chromosome of human iPSC lines using the CRISPR/Cas9 targeting system. Upon deletion of an XCI activator these cell lines will initiate XCI at a lower rate when they are induced to differentiate.

Several studies have described individuals carrying X-chromosomal aberrations that indicate that a human *trans*-acting activator is located in the region containing *RNF12* (Allderdice et al., 1978; Brown et al., 1991; Lafreniere and Willard, 1993; Leppig et al., 1993). However, one study describes an abnormal X chromosome that lacks *RNF12* but still displays XCI, indicating that other *trans*-acting activator genes might exist besides *RNF12* (Leppig et al., 1993). These alternative *trans*-acting activators must be located in the region centromeric of the *cis*-XIC, or on the short arm of the X chromosome.

In addition to genetic observations suggesting that *RNF12* might function as a *trans*-acting activator of XCI, several lines of biochemical evidence also support this. Firstly, human and mouse *RNF12/Rnf12* transgenes induce ectopic XCI equally well in male transgenic ES cells (Jonkers et al., 2009). This shows that human *RNF12* functions in a murine cellular environment, and suggests that human *RNF12* is able to target mouse *REX1* for proteasomal degradation, leading to XCI in male cells, analogous to how mouse *Rnf12* operates (Gontan et al., 2012; Jonkers et al., 2009). The experiments described in chapter 4 show that in HEK293 cells human *RNF12* ubiquitinates human *REX1*, thereby targeting the latter for proteasomal degradation. Despite this analogy in *RNF12*-induced degradation of *REX1* between mouse and human, we have not been able to show that the human *RNF12/REX1* axis also regulates human XCI. Human iPS cells generated from female carriers of mutations in *RNF12* did not contain a reactivated X chromosome, and could therefore not be used to demonstrate an effect of the identified *RNF12* mutation of XCI.

Indirect evidence that *RNF12* is involved in XCI is provided by the families described in chapter 4. Although these families carry different mutations in *RNF12*, that affect different functional domains, all three families show completely skewed XCI in females carrying the mutated allele. Skewed XCI affects blood cells, skin fibroblasts and cone cells of the retina. We

consider it unlikely that this skewed XCI is the result of secondary cell selection against cells that have inactivated the X chromosome carrying the unaffected *RNF12* allele. In fact, males inheriting this mutation are viable and display diverse phenotypes, demonstrating that cell viability is unaffected or mildly affected. Instead it seems more likely that cell functioning is affected by *RNF12* mutations, which could possibly lead to secondary cell selection. However, we consider it unlikely that such a secondary cell selection would lead to completely skewed XCI, and that this would affect all tissues analyzed. Therefore, we hypothesize that the identified mutations affect RNF12 protein functioning, and result in primary non-random skewing of XCI. This hypothesis is supported by the observation that XCI in *Rnf12*^{+/-} mice is also primary skewed towards inactivation of the mutant X chromosome.

Taken together, the experiments described in chapter 4 indicate that human REX1 is targeted for proteasomal degradation by RNF12. However, to finally prove that *RNF12* acts as a *trans*-acting activator of XCI, a repressive effect of REX1 on *XIST* expression should be demonstrated. To date, involvement of REX1 as a repressor of *XIST* has to our knowledge not been investigated yet. Demonstrating this function of REX1 is crucial to demonstrate that human *RNF12* functions as a *trans*-acting activator of XCI, analogous to mouse *Rnf12*. Unfortunately, human iPS cells do not seem suitable for this purpose. A promising experiment would be to mutate *REX1* human ES cells containing two active X chromosomes, using CRISPR technology to analyze the effect on XCI.

Although the results presented here provide evidence that *RNF12* might act as a *trans*-activator of XCI, they do not allow us to conclude this with any certainty. Instead, it should still be considered that *RNF12* might not be involved in human XCI, as several arguments support this as well. First, REX1 protein levels did not differ between wildtype and mutant *RNF12* in co-transfection experiments. Also, endogenous REX1 levels in iPS cells reprogrammed from skin fibroblasts of an affected male from family 3 did not show any differences from unaffected iPS cells (quantified immunostainings, data not shown). Second, XCI might proceed differently in humans compared to mouse. When XCI is initiated in mouse embryos *Xist* accumulates on one X chromosome, which results in the inactivation of the *Xist* coated X chromosome. Although a small percentage of cells can be observed with two *Xist* coated X chromosomes, these cells are thought to have faulty inactivated both X chromosomes (Monkhorst et al., 2008). In human embryos, the onset of XCI in early blastocysts has been studied by few studies. Two of these studies observed two *XIST* domains in the majority of cells, without accompanying characteristics of gene silencing (Okamoto et al., 2011; Teklenburg et al., 2012). Although these observations are contradicted by a third study, they provide an interesting hypothesis in light of our results. If indeed, during human XCI *XIST* RNA accumulates on both X chromosomes before gene silencing is induced, a function of RNF12 as a *trans*-acting activator might have become obsolete. Instead, such a system would require a *trans*-acting inhibitor that prevents

inactivation of both X chromosomes when actual silencing is initiated. Hypothetically *RNF12* could still perform this feedback function via inhibition of *XIST* transcription through REX1.

RNF12:REX1 titration

From previous experiments, and the experiments described in chapter 4 it can be hypothesized that correct regulation of XCI is subject to a sensitive titration between XCI activators and XCI inhibitors, which is mostly reflected by the balance between REX1 and RNF12. Previous studies performed in mouse showed that degradation of REX1 by RNF12 is dose dependent, indicating that expression of *Rnf12* and *Rex1* is well balanced during mouse XCI (Gontan et al., 2012). It can be hypothesized that also for human XCI titration between XCI activators and XCI inhibitors needs to be well balanced to correctly regulate XCI. The experiments described in chapter 4 show that degradation of human REX1 is dependent on the dose of RNF12, and that titration of these levels is very important with respect to the outcome of the experiment. In co-transfection experiments with a human *RNF12:REX1* ratio of 1:16, *RNF12* expression seems not to affect *REX1* expression, indicating that REX1 is not significantly degraded when present in excess. In contrast, at a ratio of 3:1 RNF12 completely degrades REX1, and REX1 is no longer detectable. The importance of RNF12:REX1 titration, and well titrated expression of other putative XCI activators and -inhibitors, is further illustrated by the experiments with XXY triploid ES cells described in chapter 2. In these cells the gene dosage between *RNF12* and *REX1* is 2:3, whereas in normal diploid cells this ratio is 2:2. Compared to diploid cells XXY triploid cells have a very low rate of XCI initiation, indicating that the relative level of RNF12 and other putative XCI activators in these cells only marginally exceeds the threshold required for XCI (fig. 2). Furthermore, when these cells are compared to tetraploid XXXY cells with a *RNF12:REX1* ratio of 3:4, it becomes obvious that the rate of XCI depends on the genic ratio of *RNF12:REX1*, with large differences in the rate of XCI initiation occurring as a result of small changes in the XCI activators: XCI inhibitors ratio. Taken together, these results suggest that the balance between XCI activators and XCI inhibitors, which is likely reflected by *RNF12* and *REX1* needs to be titrated precisely to ensure a well-executed XCI process.

The importance of correct titration of RNF12 and REX1 is further illustrated by the observations described in chapter 4, where mutations in *RNF12* with both a gain-of-function and a loss-of-function result in exclusive inactivation of the X chromosome carrying the mutant allele. This observation suggests that cells do not tolerate an overdose, nor a deficit in functional RNF12. Here, we present a model explaining the observation that both a hypermorphic *RNF12* allele and a hypomorphic *RNF12* allele result in primary non-random XCI of the mutant X chromosome. (Fig. 3). In mouse, before XCI is initiated there is a relatively high concentration of REX1, with a low concentration of RNF12. Upon differentiation RNF12 is upregulated leading to targeted degradation of REX1. When the concentration of REX is

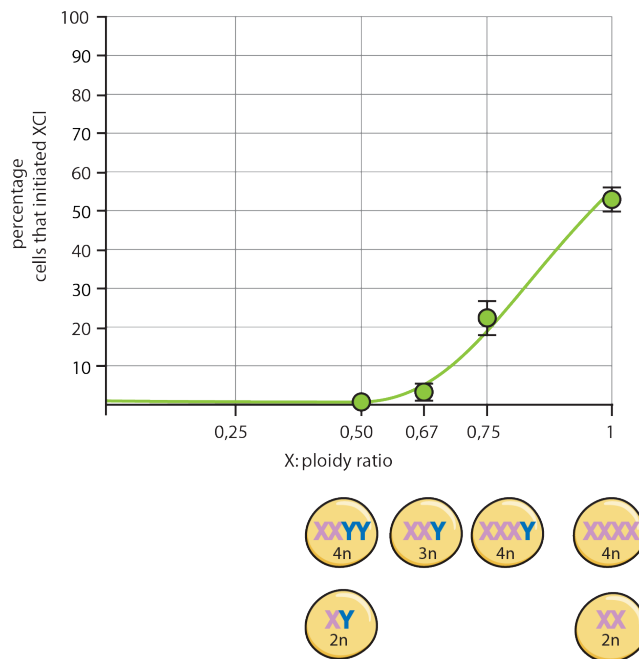


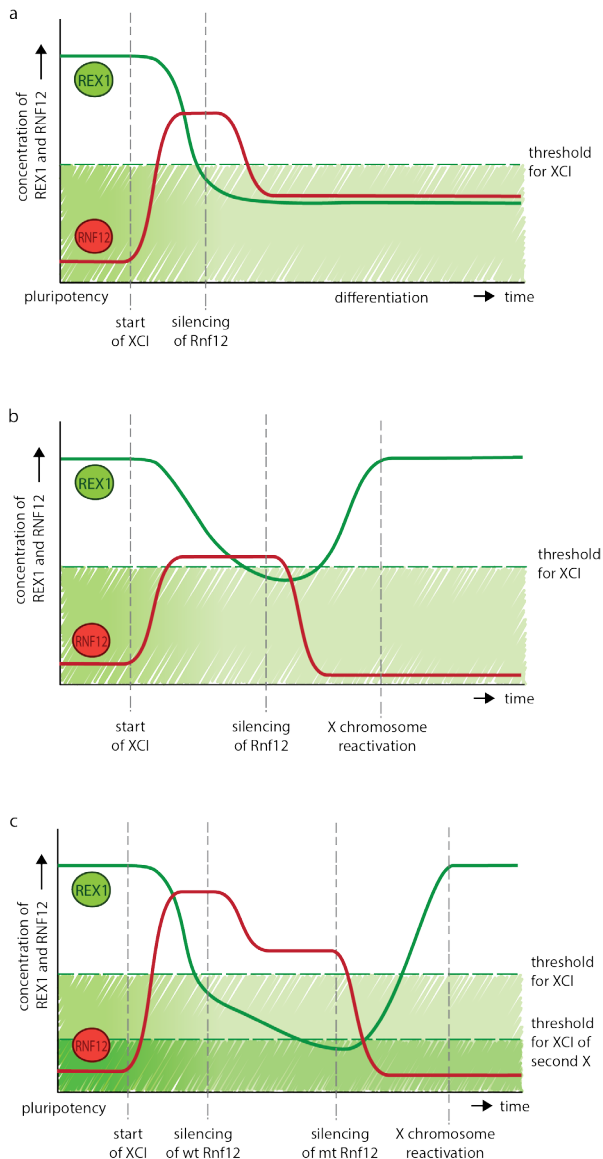
Figure 2.

XCI initiation differs by X:ploidy ratio

The percentage of cells that initiated XCI at d3 of ES cells differentiation is plotted against the X:ploidy ratio. XCI initiation is shown for XY and XX diploid cells, XXY triploid cells and XXXY, XXXY, and XXXX tetraploid cells.

reduced below a threshold where REX1 is no longer able to repress *Xist*, XCI is initiated. This results in *Xist* upregulation on both X chromosomes. The X chromosome where *Xist* silences its antisense inhibitor *Tsix* will be completely inactivated, and will be the future Xi. On this X chromosome *Xist* will also silence *Rnf12 in-cis*, leading to a reduction in the concentration of RNF12, which prevents inactivation of the second X chromosome by halting further degradation of REX1 (Fig. 3a). We hypothesize that in cells carrying a hypermorph or a hypomorph *RNF12* allele, the only possible outcome of XCI is inactivation of the mutant X chromosome, because inactivation of the wildtype *RNF12* allele will result in re-activation of the Xi in both situations. After reactivation the XCI process starts over again, repeating itself until the mutant *RNF12* allele is inactivated.

When considering cells heterozygous for a hypomorph *RNF12* allele, these cells are presented with the choice to inactivate the X chromosome carrying the mutant *RNF12* allele, or

**Figure 3.****Models of XCI in the presence of a hypermorph or hypomorph RNF12 allele**

a. Wildtype situation: Graph representing the relative concentrations of functional RNF12 and REX1 plotted against time from differentiation. In pluripotent cells REX1 concentrations are high, whereas RNF12 concentrations are low. Upon differentiation RNF12 is upregulated and targets REX1 for degradation, lowering the REX1 concentration. When REX1 concentrations drop below the XCI threshold Xist is upregulated and XCI starts on both X chromosomes. After the first X chromosome has silenced its copy of RNF12 the concentration of RNF12 decreases, which prevents a further decrease in REX1 and inactivation of the second X chromosome.

b. Hypomorph situation: If the X chromosome carrying the wildtype allele of RNF12 is inactivated the effective concentration of RNF12 from the mutant allele is insufficient to keep REX1 concentrations below the XCI threshold. Note that the

total amount of functional RNF12 is lower, and that upon inactivation of the wildtype allele, the functional dose of RNF12 is insufficient to keep REX1 below the XCI-threshold.

c. Hypermorph situation: If the X chromosome carrying the wildtype allele of RNF12 is inactivated an excessive amount of functional RNF12 remains. This excess of functional RNF12 degrades REX1 levels to below the threshold for inactivation of the second X chromosome. When both copies of RNF12 are silenced, REX1 levels increase again resulting in the reactivation of one or both X chromosomes. Note that the total amount of functional RNF12 is increased.

the X chromosome carrying the wildtype *RNF12* allele. When inactivation of the mutant X chromosome occurs, the wildtype allele will remain active, resulting in a wildtype situation. However, inactivation of the wildtype allele, means that the hypomorph allele remains active, resulting in a functional level of RNF12 that is insufficient to keep REX1 levels below the threshold required for XCI. This results in reactivation of the wildtype X chromosome, which allows the choice process to start over again until it results in inactivation of the mutant allele (Fig. 3b). When cells heterozygous for a hypermorph *RNF12*, inactivate the wildtype X chromosome an excess of functional RNF12 remains, which results in inactivation of the second X chromosome. When both alleles of *RNF12* are silenced the concentration of REX1 raises in the absence of RNF12, which results in reactivation of one or two X chromosomes (Fig 3c.). Both scenarios are characterized by an extended time period during which cells inactivate and reactivate, which eventually results in skewed XCI.

Skewing of XCI

The clinical relevance of skewed XCI is clearly demonstrated by female carriers of X-linked diseases like Rett syndrome and Fragile X syndrome, as disease severity in these females is correlated to the degree of skewed XCI (Archer et al., 2007; Knudsen et al., 2006). In chapter 5 we examined the correlation of different tissues within a female individual with regard to their XIR, and despite the good correlation between tissues, we observed considerable variation within individuals. This result is not only of relevance for clinical interpretation of XIR's determined in peripheral blood and their correlation to inaccessible disease affected tissues, but will also be important for the interpretation of X-linked variants in GWA studies. Until now, X-chromosomal data in GWA studies have been relatively neglected, due to their complexity in analysis. However, attention in this field is focused on developing new methods to properly analyze X-chromosomal data, and the first analyses dedicated to X-chromosomal variants are published (Chang et al., 2014; Wise et al., 2013). An increase in identified X-linked variants can be expected, and for the correct interpretation of these X-linked variants their relative expression will be of importance. For this reason the correlation of XIR's between tissues deserves future attention, and should preferably be aimed at identifying X chromosome wide expression profiles for multiple tissues, to detect tissue specific silencing and escape from XCI.

One phenomenon that will possibly hamper these analyses is that XIR's appear to diverge with age. An association of XCI skewing with increasing age has frequently been reported. Extrapolating from these observations we reasoned that different tissues might skew in opposite directions. The results presented in chapter 5 seem to confirm this hypothesis,

although a larger number of samples will be needed to confirm this. This divergence of tissue specific XIR's within individuals can imply that the correlation between different tissues is different in younger females compared to elderly females. When performing X chromosome-wide analysis of methylation or transcription with the intention to extrapolate to different tissues this should be taken into account.

References

- Allderdice, P.W., Miller, O.J., Miller, D.A., and Klinger, H.P. (1978). Spreading of inactivation in an (X;14) translocation. *Am J Med Genet* 2, 233-240.
- Amenduni, M., De Filippis, R., Cheung, A.Y., Disciglio, V., Epistolato, M.C., Ariani, F., Mari, F., Mencarelli, M.A., Hayek, Y., Renieri, A., *et al.* (2011). iPS cells to model CDKL5-related disorders. *Eur J Hum Genet* 19, 1246-1255.
- Ananiev, G., Williams, E.C., Li, H., and Chang, Q. (2011). Isogenic pairs of wild type and mutant induced pluripotent stem cell (iPSC) lines from Rett syndrome patients as in vitro disease model. *PLoS One* 6, e25255.
- Archer, H., Evans, J., Leonard, H., Colvin, L., Ravine, D., Christodoulou, J., Williamson, S., Charman, T., Bailey, M.E., Sampson, J., *et al.* (2007). Correlation between clinical severity in patients with Rett syndrome with a p.R168X or p.T158M MECP2 mutation, and the direction and degree of skewing of X-chromosome inactivation. *J Med Genet* 44, 148-152.
- Arnaud, D., Mattei, M.G., and Avner, P. (1993). A panel of deleted mouse X chromosome somatic cell hybrids derived from the embryonic stem cell line HD3 shows preferential breakage in the Hprt-DXHX254E region. *Genomics* 18, 520-526.
- Augui, S., Filion, G.J., Huart, S., Nora, E., Guggiari, M., Maresca, M., Stewart, A.F., and Heard, E. (2007). Sensing X chromosome pairs before X inactivation via a novel X-pairing region of the Xic. *Science* 318, 1632-1636.
- Bacher, C.P., Guggiari, M., Brors, B., Augui, S., Clerc, P., Avner, P., Eils, R., and Heard, E. (2006). Transient colocalization of X-inactivation centres accompanies the initiation of X inactivation. *Nat Cell Biol* 8, 293-299.
- Barakat, T.S., Loos, F., van Staveren, S., Myronova, E., Ghazvini, M., Grootegeed, J.A., and Gribnau, J. (2014). The trans-activator RNF12 and cis-acting elements effectuate X chromosome inactivation independent of X-pairing. *Mol Cell* 53, 965-978.

Brown, C.J., Lafreniere, R.G., Powers, V.E., Sebastio, G., Ballabio, A., Pettigrew, A.L., Ledbetter, D.H., Levy, E., Craig, I.W., and Willard, H.F. (1991). Localization of the X inactivation centre on the human X chromosome in Xq13. *Nature* **349**, 82-84.

Chang, D., Gao, F., Slavney, A., Ma, L., Waldman, Y.Y., Sams, A.J., Billing-Ross, P., Madar, A., Spritz, R., and Keinan, A. (2014). Accounting for eXentricities: analysis of the X chromosome in GWAS reveals X-linked genes implicated in autoimmune diseases. *PLoS One* **9**, e113684.

Cheung, A.Y., Horvath, L.M., Grafodatskaya, D., Pasceri, P., Weksberg, R., Hotta, A., Carrel, L., and Ellis, J. (2011). Isolation of MECP2-null Rett Syndrome patient hiPS cells and isogenic controls through X-chromosome inactivation. *Hum Mol Genet* **20**, 2103-2115.

Donohoe, M.E., Silva, S.S., Pinter, S.F., Xu, N., and Lee, J.T. (2009). The pluripotency factor Oct4 interacts with Ctfc and also controls X-chromosome pairing and counting. *Nature* **460**, 128-132.

Gontan, C., Achame, E.M., Demmers, J., Barakat, T.S., Rentmeester, E., van, I.W., Grootegoed, J.A., and Gribnau, J. (2012). RNF12 initiates X-chromosome inactivation by targeting REX1 for degradation. *Nature* **485**, 386-390.

Grumbach, M.M., Morishima, A., and Taylor, J.H. (1963). Human Sex Chromosome Abnormalities in Relation to DNA Replication and Heterochromatinization. *Proc Natl Acad Sci U S A* **49**, 581-589.

Jonkers, I., Barakat, T.S., Achame, E.M., Monkhorst, K., Kenter, A., Rentmeester, E., Grosveld, F., Grootegoed, J.A., and Gribnau, J. (2009). RNF12 is an X-Encoded dose-dependent activator of X chromosome inactivation. *Cell* **139**, 999-1011.

Kanda, N. (1973). A new differential technique for staining the heteropycnotic X-chromosome in female mice. *Exp Cell Res* **80**, 463-467.

Kim, K.Y., Hysolli, E., and Park, I.H. (2011). Neuronal maturation defect in induced pluripotent stem cells from patients with Rett syndrome. *Proc Natl Acad Sci U S A* **108**, 14169-14174.

Knudsen, G.P., Neilson, T.C., Pedersen, J., Kerr, A., Schwartz, M., Hulten, M., Bailey, M.E., and Orstavik, K.H. (2006). Increased skewing of X chromosome inactivation in Rett syndrome patients and their mothers. *Eur J Hum Genet* **14**, 1189-1194.

Lafreniere, R.G., and Willard, H.F. (1993). Pulsed-field map of Xq13 in the region of the human X inactivation center. *Genomics* **17**, 502-506.

Leppig, K.A., Brown, C.J., Bressler, S.L., Gustashaw, K., Pagon, R.A., Willard, H.F., and Disteche, C.M. (1993). Mapping of the Distal Boundary of the X-Inactivation Center in a Rearranged X-Chromosome from a Female Expressing Xist. *Human Molecular Genetics* **2**, 883-887.

- Marchetto, M.C., Carromeu, C., Acab, A., Yu, D., Yeo, G.W., Mu, Y., Chen, G., Gage, F.H., and Muotri, A.R. (2010). A model for neural development and treatment of Rett syndrome using human induced pluripotent stem cells. *Cell* 143, 527-539.
- Masui, O., Bonnet, I., Le Baccon, P., Brito, I., Pollex, T., Murphy, N., Hupe, P., Barillot, E., Belmont, A.S., and Heard, E. (2011). Live-cell chromosome dynamics and outcome of X chromosome pairing events during ES cell differentiation. *Cell* 145, 447-458.
- Migeon, B.R., Jeppesen, P., Torchia, B.S., Fu, S., Dunn, M.A., Axelman, J., Schmeckpeper, B.J., Fantes, J., Zori, R.T., and Driscoll, D.J. (1996). Lack of X inactivation associated with maternal X isodisomy: evidence for a counting mechanism prior to X inactivation during human embryogenesis. *Am J Hum Genet* 58, 161-170.
- Monkhorst, K., Jonkers, I., Rentmeester, E., Grosveld, F., and Gribnau, J. (2008). X inactivation counting and choice is a stochastic process: evidence for involvement of an X-linked activator. *Cell* 132, 410-421.
- Okamoto, I., Patrat, C., Thepot, D., Peynot, N., Fauque, P., Daniel, N., Diabangouaya, P., Wolf, J.P., Renard, J.P., Duranthon, V., *et al.* (2011). Eutherian mammals use diverse strategies to initiate X-chromosome inactivation during development. *Nature* 472, 370-374.
- Osborne, C.S., Chakalova, L., Mitchell, J.A., Horton, A., Wood, A.L., Bolland, D.J., Corcoran, A.E., and Fraser, P. (2007). Myc dynamically and preferentially relocates to a transcription factory occupied by Igh. *PLoS Biol* 5, e192.
- Pomp, O., Dreesen, O., Leong, D.F., Meller-Pomp, O., Tan, T.T., Zhou, F., and Colman, A. (2011). Unexpected X chromosome skewing during culture and reprogramming of human somatic cells can be alleviated by exogenous telomerase. *Cell Stem Cell* 9, 156-165.
- Rastan, S. (1983). Non-random X-chromosome inactivation in mouse X-autosome translocation embryos--location of the inactivation centre. *J Embryol Exp Morphol* 78, 1-22.
- Rastan, S., and Robertson, E.J. (1985). X-chromosome deletions in embryo-derived (EK) cell lines associated with lack of X-chromosome inactivation. *J Embryol Exp Morphol* 90, 379-388.
- Robertson, E.J., Evans, M.J., and Kaufman, M.H. (1983). X-chromosome instability in pluripotential stem cell lines derived from parthenogenetic embryos. *J Embryol Exp Morphol* 74, 297-309.
- Takagi, N. (1980). Primary and secondary nonrandom X chromosome inactivation in early female mouse embryos carrying Searle's translocation T(X; 16)16H. *Chromosoma* 81, 439-459.
- Takahashi, K., Tanabe, K., Ohnuki, M., Narita, M., Ichisaka, T., Tomoda, K., and Yamanaka, S. (2007). Induction of pluripotent stem cells from adult human fibroblasts by defined factors. *Cell* 131, 861-872.

Tchieu, J., Kuoy, E., Chin, M.H., Trinh, H., Patterson, M., Sherman, S.P., Aimiwu, O., Lindgren, A., Hakimian, S., Zack, J.A., *et al.* (2010). Female human iPSCs retain an inactive X chromosome. *Cell Stem Cell* 7, 329-342.

Teklenburg, G., Weimar, C.H., Fauser, B.C., Macklon, N., Geijsen, N., Heijnen, C.J., Chuva de Sousa Lopes, S.M., and Kuijk, E.W. (2012). Cell lineage specific distribution of H3K27 trimethylation accumulation in an in vitro model for human implantation. *PLoS One* 7, e32701.

Webb, S., de Vries, T.J., and Kaufman, M.H. (1992). The differential staining pattern of the X chromosome in the embryonic and extraembryonic tissues of postimplantation homozygous tetraploid mouse embryos. *Genet Res* 59, 205-214.

Wise, A.L., Gyi, L., and Manolio, T.A. (2013). eXclusion: toward integrating the X chromosome in genome-wide association analyses. *Am J Hum Genet* 92, 643-647.

Xu, N., Tsai, C.L., and Lee, J.T. (2006). Transient homologous chromosome pairing marks the onset of X inactivation. *Science* 311, 1149-1152.

CHAPTER 8



Summary
Samenvatting
Curriculum Vitae
List of Publications
PhD portfolio



Summary

The difference in sex-chromosome constitution between XY males and XX females results in an imbalance for X-encoded genes, with females having a double amount of X-encoded gene products compared to males. To compensate this difference in X-chromosomal dosage, one of the X chromosomes in every female cell is inactivated in a process called X chromosome inactivation (XCI). XCI is initiated during early female embryogenesis, and seems to differ between mouse and human. In mouse two successive forms of XCI take place, with imprinted XCI (iXCI) occurring in cells of the extraembryonic tissues, and random XCI (rXCI) in cells of the embryo proper. Imprinted XCI precedes random XCI, and results in the exclusive inactivation of the paternal X chromosome (Xp) in all cells of the morula stage embryo. Later, the cells that will comprise the embryo proper reactivate their inactive Xp to undergo rXCI, in which all cells will make an individual choice which X chromosome is inactivated. After a cell has inactivated one of its X chromosomes, this inactive state will be passed on to all daughter cells. In humans, both extra-embryonic and embryonic tissues undergo rXCI. While human rXCI is of clinical importance when a X-linked disease or trait is involved, rXCI has been most extensively studied in the mouse. In this thesis we studied the mechanism behind rXCI in mouse, and the genetic elements involved in human rXCI. In addition, we studied the correlation of XCI between different human tissues and examined the reactivation of the Xi during reprogramming of human somatic cells.

For mouse rXCI, several models explain how cells count the number of X chromosomes that are present, and determine which X chromosome is inactivated. The most fitting model is the recently postulated stochastic model, where every X chromosome is proposed to have an intrinsic chance to inactivate. This model was proposed after the observation that tetraploid XXXX cells undergo XCI at a higher rate compared to XXXY cells. [Chapter 2](#) describes experiments that support the stochastic model of XCI. The dynamics of XCI in triploid XXY embryonic stem (ES) cells were analyzed and demonstrate that the probability for an X chromosome to inactivate depends on the X:autosome ratio. In addition, it is shown that XCI is independent of cell division. Since XCI is severely delayed in triploid XXY cells, the concentration of a hypothetical *trans*-acting activator only slightly exceeds the required threshold for XCI. Computer simulation is used to show that observational experimental data of XCI match a stochastic model, where XCI is determined by the concentration of a *trans*-acting activator of XCI and an X chromosome specific threshold for XCI. Simulated data predict that the probability for an X chromosome to inactivate is not static, but changes during differentiation.

Where in the mouse the genetic locus and diffusible factors required for proper initiation of XCI have been well defined, their involvement in human XCI is less well

understood. In mouse, the genetic locus required for XCI to take place is the X-inactivation center (Xic). The mouse Xic can be divided in a *cis*-acting part and a *trans*-acting part. The *cis*-acting part is required for inactivation of the X chromosome *in-cis*, and the non-coding genes *Xist* and *Tsix* are crucial for its functioning. *Xist* produces a non-coding RNA that associates exclusively with the inactive X-chromosome (Xi). *Tsix* is located antisense to *Xist* and acts as a negative regulator of *Xist*. The *trans*-Xic is responsible for counting the number of X chromosomes in a cell and ensures that all X chromosomes but one are inactivated per diploid genome. To date, the only identified *trans*-acting activator of the *trans*-Xic is the E3 ubiquitin ligase *Rnf12*. *Rnf12* activates *Xist* by targeting the XCI-repressor REX1 for degradation. These central elements of the mouse *cis*- and *trans*-Xic are conserved from mouse to human to various degrees. Human *XIST* is moderately conserved, but functions analogous to mouse *Xist* as its RNA also associates with the Xi *in-cis*. *TSIX* is poorly conserved and seems no longer functional. *RNF12* is strongly conserved, but its involvement in human XCI has not yet been shown. Moreover, whether the human XIC contains a *cis*-acting region and a *trans*-acting region, like the mouse Xic, has not been shown. In [chapter 3](#) evidence is provided that also the human XIC can be divided in a *cis*-acting part and a *trans*-acting part. We describe a female individual with a deletion encompassing the *cis*-XIC. This deletion is mapped to the single nucleotide level, using a chromatin conformation capture based technique, and defines the *cis*-XIC. The location of a human *trans*-acting activator is defined to a small region telomeric of the *cis*-XIC, and contains *RNF12*. In addition, the described individual presented with hypergonadotrophic hypogonadism and we propose that a dosage reduction of DMRT1C by 50% causes this phenotype.

[Chapter 4](#) describes three families with missense mutations in different functional domains of *RNF12*. These different mutations all segregate with intellectual disability in males and result in exclusive XCI of the affected X chromosome in females. *In vitro* experiments show that a mutation in the interaction domain of RNF12 results in a gain of function, as ubiquitinated levels of its substrate REX1 increase. Two mutations in the RING domain of the protein result in a loss of function, with a decreased ubiquitination capacity. Although exclusive inactivation of the X chromosome carrying the *RNF12* mutant allele suggests that human *RNF12* acts as a *trans*-acting activator of XCI, analogous to mouse *Rnf12*, additional experiments are required to definitively confirm this.

As a result of XCI every female individual consists of two cell populations that have a different active X chromosome (Xa). In most females the ratio between cells with an inactive paternal X chromosome and an inactive maternal X chromosome will be around 50:50. Deviations from this 50:50 X-inactivation ratio (XIR) are common, and a situation where over 80% of all cells carry the same Xi is termed skewed XCI. In a healthy female population the XIR follows a normal distribution. The proportion of females that display skewed XCI increases with

age, probably already from neonatal life onwards. The XIR is of clinical relevance when an X-encoded trait or X-linked disease is involved. For several diseases like Rett syndrome and Fragile X syndrome it has been shown that female heterozygote carriers of the causative mutation the disease phenotype is modulated by XIR. Also several clinical conditions, for which no causative X-linked locus has been identified, are nonetheless associated with an increased prevalence of skewed XCI. Clinical testing of the XIR is often done in peripheral blood samples, which is not necessarily the disease-affected tissue. To investigate the correlation between the XIR of easily accessible tissues like blood, buccal epithelium and hair follicle, and often inaccessible disease-affected tissues we compared the XIRs of different tissues. These results are reported in [chapter 5](#), where we find that there is a good correlation between tissue-specific XIR's within an individual, although a substantial variation between tissues is present. Of the easily accessible tissues blood, hair follicles, and buccal epithelium the best correlation to inaccessible tissues was observed for buccal swab. The only inaccessible tissue with a poor correlation to buccal epithelium is ovary, which has a poor correlation to blood as well, but has a good correlation to hair follicles instead.

Despite the clinical implications of XCI, a good model system for studying human XCI is not available yet. With the generation of induced pluripotent stem (iPS) cells, such a model system seemed at hand, as these new pluripotent cells might contain two active X chromosomes. However, reprogramming cells to a naïve state that is associated with two active X chromosomes is difficult, and many studies have reported different outcomes regarding the activity of the X chromosomes. In [chapter 6](#) the reactivation of the Xi is analyzed when cells are being reprogrammed from skin fibroblasts to iPS cells. Although the Xi seems to be reactivated during the early stages of the reprogramming process, the reactivated state is unstable, resulting in re-inactivation. As a result a cell population is a mixture of cells that have two Xa's and cells with one Xi and one Xa. Culturing these cells in naïve medium seems to stabilize the reactivation-inactivation process and allows expansion of clones with two Xa's. These results show that although very inefficient human iPS cells might provide a model system for studying XCI.

Samenvatting

Door het verschil in geslachtschromosomen tussen XY mannen en XX vrouwen hebben vrouwen een dubbele hoeveelheid van X-chromosomale genproducten in vergelijking met mannen. Om te compenseren voor deze relatieve overdosering van het X chromosoom in vrouwen wordt in iedere vrouwelijke cel een X chromosoom geïnactiveerd in een proces genaamd X chromosoom inactivatie (XCI). XCI vindt plaats tijdens de vroege embryogenese en is waarschijnlijk verschillend tussen mens en muis. In de muis treden er twee opeenvolgende vormen van XCI op, waarbij de cellen van de extra-embryonale weefsels een geïmprinte vorm van XCI (iXCI) ondergaan, terwijl de cellen van het embryo random XCI (rXCI) ondergaan. Geïmprinte XCI treedt als eerste op en resulteert in de inactivatie van uitsluitend het paternale X chromosoom in alle cellen van het morula-stadium embryo. Later tijdens de embryonale ontwikkeling reacteren de cellen van het embryo proper hun inactieve paternale X chromosoom, om vervolgens rXCI te kunnen ondergaan, waarbij iedere cel een individuele keuze maakt welk X chromosoom geïnactiveerd wordt. Nadat een cel één van zijn X chromosomen geïnactiveerd heeft, wordt deze inactieve status doorgegeven aan alle dochtercellen. In de mens treedt in zowel de embryonale weefsels als de extra-embryonale weefsels rXCI op. Ondanks dat humaan rXCI van klinisch belang is, wanneer er sprake is van een X-chromosomale aandoening of eigenschap, is rXCI het meest uitvoerig bestudeerd in de muis. In dit proefschrift hebben we het mechanisme achter rXCI in de muis en de genetische elementen die betrokken zijn bij humane rXCI bestudeerd. Daarnaast hebben we de correlatie van XCI tussen verschillende humane weefsels onderzocht en hebben we de reactivatie van het inactieve X chromosoom tijdens de reprogrammering van humane somatische cellen geanalyseerd.

Er bestaan verschillende modellen die voor rXCI in de muis verklaren hoe een cel bepaald hoeveel X chromosomen er aanwezig zijn en hoe bepaald wordt welk X chromosoom geïnactiveerd wordt. Het meest plausibele model is het recent gepostuleerde stochastische model, waarin voorgesteld werd dat ieder X chromosoom een intrinsieke kans heeft om te inactiveren. Dit model is gebaseerd op de observatie dat XCI sneller verloopt in XXXX tetraploïde cellen, in vergelijking met XXXY tetraploïde cellen. In **hoofdstuk 2** worden experimenten beschreven die het stochastisch model van XCI bevestigen. De dynamiek van XCI werd bestudeerd in XXY triploïde embryonale stam (ES) cellen en deze laat zien dat de intrinsieke kans van een X chromosoom om te inactiveren afhankelijk is van de ratio tussen X chromosomen en autosomen. Daarnaast wordt gedemonstreerd dat XCI onafhankelijk is van celdeling. Omdat XCI in triploïde cellen plaatsvindt met een erg vertraagd tempo, moet de concentratie van een hypothetische activator van XCI maar minimaal de vereiste threshold voor initiatie van XCI overstijgen. Computer simulatie wordt gebruikt om te demonstreren dat

observationele experimentele data van XCI compatibel zijn met een stochastisch model, waarin XCI wordt gereguleerd door de concentratie van een activator van XCI en een X chromosoom-specifieke threshold voor XCI. De gesimuleerde data voorspellen dat de kans van een X chromosoom om te inactiveren niet statisch is, maar in plaats daarvan veranderd tijdens cel-differentiatie.

De genetische elementen en diffundeerbare factoren die nodig zijn voor een correctie initiatie van XCI zijn geïdentificeerd in de muis, maar of deze elementen ook een rol spelen in humane XCI is vaak onbekend. In de muis is het genetische locus wat noodzakelijk is om XCI op te laten treden het X-inactivatie centrum (Xic). Het Xic van de muis kan onderverdeeld worden in een *in-cis* werkend gedeelte en een *in-trans* werkend gedeelte. Het *cis*-werkende gedeelte is noodzakelijk voor inactivatie van een X chromosoom *in-cis* en de niet-coderende genen *Xist* en *Tsix* zijn cruciaal voor het juist functioneren van dit gedeelte. *Xist* produceert een niet-coderend RNA, dat uitsluitend associeert met het inactieve X chromosoom (Xi). *Tsix* is antisense ten opzichte van *Xist* georiënteerd en functioneert als een negatieve regulator van *Xist*. De *trans*-Xic telt het aantal X chromosomen in een cel en zorgt ervoor dat er per diploid genoom maar één X chromosoom niet geïnactiveerd wordt. Op dit moment is de enige geïdentificeerde *trans*-werkende activator van de *trans*-Xic het E3 ubiquitine-ligase *Rnf12*. *Rnf12* activeert *Xist* indirect, door de XCI-repressor REX1 te markeren voor afbraak door het proteasoom. Deze elementen die essentieel zijn voor de Xic van de muis, zijn in verschillende mate geconserveerd in de mens. Humaan *XIST* is matig geconserveerd, maar functioneert analoog aan muizen *Xist* waarbij het *XIST* RNA ook associeert met de Xi *in-cis*. *TSIX* is slecht geconserveerd en lijkt niet langer functioneel. *RNF12* is sterk geconserveerd, maar of *RNF12* een functie heeft in humane XCI is nog onbekend. Ook was het nog onbekend of de humane XIC, net als de Xic in muis, onderverdeeld kan worden in een *cis*-werkend gedeelte en een *trans*-werkend gedeelte. In **hoofdstuk 3** worden resultaten getoond, die laten zien dat ook de humane XIC in een *cis*-werkend gedeelte en een *trans*-werkend gedeelte kan worden onderverdeeld. Dit hoofdstuk beschrijft een vrouw, waarbij een deletie van de XIC werd geïdentificeerd. Deze deletie werd tot op de nucleotide nauwkeurig geïdentificeerd met een techniek gebaseerd op chromatin conformation capture, en representeert de *cis*-XIC. Een humane *trans*-werkende activator van XCI moet gelokaliseerd zijn in een kleine regio telomerisch ten opzichte van de *cis*-XIC, waarin ook *RNF12* gelokaliseerd is. Daarnaast is er bij de vrouw die in dit hoofdstuk beschreven wordt sprake van een hypergonadotroop hypogonadisme. Dit fenotype wordt volgens ons mogelijk verklaart door een reductie van 50% in de dosering *DMRT1C*.

Hoofdstuk 4 beschrijft drie families met missense mutaties in verschillende functionele domeinen van *RNF12*. Deze verschillende mutaties segregeren in mannen met verstandelijke beperking en leiden in vrouwen tot XCI met inactivatie van uitsluitend het aangedane X

chromosoom. De in vitro experimenten die worden beschreven laten zien dat een mutatie in het interactiedomein van RNF12 leidt tot toegenomen functionele capaciteit, wat blijkt uit de toename in de hoeveelheid geubiquitineerd REX1. Twee mutaties in het RING domein van RNF12 leiden tot een afgenomen functionele capaciteit, met een verminderd vermogen tot ubiquitinatie. Omdat bij draagsters van deze *RNF12* mutaties uitsluitend het X chromosoom met het aangedane RNF12 geïnactiveerd is, is het niet onwaarschijnlijk dat humaan *RNF12*, net als muizen *Rnf12*, functioneert als een *trans*-activator van XCI. Om een *trans*-activerende functie van *RNF12* aan te tonen zijn echter verdere experimenten nodig.

Als gevolg van XCI bestaat iedere vrouw uit twee cel populaties, die ieder een ander actief X chromosoom (Xa) hebben. In de meeste vrouwen zal de verhouding tussen de cellen met een actief paternaal X chromosoom (Xp) en de cellen met een actief maternaal X chromosoom (Xm) ongeveer 50:50 zijn. Deviatie van deze 50:50 X-inactivatie ratio (XIR) komt frequent voor en de situatie waar meer dan 80% van alle cellen dezelfde Xi hebben, wordt skewed XCI genoemd. In een gezonde vrouwelijke populatie volgt de XIR een normale verdeling. Het percentage vrouwen met skewed XCI in een populatie neemt toe met de leeftijd, waarschijnlijk al vanaf de geboorte. De XIR is klinisch relevant, wanneer er sprake is van een X-gecodeerde eigenschap, of X-chromosomale aandoening. Voor een aantal aandoeningen, zoals Rett syndroom en Fragiele X syndroom, wordt het fenotype in vrouwelijke draagsters van deze aandoening gemoduleerd door de XIR. Daarnaast zijn er een aantal aandoeningen waar geen X-chromosomale oorzaak voor geïdentificeerd is, die geassocieerd zijn met een verhoogde prevalentie van skewed XCI. Klinische testen gericht op het bepalen van de XIR worden vaak uitgevoerd op perifere bloedsamples, ook al is dit niet altijd het aangedane weefsel. Om de correlatie te testen tussen de XIR van makkelijk toegankelijke weefsels zoals bloed, wangslijmvlies en haarfollikel, en de XIR van de vaak ontoegankelijke aangedane weefsels, hebben we de XIR van verschillende weefsels met elkaar vergeleken. De resultaten hiervan worden beschreven in [hoofdstuk 5](#), waar we een goede correlatie vinden tussen de weefselspecifieke XIR's van een vrouw, ook al is er een substantiële variatie aanwezig. Van de gemakkelijk toegankelijke weefsels bloed, wangslijmvlies en haarfollikel had wangslijmvlies de beste correlatie met de ontoegankelijke weefsels. Het enige ontoegankelijke weefsel met een slechte correlatie met wangslijmvlies was ovarium, waarvoor wel een goede correlatie met haarfollikel gevonden werd.

Ondanks de klinische implicaties van XCI, is er geen goed modelsysteem beschikbaar om humaan XCI te bestuderen. Na de beschrijving van de eerste geïnduceerde pluripotente stamcellen (iPSC) leek dit modelsysteem aanstaande, omdat deze nieuwe pluripotente stamcellen mogelijk twee actieve X chromosomen bevatten. Maar het reprogrammeren van somatische cellen naar een naïeve staat, waarbij beide X chromosomen actief zijn, is moeizaam gebleken en vele studies hebben verschillende uitkomsten beschreven wat betreft de activiteit

van de twee X chromosomen. In **hoofdstuk 6** is de reactivatie van de Xi geanalyseerd tijdens het reprogrammeren van huidfibroblasten naar iPS cellen. De Xi wordt inderdaad gereactiveerd vroeg tijdens het proces van reprogrammeren, maar deze reactivatie is instabiel en leidt tot re-inactivatie. Als gevolg hiervan bestaat een gereprogrammeerde cel populatie uit zowel cellen met twee Xa's als cellen met een Xi en een Xa. Wanneer deze gereprogrammeerde cellen in naïef medium gekweekt worden, wordt het reactivatie-inactivatie proces van de Xi gestabiliseerd. Hierdoor is expansie van de cel-klonen met twee Xa's mogelijk. Deze resultaten laten zien dat humane iPS cellen een modelsysteem voor XCI zijn, ook al is het genereren van deze cellen een inefficiënt proces.

List of Publications

Frints S*, De Hoon B*, Gontan C*, Gecz J, Laven JS and Gribnau J. (manuscript in preparation). Mutations in RNF12 segregate with X-linked intellectual disability and result in hypomorphic alleles

Maduro C, De Hoon B, Gribnau J (Submitted). Fitting the puzzle pieces: the bigger picture of XCI

De Hoon B, Splinter E, Eussen B, Douben JCW, Rentmeester E, van de Heijning M, de Klein JEMM, Laven JS, Liebelt J* and Gribnau J*. (Submitted). X chromosome inactivation in a female carrier of a 1.28 Mb deletion encompassing the human X inactivation center

De Hoon B, Monkhorst K, Riegman P, Laven JS, Gribnau J (2015). Buccal swab as a reliable predictor for X-inactivation ratio in inaccessible tissues. *Journal of Medical Genetics*, 2015 Jul 28

Barakat TS, Ghazvini M, de Hoon B, Li T, Eussen B, Douben H, van der Linden R, van der Stap N, Boter M, Laven JS, Galjaard RJ, Grootegeod JA, de Klein A, Gribnau J (2015). Stable X chromosome reactivation in female human induced pluripotent stem cells. *Stem Cell Reports*, vol. 4(2): pp. 199-208.

Rottenberg S, Vollebergh MA, de Hoon B, de Ronde J, Schouten PC, Kersbergen A, Zander SA, Pajic M, Jaspers JE, Jonkers M, Lodén M, Sol W, van der Burg E, Wesseling J, Gillet JP, Gottesman MM, Gribnau J, Wessels L, Linn SC, Jonkers J, Borst P (2012). Impact of intertumoral heterogeneity on predicting chemotherapy response of BRCA1-deficient mammary tumors. *Cancer Research*, vol. 72(9): pp. 2350-2361.

Monkhorst K*, De Hoon B*, Jonkers I, Mulugeta Achame E, Monkhorst W, Hoogerbrugge J, Rentmeester E, Westerhoff HV, Grosveld F, Grootegeod JA, Gribnau J (2009). The probability to initiate X chromosome inactivation is determined by the X to autosomal ratio and X chromosome specific allelic properties. *PLoS One*, vol. 4(5): 5616.

Curriculum Vitae

Personal Information

Bas de Hoon

Date of Birth: 27-10-1983, Oosterhout, the Netherlands

Education

- 2010 - 2015: PhD research, Dept. of Obstetrics and Gynaecology, Dept of Developmental Biology,
Erasmus MC Rotterdam
- 2003 - 2007: Master of Science: Molecular Medicine, Erasmus MC Rotterdam
- 2002 - 2009: Medicine, Erasmus Mc Rotterdam
- 1996 - 2002: Gymnasium, Sint-Oelbert, Oosterhout

Employment history

- 2009 - 2010: Internship gynaecologie (ANIOS), Amphia Ziekenhuis Breda

Research experience

- 2006: Scientific internship of 6 months at the Department of Cell Biology, Erasmus MC Rotterdam. During this internship I investigated the function of the transcriptional regulator CTCF using an in vitro model.
- 2006: Scientific internship of 3 months at the Department of Internal Medicine, Erasmus MC Rotterdam. This research explored the function of the calcium channel TRPV5 using a mouse model.
- 2007: Scientific internship of 10 months at the Department of Developmental Biology, Erasmus MC Rotterdam. This research focused on the molecular mechanism of X chromosome inactivation.
- 2010 - now: PhD research at the Department of Obstetrics and Gynaecology, subdivision of Reproductive medicine, and the Department of Developmental Biology. This research focusses on the molecular mechanisms and clinical implications of human X chromosome inactivation.

PhD Portfolio

Name: Bas de Hoon
Department: Developmental Biology
 Obstetrics and Gynaecology
PhD period: 2011-2015
Promotor: Prof. dr. J. Gribnau
 Prof. dr. J.S. Laven

1. PhD training	year	workload (ECTS)
General courses		
Biostatistics for clinicians	2011	0,6
Laboratory animal science (art.9/FELASA-C)	2011	1
Handling of laboratory animals (IVC)	2012	
Specific courses		
Cell and Developmental Biology course	2011	1
Genetics course	2011	1
Biochemistry and Biophysics course	2011	1
Literature discussion course	2011	0,2
Heard-Gribnau lab retreat	2012	1
Heard-Gribnau lab retreat	2013	1
Refereeravonden Rotterdams Gynaecologen Opleidings Cluster	2010-2015	0,4
Seminars and workshops		
Department journal club	2011-2015	1
Presentations		
Reproduction and Development work discussions	2010-2015	1
Obstetrics and Gynaecology, Reproductive Medicine work discussions	2010-2015	0,6
Heard-Gribnau lab retreat	2012	1
TRR81 Winter School	2012	1
Heard-Gribnau lab retreat	2013	1
International conferences		
TRR81 Symposium on Chromatin Changes in Differentiation and Malignancy	2011	0,6
10 th Dutch Chromatin Meeting	2012	0,2
TRR81 Winter School (oral presentation)	2012	1
Stem Cells, Development and Regulation	2012	1
TRR81 Symposium on Chromatin Changes in Differentiation and Malignancy	2013	0,6
Society of Reproductive Investigations (oral presentation)	2014	1
Society of Reproductive Investigations (poster presentation)	2015	1
2. Teaching	year	workload (ECTS)
Supervising Junior Science project	2011	0,8
Supervising Master of Science Lab rotation	2012	1
VO: Vroege embryo's, klonen en transgenese	2011-2014	0,8

Dankwoord

Lieve vrienden, familie en collega's, mijn promotietraject zit er nu bijna op en het is geweldig om dit te kunnen afsluiten met dit proefschrift. Ik wil iedereen bedanken die mij geholpen heeft bij het tot stand komen van dit proefschrift. Even dankbaar ben ik voor alle hulp bij de experimenten die dit proefschrift niet bereikt hebben. Ik wil jullie allemaal heel erg bedanken voor deze onvergetelijke tijd.

Beste Professor Gribnau, beste Joost, dit promotietraject is voor mij al begonnen toen ik als master student bij jouw groep kwam. Ik heb je leren kennen als een goede wetenschapper, maar bovenal als iemand met een hartelijke persoonlijkheid. Sinds dat begin is er veel veranderd, maar voor mij ben jij altijd die begeleider gebleven met wie ik pipetteer-helmen moest maken om te celkweken. In de afgelopen jaren heeft jouw deur altijd voor mij open gestaan. Bedankt voor je opbeurende gesprekken wanneer ik deze nodig had. Bedankt ook, voor je geduld met mij als ik weer een keer onaangekondigd je kamer binnenliep, of als je mij bij herhaling iets uit moest leggen, omdat ik het na een paar slapeloze nachten met de kinderen weer vergeten was. Ik hoop dat onze paden elkaar in de toekomst nog vaak mogen kruisen.

Beste Professor Laven, beste Joop, ik heb je de afgelopen jaren leren kennen als een begeleider die volledig achter zijn promovendi staat. Het was mooi om jou de resultaten van mijn basale experimenten voor te leggen en te zien hoe jij deze in een ander daglicht plaatste. Ook al hebben we misschien niet zo vaak overleg gehad als we gewild zouden hebben, ik heb me altijd één van jouw team gevoeld. Dank je voor je steun en je mentorschap op de momenten dat ik deze nodig had.

In het bijzonder wil ik ook de leden van mijn kleine commissie bedanken voor het nauwkeurig lezen van dit proefschrift. Dank ook aan de leden van de grote commissie dat u hier deel van uit wilt maken.

Beste Professor Grootegoed, beste Anton, zonder jou was dit proefschrift er nooit gekomen. En wie weet hoe mijn loopbaan zich dan gevormd zou hebben. Toen ik als master student het niet zag zitten om de master verder af te maken, was jij degene die me overtuigt heeft om dit toch te doen. Die keuze heeft me uiteindelijk geleid naar dit promotie-traject, waarvoor ik je nu nog dankbaar ben.

Lieve collega's van het Albert Schweitzer ziekenhuis, bedankt voor jullie warme ontvangst. Ik geniet er nog iedere dag opnieuw van terug te zijn in de kliniek en met jullie samen te mogen werken.

Dear members of lab 902, Adna, Andrea, Azi, Daphne, Dimitar, Esther, Elvira, Gaby, Joachim, Joke, Marja, Nilhan, Peng and Stefan. It has been a great pleasure to work together with all of you! Thank you for all the fun, the interesting discussions and your help with experiments. Ruben, Ruby! Jij weet als geen ander hoe het is om te promoveren bij een klinische en een basaal wetenschappelijke afdeling. Jouw ontspannen manier van werken is altijd een mooie compensatie geweest voor mijn gehaastheid. Kim, bedankt voor je hulp en je altijd kritische beschouwing van bijna elke situatie. Het was mooi om in verschillende fasen van onze carrières samen te mogen werken. Hopelijk krijgen we deze kans in de toekomst nog een keer. Jos en Evelyne, jullie zijn vanaf het begin mijn buurtjes geweest. Ik heb genoten van de vele gezellige momenten die daarbij hoorden. Catherine, roomie, door jou denk ik soms nog steeds dat ik kattengeluiden achter me hoor. Cheryl, misschien heb je in het begin even moeten wennen aan mijn grappen, maar ik heb ervan genoten steeds meer weerwoord van jou te krijgen. Eskeww, it is a pity that we did not work together for a longer time. I always enjoyed our serious and also our hilarious conversations. Cristina, I think everything I learned from working with protein, I learned from you! Friedemann, thank you for our great discussions. Fabrizia, thank you for all your great stories. I am afraid I won't remember them as accurately as you probably can. Agnese, it is great to see your enthusiasm for science. But please don't talk to the closet anymore. Hegias, thanks for all the laughs we had. Fede, your cheerfulness seems to make all people around you happy. Godfried, soms mis ik onze gesprekken, die ineens een bizarre wending konden nemen. Aristeia, thank you for helping me out so many times. Without you my cloning would still be unfinished. Willy, bedankt voor je kritische beschouwingen en suggesties tijdens onze onderzoeksbesprekingen. Maureen, jij was voor mij soms een extra begeleider. Dankjewel voor je steun en adviezen.

Beste Guido, Bianca en Marialuisa, ontzettend bedankt voor al jullie hulp met de ABI genetic analyzer. Zonder jullie hulp was de HumARA nooit van de grond gekomen. Josja, je zal wel blij zijn dat je je computer weer helemaal voor jezelf hebt. Bert, Erwin en Hannie, bedankt voor al jullie hulp met experimenten. Jullie expertise is onmisbaar geweest.

Jaap en Jaap, van de pathologie, bedankt voor de opvrolijkende telefoontjes iedere ochtend, zoveel dagen en jaren achter elkaar.

Beste Cindy, Esther, Hikke, Ilse, bedankt voor het meedenken en de hulp bij experimenten.

Mehrnaz, Tracy, Dorota and Alex, many thanks for your advices and help with cell culture. Also many thanks to all other great people of the ErasmusMC that I have met over the past years and that I have forgotten to mention.

Lieve (oud) arts-onderzoekers van de gynaecologie: Aleid, Amber, Anke, Babs, Babette, Caroline, Christine, Cindy, Eline, Emilie, Evelyne, Fatima, Hein, Irene, Jashvant, Jacky, Jinke, John, Leonie, Lindy, Matthijs, Meertien, Melek, Nicole, Olivier, Paulien, Sabine, Wendy, Yvonne, en Zoe, bedankt voor alle gezellige momenten! Sam, ook al was jij al klaar met je promotie, bedankt voor je steun en interesse als mede-arts in de basale wetenschap. Ik heb je enthousiasme en adviezen altijd erg gewaardeerd.

Lieve Annegien en Eveline, bedankt dat jullie naast mij willen staan als mijn paranimfen. Eveline, (ik zal je naam nu een keer goed spellen) we kennen elkaar al sinds mijn begin op het lab als master student. Als mede-Breda-naars hadden wij elkaar al snel gevonden en in de jaren daarna hebben we vele gezellige momenten beleefd. Daarnaast is je enorme hulp bij mijn experimenten van onschatbare waarde geweest. Annegien, jij kwam pas halverwege mijn promotie, maar wij zaten al meteen op één lijn. Ik heb genoten van onze discussies en grappen. Dankjewel voor alle gezellige momenten. Het was inspirerend om te zien hoe gemotiveerd en gedreven jij met je onderzoek bezig bent. Vergeet je niet om onze plant nog terug te brengen?

Bart en Bart, jongens van de co-groep Tilburg, bedankt voor het regelmatig bijpraten op persoonlijk vlak en vakinhoudelijk, natuurlijk onder het genot van een Belgisch biertje. Jongens van de Mojo Tilburg: Bart, Bob, Jaap, Jordi, Niek, Rick, Rob B en Rob V. Bedankt voor de momenten van ontspanning en ongein tussen het werken door.

Lieve schoonfamilie: oma Jet, Bert, Jos, Marloes, Emiel, Lauran, Joes, Quint, Jos, Carla, Anne en Marleen. Dankjewel voor jullie interesse en steun de afgelopen jaren. Lieve Ad en Rian, soms voel ik me echt als een zoon van jullie. Bedankt voor jullie enorme steun in de afgelopen jaren. Jullie zijn als een rots in de branding geweest tijdens de, soms onstuimige, gebeurtenissen de afgelopen jaren.

Lieve papa en mama, jullie zijn mijn thuisbasis, waarop ik altijd kan terugvallen. Ook al is ons familieleven de afgelopen jaren behoorlijk druk geweest, jullie hebben altijd voor mij klaar gestaan. Dankjewel voor alle hulp en jullie steun in al mijn keuzes. Ben, broertje, het was mooi om te zien hoe snel jij begreep waar ik soms mee bezig was. Mariëlle, bedankt voor het beheren van de sociale agenda van mijn broertje, waardoor er vaker gezellige familie avonden zijn. Lieve Dorien, ik heb je de afgelopen jaren erg zien groeien. Houdt daar niet mee op, hoor!

Alice en Celeste, ik hoop dat jullie altijd zo open en spontaan mogen blijven en dat er nog vele speelmomenten met Stijn en Nina mogen zijn.

Lieve Stijn en Nina, ik ben er ontzettend trots op om jullie papa te mogen zijn. Het is geweldig om jullie je eigen persoonlijkheid te zien ontwikkelen. Ik ben benieuwd naar wat er allemaal nog komen gaat en ik kijk ernaar uit om daar getuige van te mogen zijn.

Lieve Judith, met jouw steun kan ik écht de hele wereld aan! Voor jou zijn de afgelopen jaren niet makkelijk geweest. Dankjewel voor je oneindige geduld, als ik thuis weer eens een experiment niet los kon laten. Er zal, naast mij, niemand zo naar het einde van dit boekje toegeleefd hebben als jij. Dankjewel voor je nooit aflatende steun. Ik hou van jou!

